CONFIDENTIAL

B.S.R.A. Report NS. 333
Naval Architecture Report No. 89

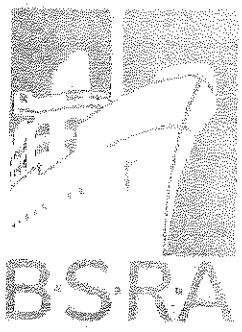

THE BRITISH SHIP RESEARCH ASSOCIATION

Methodical Series Experiments on Single-Screw Ocean-Going Merchant-Ship Forms. Extended and Revised Overall Analysis

(Project No. D1(NA)1)

Part I. Geometry of Forms and Variation of Resistance with Block Coefficient

R. N. M. PATTULLO, C.Eng., F.R.I.N.A.
(Vickers Limited)

Part II. Variation of Resistance with Beam-Draught Ratio, Length-Displacement Ratio and Longitudinal Position of Centre of Buoyancy

B. D. W. WRIGHT, C.Eng., M.R.I.N.A.
(B.S.R.A.)
R. N. M. PATTULLO

Part III. Propulsion Factors

B. D. W. WRIGHT

1971

WALLSEND RESEARCH STATION, WALLSEND,
NORTHUMBERLAND, NE28 6UY

B.S.R.A. REPORT NS. 333

NAVAL ARCHITECTURE REPORT NO. 89

THE BRITISH SHIP RESEARCH ASSOCIATION

Methodical Series Experiments on Single-Screw Ocean-Going Merchant-Ship Forms. Extended and Revised Overall Analysis

Part I. Geometry of Forms and Variation of Resistance with Block Coefficient

R. N. M. PATTULLO, C.Eng., F.R.I.N.A.
(Vickers Limited)

Part II. Variation of Resistance with Beam-Draught Ratio, Length-Displacement Ratio and Longitudinal Position of Centre of Buoyancy

B. D. W. WRIGHT, C.Eng., M.R.I.N.A.
(B.S.R.A.)
R. N. M. PATTULLO

Part III. Propulsion Factors

B. D. W. WRIGHT

1971

WALLSEND RESEARCH STATION, WALLSEND, NORTHUMBERLAND

CONTENTS

PART III. PROPULSION FACTORS

NOMENCLATURE AND SYMBOLS*

A_D/A_O	Developed blade area ratio
B	Beam (m)
Ⓑ	Froude breadth coefficient $= B/\nabla^{1/3}$
C_B	Block coefficient
Ⓒ	Froude resistance coefficient
	$= \frac{250}{\pi} \cdot \frac{R_T}{\rho V^2 \nabla^{2/3}}$ where R_T, ρ, V, and ∇ are in any consistent system of units,
	$= \frac{2924 R_T}{\Delta^{2/3} V^2} = \frac{579{\cdot}9 P_E}{\Delta^{2/3} V^3}$ where R_T is in tonnes Δ is in tonnes salt water V is in knots P_E is in kilowatts
D	Diameter of propeller (m)
D_t	Thrust deduction parameter $= B/\nabla^{1/3} \cdot D/\nabla^{1/3}$
D_W	Wake fraction parameter $= B/\nabla^{1/3} \cdot \sqrt{\nabla^{1/3}/D}$
F_n	Froude number
	$= v/\sqrt{gL_{PP}}$ in any consistent system of units,
	$= 0{\cdot}164\ V/\sqrt{L_{PP}}$ where V is in knots L_{PP} is in metres
L_{PP}	Length between perpendiculars (m)
LCB	Longitudinal position of centre of buoyancy from midships (m). The LCB value is considered positive when forward of midships
Ⓛ	Froude speed-length coefficient
	$= \sqrt{4\pi}\ F_n = 3{\cdot}545\ F_n$
Ⓜ	Froude length coefficient or length-displacement ratio $= L/\nabla^{1/3}$
N	Revolutions per minute
P_E	Effective power (kW)
P/D	Mean face-pitch ratio
R_T	Total resistance (tonnes)
Ⓢ	Froude wetted surface coefficient $= S/\nabla^{2/3}$
S	Wetted surface area (m^2)
t	Thrust-deduction fraction
T	Draught (m)
V	Ship speed (knots)
V_A	Speed of advance of propeller (knots)

** The symbols used conform in general to those recommended in International Towing Tank Conference Standard Symbols 1971, B.S.R.A. Technical Memorandum No. 400. 1971. Other symbols are defined as they appear in the text.*

w_T	Taylor wake fraction
δ	Taylor advance coefficient = ND/V_A
Δ	Displacement (tonnes)
∇	Volume of displacement (m^3)
η_D	Quasi-propulsive coefficient = $\eta_H \cdot \eta_R \cdot \eta_O$
η_H	Hull efficiency = $(1 - t)/(1 - w_T)$
η_O	Open-water efficiency of propeller
η_R	Relative rotative efficiency
$(1 + x)$	Power prediction load factor where x is the overload fraction

Methodical Series Experiments on Single-Screw Ocean-Going Merchant-Ship Forms. Extended and Revised Overall Analysis

§ 1. INTRODUCTION AND SUMMARY

The B.S.R.A. Methodical Series originally consisted of four single-screw parent forms of block coefficient, 0·65, 0·70, 0·75, and 0·80 on each of which the effect of systematic changes in proportions and LCB position was investigated by resistance and propulsion tests on models. In addition to the load draught, tests were also carried out at a number of reduced draughts including a ballast draught trimmed by the stern. An overall analysis was then carried out to facilitate interpolation at intermediate block coefficients for both hull geometry and resistance and propulsion performance.

Since this analysis was made, further systematic model testing for the load condition only has been carried out at Ship Division, N.P.L., and Vickers Experiment Tank, St. Albans, which has extended the scope of the work as follows:-

(i) The range of fullness has been extended down to 0·55 and up to 0·85 block coefficient. For this purpose new parent forms were developed at block coefficients of 0·55, 0·60 and 0·85.

(ii) Several of the parent forms in the intermediate range covered by the original analysis have been redesigned and a considerable improvement in performance obtained.

(iii) Bulbous and non-bulbous forms are now covered.

A new overall analysis incorporating these later developments has been carried out for the load condition and is the subject of the present report. This analysis has been made on generally the same lines as the earlier analysis and the presentation is again in the form of design charts.

These charts enable a hull form, with or without a bulbous bow, and the corresponding resistance and propulsion characteristics at load draught to be readily determined for any block coefficient, beam-draught ratio, length-displacement ratio and LCB position within the scope of the series.

The report is in three parts as follows:-

PART I **Geometry of Forms and Variation of Resistance with Block Coefficient.**
Part I gives, on a base of block coefficient, details of the hull geometry for standard proportions and LCB position together with the corresponding resistance data.

PART II **Variation of Resistance with Beam-Draught Ratio, Length-Displacement Ratio and Longitudinal Position of Centre of Buoyancy.**
Part II gives, also on a base of block coefficient,

correction factors to be applied to the basic resistance given in Part I to allow for changes from the standard values of B/T, $L/\nabla^{1/3}$ and LCB position.

PART III **Propulsion Factors**
Part III gives, also in graphical form, the corresponding propulsion data to be used in conjunction with the information given in Parts I and II. The factors presented include wake fraction, thrust-deduction fraction, relative rotative efficiency, together with quasi-propulsive coefficient.

The use of the design charts is illustrated by worked examples.

The extended and revised overall analysis of the B.S.R.A. Methodical Series data for the load condition given in this report supersedes the earlier one given in References 1, 8, 10, and 21. It is expected that the new presentation of data will meet most requirements for the load condition. If estimates of performance at reduced draughts are required, it is suggested that guidance be obtained from the relative performance at load and fractional draughts given by the earlier analysis for the block coefficient range 0·65 to 0·80. Alternatively use could be made of Moor's analysis of performance at fractional draught[31] which goes beyond this range of block coefficient. It should be noted that both these methods apply to non-bulbous forms and should be used with caution in the case of bulbous forms.

The resistance performance presented in this extended and revised analysis may be compared with the average and optimum 1969 standards of attainment in Reference 32. In particular, for most practical combinations of block coefficient and speed-length ratio the resistance performance lies between the average and optimum. The forms without bulbous bows give near optimum performance for fine and moderately full ships at moderate speeds. The forms with bulbous bows give near optimum performance for ships with fine block coefficients and high speeds and for full ships at low speeds. The differences are generally within two per cent and not more than four per cent above the 1969 optimum in way of the practical speed range.

In accordance with B.S.R.A. policy on metrication, this report has been produced in metric units, chosen as advised in B.S.I. publication PD 6430. 'The Adoption of the Metric System in the Marine Industry.' A sheet of conversion factors is included at the back of the report to assist comparison with Imperial units.

PART I. GEOMETRY OF FORMS AND VARIATION OF RESISTANCE WITH BLOCK COEFFICIENT

R. N. M. PATTULLO, C.Eng., F.R.I.N.A.

§ 2. INTRODUCTION

1 The B.S.R.A. Methodical Series originally consisted of a number of independent groups of models in each of which a parent form was varied geometrically. The parent forms had block coefficients of 0·65, 0·70, 0·75 and 0·80.

2 To enhance the use of these independent groups and to enable precise forms other than the parents to be obtained by interpolation, four forms were taken as the basis for the derivation of a set of geometric cross curves covering a range of block coefficients 0·625 to 0·825.[1] *

3 Since the first analysis[1] was made, several new normal forms and bulbous-bow forms have been developed for B.S.R.A. at St. Albans and N.P.L., extending the range of block coefficients covered by the original experiments downwards to 0·55 and upwards to 0·85, and considerable improvements in the performance of some of the forms covered by the original analysis have been made.

4 The analysis described in this report has been made to extend the range of block coefficients covered by the cross curves from 0·525 to 0·875 and to take advantage of the improvement in resistance performance already mentioned, notably at a block coefficient of 0·80. The best of the new forms, bearing in mind stability requirements at the lower block coefficients, have been used as bases for the derivation of sets of cross curves of geometry and resistance coefficient ©.

5 From the cross curves, offsets may be obtained for a normal or bulbous-bow form of any block coefficient between 0·525 and 0·875. Each block coefficient is associated with a unique position of longitudinal centre of buoyancy. Variations from this position may be made by the standard method of swinging the sectional area curve, ordinates of which may be read off the curves given.

6 For the load condition estimates of the resistance coefficient ©, for a normal or bulbous form, or a comparison of the two may be made from the curves provided. It should be remembered that with large block coefficients, bulbous bows are fitted because of the greater advantage to be gained in the ballast rather than the load condition.

RELATION BETWEEN LCB AND BLOCK COEFFICIENT

7 For block coefficients between 0·525 and 0·725, the relation between LCB position and block coefficient in the load condition is:-

$$\text{LCB, per cent } L_{PP} \text{ from midships} = 20(C_B - 0{\cdot}675)$$

(LCB forward of midships being considered positive)

This line will be recognised as that chosen for the D.T.M.B. Series 57[2] and 60[3], that used in an early cross fairing of some B.S.R.A. Methodical Series results by Ferguson and Parker[4], and also used in the first overall analysis of the B.S.R.A. Methodical Series by Moor and Pattullo.[1]

---

* *References are given on p 117.*

8 Where necessary, parent forms have been swung to give positions of LCB consistent with this line.

9 For block coefficients above 0·725 the LCB position has been fixed at 2% L_{pp} forward of midships.

10 Figs. 1 and 32* show the basic models in relation to the chosen LCB line for normal and bulbous bows respectively.

§ 3. GEOMETRY OF FORMS

(1) BASIC FORMS USED

11 The models of each block coefficient used as basic forms in the cross fairing of the geometry are given in Table 1.

TABLE 1

Models Used for Cross Fairing of Geometry

C_B	LCB	Model No.	Remarks
Normal bows			
0·55	2½% A	STA 1672	derived from NPL 4701 by swinging the area curve
0·60	1½% A	NPL 4632C	—
0·65	½% A	NPL 3797	—
0·70	½% F	STA 1673	derived from STA 1174 by swinging the area curve
0·75	2% F	STA 1187	—
0·80	2% F	STA 1235	—
0·85	2% F	STA 1257A	—
Bulbous bows			
0·55	2½% A	STA 1718	derived from NPL 4780 by swinging the area curve
0·60	1½% A	NPL 4632D	—
0·65	½% A	STA 1173	—
0·70	½% F	STA 1695	—
0·75	2% F	STA 1708	—
0·80	2% F	STA 1234A	—
0·825	2% F	STA 1238	—
0·85	2% F	STA 1257A	—

* Figs. 1 to 67(b) relative to this part of the report will be found on pp. 22 to 95.

(2) CROSS CURVES OF OFFSETS

12 Figs. 2 to 19 show cross curves of waterline offsets for normal forms on a base of block coefficient. The offsets are presented in terms of the ratio (waterline ordinate/ full half-breadth) for each of the standard B.S.R.A. waterlines shown in Table 2.

TABLE 2

Waterline	A	B	C	D	E
% of load draught	7·69	15·38	23·08	38·46	53·85
Waterline	F	G	H	J	K
% of load draught	69·23	84·62	100·00	115·38	130·77

Similar cross curves for bulbous bow forms are given in Figs. 33 to 50. To assist the definition of the body sections below waterline A, the fractional half-breadths of tangent to flat of bottom, for both bulbous and non-bulbous forms, are given in Tables 3 to 6.

13 It will be seen that there is a dichotomy at $C_B = 0{\cdot}725$, and this persists throughout the geometry and hydrostatic particulars. It is possible, therefore, to obtain two forms at $C_B = 0{\cdot}725$, one derived from the cargo-liner range and one derived from the tanker range. Where a form with $C_B = 0{\cdot}725$ is required it is recommended that the form derived from the low C_B side of the cross curves should be used, since this form has more 'U' shaped sections aft and is likely to have better propulsion qualities than the more 'V' shaped form derived from the high C_B side of the cross curves.

(3) STEM AND STERN PROFILES

14 Stem and stern-profile offsets are presented in terms of per cent L_{PP} relative to stations 10 and 0 plotted on a base of block coefficient in Figs. 20 and 21 respectively for normal forms and Figs. 51 and 52 for bulbous forms.

(4) MIDSHIP SECTION

15 The midship section varies throughout the series and should be drawn from the offsets given for station 5 and from the rise of floor derived from the following relation:-

Rise of floor $= 0{\cdot}25\,(0{\cdot}725 - C_B)T$ for $C_B < 0{\cdot}725$.

There is no rise of floor for $C_B \geqslant 0{\cdot}725$.

(5) PARALLEL MIDDLE BODY AND HALF ANGLE OF ENTRANCE

16 To assist in the drawing of new lines plans the curves in Fig. 22 for normal bows, and Fig. 53 for bulbous bows, give the total percentage of parallel middle body with its extent forward and aft of midships, and of half angle of entrance all on the base of block coefficient.

(6) SECTIONAL AREA CURVE

17 Cross curves of sectional area curve ordinates on a base of block coefficient are given in Figs. 23 and 54 for normal and bulbous bows respectively. The ordinates are presented in terms of the ratio (sectional area/midship area) for each of the sections for which offsets are given.

TABLE 3

Offsets of Tangent to Flat of Bottom: Normal Forms
(Expressed as the Ratio of Ordinate/Full Half-Breadth)

C_B	0·52	0·54	0·56	0·58	0·60	0·62	0·64	0·66	0·68	0·70	0·72
Stn											
1/4	0·016	0·016	0·016	0·016	0·016	0·016	0·016	0·017	0·017	0·017	0·018
1/2	0·016	0·016	0·016	0·016	0·016	0·016	0·016	0·017	0·017	0·017	0·018
3/4	0·016	0·016	0·016	0·016	0·016	0·016	0·016	0·017	0·017	0·017	0·018
1	0·016	0·027	0·030	0·030	0·023	0·021	0·020	0·020	0·020	0·031	0·052
1 1/2	0·016	0·033	0·042	0·044	0·042	0·037	0·030	0·026	0·030	0·058	0·127
2	0·017	0·044	0·062	0·072	0·076	0·075	0·070	0·069	0·080	0·120	0·235
2 1/2	0·026	0·064	0·093	0·113	0·128	0·139	0·147	0·164	0·193	0·245	0·362
3	0·150	0·163	0·179	0·198	0·223	0·250	0·285	0·326	0·375	0·435	0·500
3 1/2	0·482	0·432	0·396	0·377	0·380	0·411	0·473	0·543	0·598	0·630	0·627
4	0·762	0·662	0·594	0·560	0·562	0·591	0·637	0·687	0·724	0·737	0·727
5	0·647	0·681	0·711	0·733	0·754	0·768	0·781	0·792	0·800	0·807	0·813
6	0·249	0·363	0·454	0·527	0·588	0·640	0·684	0·703	0·755	0·783	0·806
6 1/2	0·058	0·162	0·260	0·347	0·427	0·498	0·564	0·625	0·680	0·734	0·783
7	—	0·060	0·120	0·187	0·257	0·330	0·408	0·486	0·568	0·651	0·734
7 1/2	—	—	0·040	0·082	0·131	0·186	0·250	0·327	0·415	0·517	0·642
8	—	—	—	0·021	0·049	0·082	0·123	0·178	0·248	0·348	0·482
8 1/2	—	—	—	—	0·003	0·015	0·034	0·063	0·106	0·170	0·268
9	—	—	—	—	—	—	—	—	0·005	0·028	0·065

TABLE 4

Offsets of Tangent to Flat of Bottom: Normal Forms
(Expressed as the Ratio of Ordinate/Full Half-Breadth)

C_B	0·72	0·74	0·76	0·78	0·80	0·82	0·84	0·86	0·88
Stn									
1/4	0·004	0·010	0·015	0·018	0·019	0·020	0·020	0·020	0·020
1/2	0·006	0·010	0·015	0·018	0·020	0·024	0·026	0·027	0·027
3/4	0·008	0·012	0·016	0·020	0·025	0·029	0·035	0·041	0·049
1	0·012	0·014	0·018	0·025	0·036	0·050	0·067	0·094	0·127
1 1/2	0·022	0·034	0·052	0·077	0·111	0·154	0·206	0·268	0·340
2	0·038	0·107	0·174	0·239	0·304	0·368	0·431	0·494	0·557
2 1/2	0·132	0·268	0·378	0·466	0·539	0·599	0·651	0·695	0·733
3	0·539	0·587	0·632	0·674	0·714	0·748	0·779	0·807	0·830
3 1/2	0·773	0·777	0·783	0·792	0·803	0·821	0·839	0·856	0·866
4	0·814	0·814	0·814	0·817	0·827	0·845	0·860	0·867	0·870
5	0·814	0·813	0·814	0·817	0·827	0·845	0·860	0·867	0·870
6	0·803	0·807	0·811	0·817	0·827	0·845	0·860	0·867	0·870
6 1/2	0·768	0·795	0·810	0·817	0·827	0·845	0·860	0·867	0·870
7	0·681	0·746	0·788	0·813	0·827	0·845	0·860	0·867	0·870
7 1/2	0·500	0·627	0·716	0·778	0·817	0·842	0·860	0·867	0·870
8	0·218	0·432	0·581	0·683	0·758	0·812	0·845	0·862	0·870
8 1/2	—	0·168	0·386	0·509	0·598	0·674	0·737	0·788	0·833
9	—	—	0·160	0·272	0·364	0·444	0·514	0·575	0·628
9 1/4	—	—	0·051	0·143	0·222	0·290	0·350	0·400	0·445
9 1/2	—	—	—	0·012	0·065	0·110	0·148	0·178	0·205

TABLE 5

Offsets of Tangent to Flat of Bottom: Bulbous Forms
(Expressed as the Ratio of Ordinate/Full Half-Breadth)

C_B	0·52	0·54	0·56	0·58	0·60	0·62	0·64	0·66	0·68	0·70	0·72
Stn											
1/4	0·015	0·015	0·015	0·015	0·015	0·015	0·015	0·015	0·015	0·015	0·015
1/2	0·015	0·015	0·015	0·015	0·015	0·015	0·015	0·015	0·015	0·015	0·015
3/4	0·015	0·015	0·015	0·015	0·015	0·015	0·015	0·015	0·015	0·015	0·015
1	0·015	0·017	0·019	0·020	0·020	0·020	0·019	0·019	0·020	0·022	0·026
1 1/2	0·015	0·022	0·030	0·033	0·034	0·030	0·024	0·024	0·028	0·038	0·058
2	0·015	0·043	0·062	0·074	0·078	0·075	0·070	0·065	0·064	0·080	0·132
2 1/2	0·040	0·099	0·133	0·152	0·159	0·158	0·150	0·143	0·149	0·178	0·253
3	0·230	0·257	0·272	0·279	0·280	0·280	0·281	0·286	0·301	0·344	0·417
3 1/2	0·552	0·502	0·465	0·440	0·429	0·427	0·437	0·462	0·496	0·534	0·569
4	0·697	0·653	0·615	0·587	0·570	0·566	0·579	0·610	0·656	0·690	0·700
5	0·594	0·649	0·693	0·725	0·744	0·751	0·757	0·766	0·775	0·786	0·799
6	0·166	0·292	0·407	0·511	0·600	0·666	0·708	0·737	0·756	0·766	0·770
6 1/2	—	0·119	0·249	0·363	0·460	0·540	0·601	0·647	0·674	0·683	0·670
7	—	0·030	0·126	0·214	0·294	0·365	0·415	0·473	0·509	0·523	0·509
7 1/2	—	—	0·050	0·107	0·158	0·205	0·243	0·275	0·296	0·307	0·303
8	—	—	0·020	0·048	0·075	0·099	0·119	0·134	0·143	0·144	0·135
8 1/2	—	—	—	0·012	0·031	0·046	0·058	0·063	0·064	0·060	0·054
9	—	—	—	—	0·005	0·018	0·028	0·033	0·035	0·032	0·024
9 1/4	—	—	—	—	0·003	0·012	0·020	0·025	0·028	0·027	0·020
9 1/2	—	—	—	—	—	0·004	0·013	0·020	0·022	0·022	0·015
9 3/4	—	—	—	—	—	—	0·011	0·017	0·020	0·018	0·010

TABLE 6

Offsets of Tangent to Flat of Bottom: Bulbous Forms
(Expressed as the Ratio of Ordinate/Full Half-Breadth)

C_B	0·72	0·74	0·76	0·78	0·80	0·82	0·84	0·86	0·88
Stn									
1/4	0·013	0·014	0·015	0·016	0·017	0·018	0·020	0·021	0·023
1/2	0·015	0·015	0·015	0·016	0·018	0·020	0·024	0·029	0·035
3/4	0·017	0·017	0·018	0·020	0·024	0·031	0·041	0·054	0·069
1	0·025	0·027	0·030	0·036	0·046	0·059	0·077	0·099	0·126
1 1/2	0·056	0·071	0·090	0·114	0·143	0·177	0·217	0·264	0·318
2	0·118	0·166	0·216	0·267	0·321	0·375	0·431	0·492	0·556
2 1/2	0·223	0·315	0·397	0·473	0·537	0·592	0·640	0·683	0·721
3	0·373	0·484	0·573	0·646	0·703	0·746	0·778	0·801	0·814
3 1/2	0·546	0·632	0·701	0·754	0·795	0·824	0·843	0·854	0·857
4	0·687	0·739	0·780	0·813	0·835	0·851	0·860	0·865	0·870
5	0·785	0·799	0·813	0·829	0·840	0·851	0·860	0·865	0·870
6	0·770	0·795	0·813	0·829	0·840	0·851	0·860	0·865	0·870
6 1/2	0·640	0·736	0·790	0·822	0·840	0·851	0·860	0·865	0·870
7	0·463	0·640	0·744	0·803	0·836	0·851	0·860	0·865	0·870
7 1/2	0·288	0·505	0·662	0·757	0·815	0·845	0·860	0·865	0·870
8	0·150	0·346	0·522	0·651	0·746	0·810	0·848	0·865	0·870
8 1/2	0·056	0·196	0·333	0·463	0·580	0·665	0·733	0·786	0·819
9	0·010	0·084	0·168	0·260	0·345	0·427	0·500	0·566	0·620
9 1/4	0·010	0·053	0·100	0·153	0·209	0·267	0·328	0·390	0·450
9 1/2	0·010	0·030	0·050	0·071	0·095	0·122	0·153	0·190	0·236
9 3/4	0·010	0·012	0·015	0·020	0·023	0·028	0·032	0·038	0·046

§ 4. HYDROSTATIC PARTICULARS

18 Figs. 24 to 30, normal bows and Figs. 55 to 61, bulbous bows, (See Table 7), show cross curves of the following hydrostatic particulars plotted on a base of block coefficient in the design load condition. Displacement, Ⓢ, and Ⓜ refer to ships 121·92-m L_{PP} × 16·76-m moulded breadth × 7·32-m moulded draught for $C_B \leq 0{\cdot}725$ and 121·92-m L_{PP} × 16·76-m moulded breadth × 6·71-m moulded draught for $C_B \geq 0{\cdot}725$.

TABLE 7.

Normal bows		Bulbous bows
Fig. 24	Moulded displacement, tonnes salt water	Fig. 55
25	Longitudinal position of centre of buoyancy and longitudinal position of centre of flotation, per cent L_{PP} from midships	56
26	Longitudinal position of centre of buoyancy of forward and after bodies, per cent L_{PP} from midships	57
27	Prismatic coefficient C_P using L_{PP} and prismatic coefficient of fore and after bodies using $\frac{1}{2}L_{PP}$	58
28	Waterplane area coefficient, C_W and transverse inertia coefficient, C_{IT}, using wetted length	59
29	Wetted surface coefficient, Ⓢ $= S/\nabla^{2/3}$ and length-displacement coefficient, Ⓜ $= L/\nabla^{1/3}$	60
30	Wetted length and height of centroid of sectional area curve, fraction of ordinate at station 5, midships of L_{PP}	61

§ 5. CHANGE OF LCB

19 If the desired form is required to have an LCB position different from the standard, it is necessary to move the transverse sections by the standard method of swinging the sectional area curve, which is fully described in B.S.R.A. Report No. 12.[5]

20 Fig. 31 shows for normal forms cross curves of the movement of each section required to produce a change in position of LCB equal to one per cent L_{PP}. The movement is itself expressed as a percentage of L_{PP}. The movement of each section required to produce a change in position of LCB other than one per cent is in direct proportion to that shown in Fig. 31. Similar information for bulbous bow forms is given in Fig. 62.

§ 6. APPLICATION OF CROSS CURVES

21 A worked example, prepared by B.S.R.A. Staff, is given in Fig. 95 in Appendix II, in which the lines of a ship 330-m L_{PP}, 293 750-tonnes displacement and LCB position 8·25 m forward of midships have been derived from the cross curves.

§ 7. VARIATION OF RESISTANCE WITH BLOCK COEFFICIENT

(1) DATA EMPLOYED

22 The resistance data used in the cross fairing was derived from tests made with the models listed in Table 1. Additional models, given in Table 8 were run to provide information at 0·725 block coefficient.

TABLE 8

Additional Models Used in Resistance Cross Fairing

C_B	LCB	Model No.	Remarks
Normal bows			
0·725	1% F	STA 1669	Derived from cross curves
0·725	2% F	STA 1674	Derived from cross curves
Bulbous bows			
0·725	1% F	STA 1716	Derived from cross curves
0·725	2% F	STA 1719	Derived from cross curves

23 The data refer to ships 121·92-m L_{PP} × 16·76-m moulded breadth × 7·32-m moulded draught for $C_B \leq 0{\cdot}725$ and 121·92-m L_{PP} × 16·76-m moulded breadth × 6·71-m moulded draught for $C_B \geq 0{\cdot}725$. Models NPL 4632C and NPL 4632D had dimensions of 121·92-m L_{PP} × 18·3-m moulded breadth × 7·26-m moulded draught while model NPL 3797 had dimensions 121·92-m L_{PP} × 16·76-m moulded breadth × 7·93-m moulded draught. The resistance data for models NPL 4632C and 4632D were therefore corrected to standard dimensions using Mumford indices given by Moor[6] and those for model NPL 3797 by the method given by Moor and Small.[7]

(2) PRESENTATION OF DATA

24 The values of the resistance coefficient © used in the cross fairing are given in Tables 9 to 12.

25 Cross curves of resistance coefficient ©, for a range of speeds, plotted on a base of block coefficient are shown in Figs. 63 and 64 for normal and bulbous bows respectively. On each sheet the base scale is block coefficient and the © for each block coefficient is that corresponding to the standard LCB position for that fullness. The relation between LCB position and block coefficient is given in paras. 7 and 9.

26 Where estimates of © are required for ships with proportions and LCB position differing from those stated, corrections may be made to the basis © by applying the correction factors given in Part II of this report.

(3) SKIN-FRICTION CORRECTION

27 The © values presented are for 121·92-m L_{PP} ships and they have been calculated using the R.E. Froude friction coefficients. To obtain © values for ships other than 121·92-m L_{PP} the Froude skin-friction correction may be made using the formula

$$©_{121.9} - ©_L = (0_{121.9} - 0_L)\, Ⓢ\, Ⓛ^{-0.175}$$

where $0_{121\cdot9}$ and 0_L are R. E. Froude's skin-friction 0-values for 121·92m and the actual length required[9]. The wetted surface coefficient Ⓢ may be obtained from Figs. 29 and 60 for normal and bulbous-bow forms respectively, provided they have the basis proportions stated. In the case of designs having different basis proportions the value of Ⓢ can be obtained from either of the approximate formulae given in para. 40. For convenience a diagram for determining the skin-friction correction for ranges of length, Ⓢ, and speed in knots corresponding to 121·92-m L_{PP} is given in Fig. 65.

TABLE 9

Values of © Used in Cross Plotting: Normal Bows

S.S. 121·92-m L_{PP} × 16·76-m B. Mld × 7·32-m T. Mld					
C_B	0·548	0·601	0·650	0·696	0·725
LCB, % L_{PP}	2½A	1½A	½A	½F	1F
Model No.	STA 1672	NPL 4632C	NPL 3797	STA 1673	STA 1669
Speed (knots)	©				
8	—	—	—	—	0·643
8·5	—	—	—	—	0·645
9	—	—	—	0·643	0·649
9·5	—	—	—	0·640	0·654
10	—	—	0·636	0·638	0·661
10·5	—	—	0·637	0·640	0·666
11	—	—	0·641	0·644	0·671
11·5	—	—	0·647	0·652	0·678
12	—	—	0·657	0·661	0·686
12·5	—	—	0·665	0·670	0·695
13	0·653	—	0·673	0·673	0·706
13·5	0·657	0·644	0·680	0·672	0·718
14	0·661	0·657	0·684	0·673	0·732
14·5	0·665	0·663	0·687	0·685	0·762
15	0·667	0·671	0·688	0·713	0·819
15·5	0·667	0·676	0·692	0·768	0·919
16	0·667	0·683	0·700	0·845	1·045
16·5	0·669	0·691	0·720	0·907	1·161
17	0·675	0·704	0·753	0·951	1·293
17·5	0·683	0·727	0·805	1·022	—
18	0·700	0·764	0·894	1·132	—
18·5	0·729	0·823	—	—	—
19	0·761	0·899	—	—	—
19·5	0·792	0·985	—	—	—
20	0·814	1·059	—	—	—
20·5	0·822	1·115	—	—	—
21	0·826	1·151	—	—	—
21·5	0·845	1·166	—	—	—
22	0·880	1·161	—	—	—

28 The resistance values may be converted to a basis of I.T.T.C. 1957 model-ship correlation line[29] by means of the conversion chart, Fig. 66.

29 Fig. 67 gives contours of the ratio $\frac{\text{© bulbous form}}{\text{© normal form}}$, at the load draught, and may be used to decide whether to adopt a normal or bulbous form for the particular C_B and speed under consideration. It is emphasised that the ratios quoted apply strictly to the forms presented in this report and will not necessarily apply to independent forms, nor to cases where a bulbous bow is simply added to an existing normal form.

TABLE 10

Values of © Used in Cross Plotting: Normal Bows

S.S. 121·92-m L_{PP} × 16·76-m B. Mld × 6·71-m T. Mld				
C_B	0·723	0·743	0·798	0·846
LCB, % L_{PP}	2F	2F	2F	2F
Model No.	STA 1674	STA 1187	STA 1235	STA 1257A
Speed (knots)	©			
8	0·657	0·659	0·678	0·707
8·5	0·654	0·653	0·683	0·698
9	0·650	0·652	0·686	0·692
9·5	0·648	0·655	0·689	0·692
10	0·648	0·660	0·691	0·693
10·5	0·650	0·664	0·693	0·696
11	0·654	0·668	0·696	0·705
11·5	0·661	0·673	0·704	0·730
12	0·670	0·681	0·717	0·770
12·5	0·684	0·694	0·739	0·824
13	0·704	0·713	0·774	0·902
13·5	0·730	0·740	0·829	1·017
14	0·765	0·786	0·909	1·134
14·5	0·814	0·849	0·991	—
15	0·877	0·934	1·077	—
15·5	0·967	1·036	—	—
16	1·057	1·140	—	—
16·5	1·123	—	—	—
17	1·191	—	—	—

TABLE 11

Values of © Used in Cross Plotting: Bulbous Bows

S.S. 121·92-m L_{PP} × 16·76-m B. Mld × 7·32-m T. Mld					
C_B	0·555	0·603	0·644	0·701	0·723
LCB, % L_{PP}	2½A	1½A	½A	½F	1F
Model No.	STA 1718	NPL 4632D	STA 1173	STA 1695	STA 1716
Speed (knots)	©				
8	—	—	—	—	0·698
8·5	—	—	—	—	0·698
9	—	—	—	0·687	0·696
9·5	—	—	—	0·680	0·693
10	—	—	—	0·676	0·693
10·5	—	—	—	0·674	0·695
11	—	—	—	0·672	0·700
11·5	—	—	—	0·674	0·709
12	—	—	0·664	0·678	0·719
12·5	—	—	0·668	0·683	0·730
13	—	—	0·674	0·688	0·738
13·5	—	—	0·681	0·692	0·743
14	0·683	—	0·688	0·698	0·750
14·5	0·692	0·663	0·693	0·711	0·760
15	0·700	0·668	0·693	0·734	0·789
15·5	0·704	0·678	0·692	0·768	0·839
16	0·707	0·687	0·695	0·805	0·897
16·5	0·707	0·696	0·704	0·842	0·942
17	0·708	0·698	0·724	0·875	0·984
17·5	0·713	0·709	0·773	0·939	—
18	0·723	0·731	0·859	1·062	—
18·5	0·739	0·777	0·987	—	—
19	0·760	0·835	1·135	—	—
19·5	0·782	0·904	—	—	—
20	0·794	0·955	—	—	—
20·5	0·797	0·996	—	—	—
21	0·804	1·018	—	—	—
21·5	0·819	1·030	—	—	—
22	0·841	1·034	—	—	—

TABLE 12

Values of © Used in Cross Plotting: Bulbous Bows

S.S. 121·92-m L_{PP} × 16·76-m B. Mld × 6·71-m T. Mld					
C_B	0·725	0·749	0·798	0·822	0·846
LCB, % L_{PP}	2F	2F	2F	2F	2F
Model No.	STA 1719	STA 1708	STA 1234A	STA 1238	STA 1257A
Speed (knots)	©				
8	0·685	0·676	0·681	0·711	0·707
8·5	0·681	0·674	0·680	0·703	0·698
9	0·677	0·673	0·679	0·697	0·692
9·5	0·675	0·671	0·678	0·694	0·692
10	0·677	0·671	0·676	0·692	0·693
10·5	0·681	0·673	0·675	0·694	0·696
11	0·685	0·679	0·677	0·699	0·705
11·5	0·689	0·686	0·686	0·709	0·730
12	0·695	0·693	0·697	0·724	0·770
12·5	0·704	0·704	0·716	0·755	0·824
13	0·717	0·720	0·750	0·806	0·902
13·5	0·737	0·744	0·802	0·874	1·017
14	0·764	0·780	0·871	0·949	1·134
14·5	0·795	0·832	0·940	1·035	—
15	0·830	0·897	1·034	—	—
15·5	0·881	0·970	—	—	—
16	0·947	1·058	—	—	—
16·5	1·015	—	—	—	—
17	1·083	—	—	—	—

Geometry of Forms
and
Hydrostatic Particulars
Normal Bows

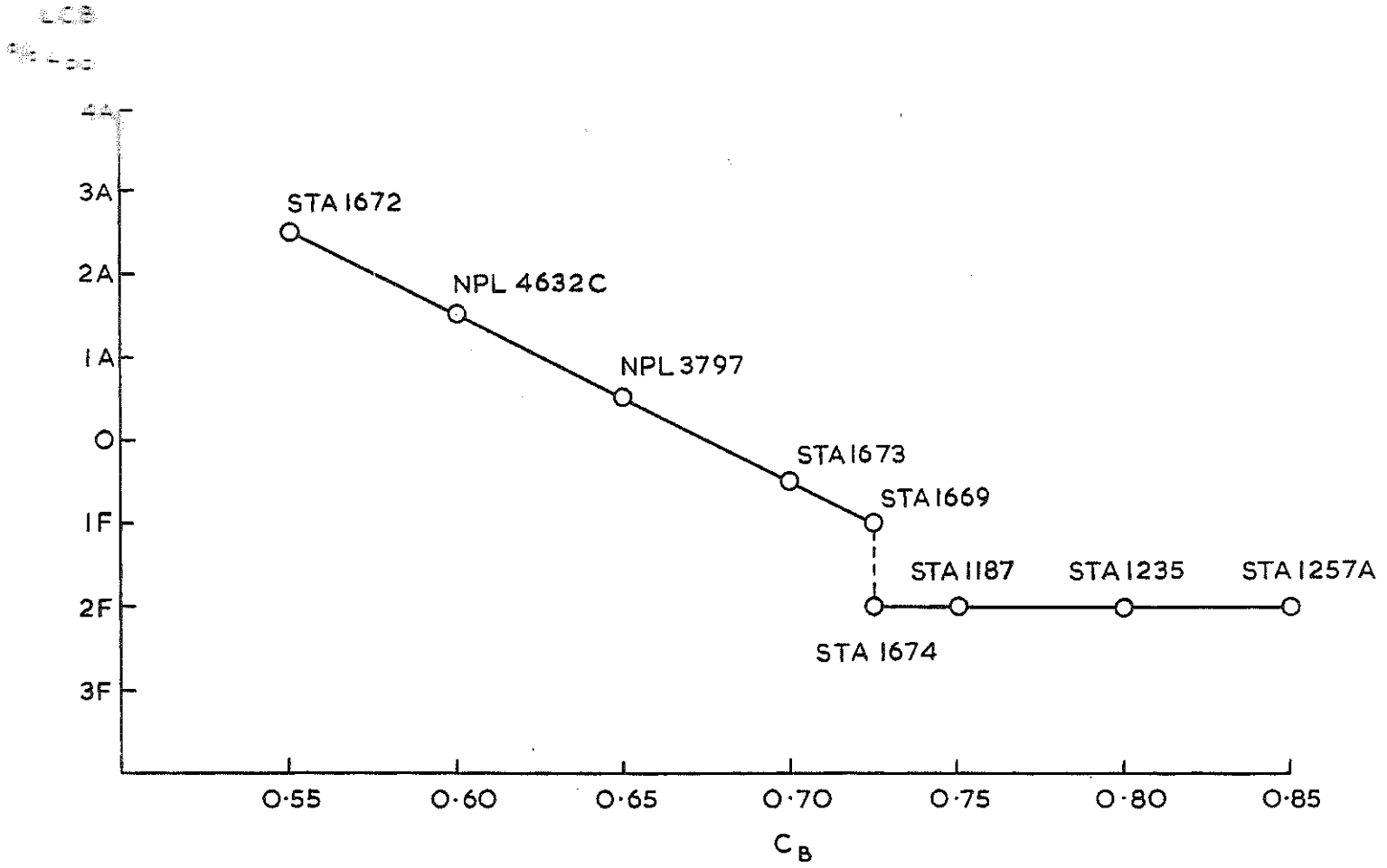

Fig. 1—Basic Models Relative to LCB Line: Normal Forms.

ORDINATE / FULL HALF-BREADTH

STATION O

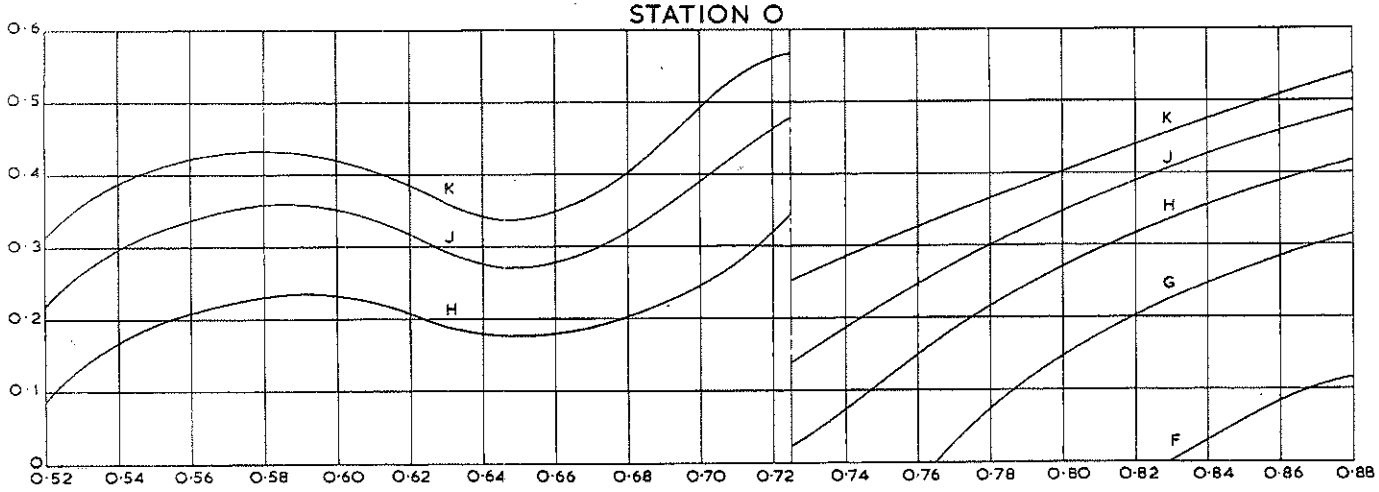

C_B

ORDINATE / FULL HALF-BREADTH

STATION ¼

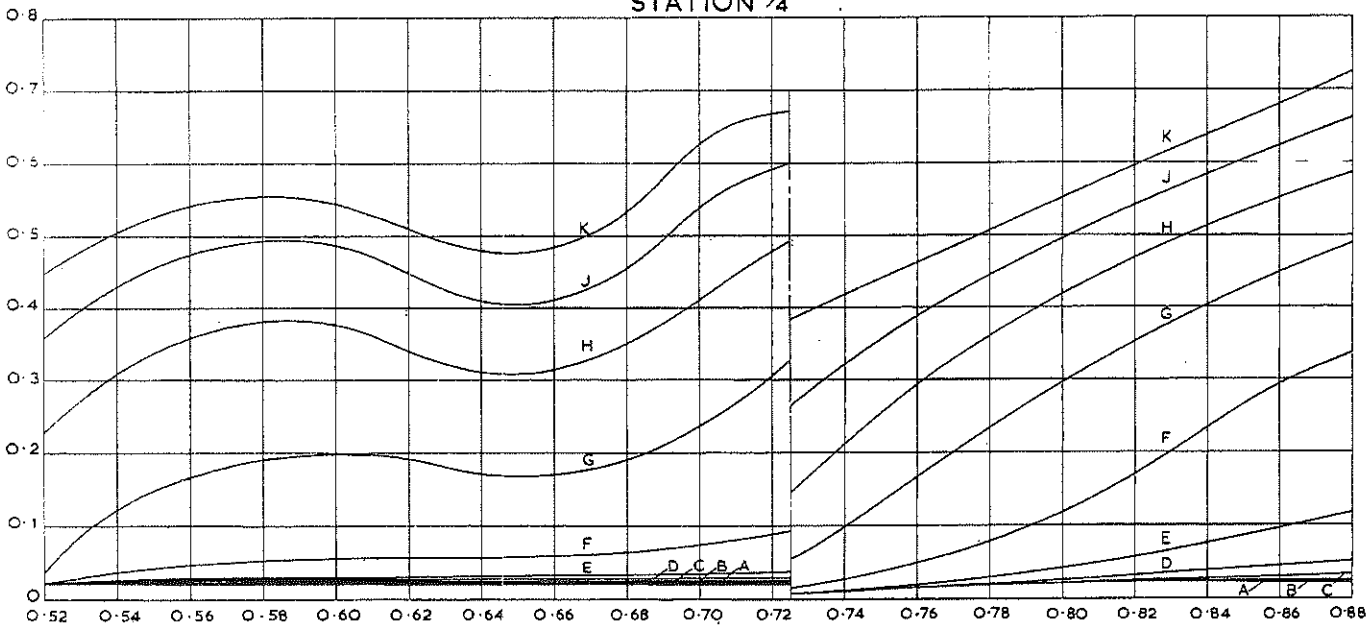

Fig. 2—Stations 0 and 1

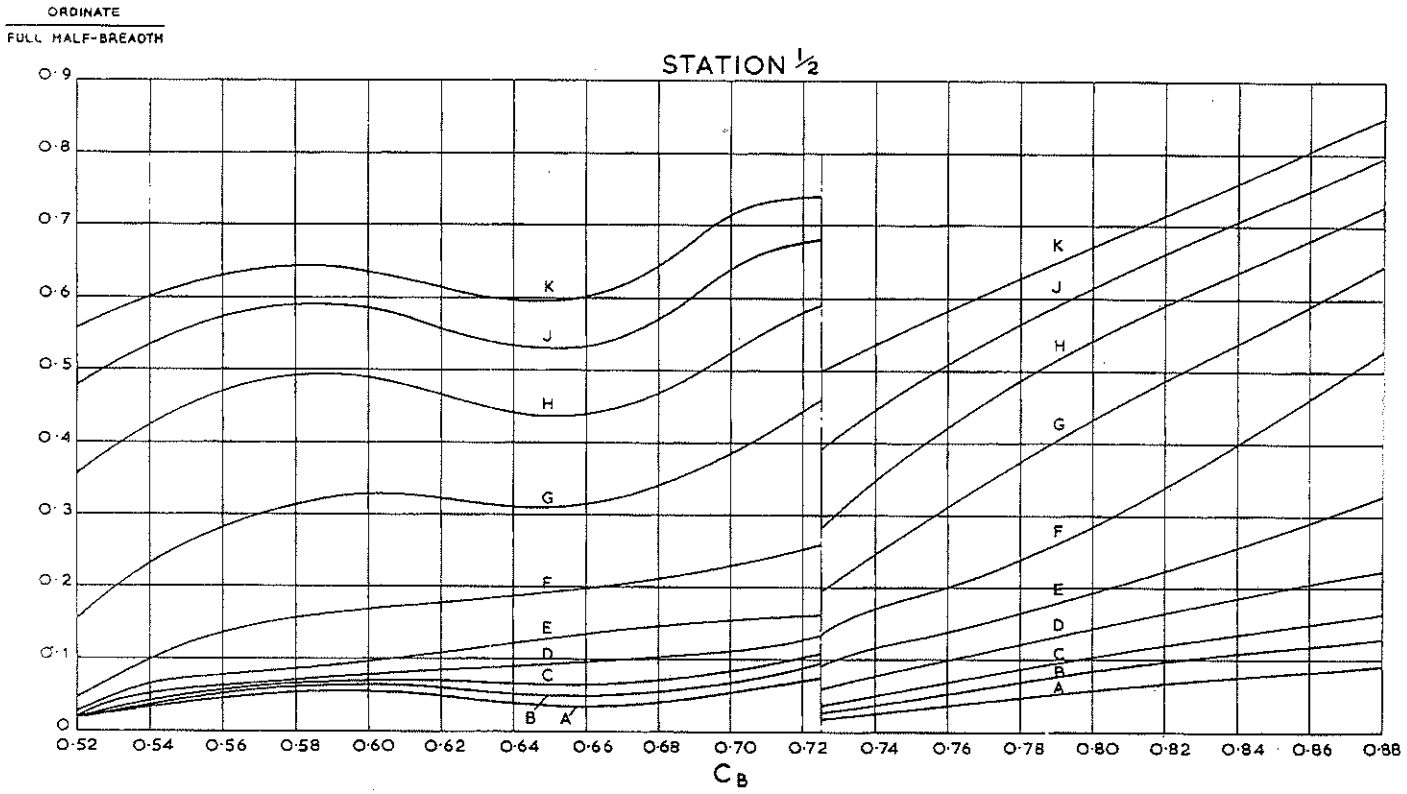

Fig. 3—Station ½.
Waterline Offsets Expressed as the Ratio of Waterline Ordinate/Full Half-Breadth.

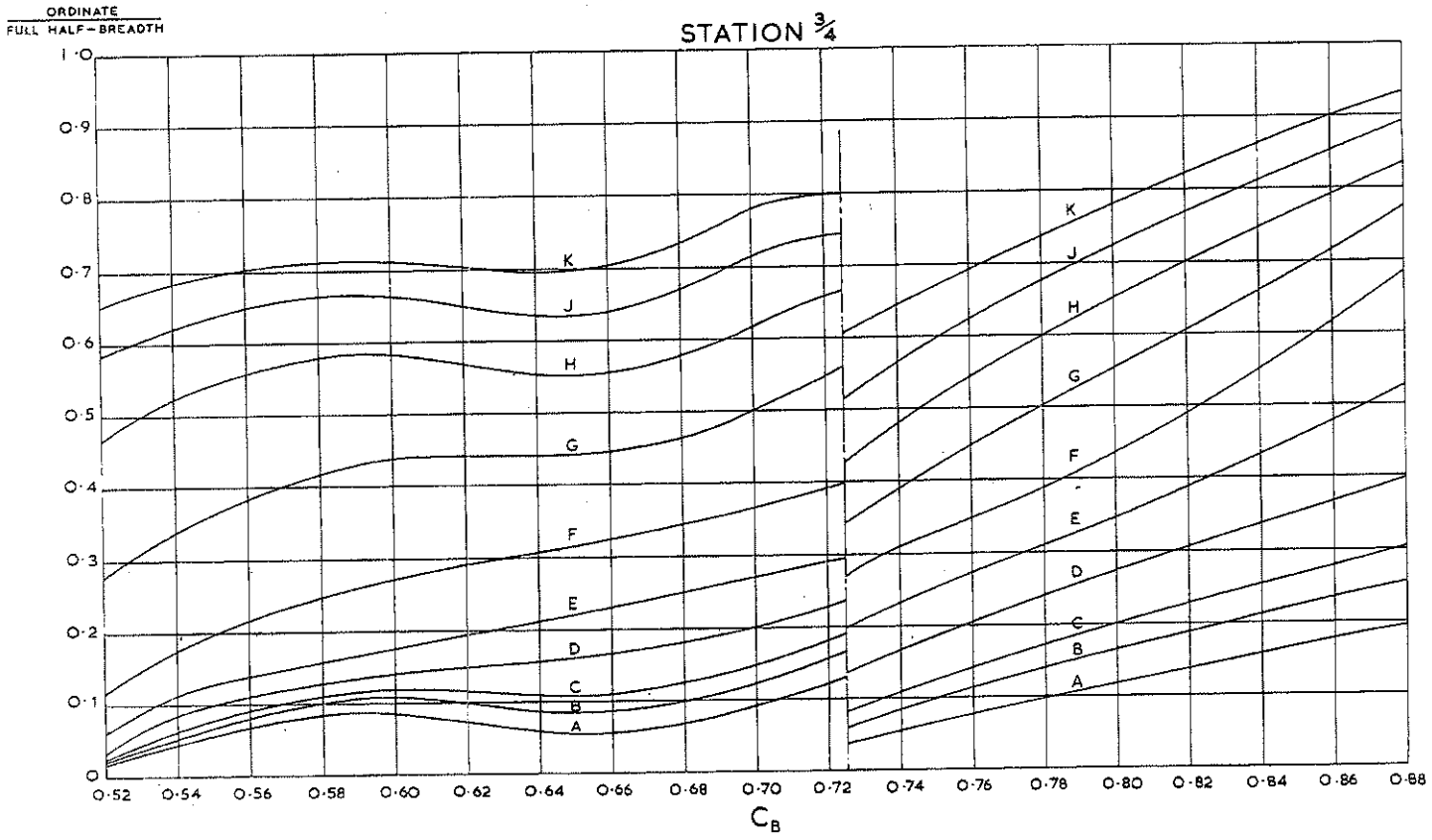

Fig. 4—Station 3/4.
Waterline Offsets Expressed as the Ratio of Waterline Ordinate/Full Half-Breadth.

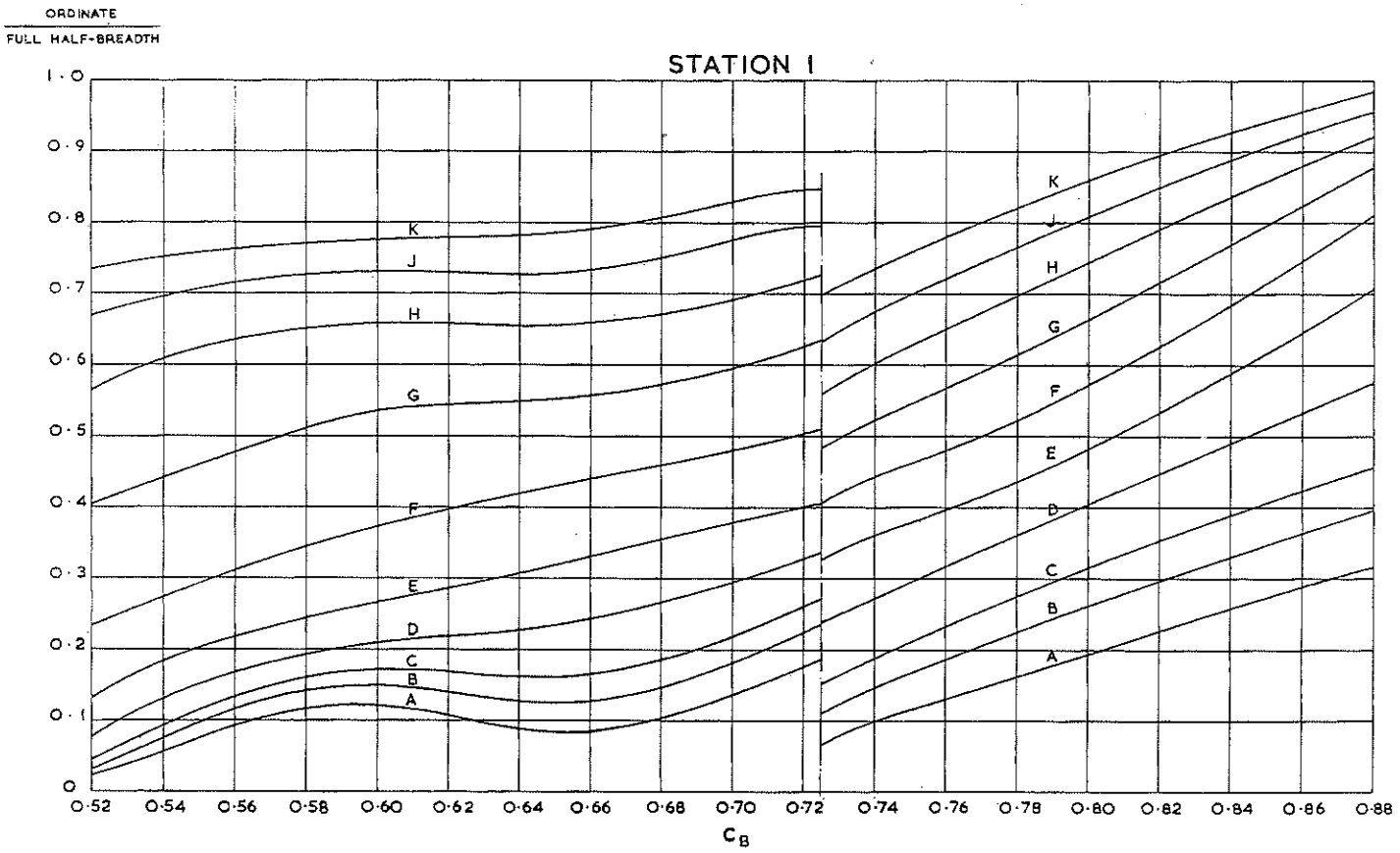

Fig. 5—Station 1.
Waterline Offsets Expressed as the Ratio of Waterline Ordinate/Full Half-Breadth.

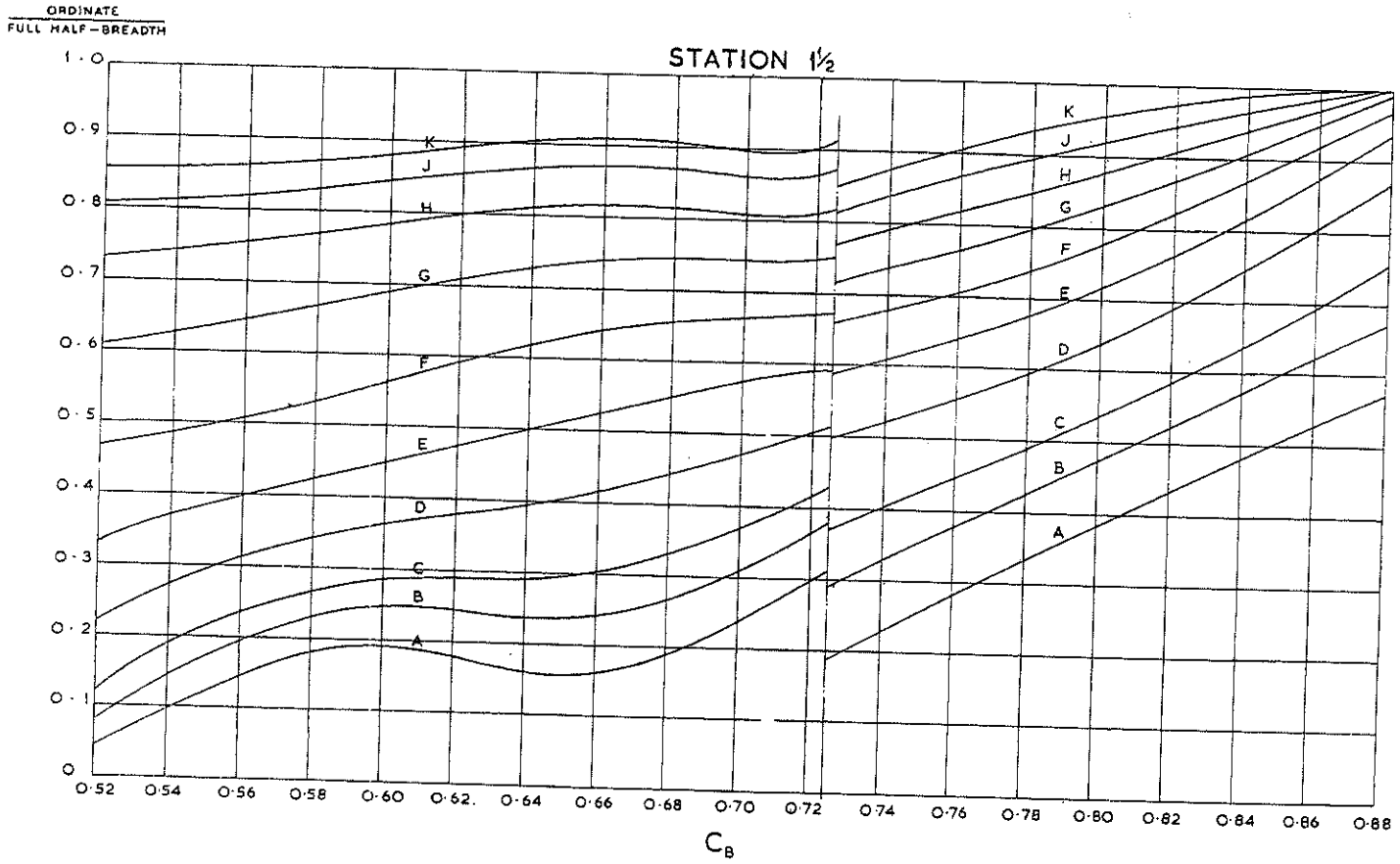

Fig. 6—Station 1½.
Waterline Offsets Expressed as the Ratio of Waterline Ordinate/Full Half-Breadth.

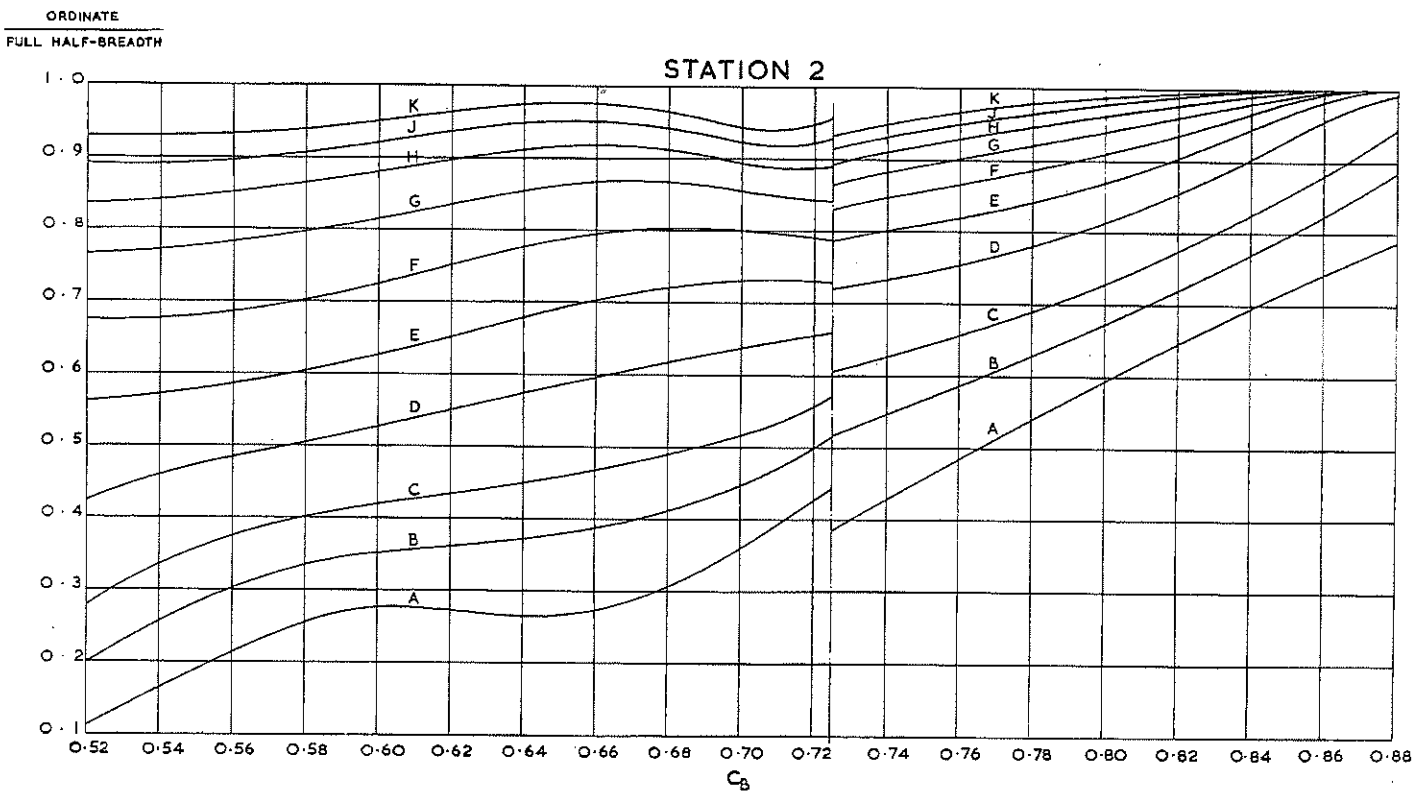

Fig. 7—Station 2.
Waterline Offsets Expressed as the Ratio of Waterline Ordinate/Full Half-Breadth.

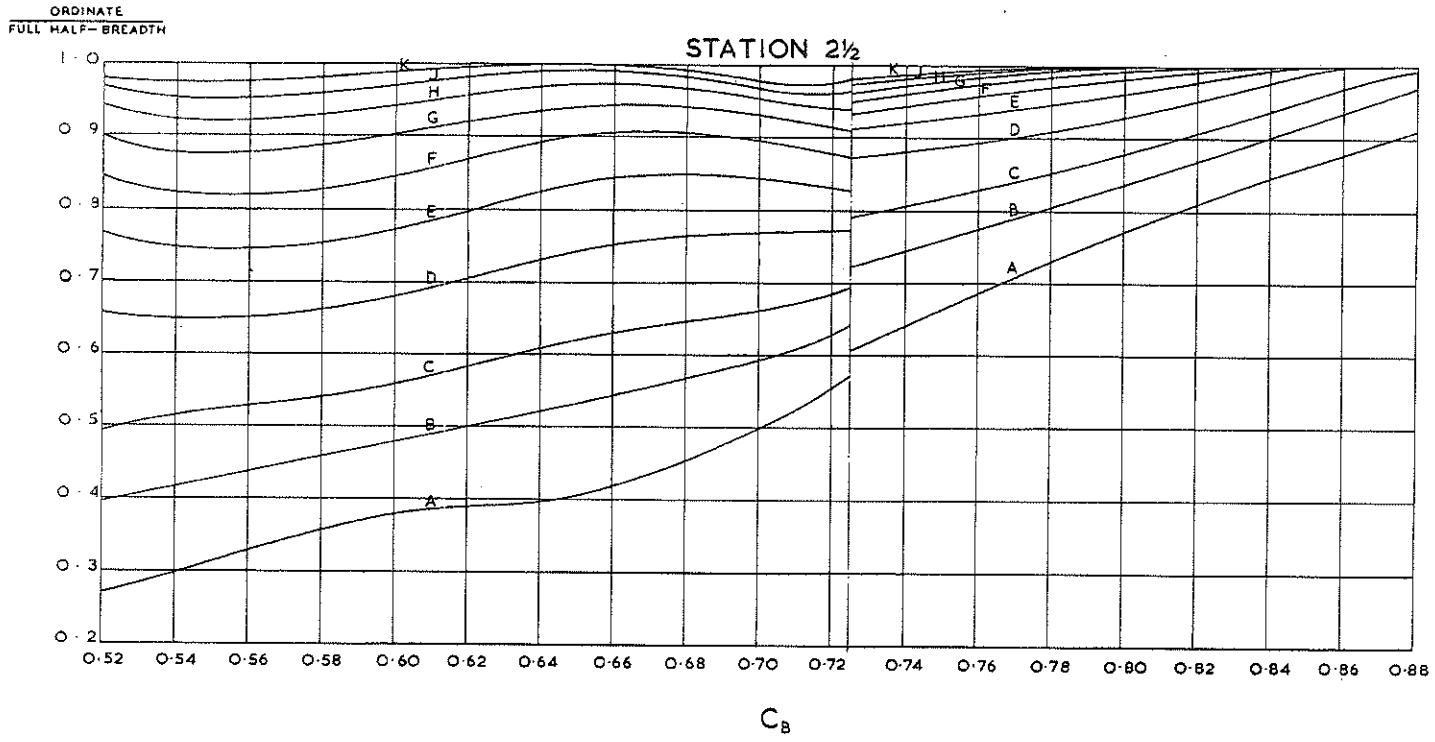

Fig. 8—Station 2½.
Waterline Offsets Expressed as the Ratio of Waterline Ordinate/Full Half-Breadth.

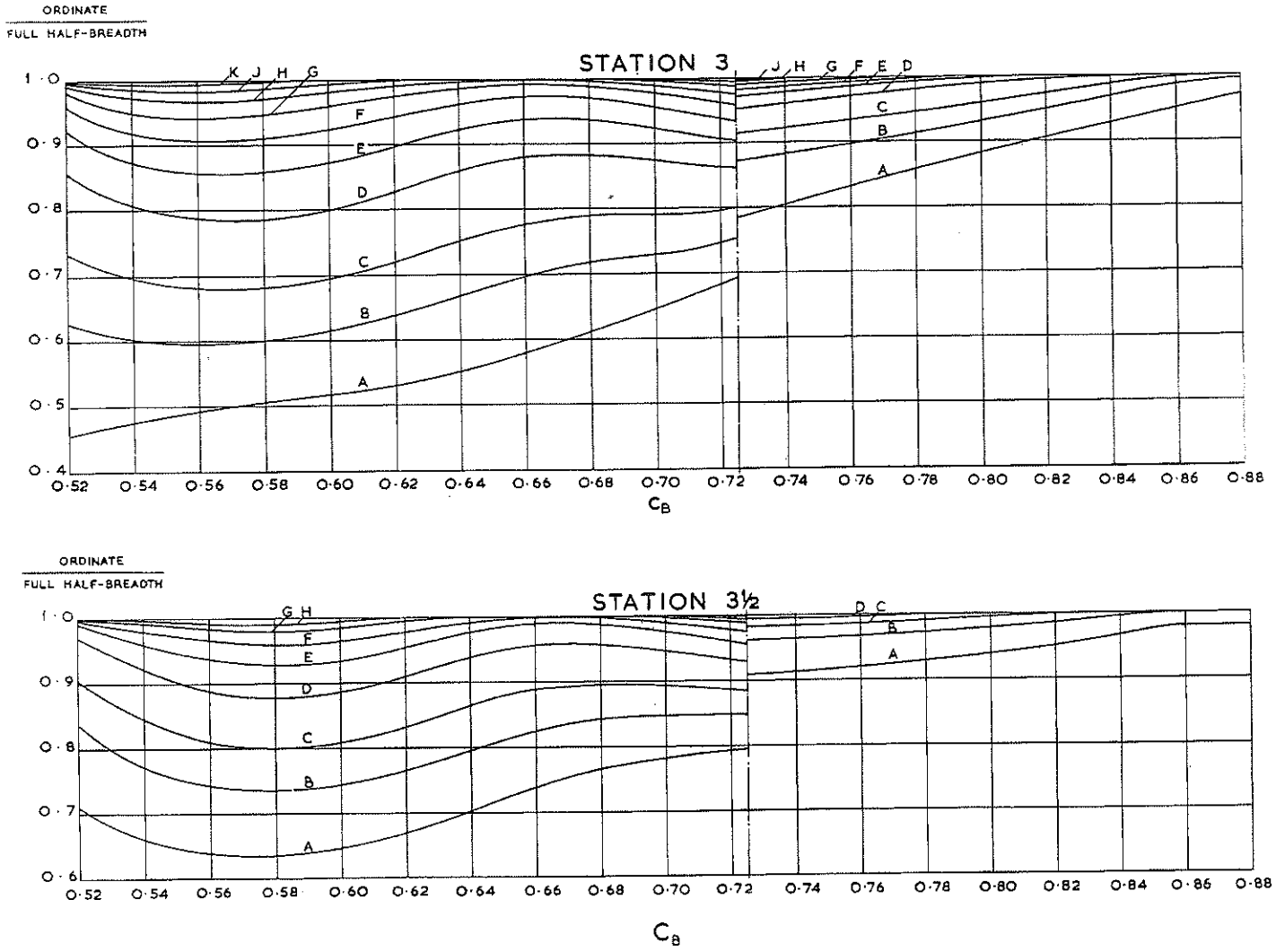

Fig. 9—Stations 3 and 3½.
Waterline Offsets Expressed as the Ratio of Waterline Ordinate/Full Half-Breadth.

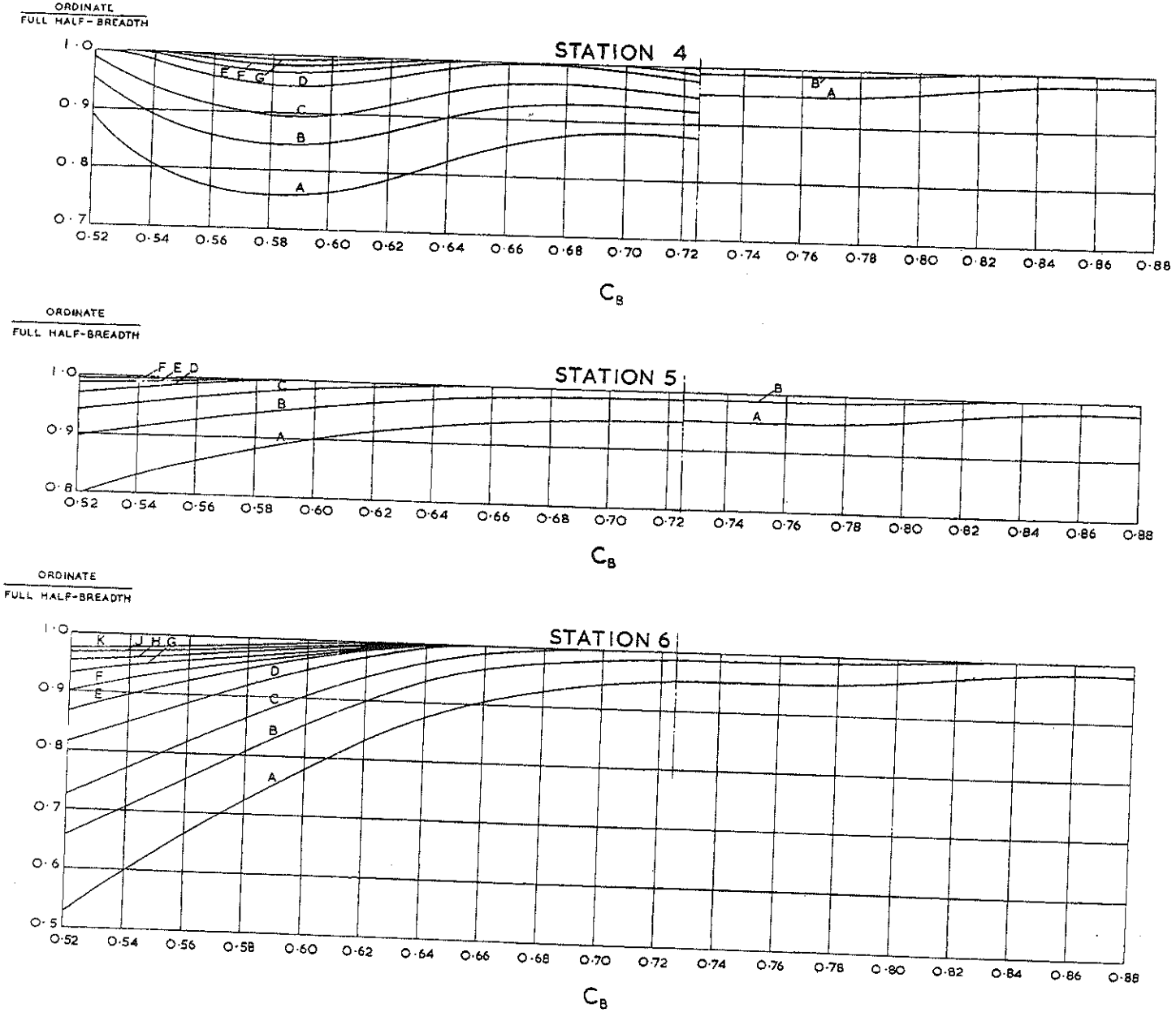

Fig. 10—Stations 4, 5 and 6

Variable Offsets Expressed as the Ratio of Waterline Ordinate (Full H...

Fig. 10—Stations 4, 5 and 6
Waterline Offsets Expressed as the Ratio of Waterline Ordinate/Full Half-Breadth

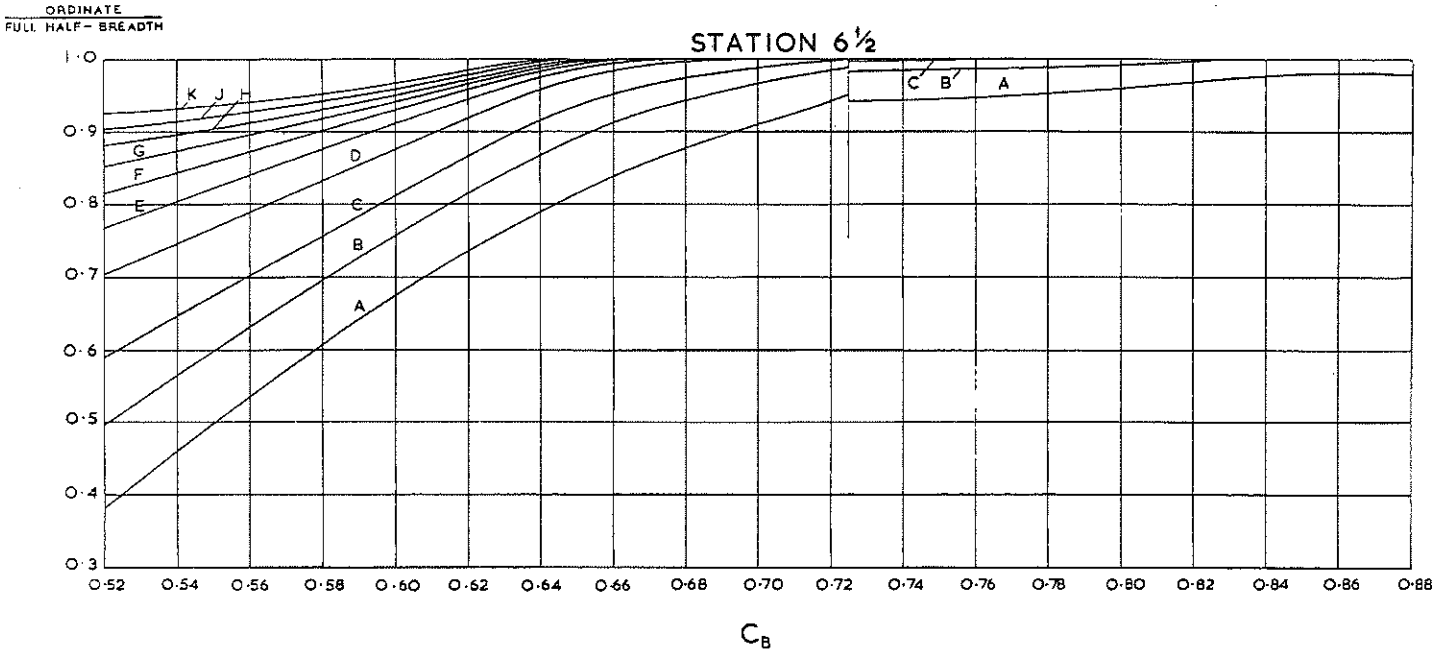

Fig. 11—Station 6½.
Waterline Offsets Expressed as the Ratio of Waterline Ordinate/Full Half-Breadth.

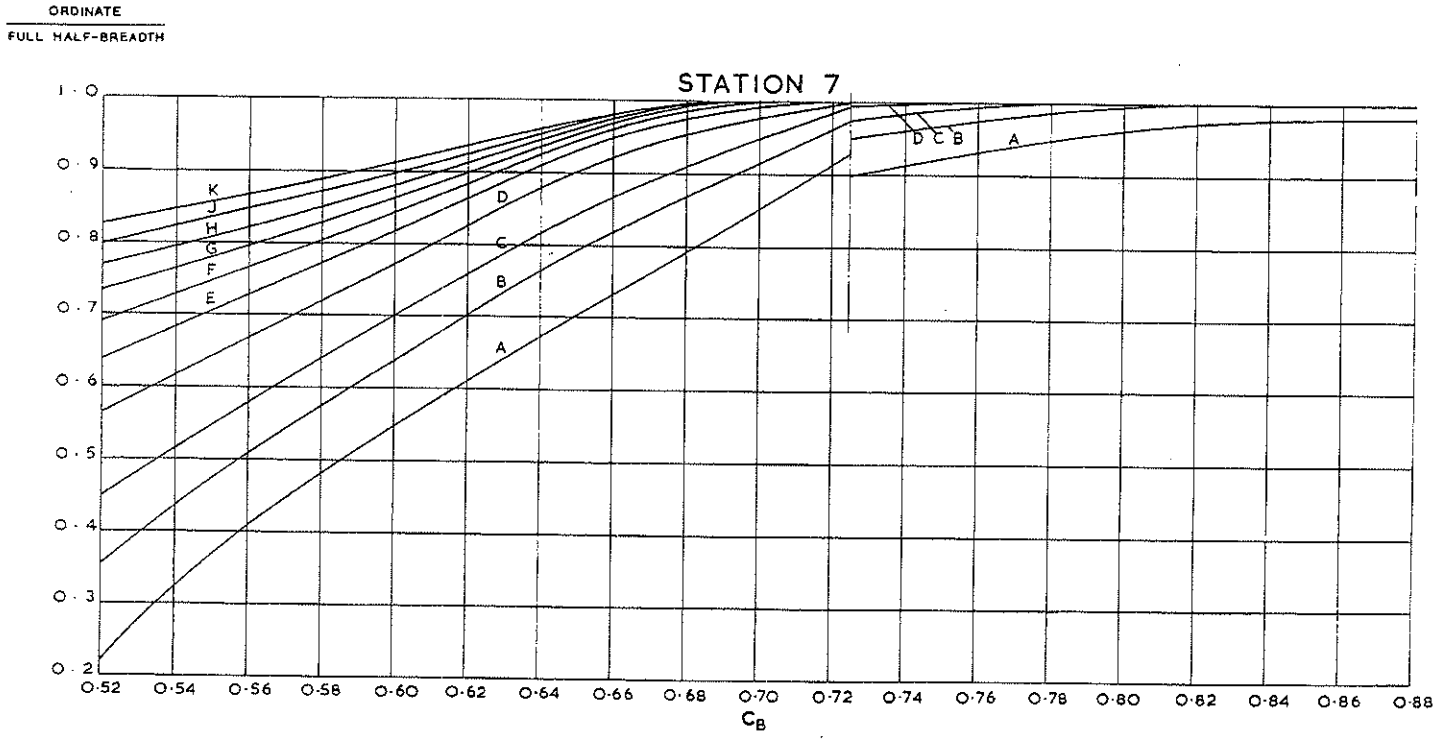

Fig. 12—Station 7.
Waterline Offsets Expressed as the Ratio of Waterline Ordinate/Full Half-Breadth.

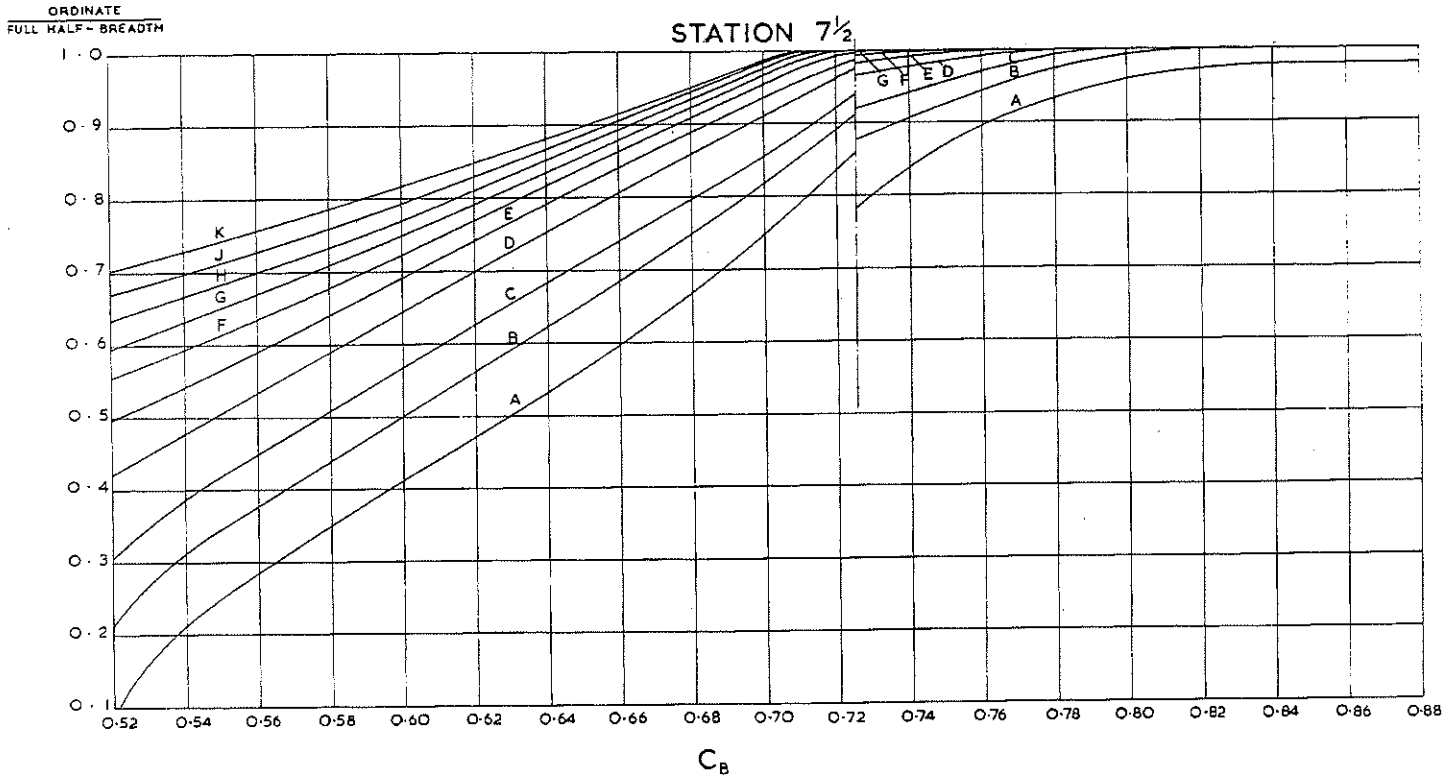

Fig. 13—Station 7½.
Waterline Offsets Expressed as the Ratio of Waterline Ordinate/Full Half-Breadth.

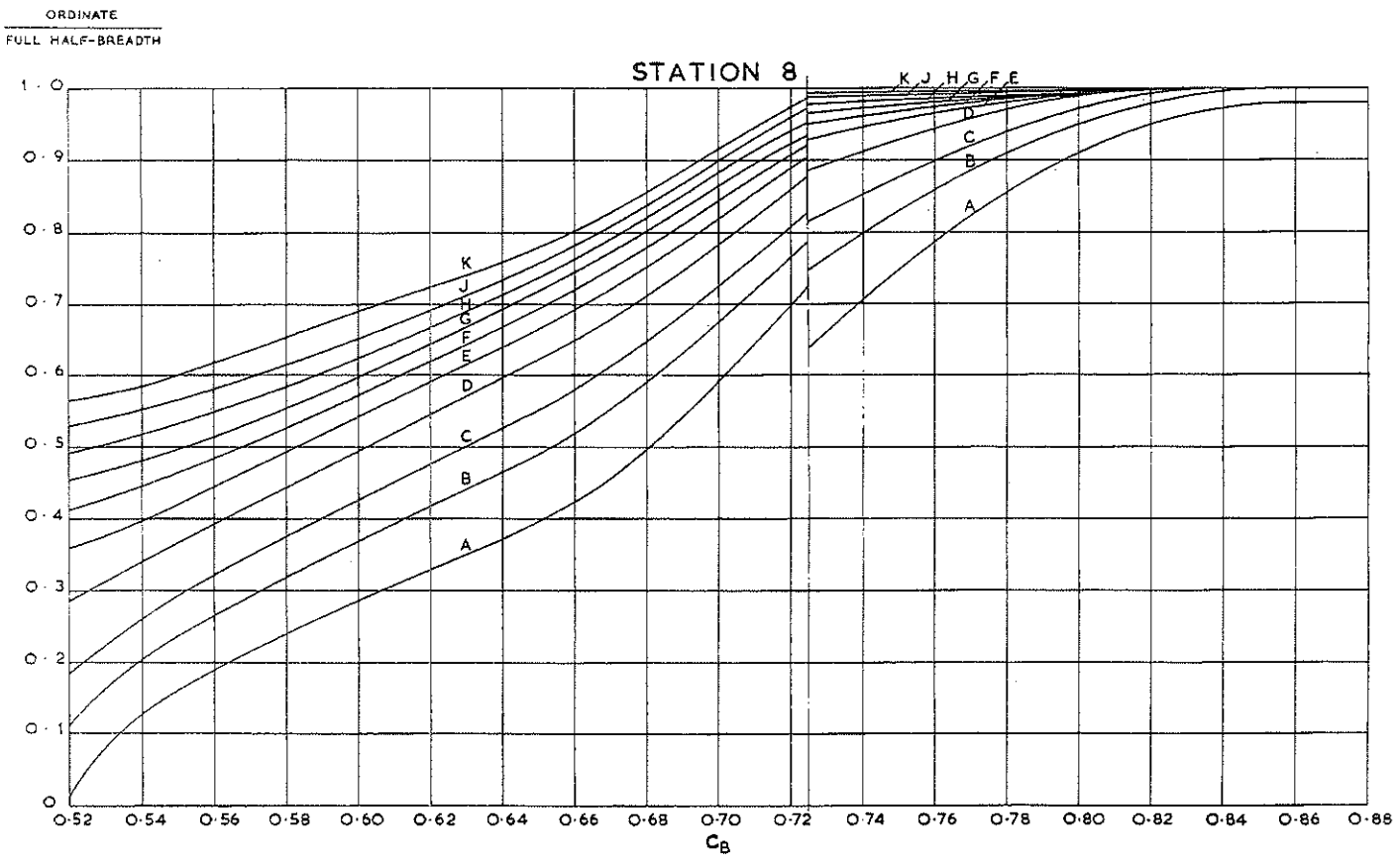

Fig. 14—Station 8.
Waterline Offsets Expressed as the Ratio of Waterline Ordinate/Full Half-Breadth.

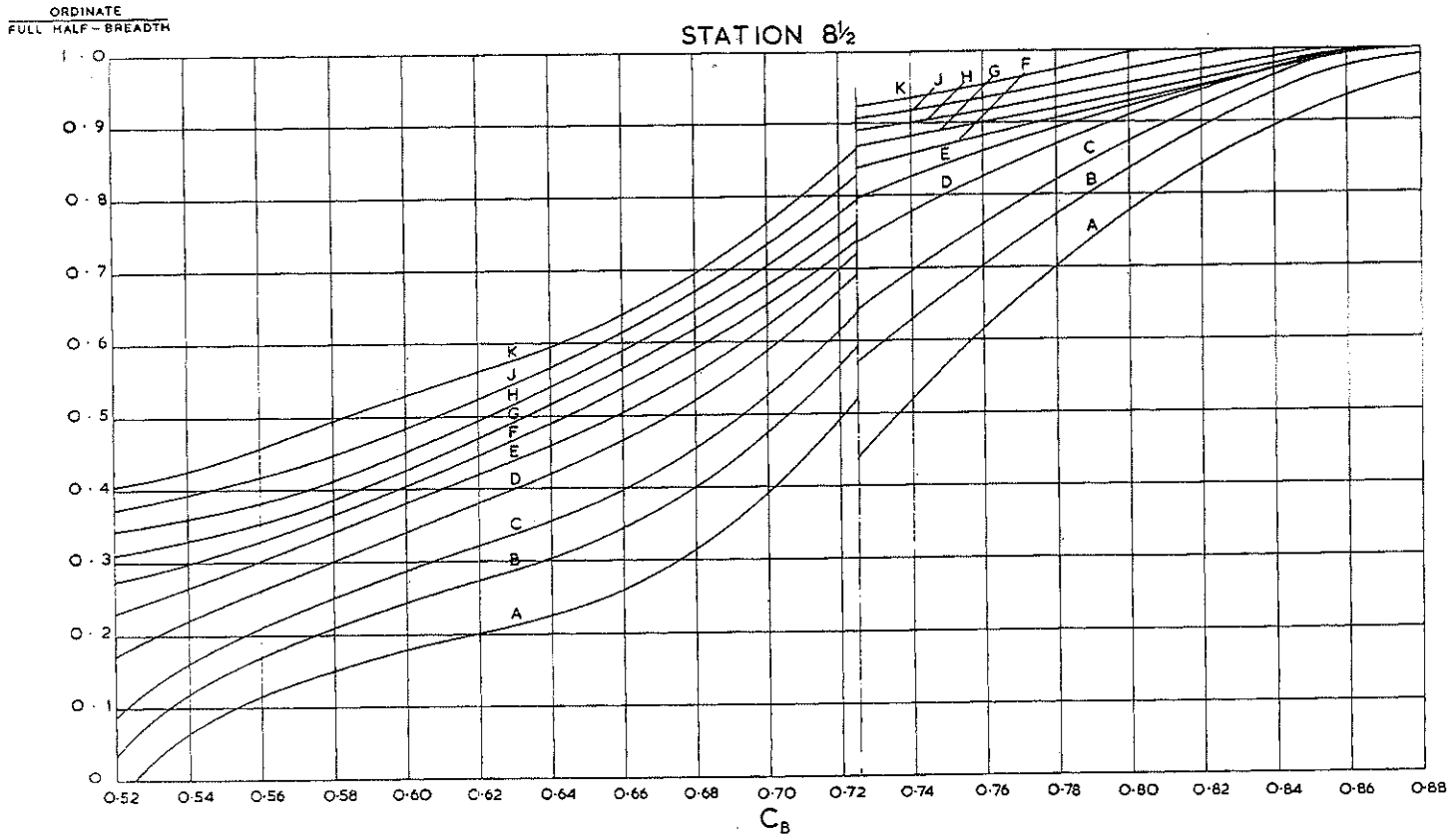

Fig. 15—Station 8½.
Waterline Offsets Expressed as the Ratio of Waterline Ordinate/Full Half-Breadth.

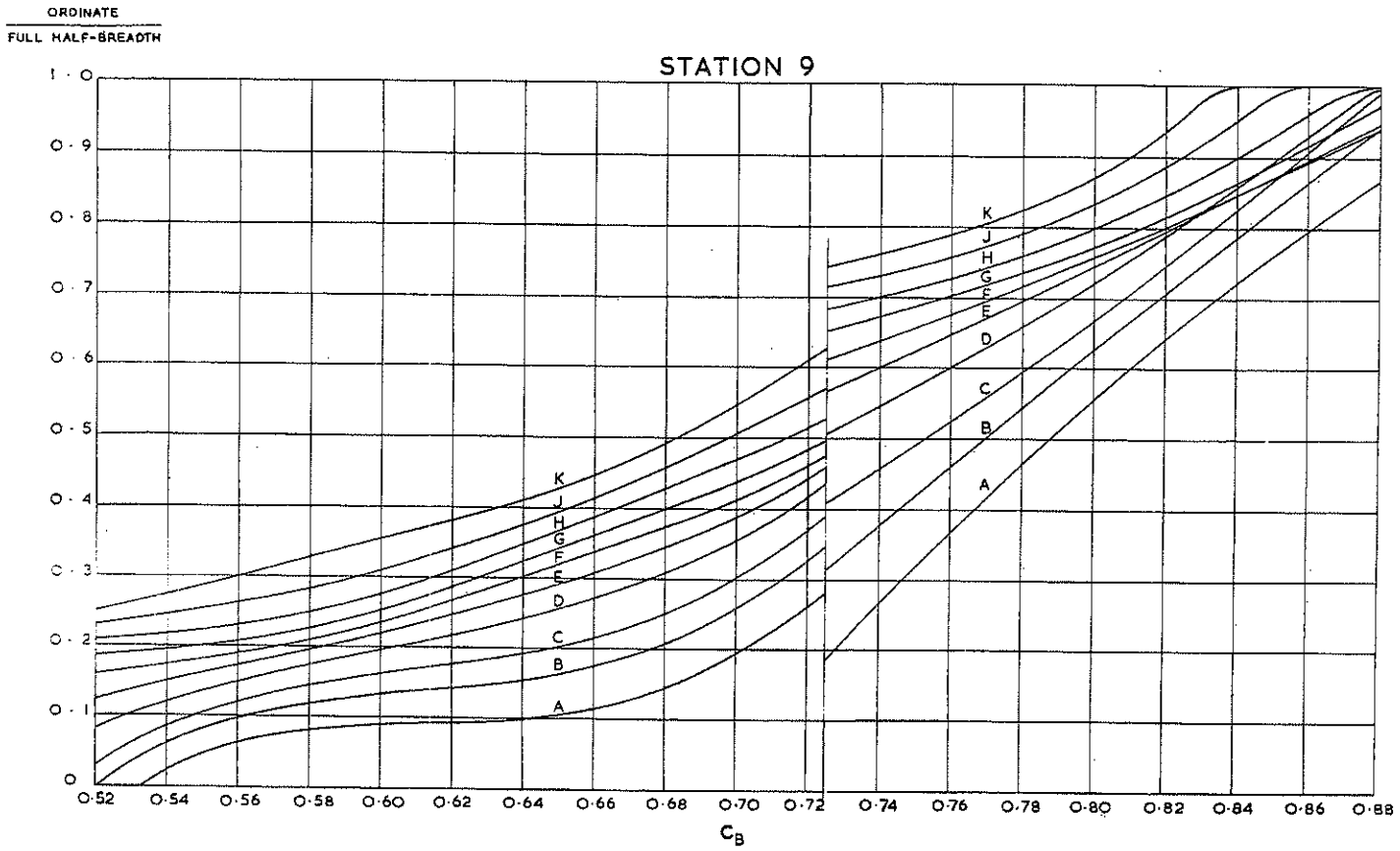

Fig. 16—Station 9.
Waterline Offsets Expressed as the Ratio of Waterline Ordinate/Full Half-Breadth.

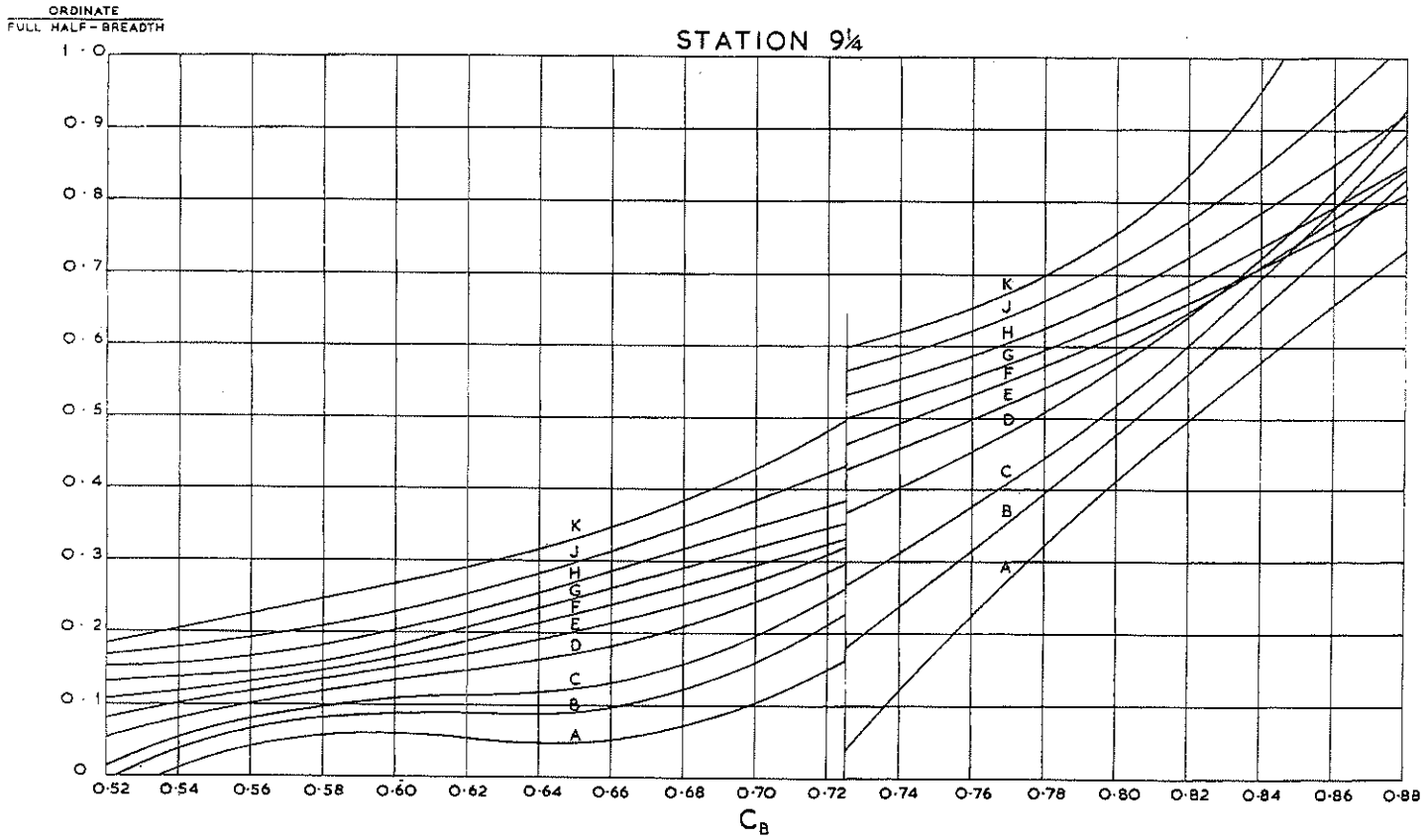

Fig. 17—Station 9¼.
Waterline Offsets Expressed as the Ratio of Waterline Ordinate/Full Half-Breadth.

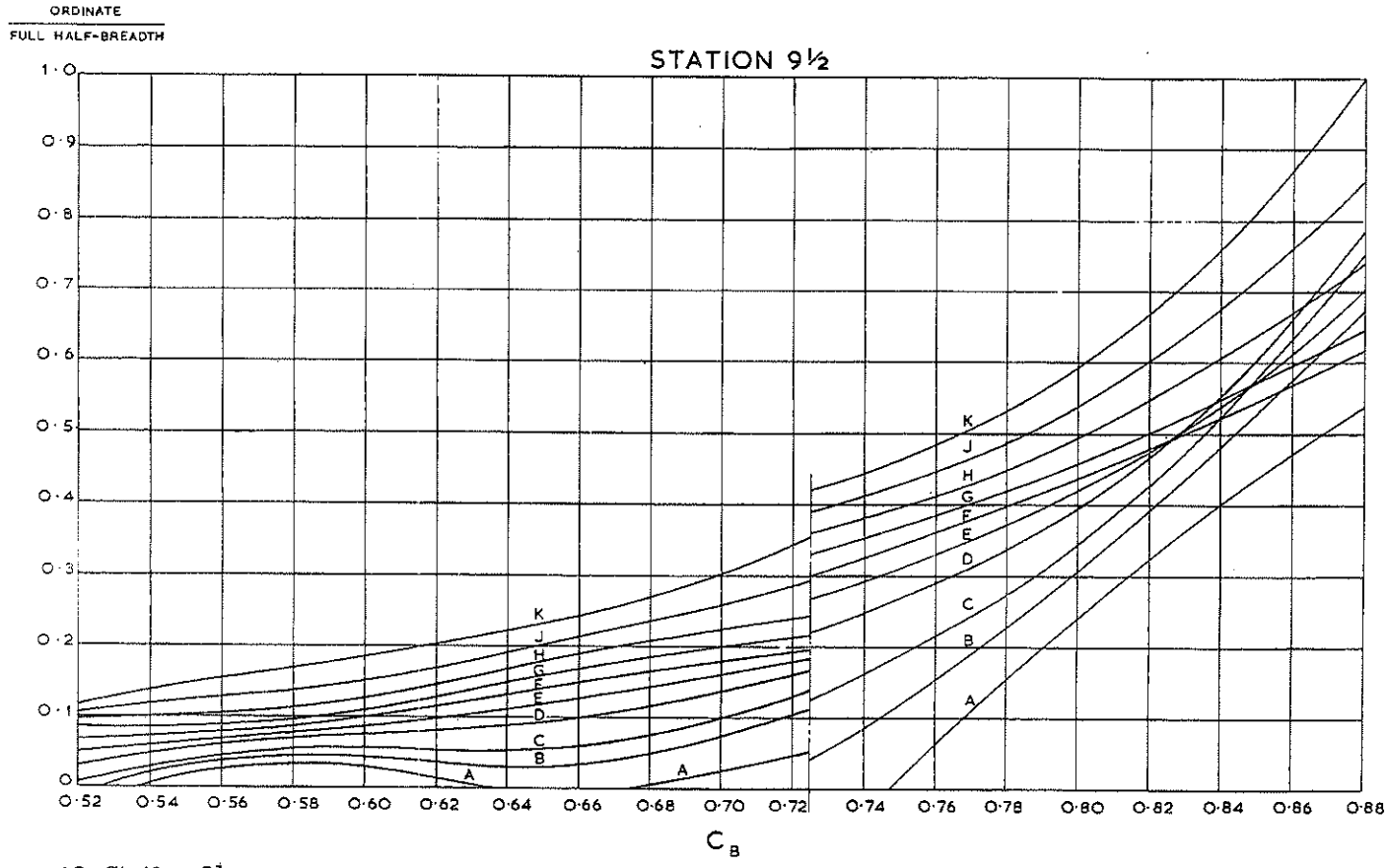

Fig. 18—Station 9½.
Waterline Offsets Expressed as the Ratio of Waterline Ordinate/Full Half-Breadth.

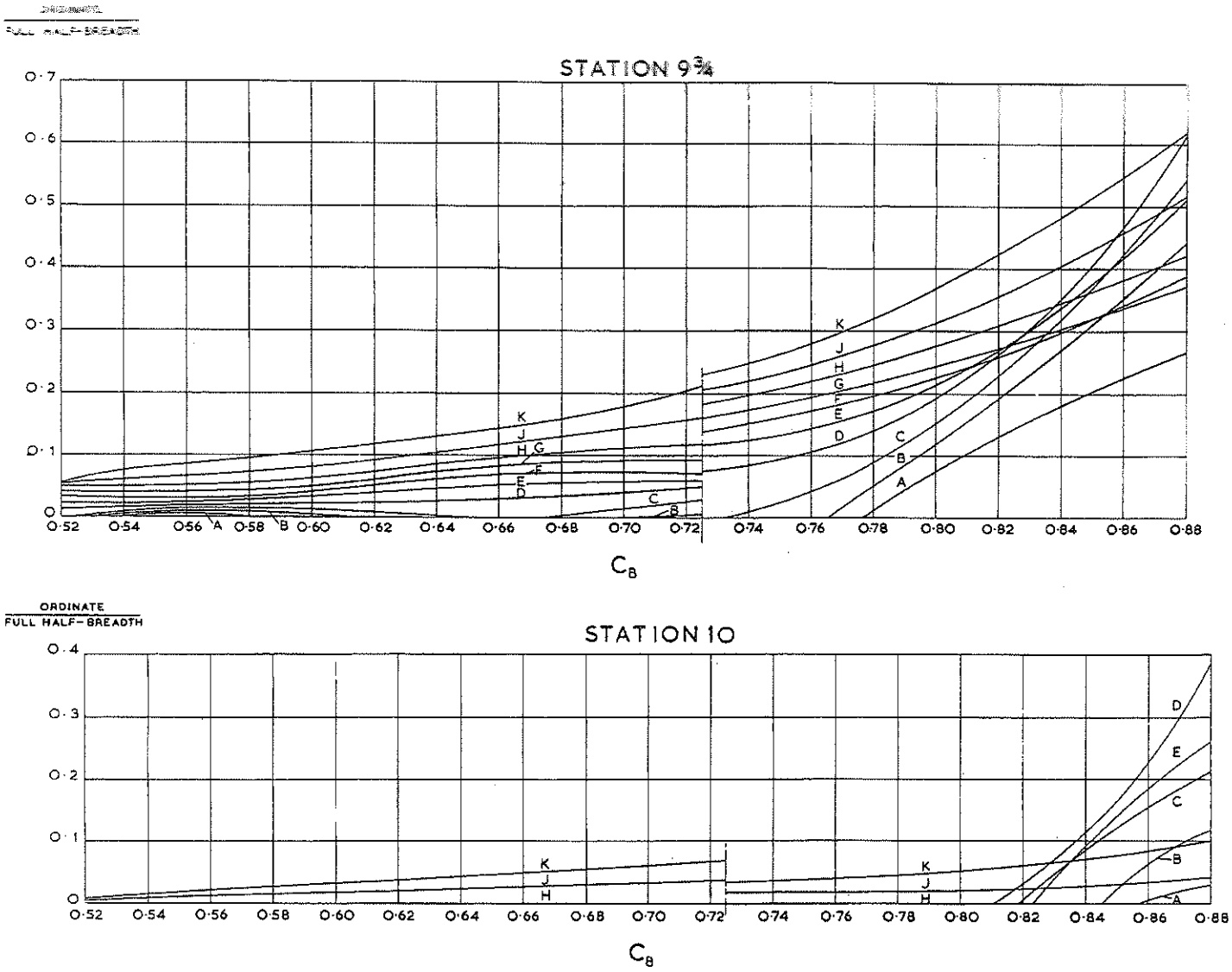

Fig. 19—Stations 9¾ and 10.
Waterline Offsets Expressed as the Ratio of Waterline Ordinate/Full Half-Breadth.

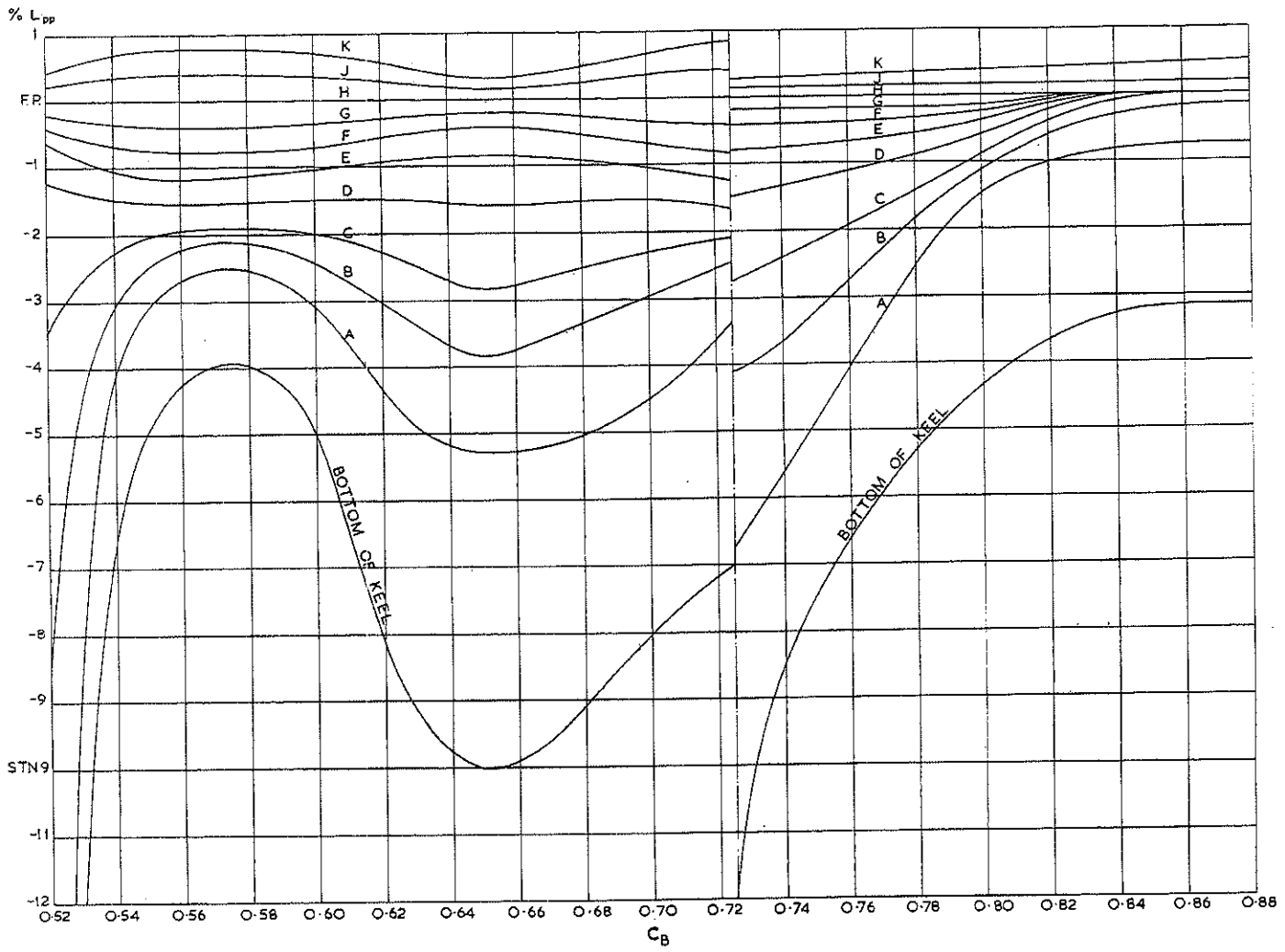

Fig. 20—Stem Profile Offsets.
Expressed as a Percentage of L_{PP} Relative to Station 10.

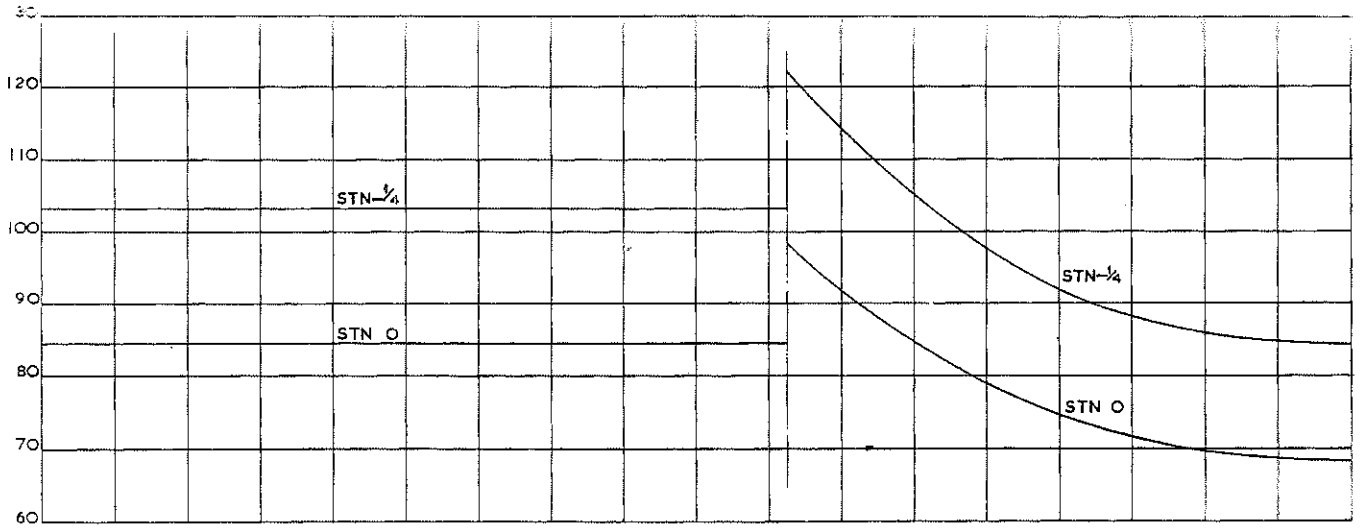

Waterline height above keel expressed as percentage of load draught

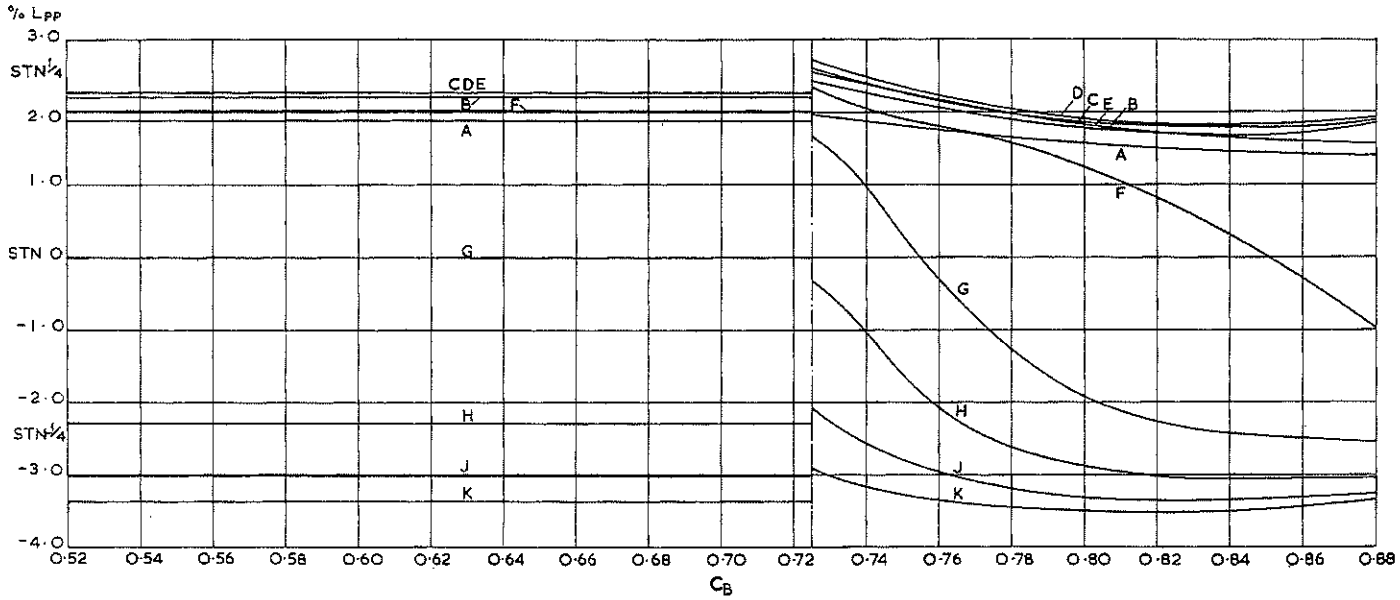

Ordinate expressed as percentage L_{PP} relative to station O

Fig. 21—Stern Profile Offsets.

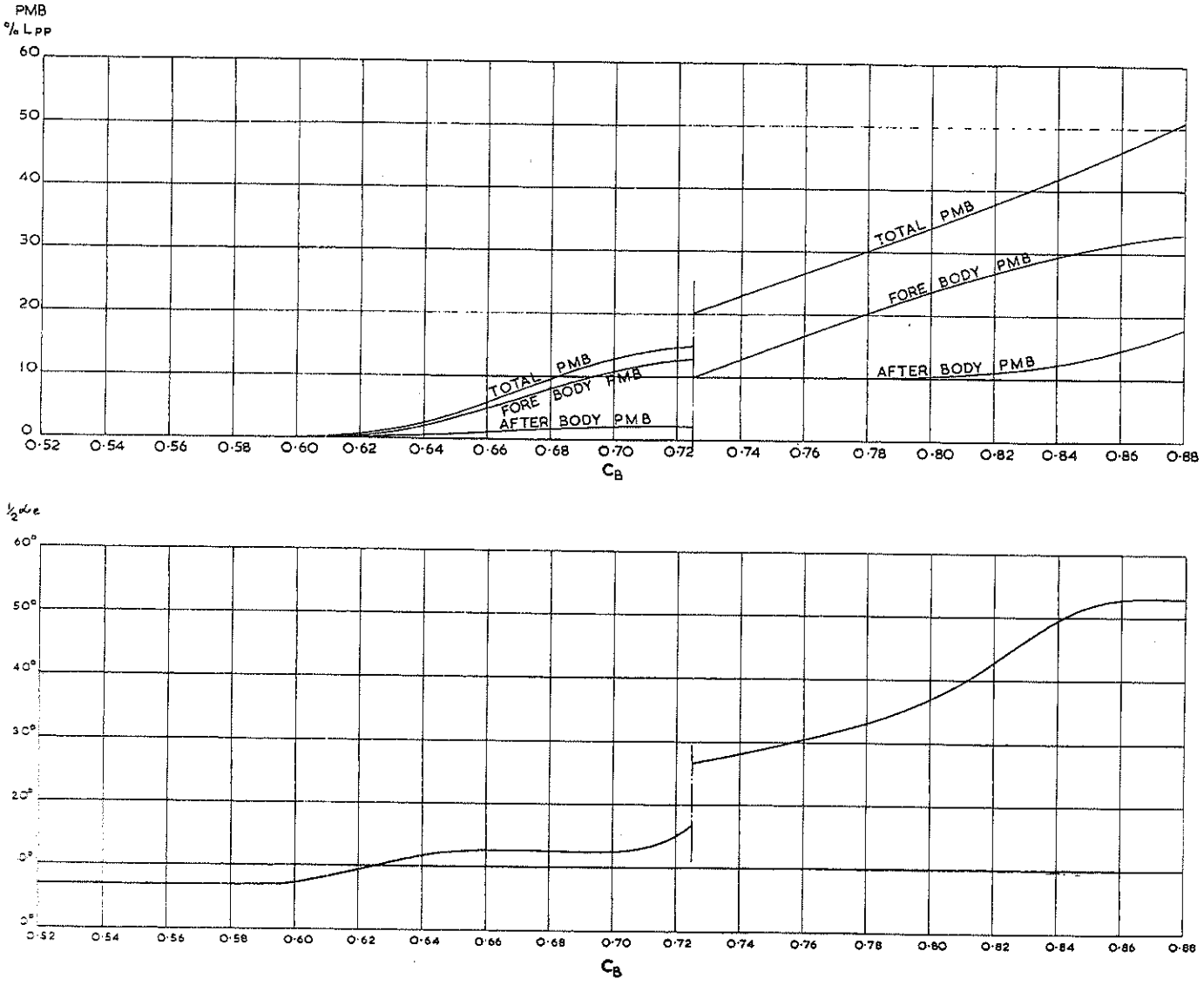

Fig. 22—Parallel Middle-Body and Half Angle of Entrance.

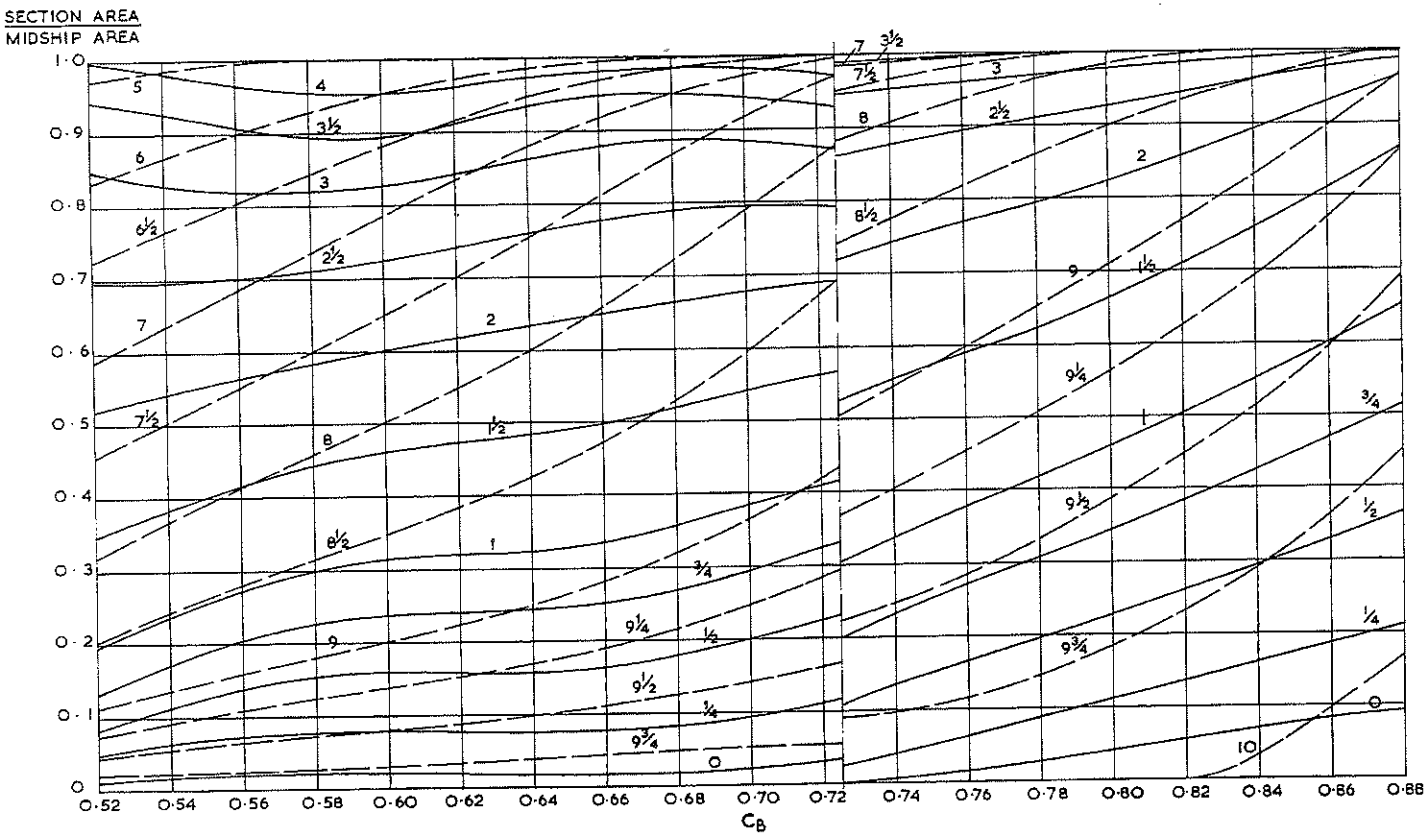

Fig. 23—Sectional Area Curve Ordinates for Load Draught.
Expressed as the Ratio of Sectional Area/Midship Area.

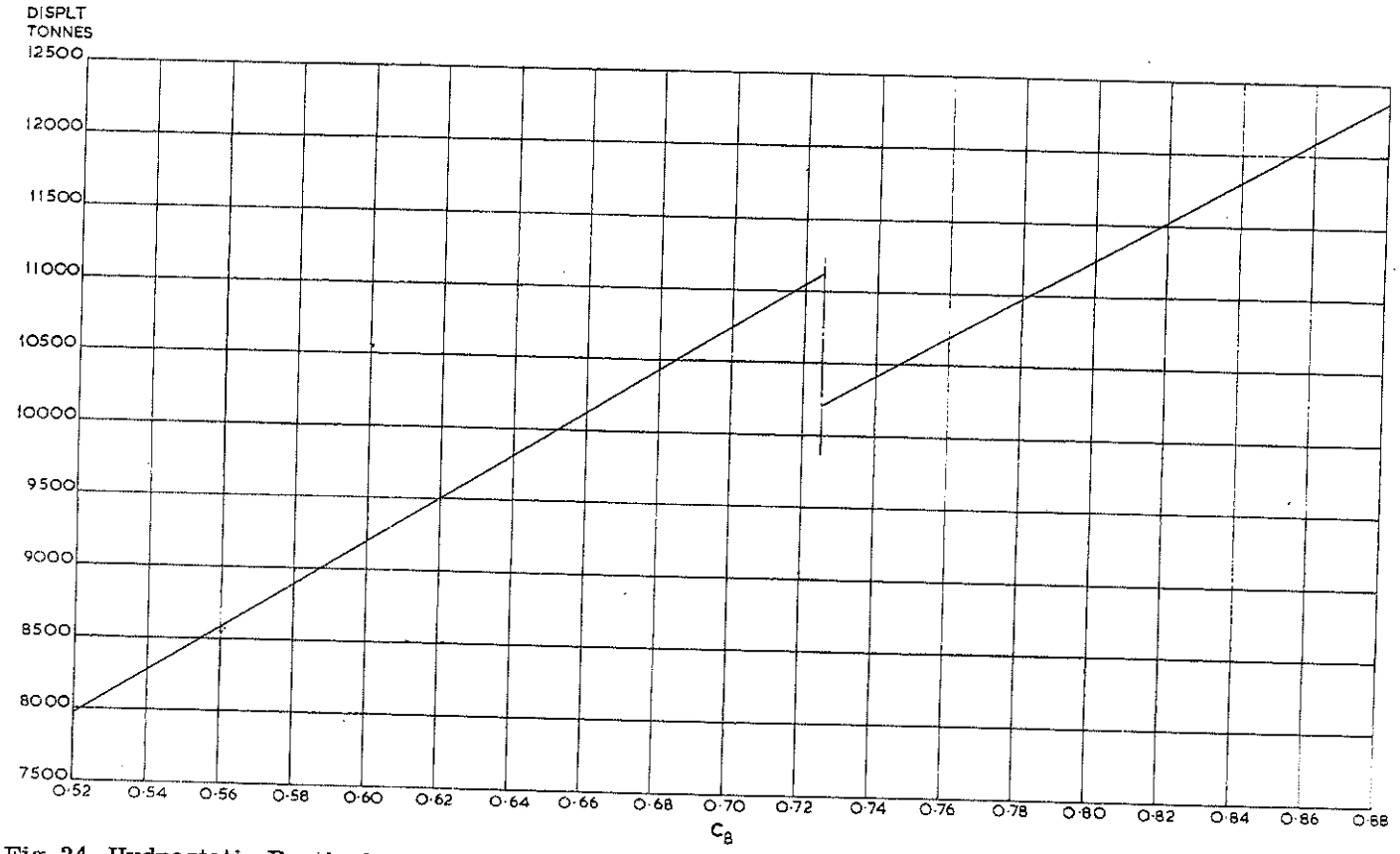

Fig. 24—Hydrostatic Particulars.
Displacement, Tonnes Salt Water.

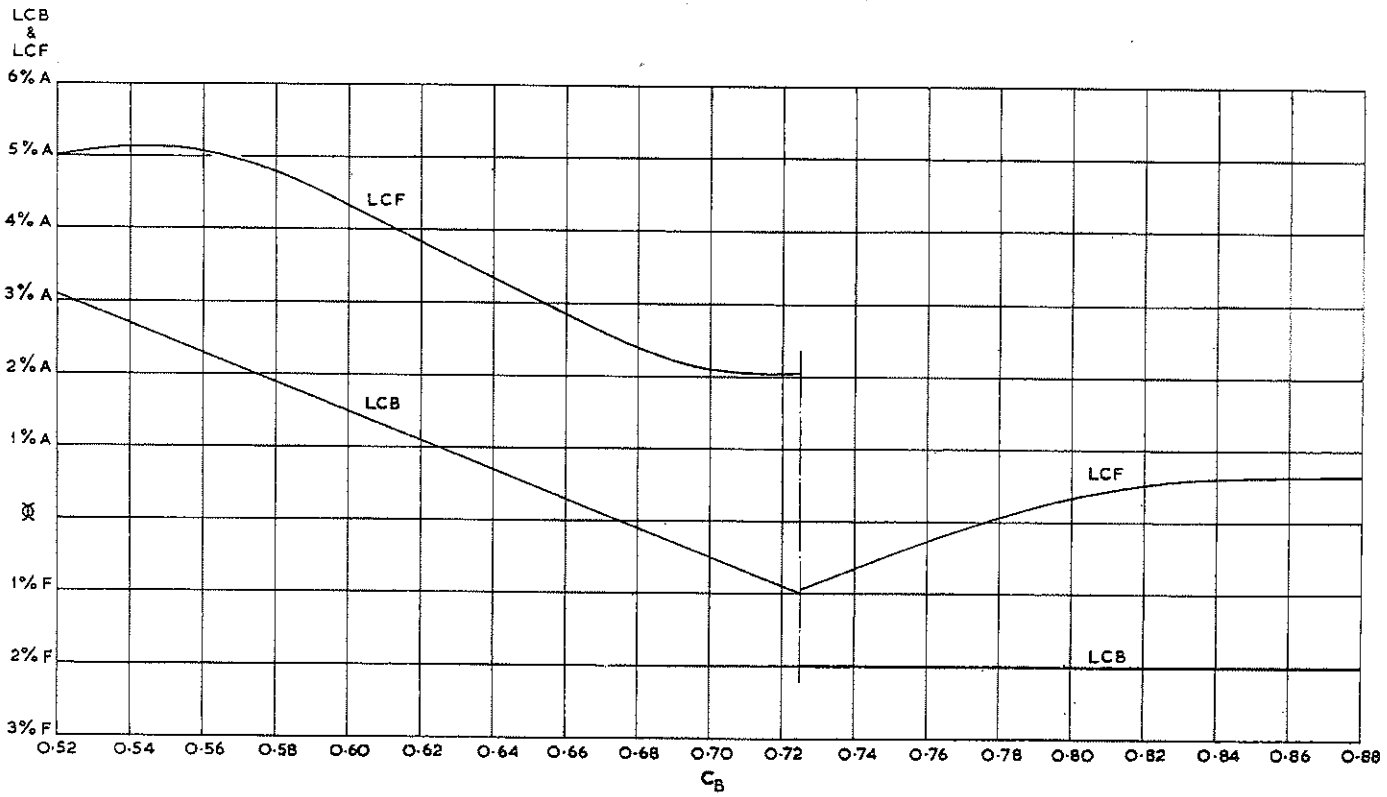

Fig. 25—Hydrostatic Particulars.
Longitudinal Centre of Buoyancy and Longitudinal Centre of Flotation.
Expressed as a Percentage of L_{pp} Forward or Aft of Midships.

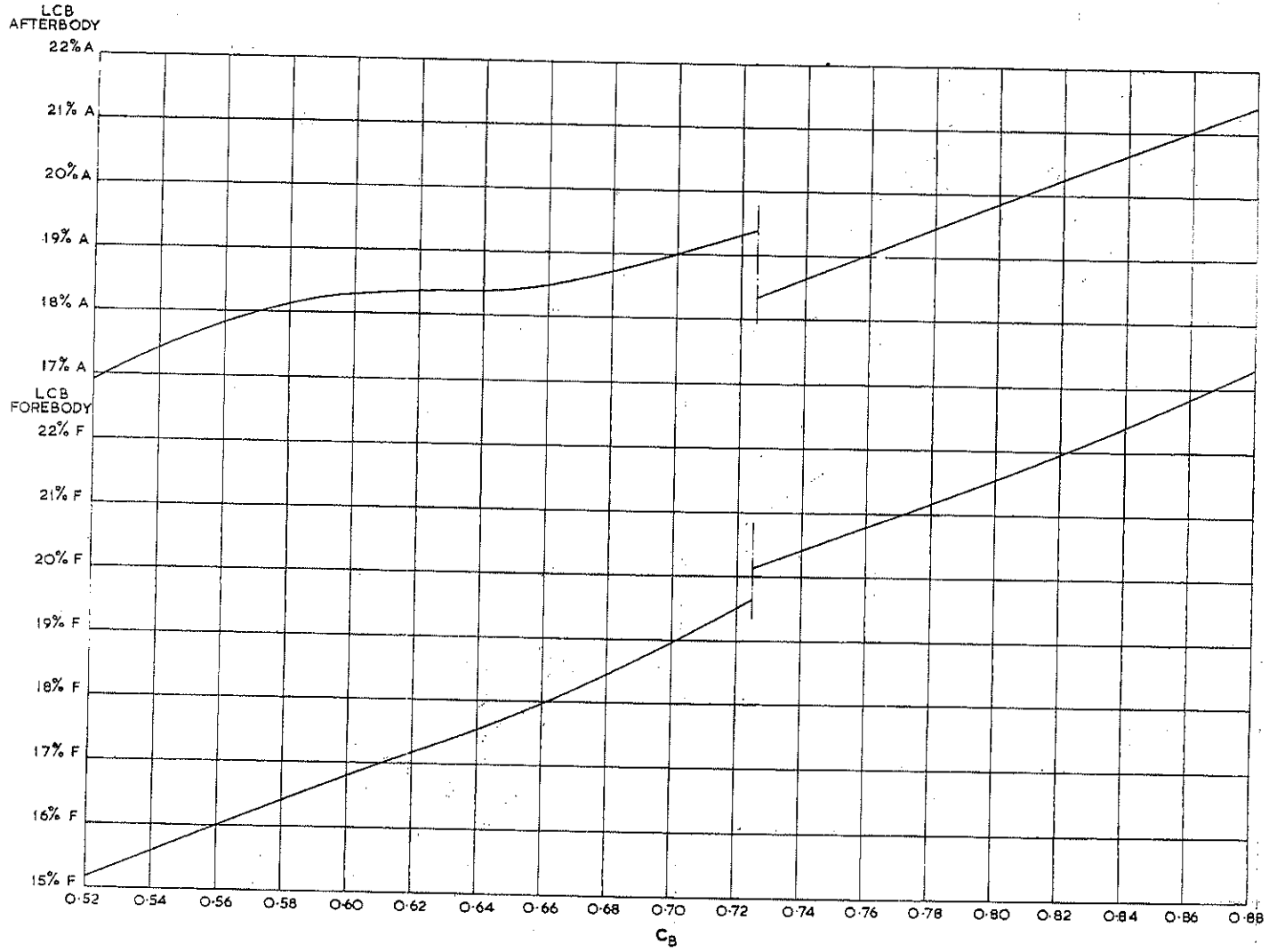

Fig. 26—Hydrostatic Particulars.
Longitudinal Centre of Buoyancy for Forward and After Bodies. Expressed as a Percentage of L_{pp} from Midships.

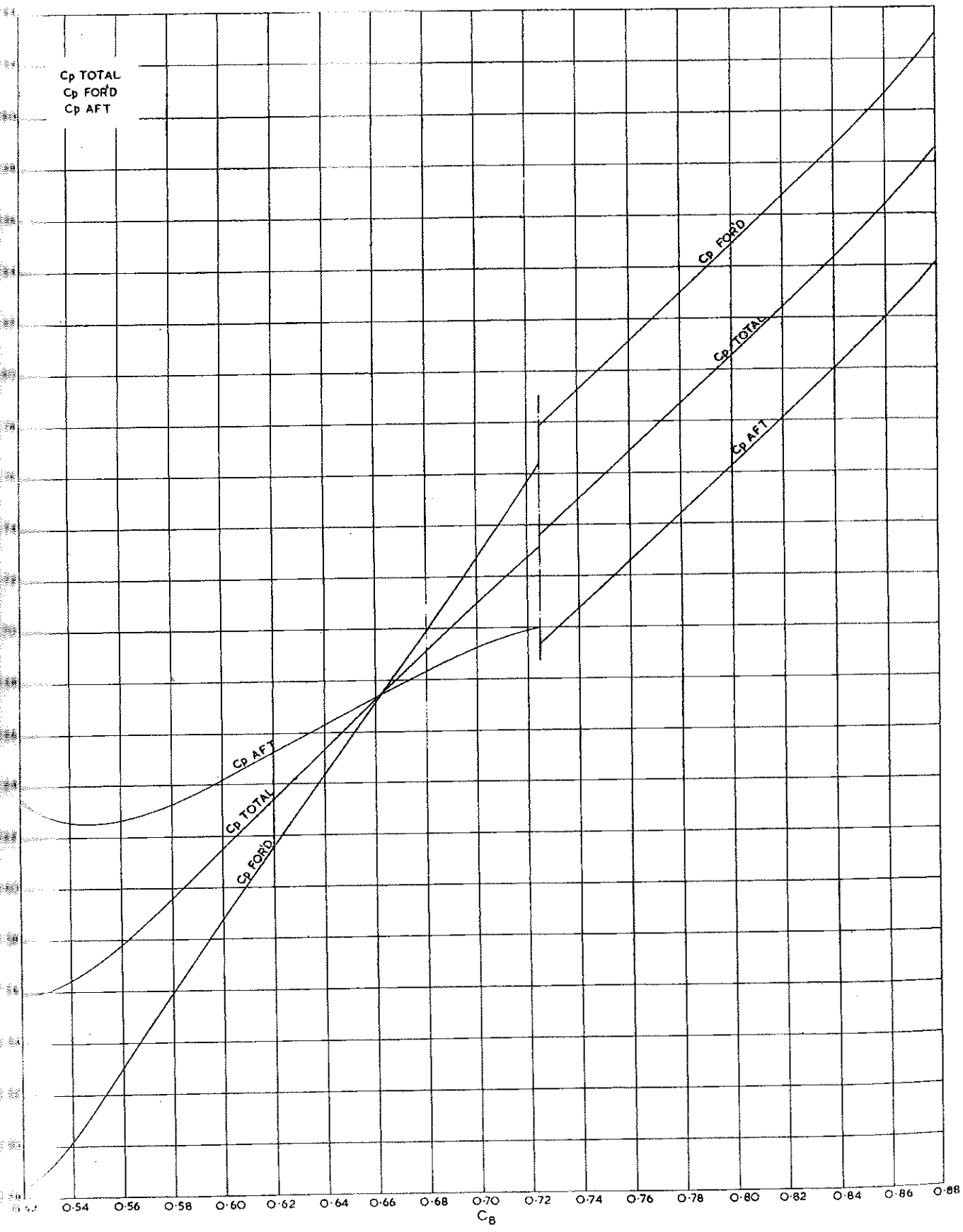

FIG. 27—**Hydrostatic Particulars.**
Prismatic Coefficient Total Based on L_{PP}, Fore Body and After Body Based on $\frac{1}{2}$ L_{PP}.

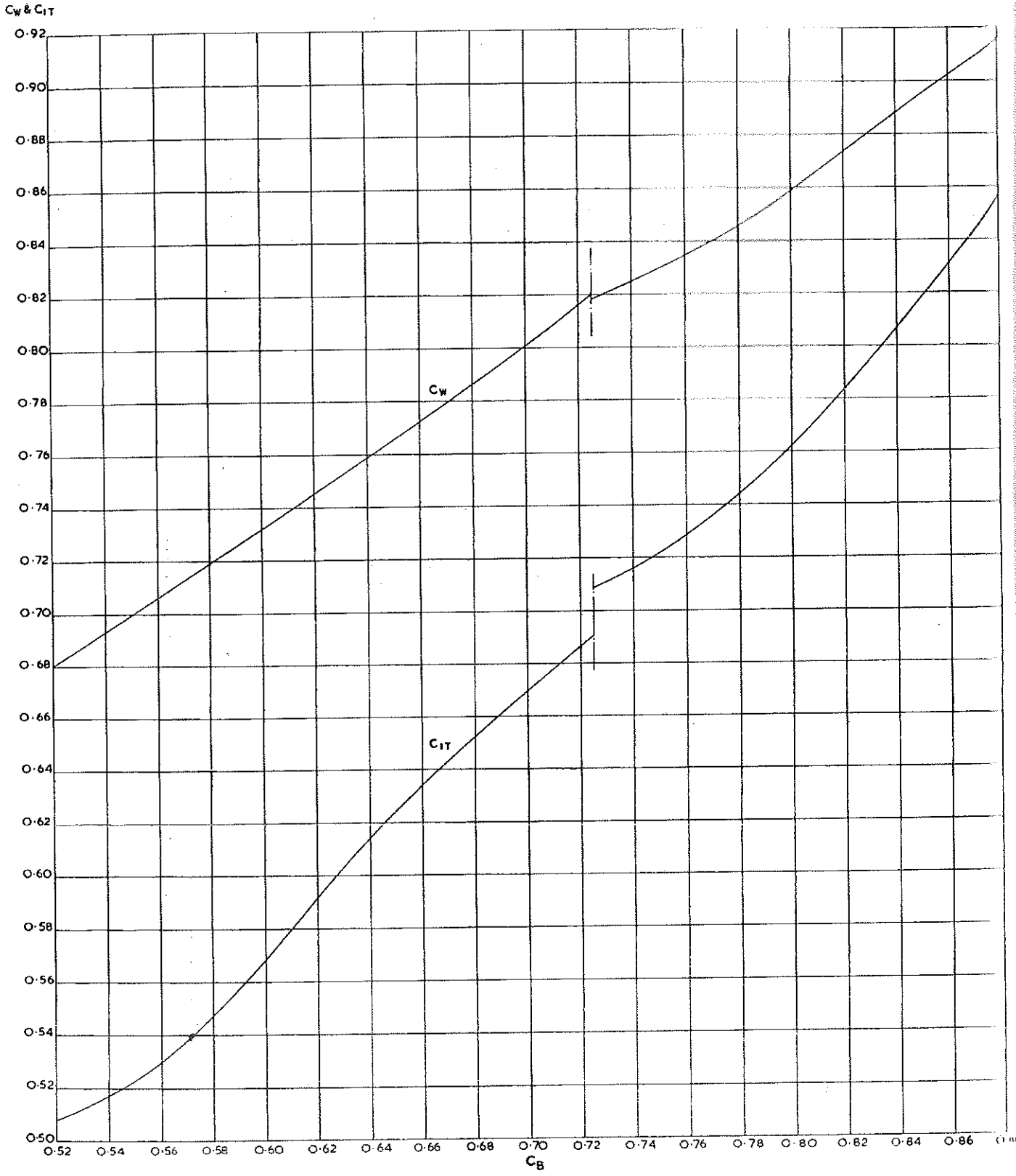

Fig. 28—Hydrostatic Particulars.
Waterplane Area and Transverse Inertia Coefficients Based on Wetted Length.

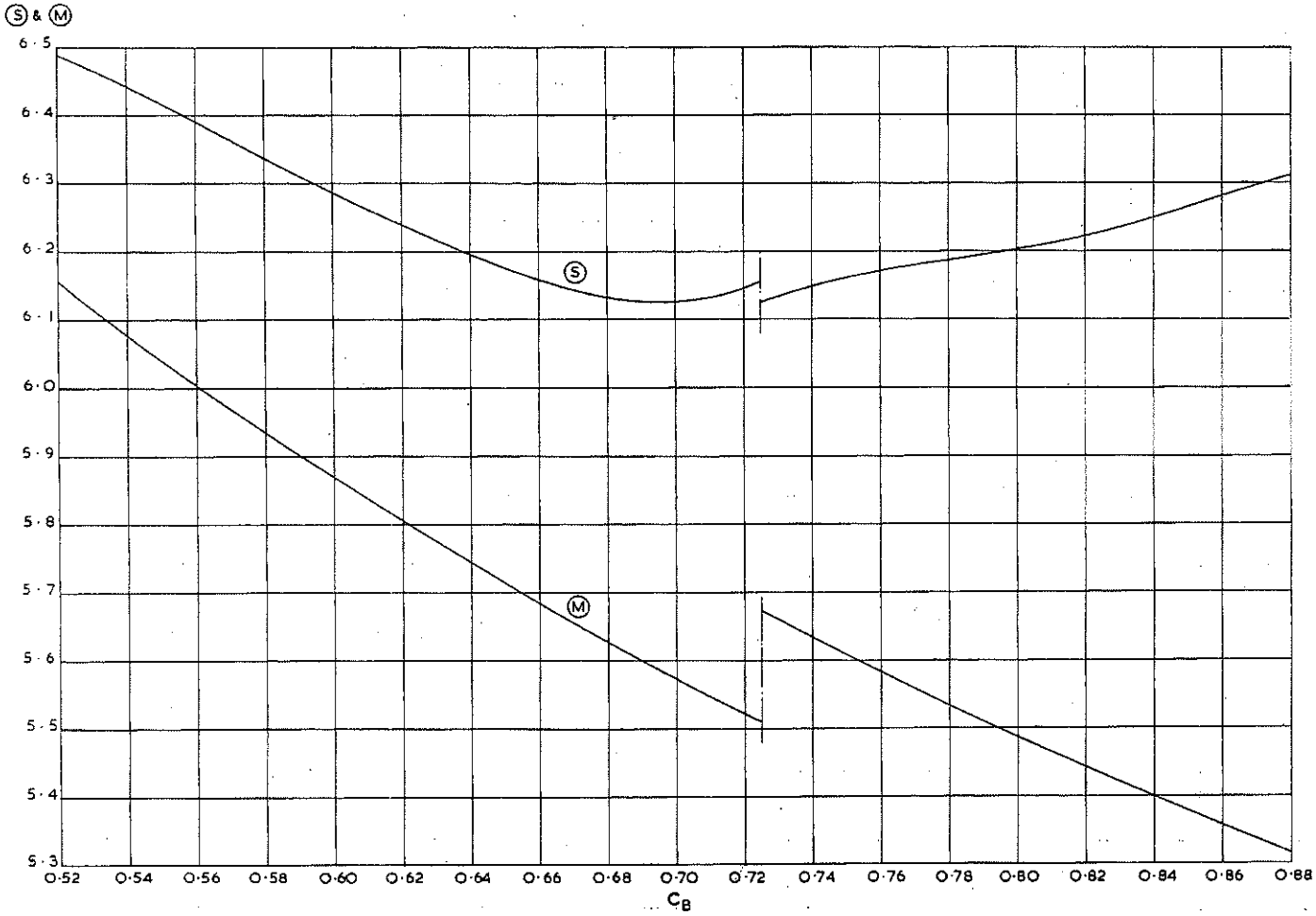

Fig. 29—Hydrostatic Particulars.
Wetted Surface Coefficient Ⓢ and Length-Displacement Ratio Ⓜ.

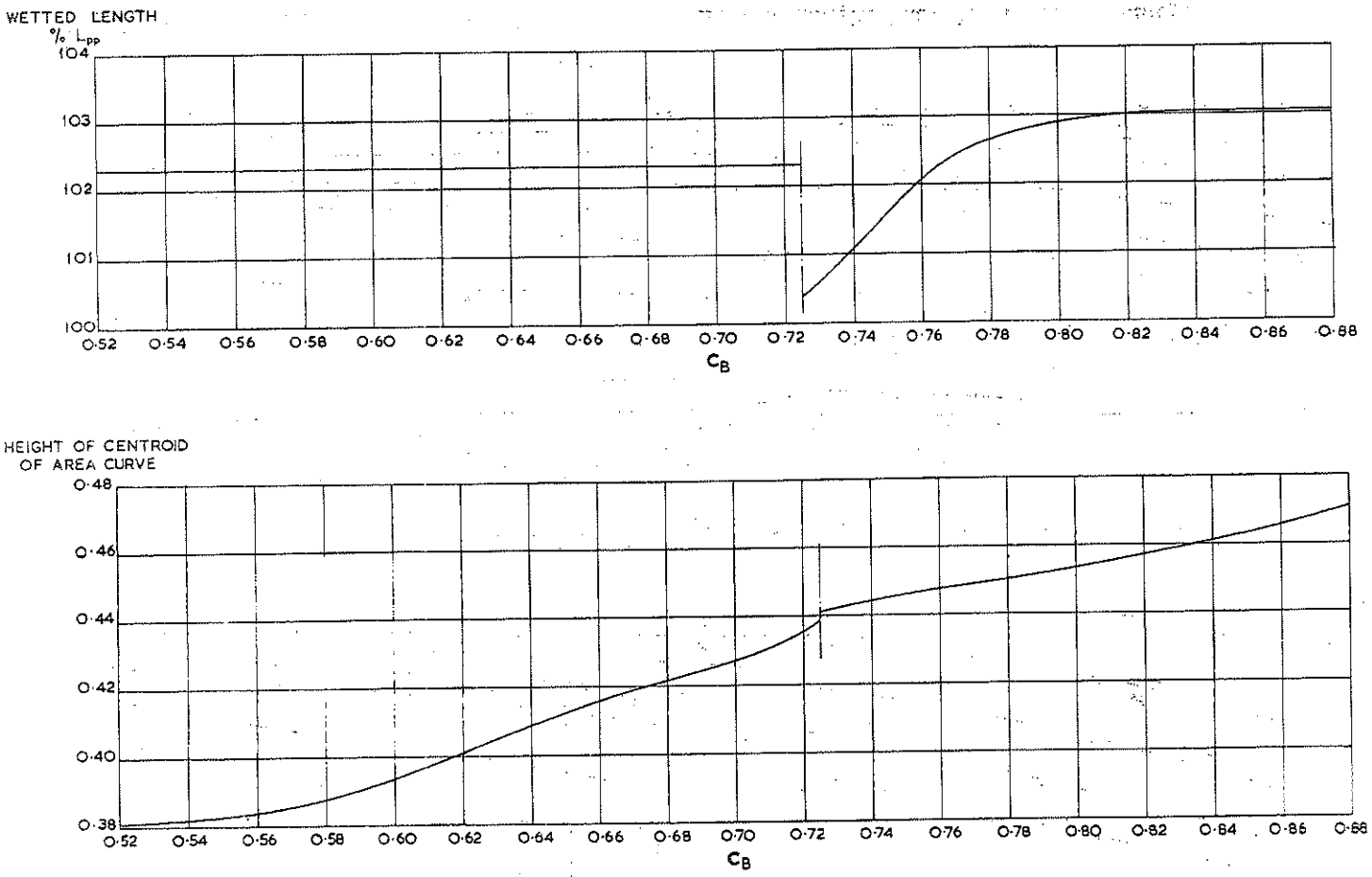

Fig. 30—Hydrostatic Particulars.
Wetted Length and Height of Centroid of Sectional Area Curve.

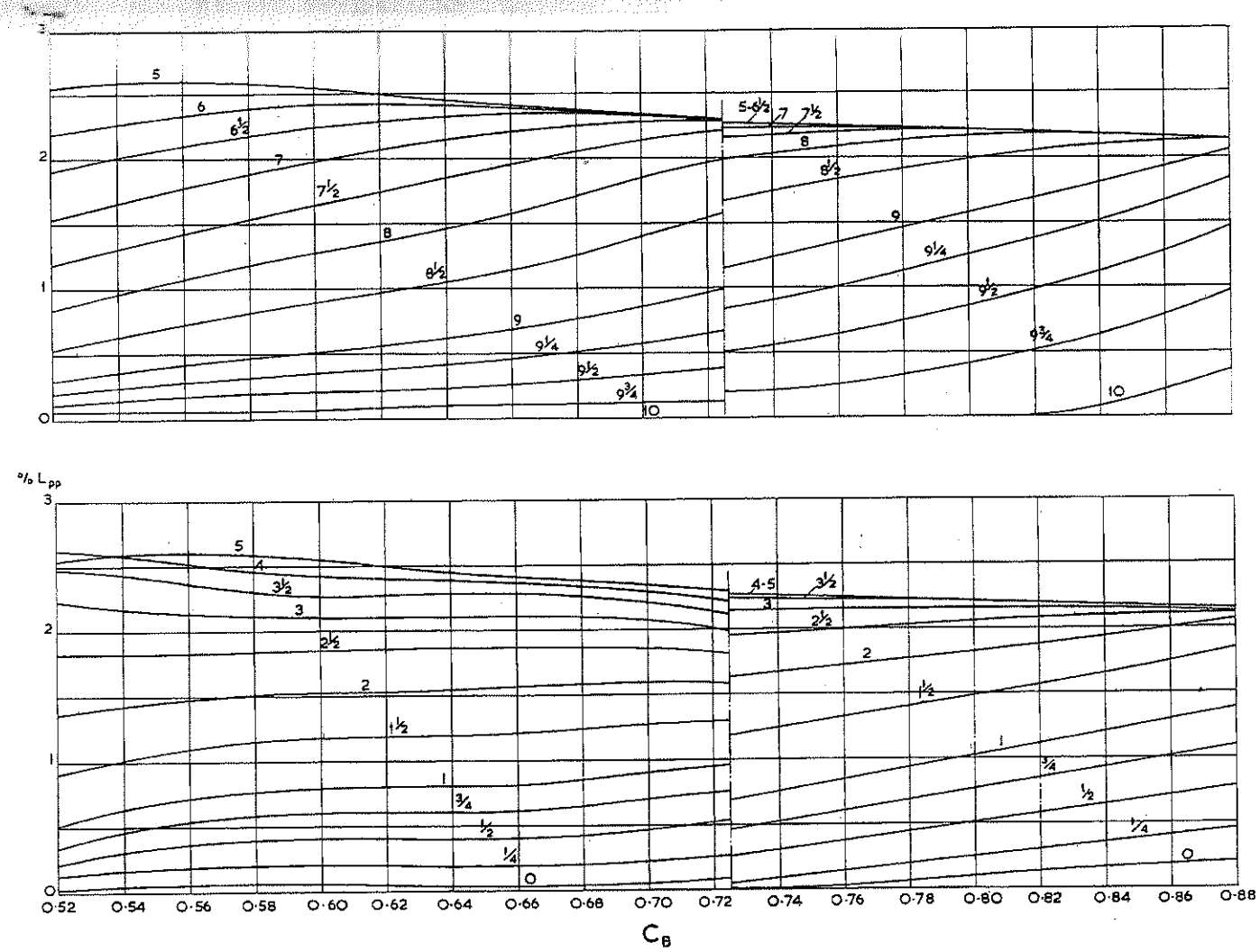

Fig. 31—Shift of Station For One Per Cent L_{pp} Movement of Longitudinal Centre of Buoyancy.

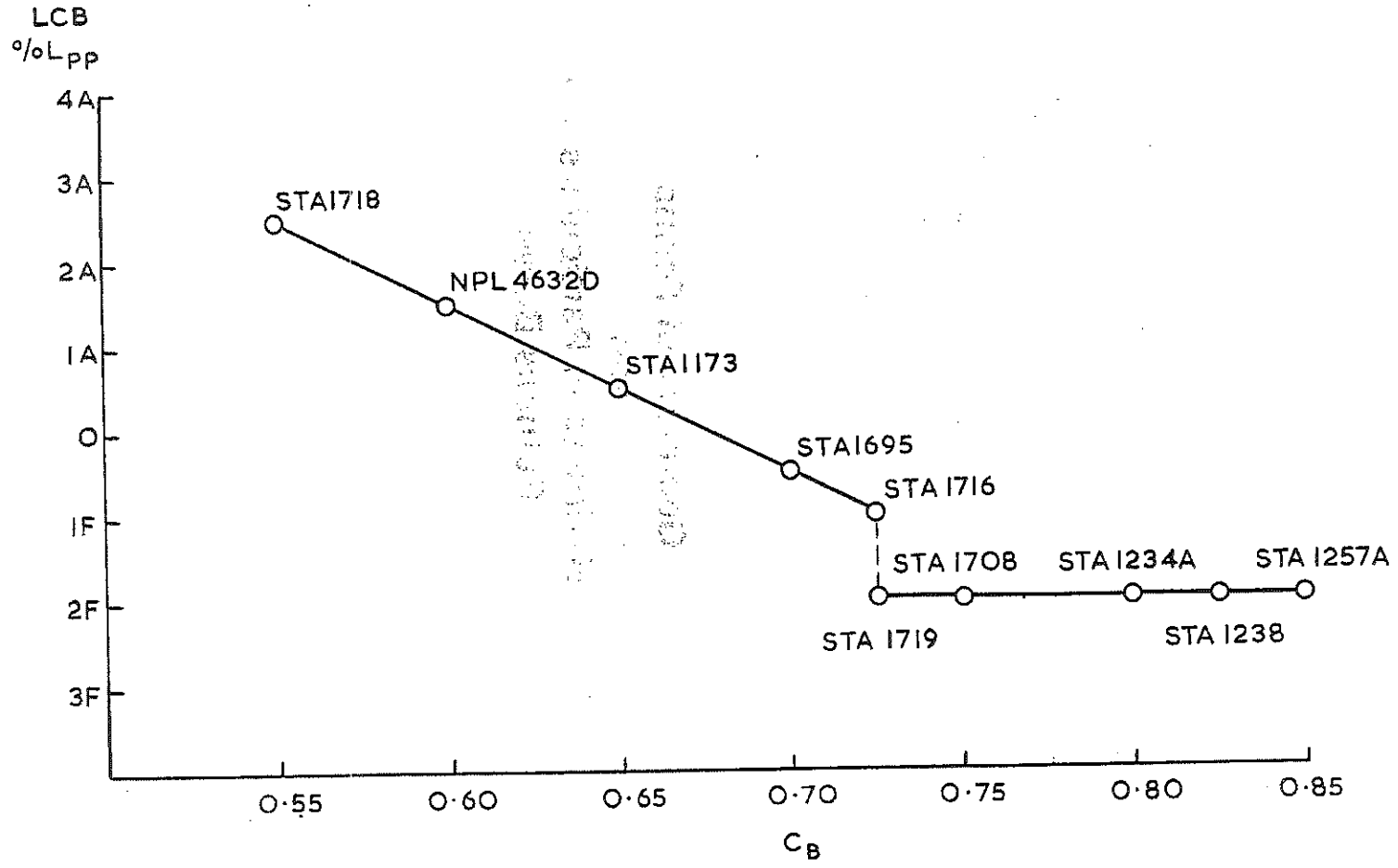

Fig. 32—Basic Models Relative to LCB Line; Bulbous Bows

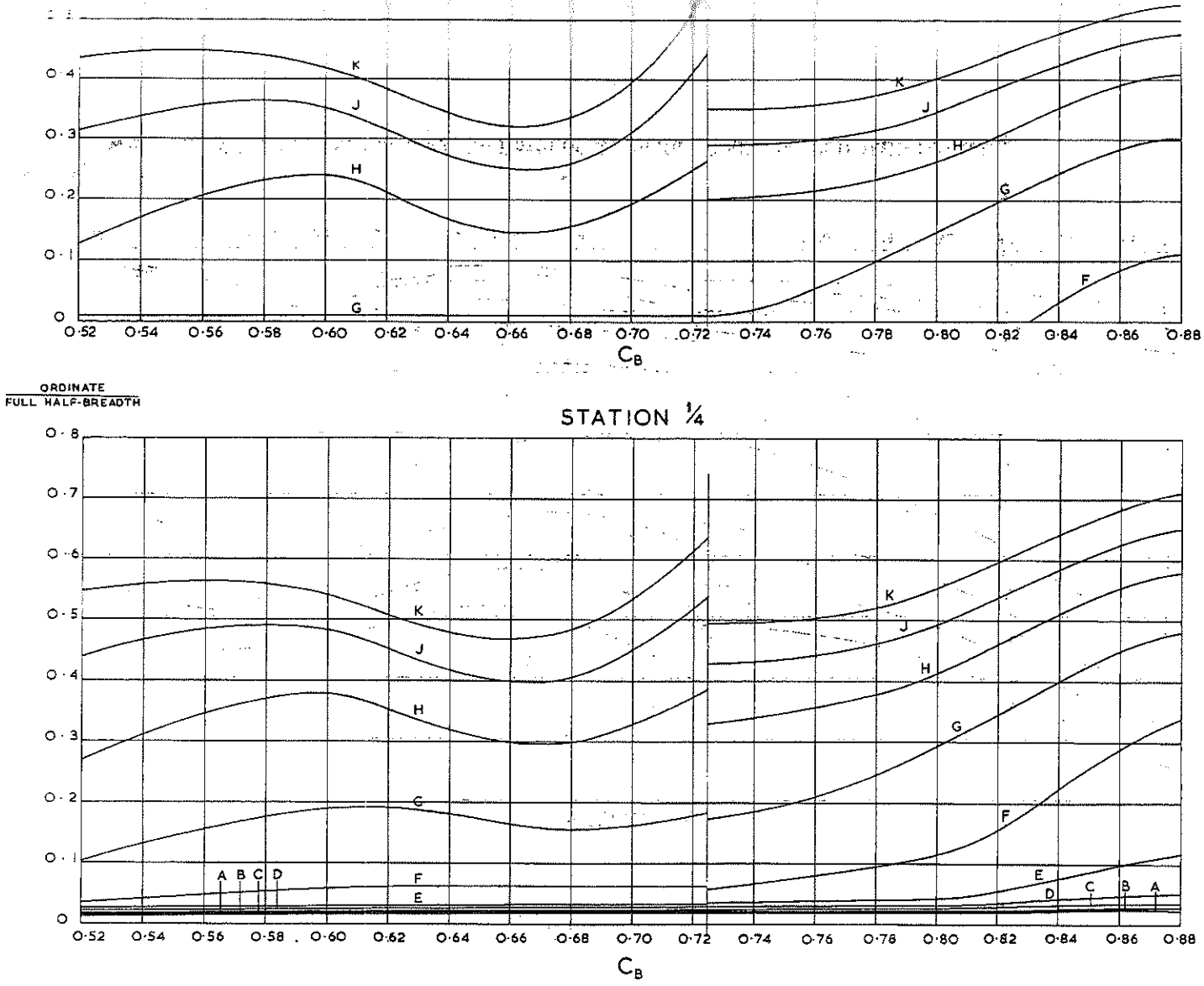

Fig. 33—Stations O and ¼.
Waterline Offsets Expressed as the Ratio of Waterline Ordinate/Full Half-Breadth.

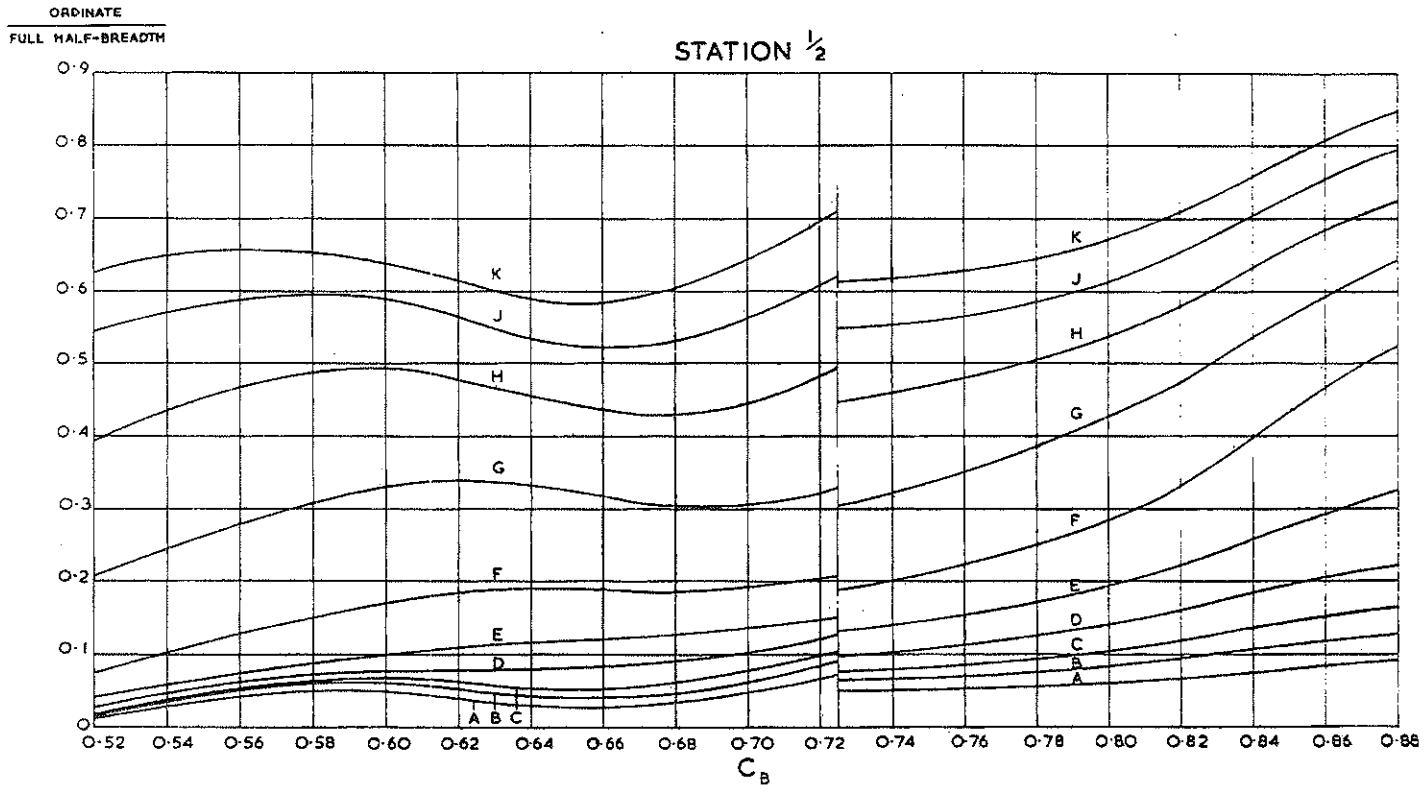

Fig. 34—Station ½.
Waterline Offsets Expressed as the Ratio of Waterline Ordinate/Full Half-Breadth.

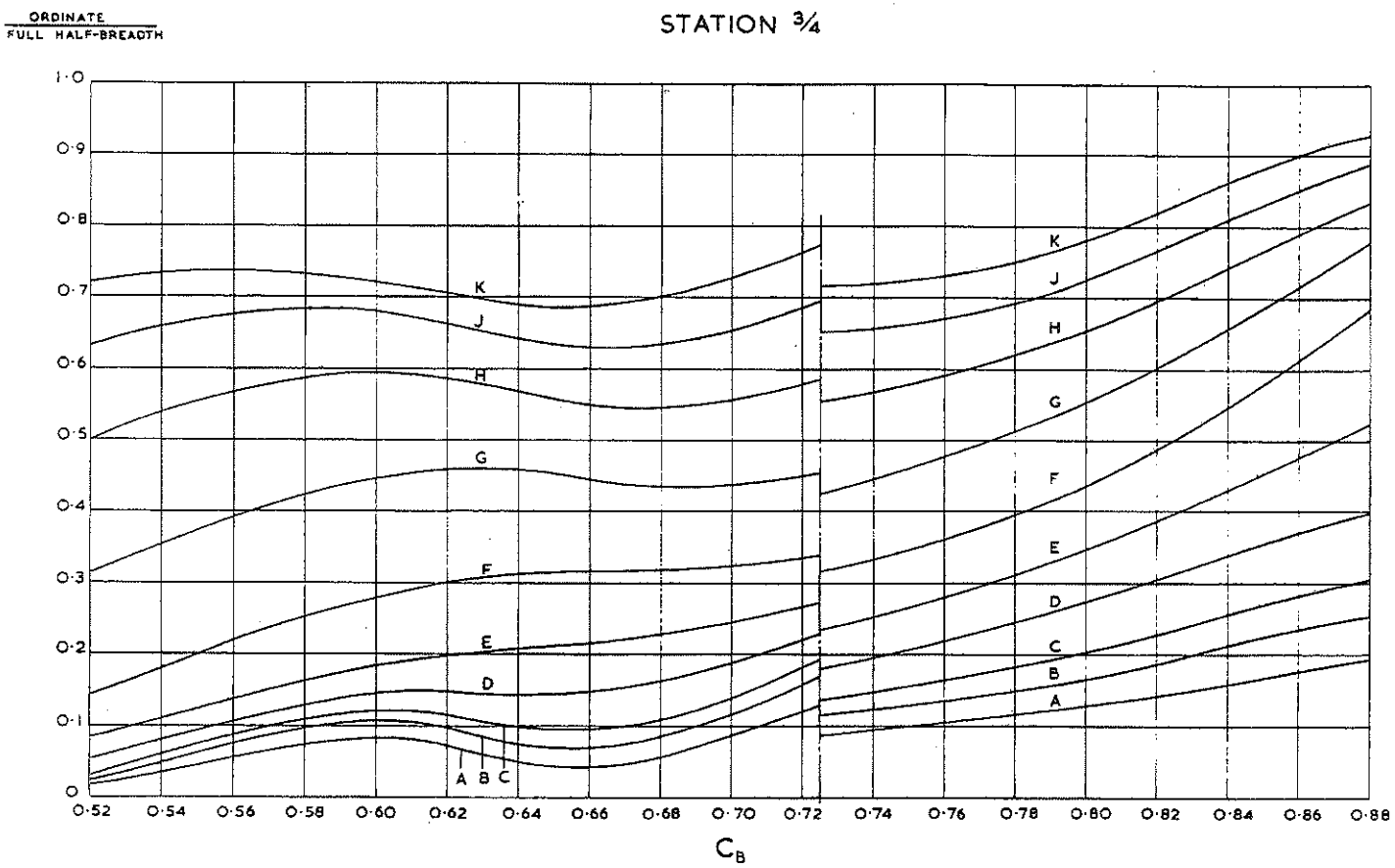

Fig. 35—Station ¾.
Waterline Offsets Expressed as the Ratio of Waterline Ordinate/Full Half-Breadth.

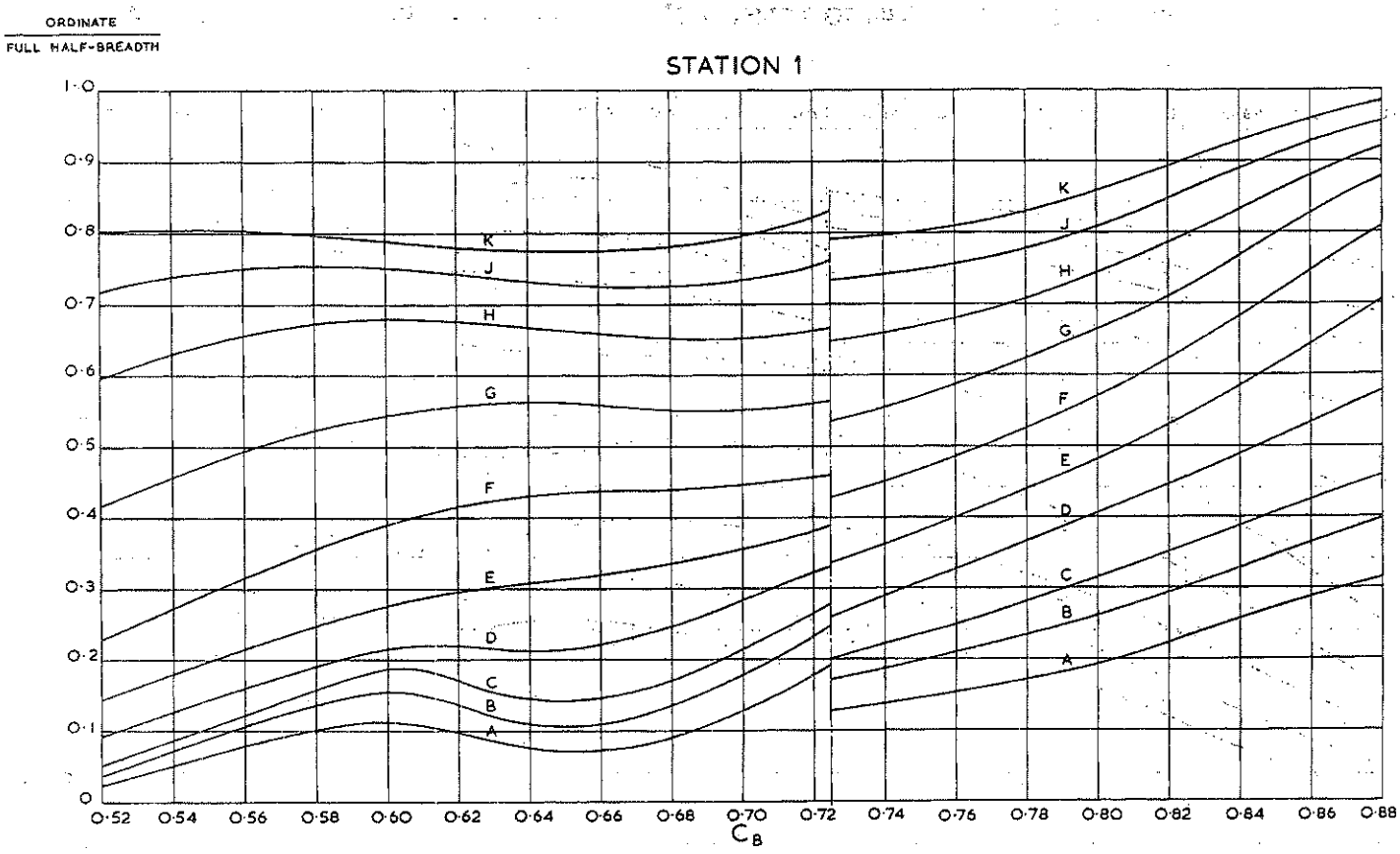

Fig. 36—Station 1.
Waterline Offsets Expressed as the Ratio of Waterline Ordinate/Full Half-Breadth.

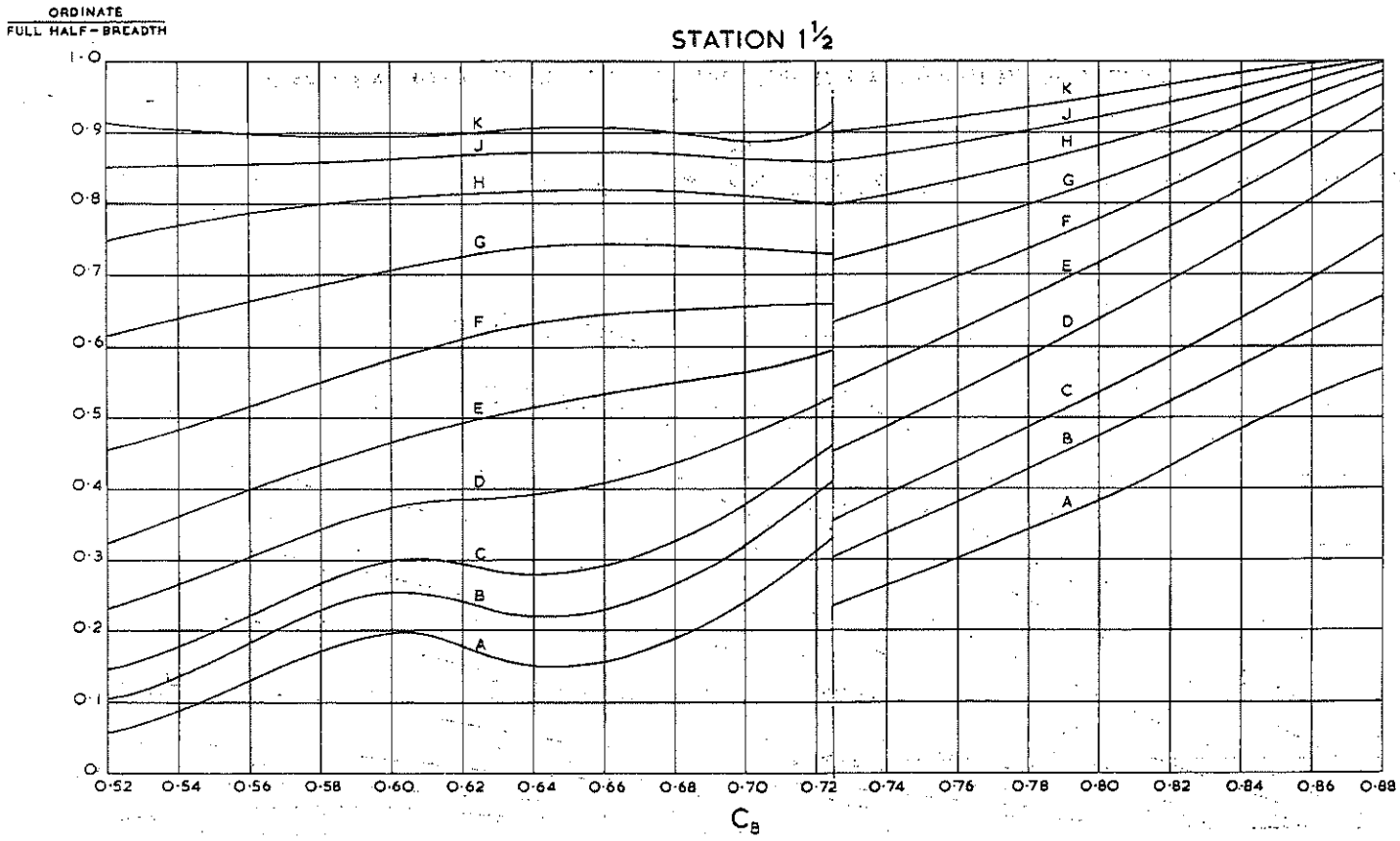

Fig. 37—Station 1½.
Waterline Offsets Expressed as the Ratio of Waterline Ordinate/Full Half-Breadth.

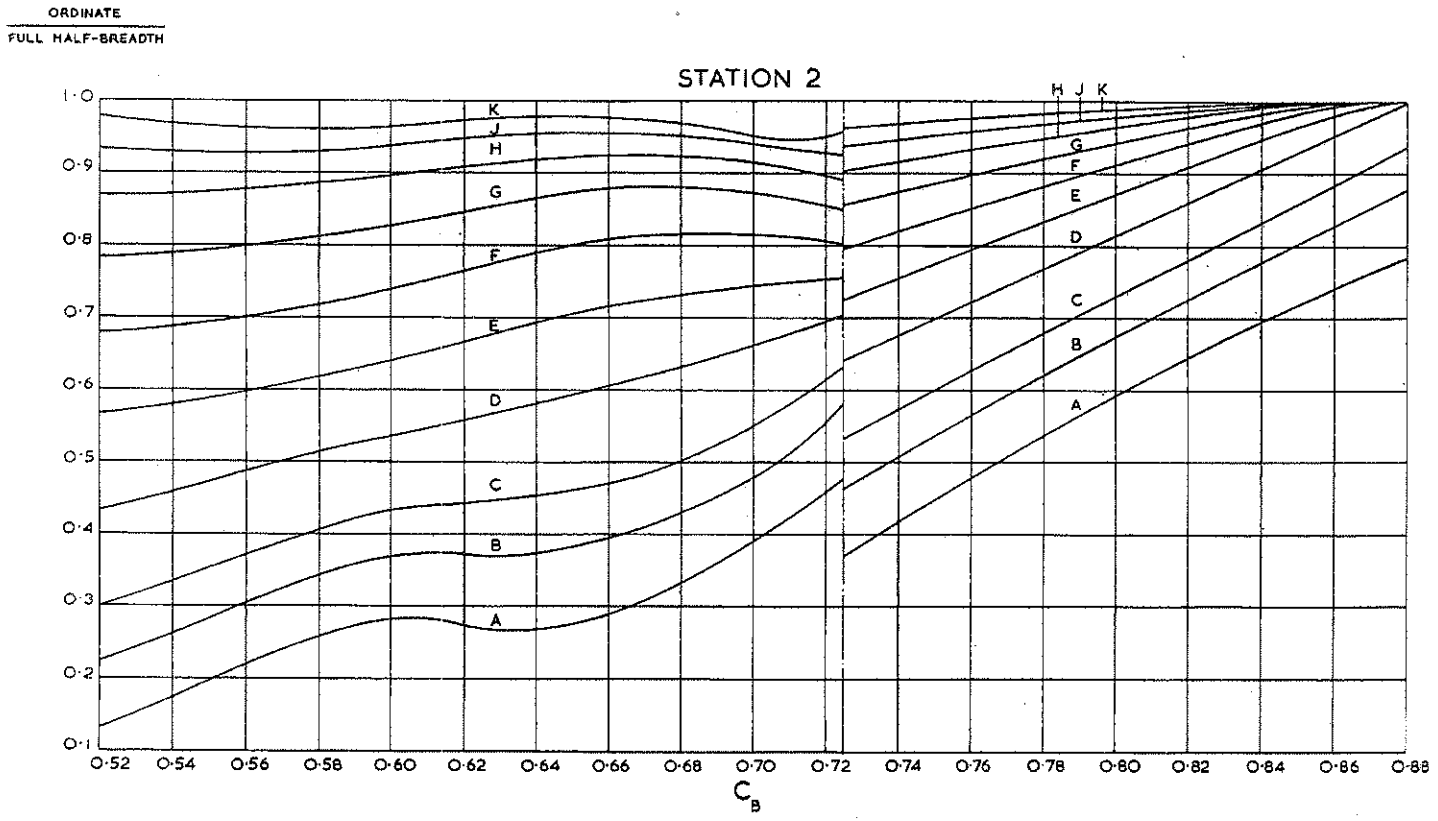

Fig. 38—Station 2.
Waterline Offsets Expressed as the Ratio of Waterline Ordinate/Full Half-Breadth.

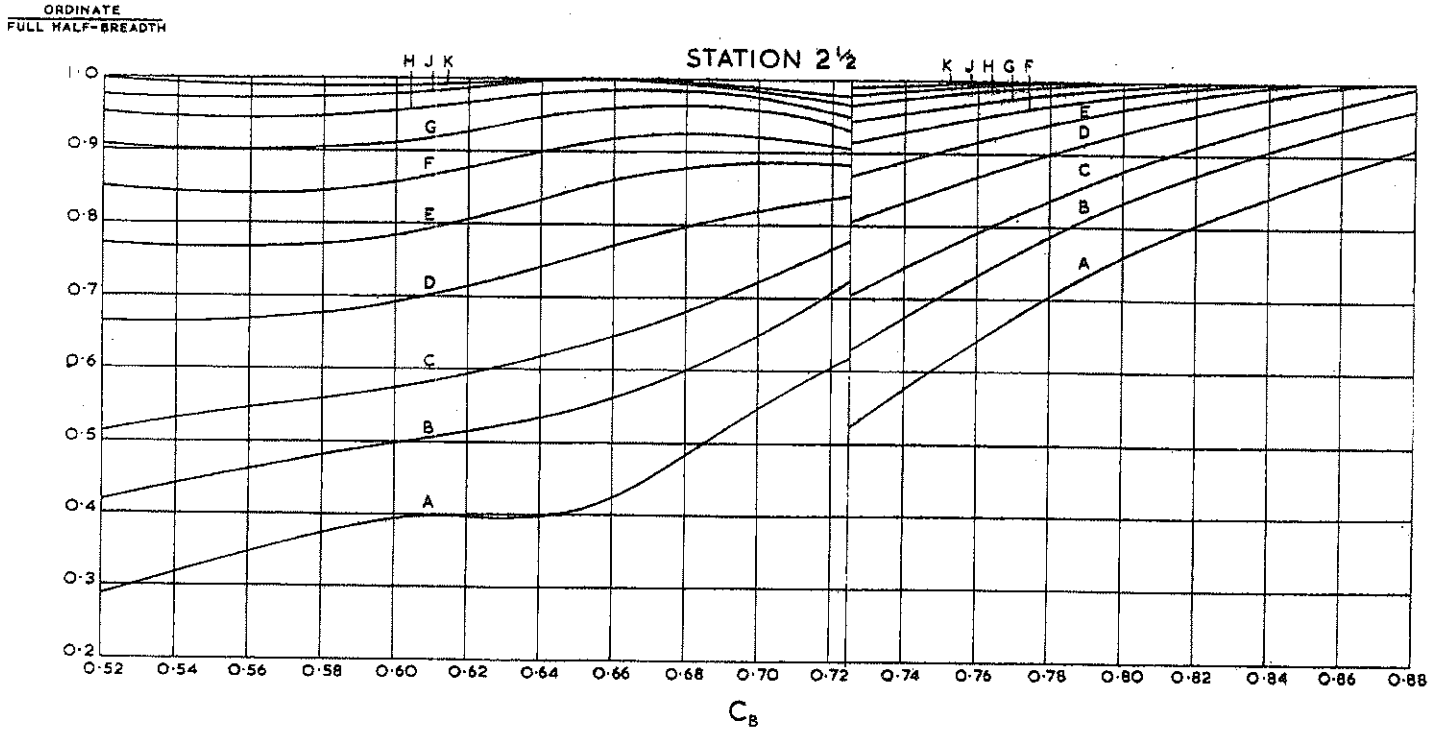

Fig. 39—Station 2½
Waterline Offsets Expressed as the Ratio of Waterline Ordinate/Full Half-Breadth.

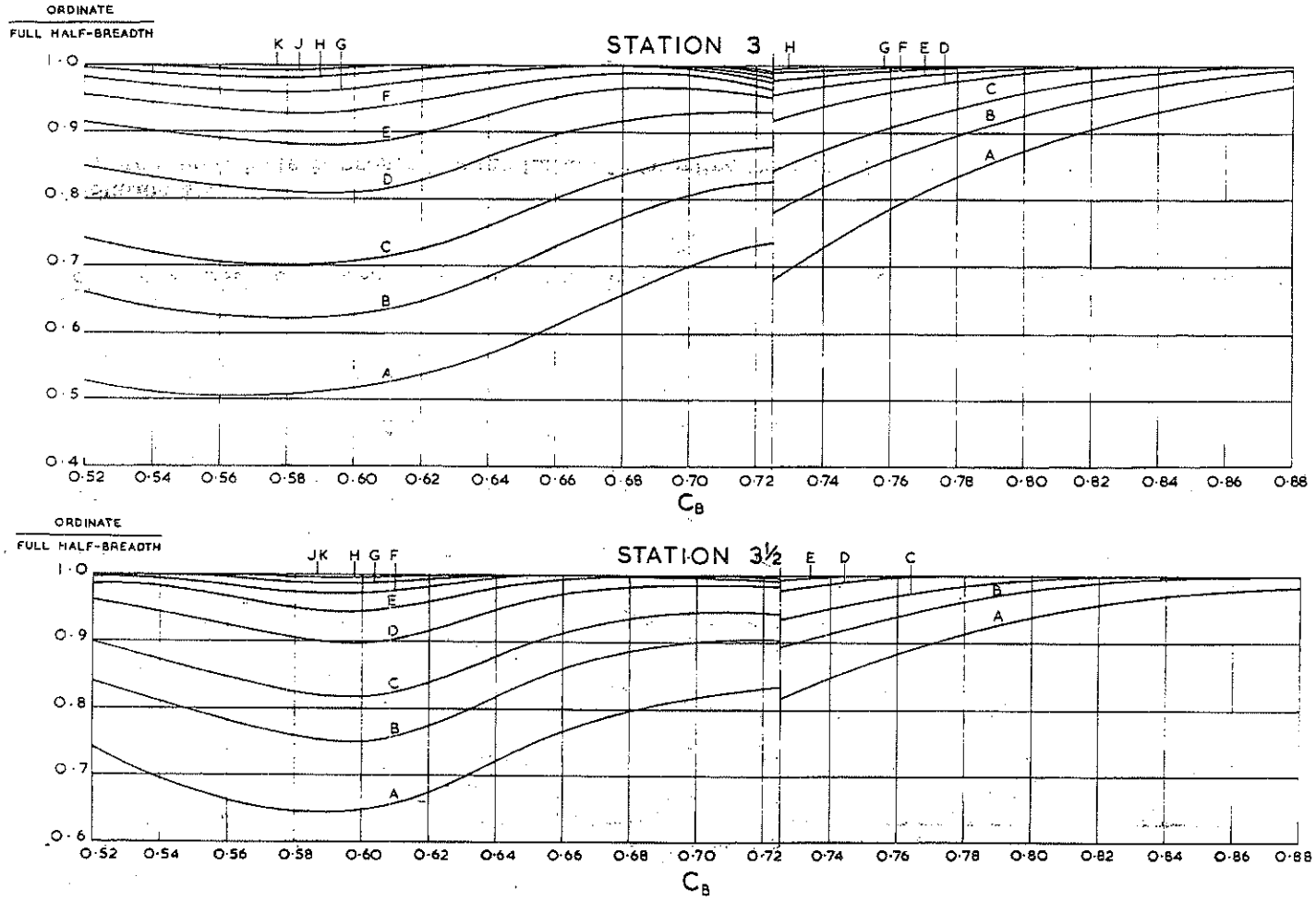

Fig. 40—Stations 3 and 3½.
Waterline Offsets Expressed as the Ratio of Waterline Ordinate/Full Half-Breadth.

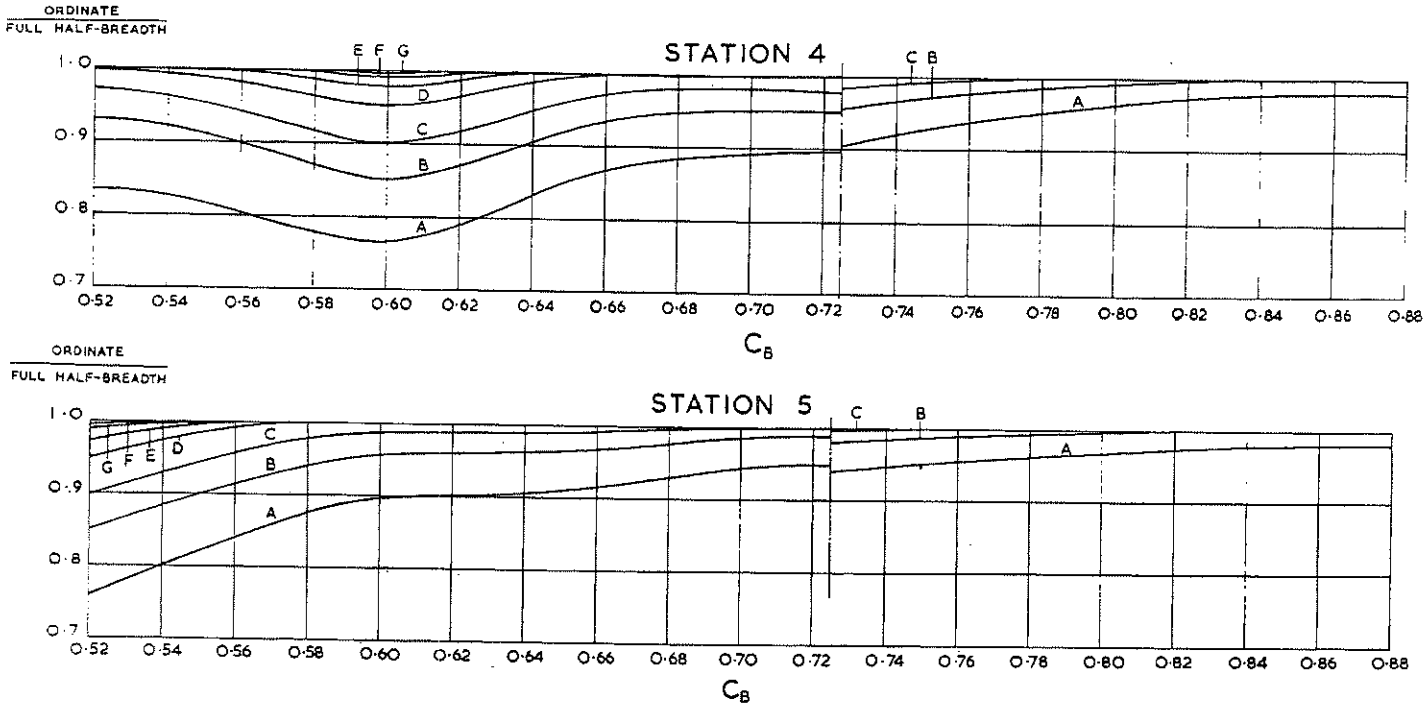

Fig. 41—Stations 4 and 5.
Waterline Offsets Expressed as the Ratio of Waterline Ordinate/Full Half-Breadth.

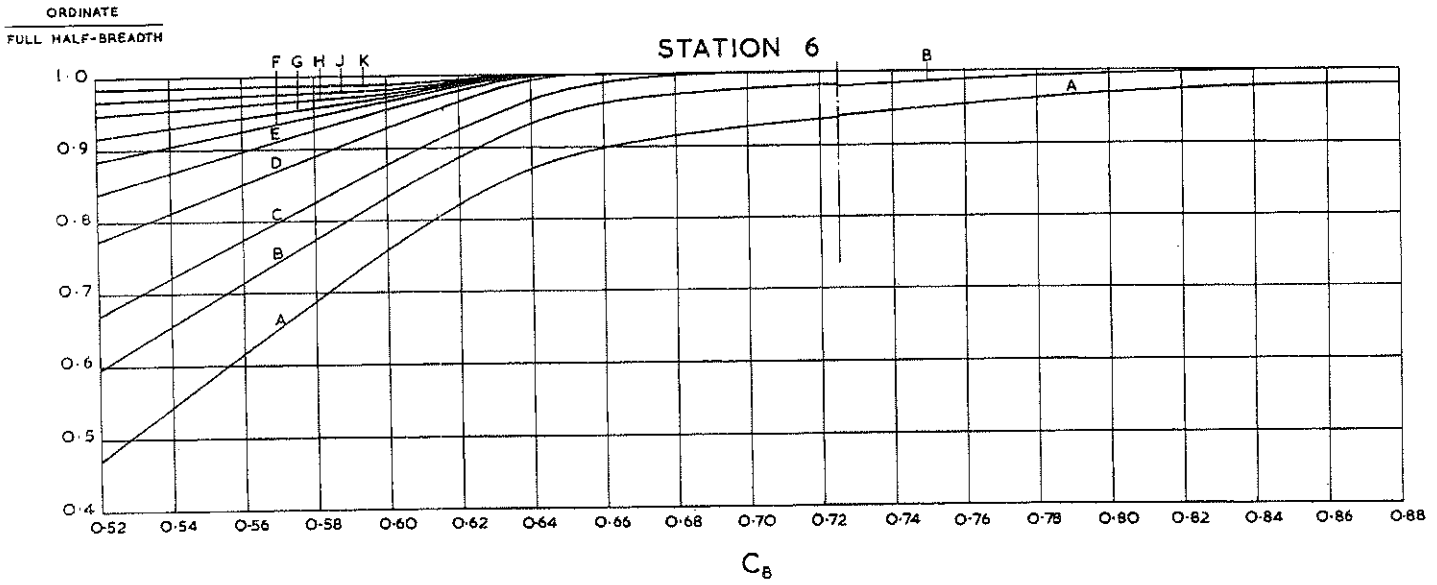

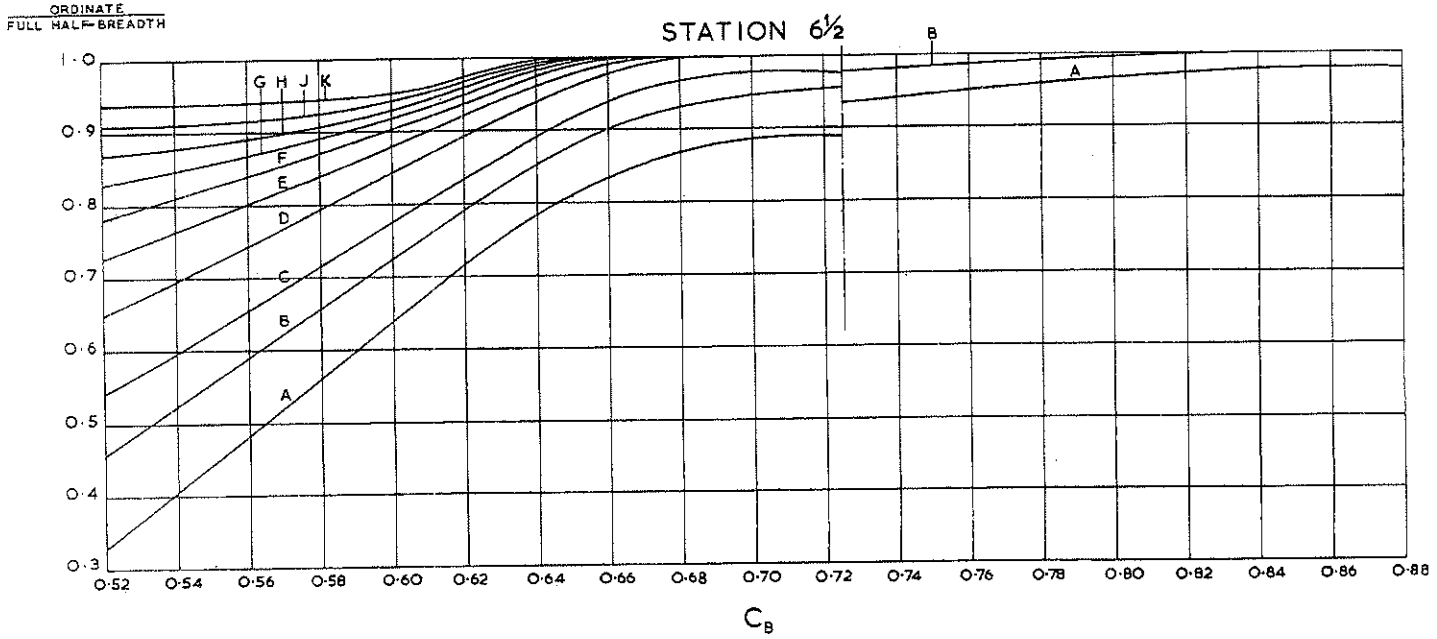

Fig. 42—Stations 6 and 6½.

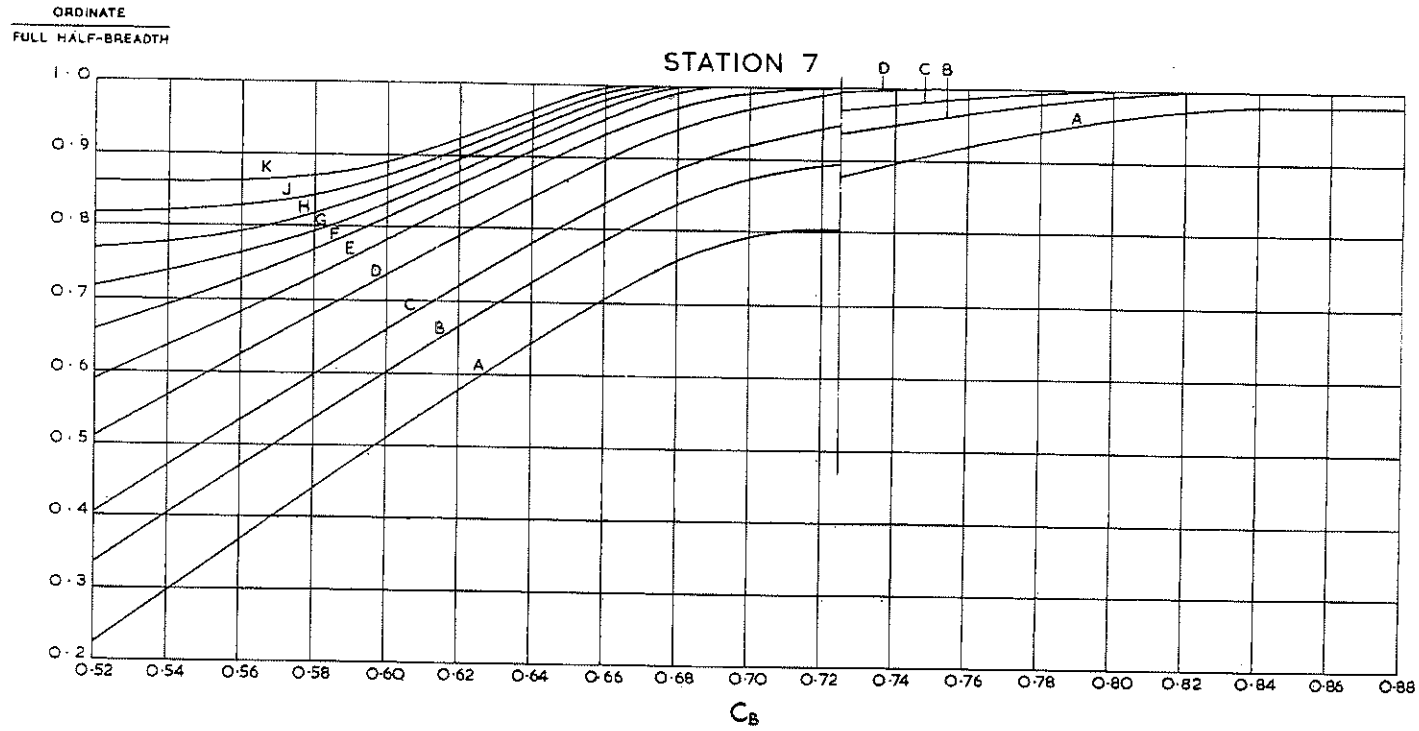

Fig. 43—Station 7.
Waterline Offsets Expressed as the Ratio of Waterline Ordinate/Full Half-Breadth.

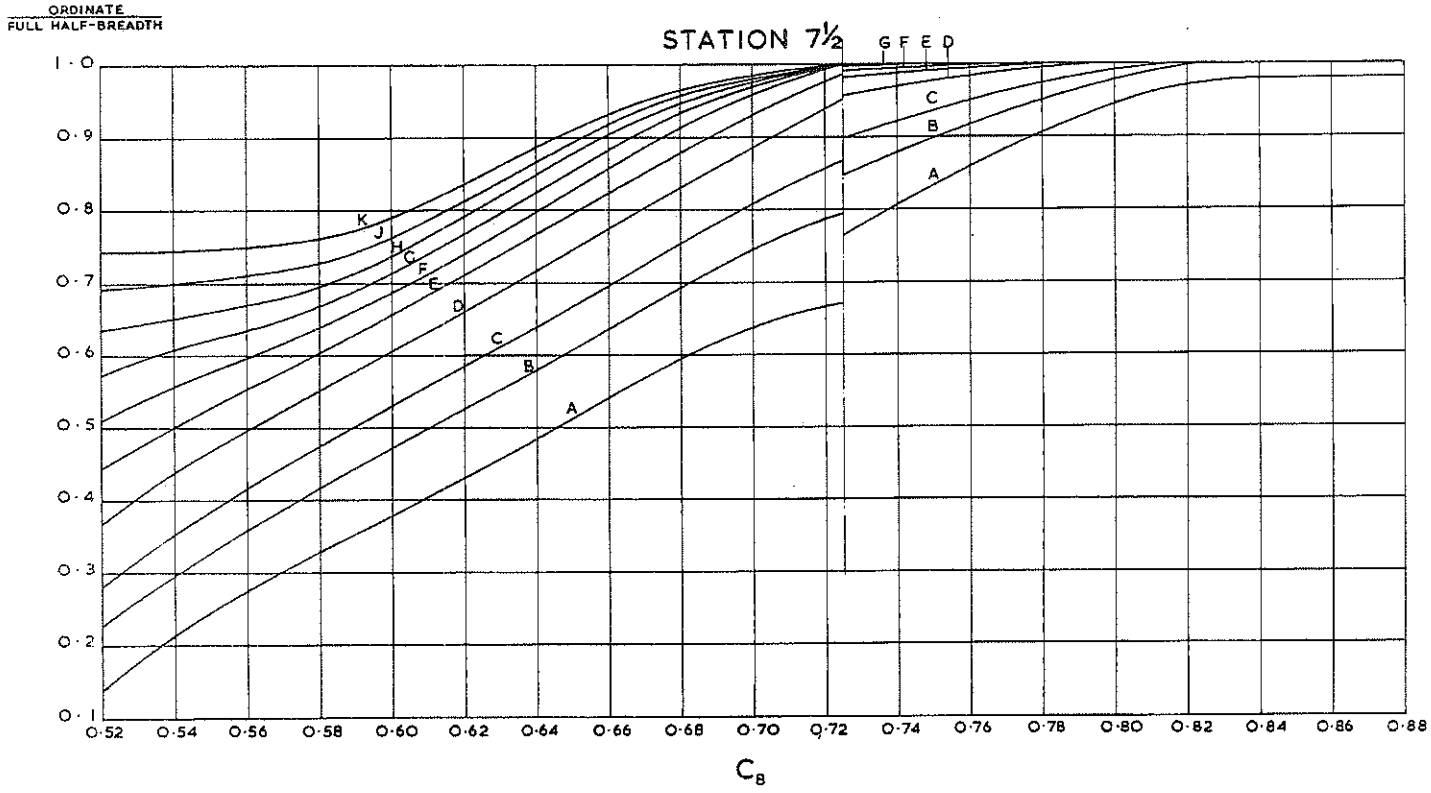

Fig. 44—Station 7½.
Waterline Offsets Expressed as the Ratio of Waterline Ordinate/Full Half-Breadth.

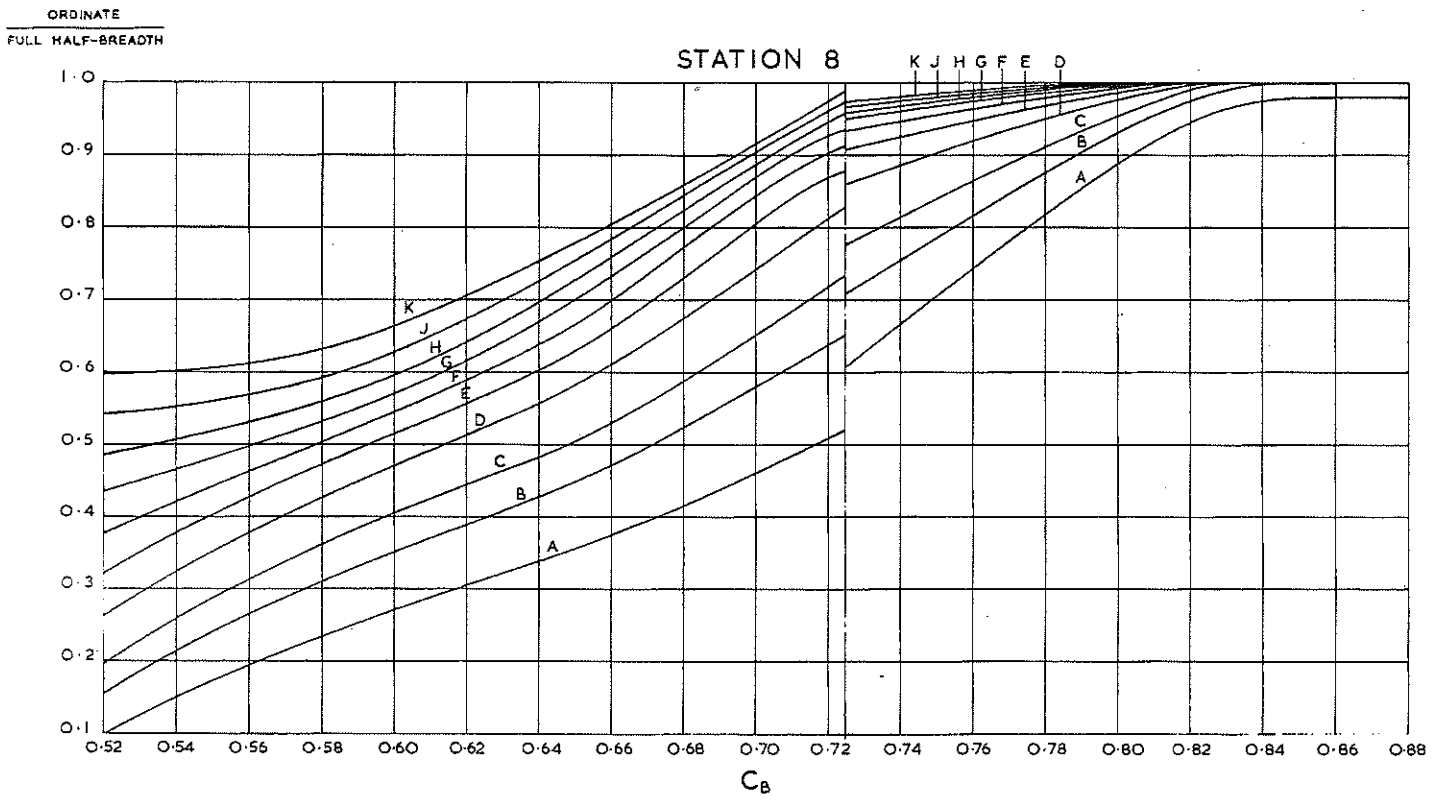

Fig. 45—Station 8.
Waterline Offsets Expressed as the Ratio of Waterline Ordinate/Full Half-Breadth.

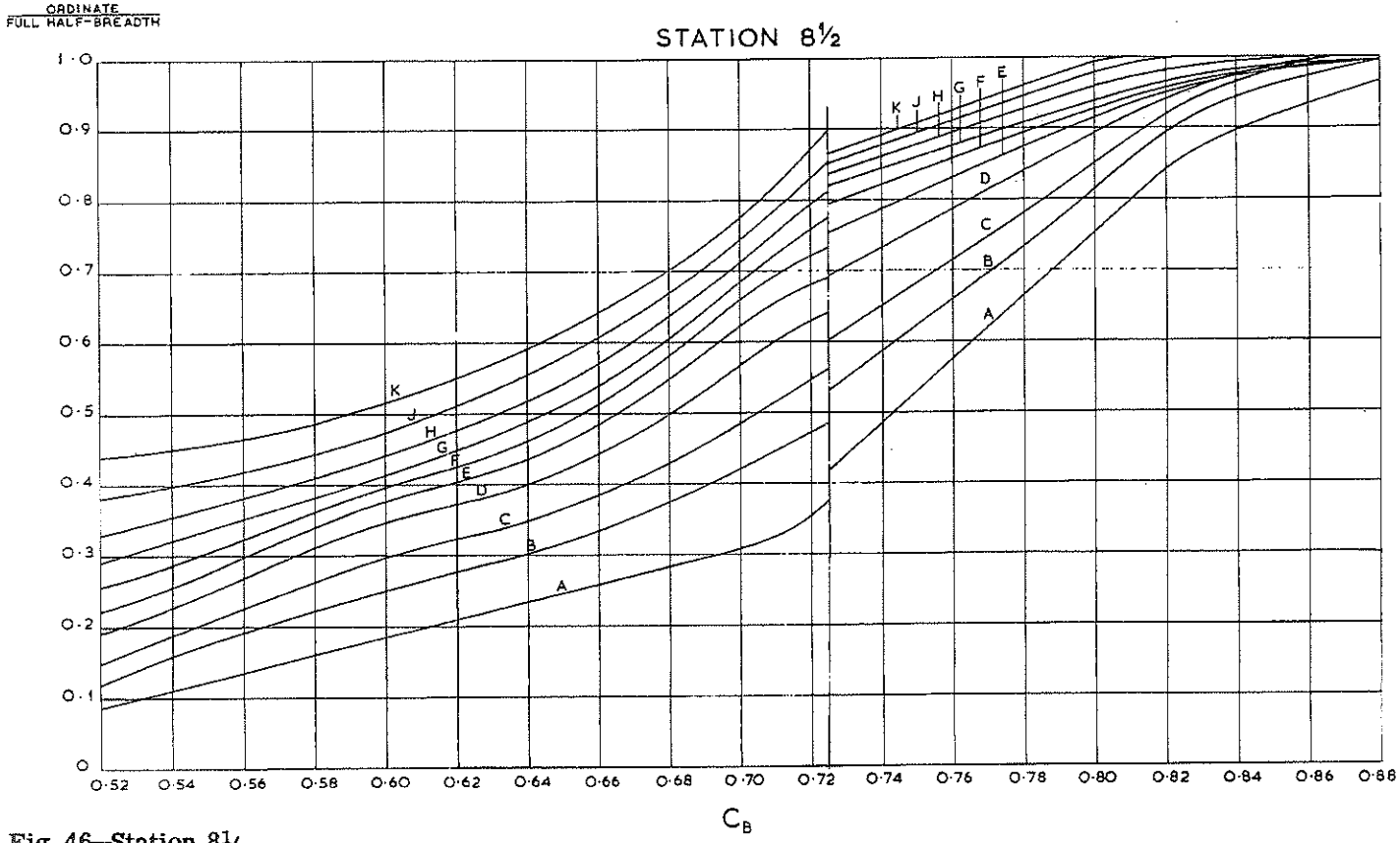

Fig. 46—Station 8½.
Waterline Offsets Expressed as the Ratio of Waterline Ordinate/Full Half-Breadth.

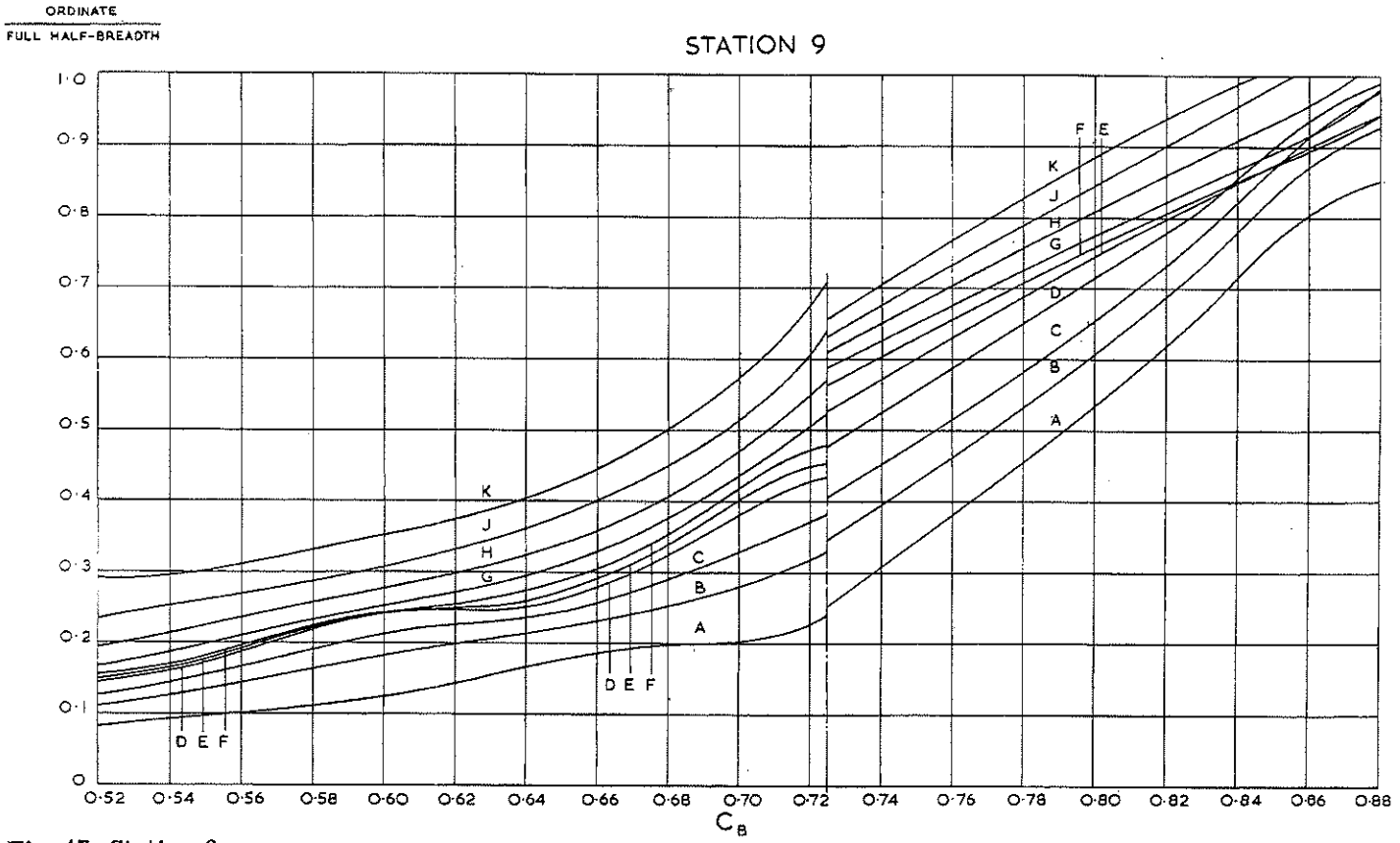

Fig. 47—Station 9.
Waterline Offsets Expressed as the Ratio of Waterline Ordinate/Full Half-Breadth.

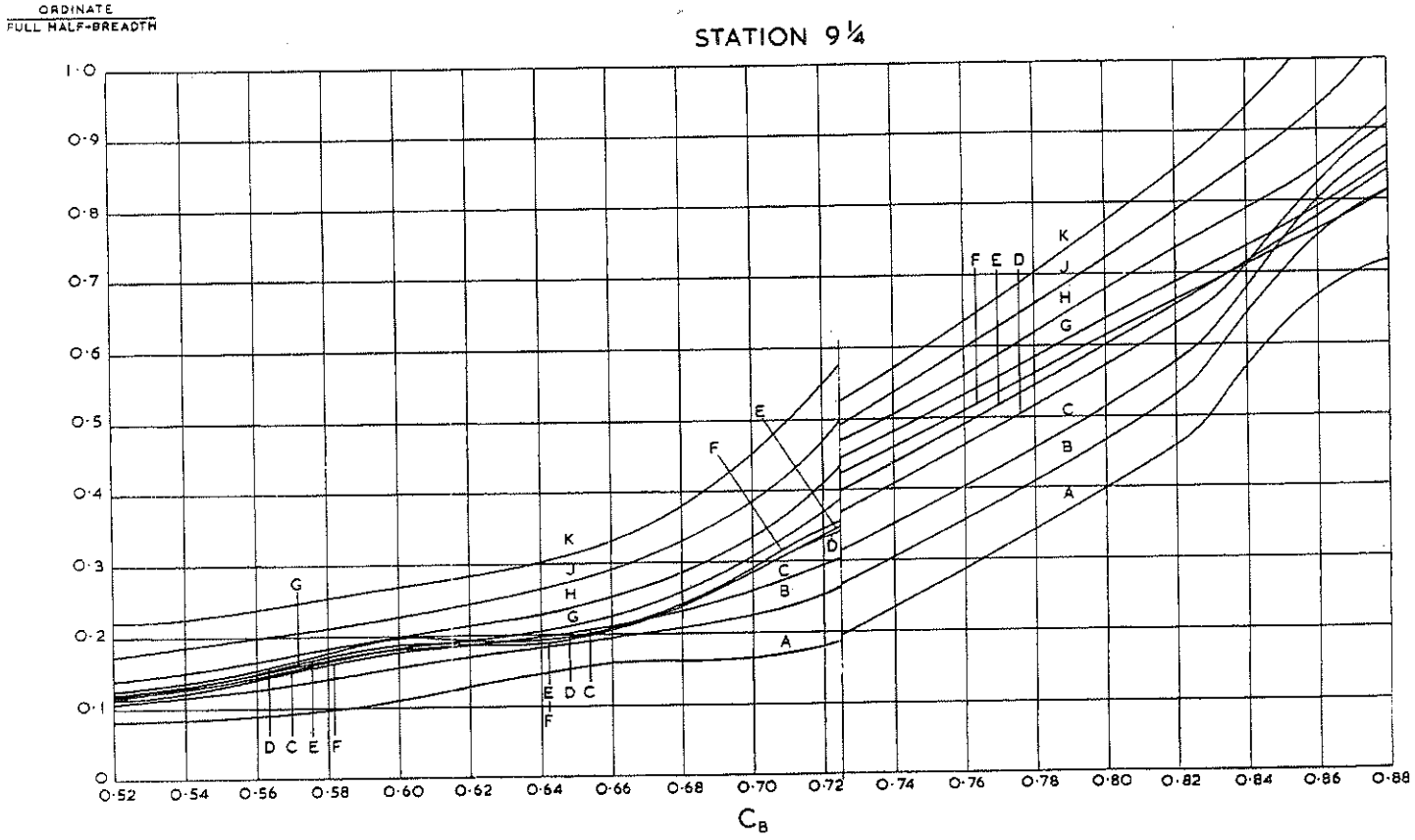

Fig. 48—Station 9¼.
Waterline Offsets Expressed as the Ratio of Waterline Ordinate/Full Half-Breadth.

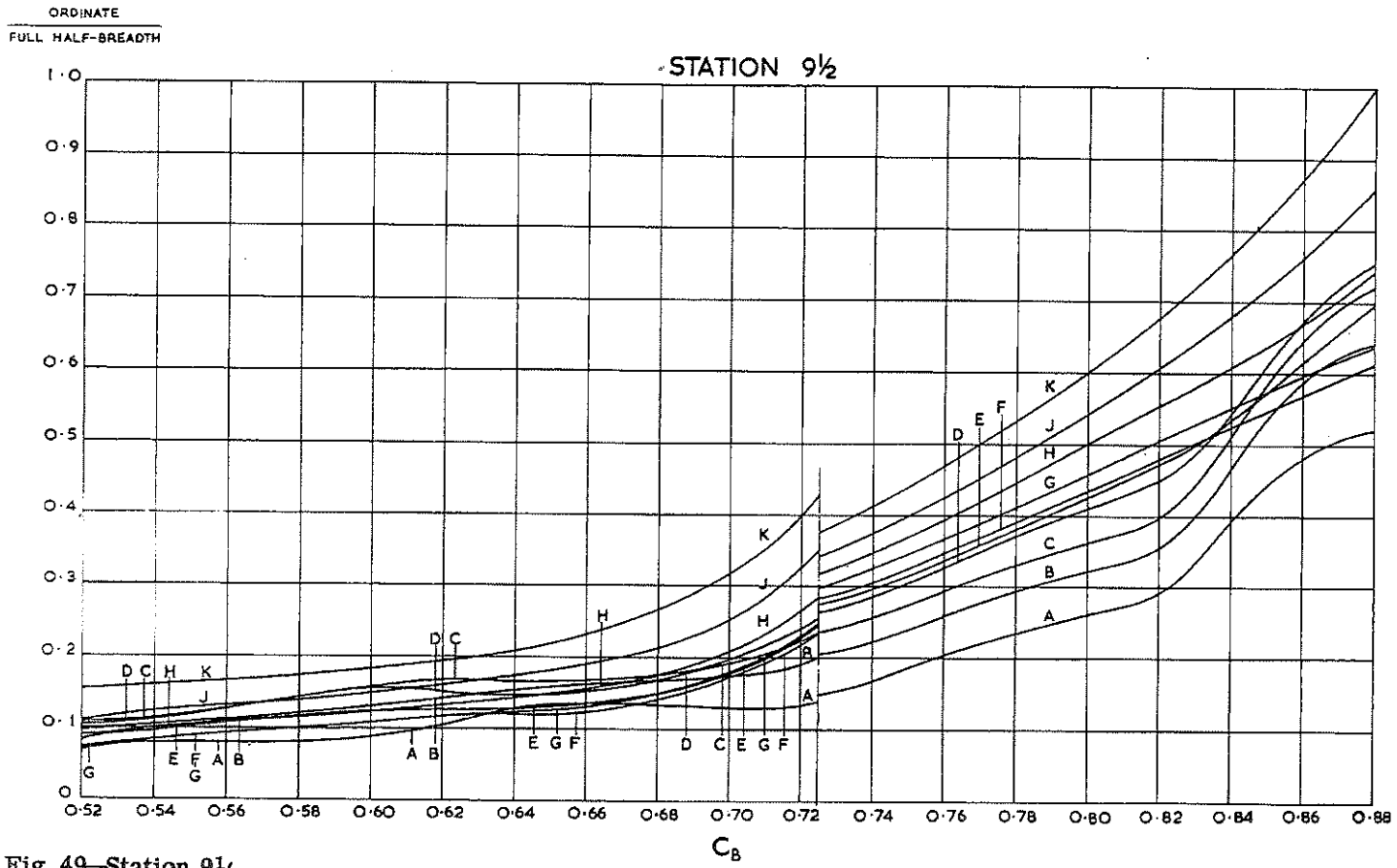

Fig. 49—Station 9½.
Waterline Offsets Expressed as the Ratio of Waterline Ordinate/Full Half-Breadth.

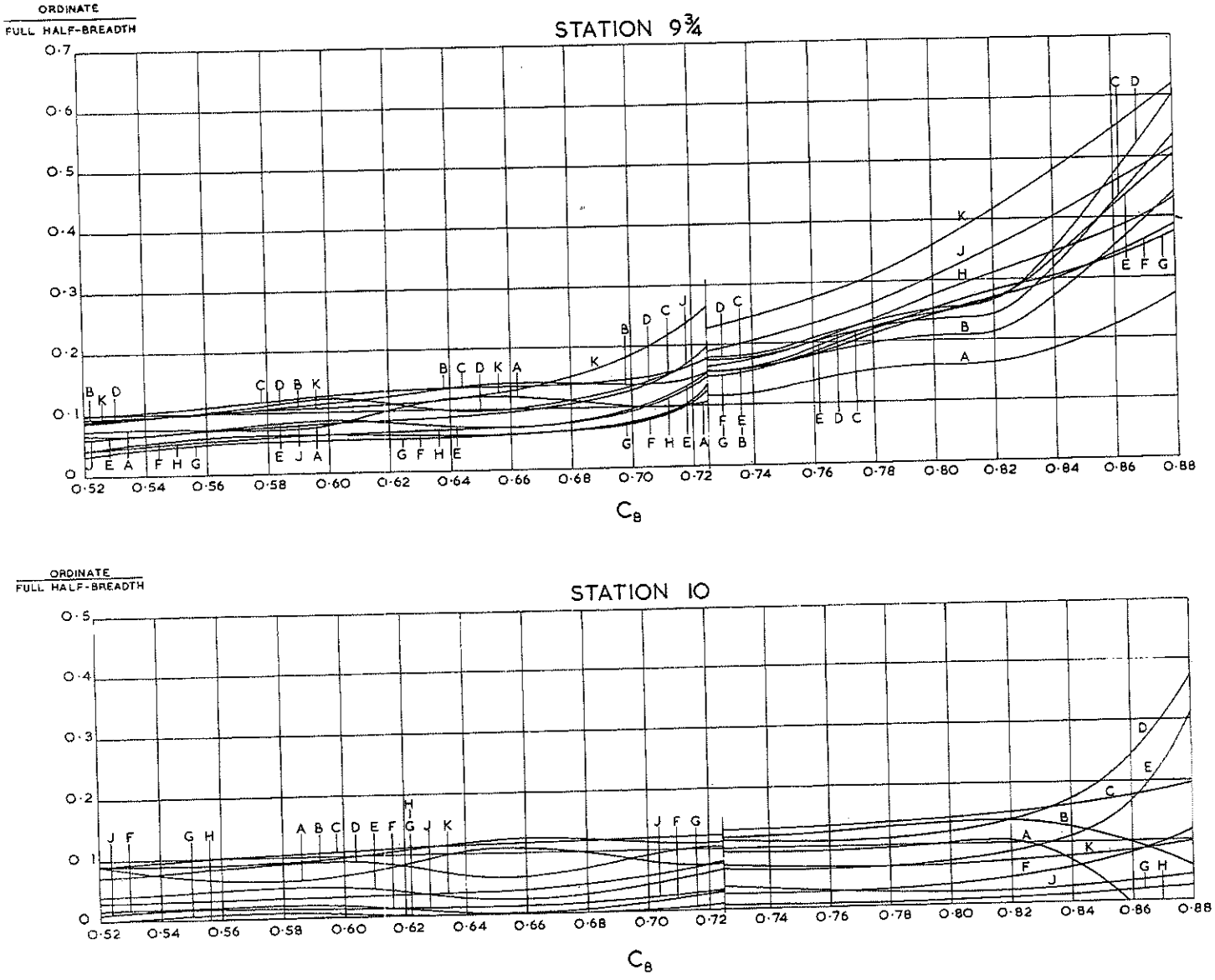

Fig. 50—Stations 9¾ and 10.
Waterline Offsets Expressed as the Ratio of Waterline Ordinate/Full Half-Breadth.

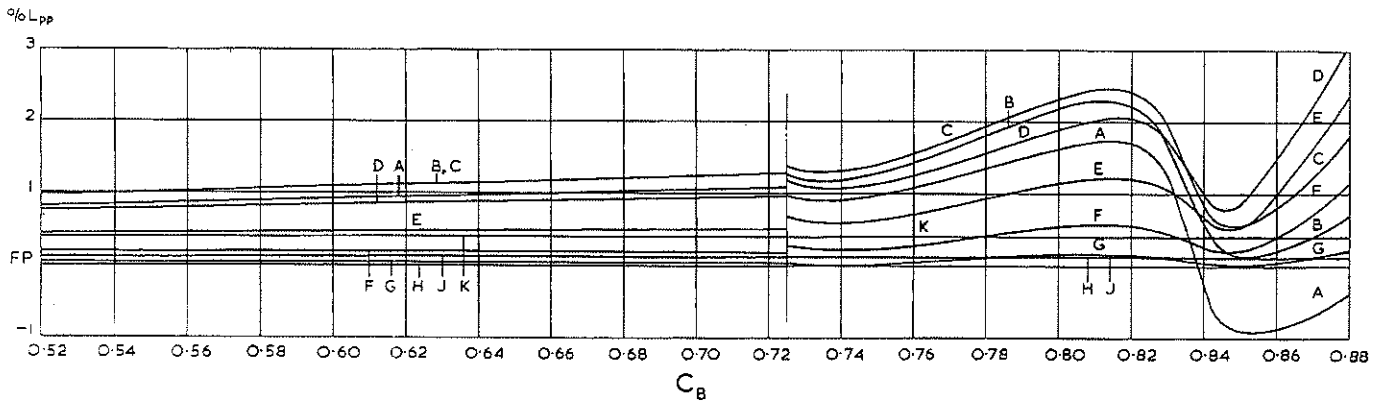

Fig. 51—Stem Profile Offsets.
Expressed as Percentage of L_{pp} Relative to Station 10.

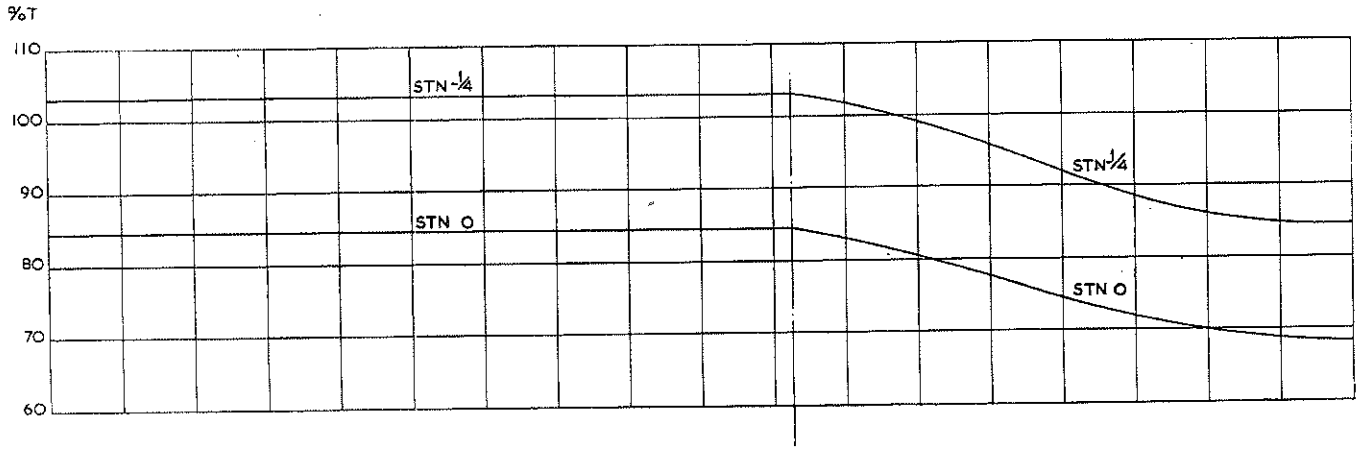

Waterline height above keel expressed as percentage of load draught.

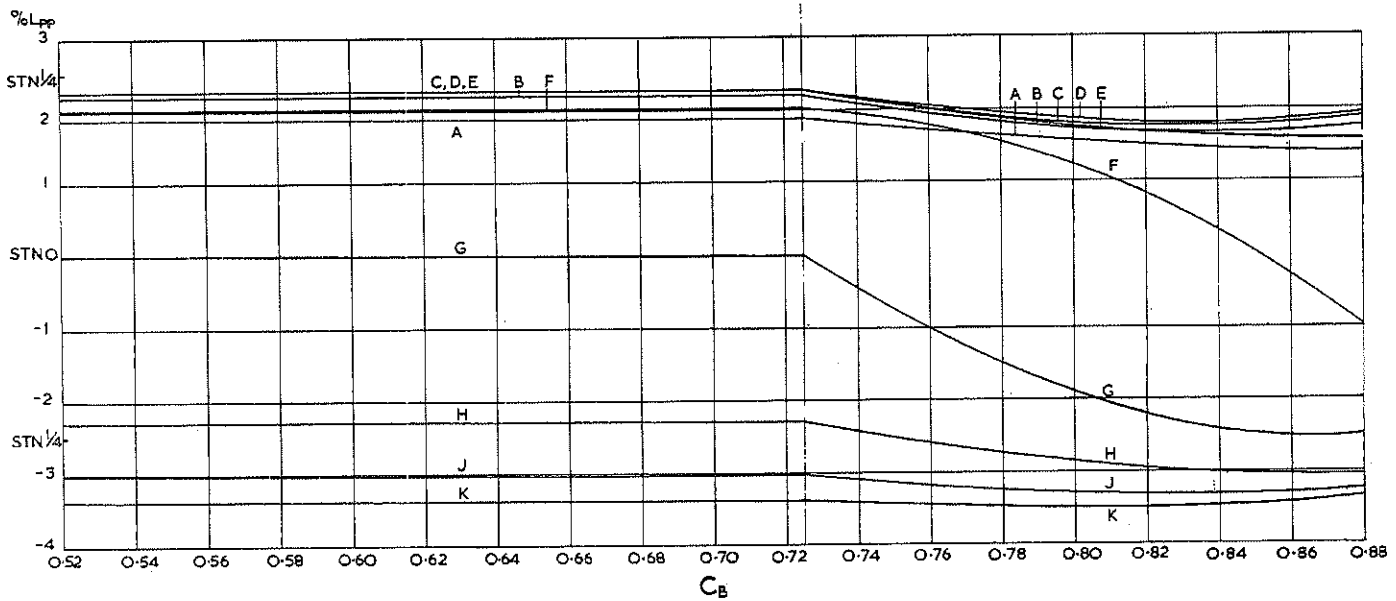

Ordinate expressed as percentage of L_{PP} relative to station O.

Fig. 52—Stern Profile Offsets.

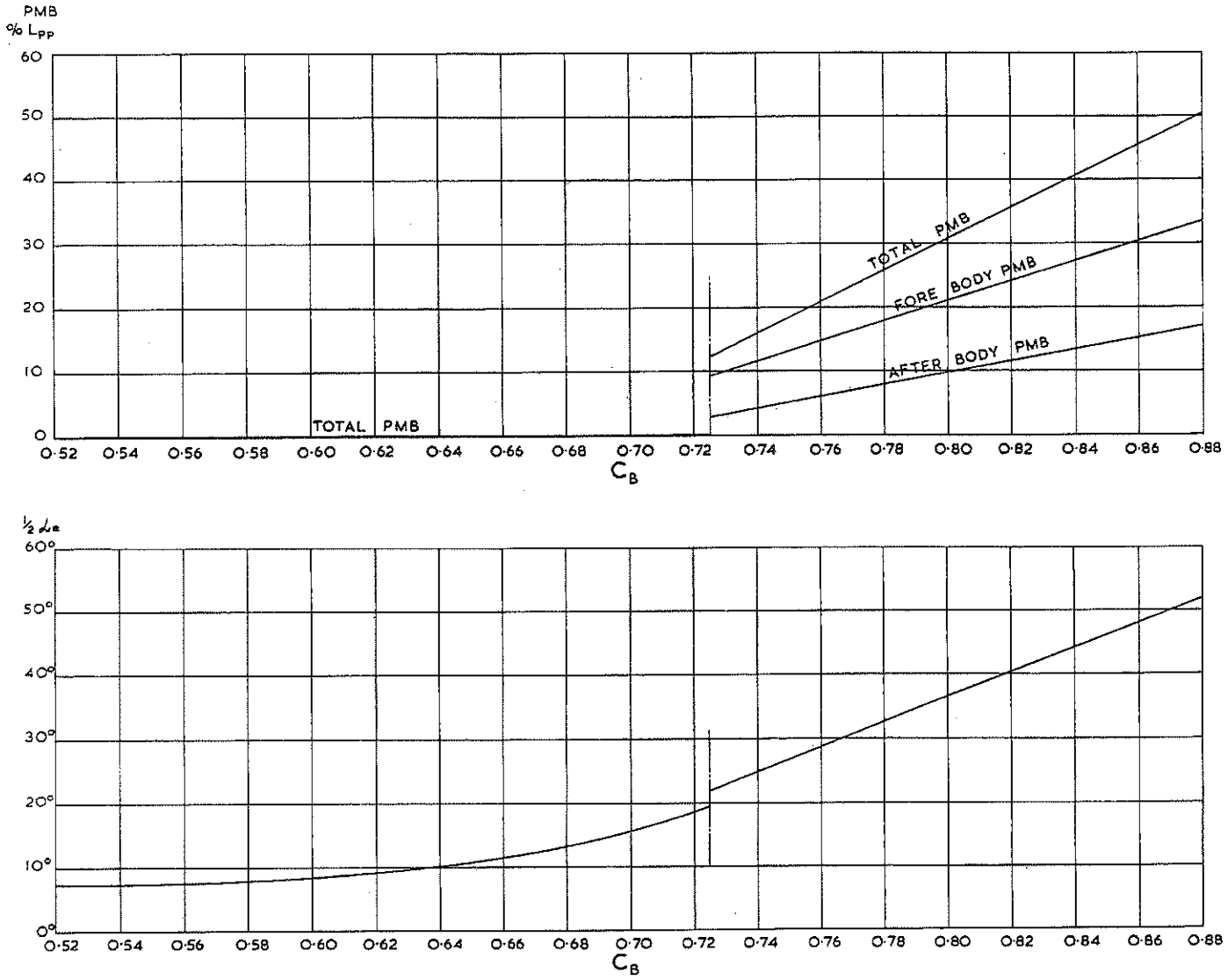

Fig. 53—Parallel Middle Body and Half Angle of Entrance.

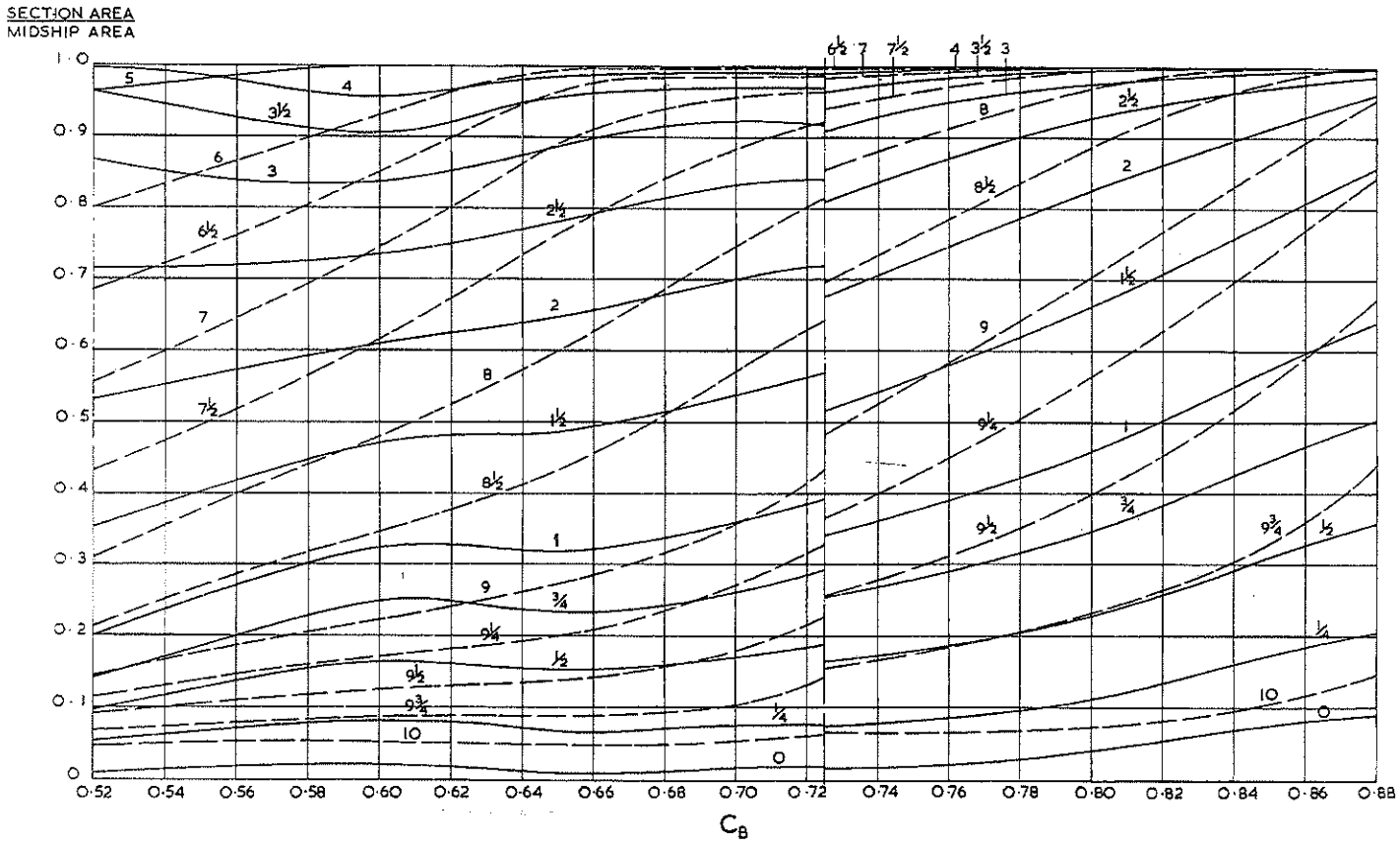

Fig. 54—Sectional Area Curve Ordinates for Load Draught. Expressed as the Ratio of Sectional Area/Midship Area.

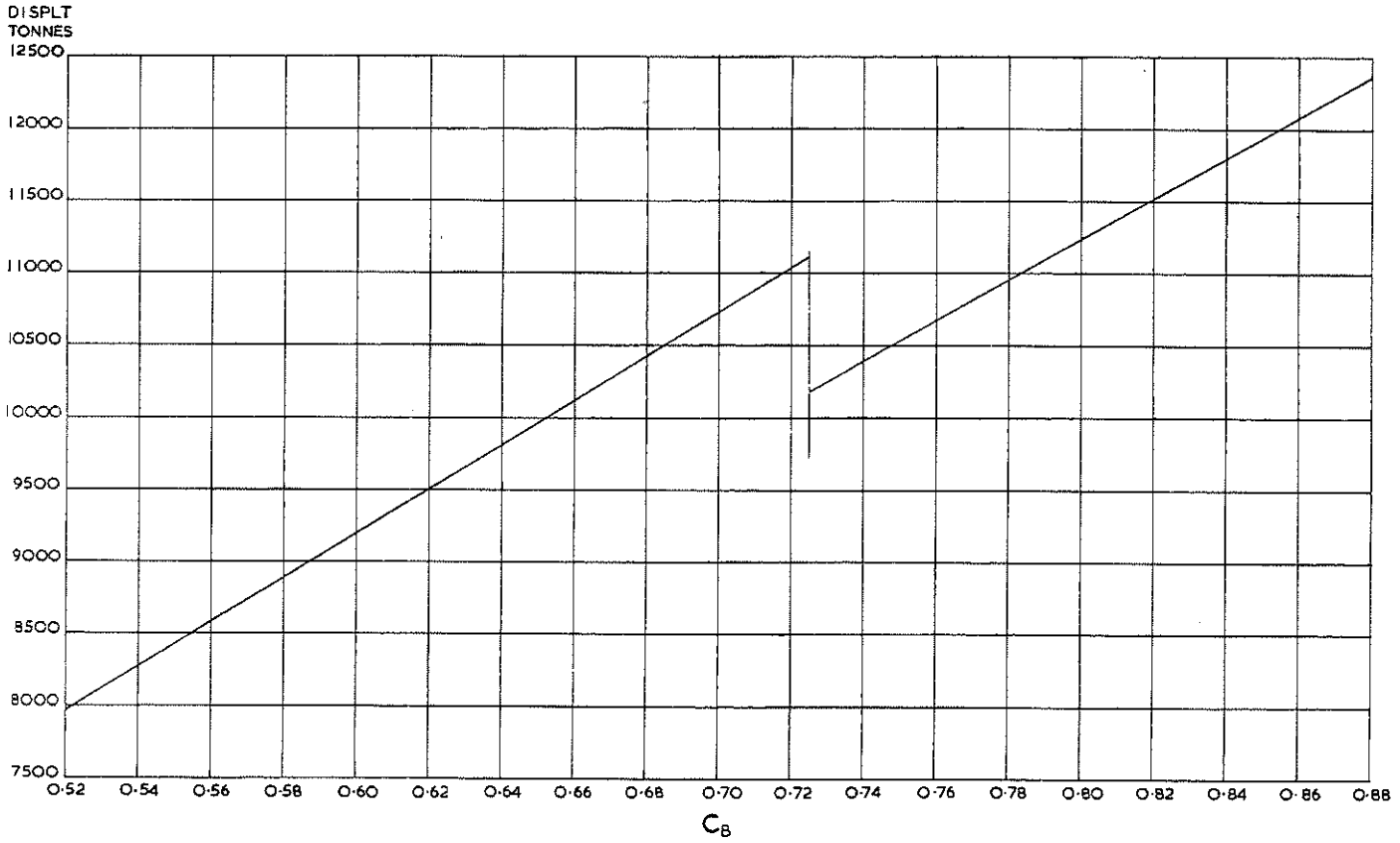

Fig. 55—Hydrostatic Particulars.
Displacement, Tonnes Salt Water.

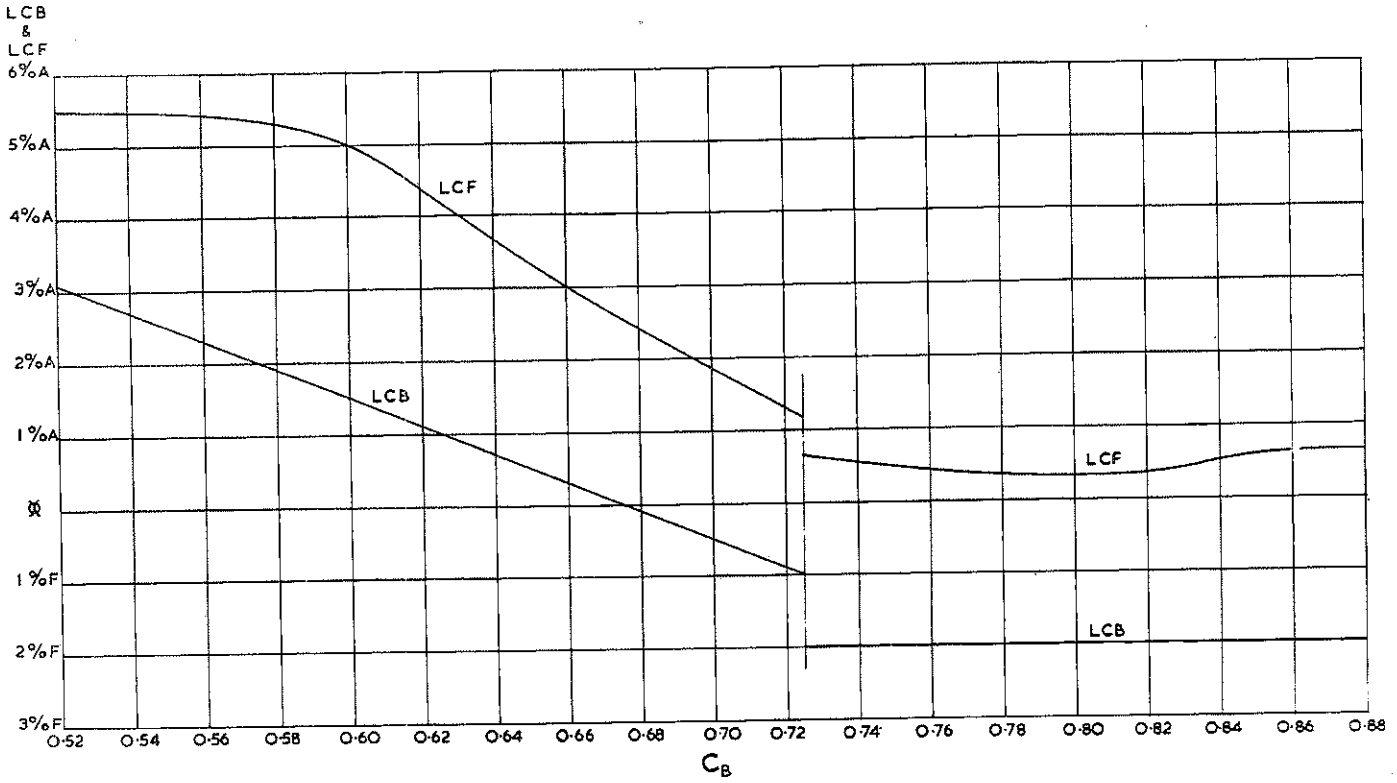

Fig. 56—Hydrostatic Particulars.
Longitudinal Centre of Buoyancy and Longitudinal Centre of Flotation Expressed as Percentage of L_{pp} Forward or Aft of Midships.

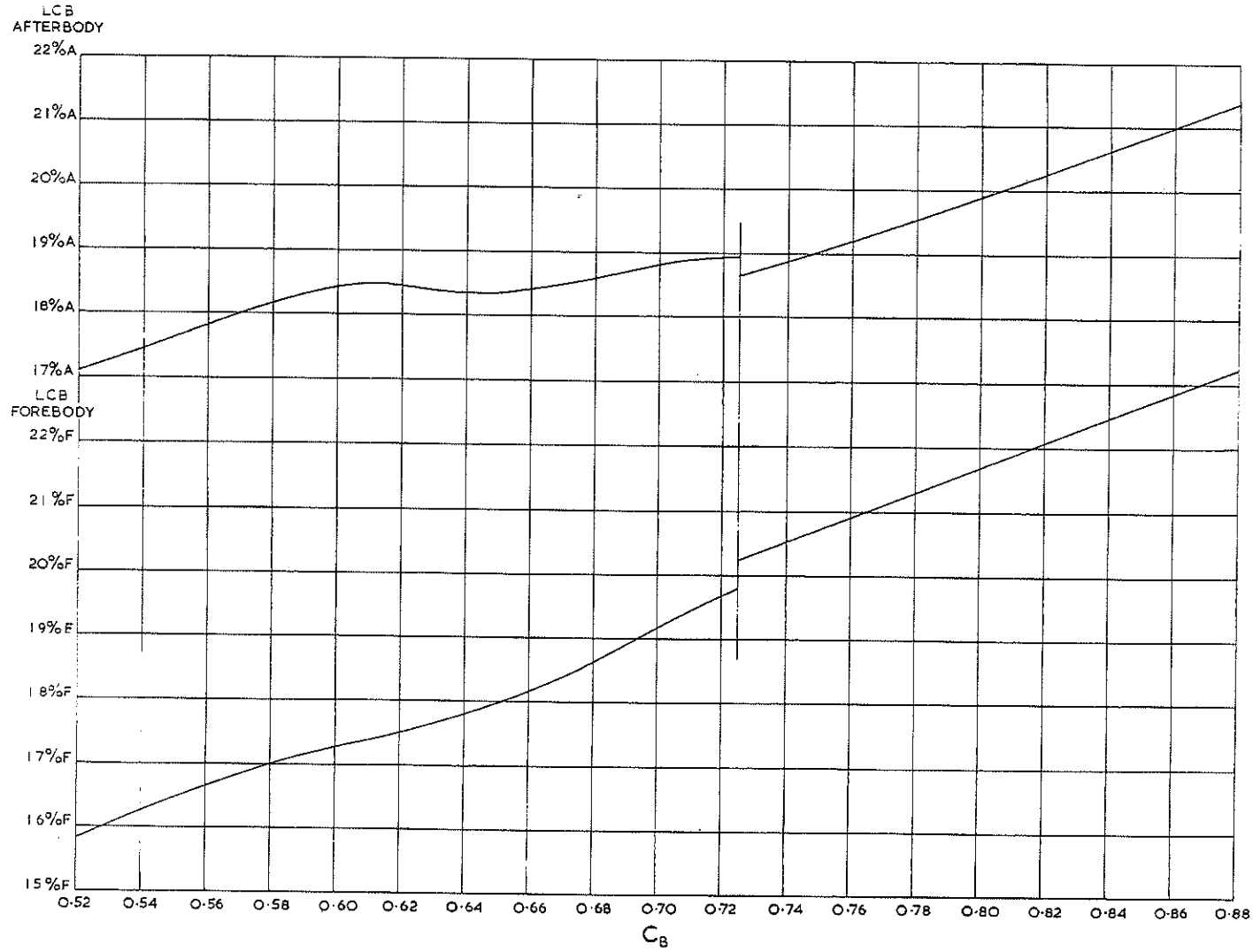

Fig. 57—Hydrostatic Particulars.
Longitudinal Centre of Buoyancy for Forward and After Bodies Expressed as Percentage of L_{pp} from Midships.

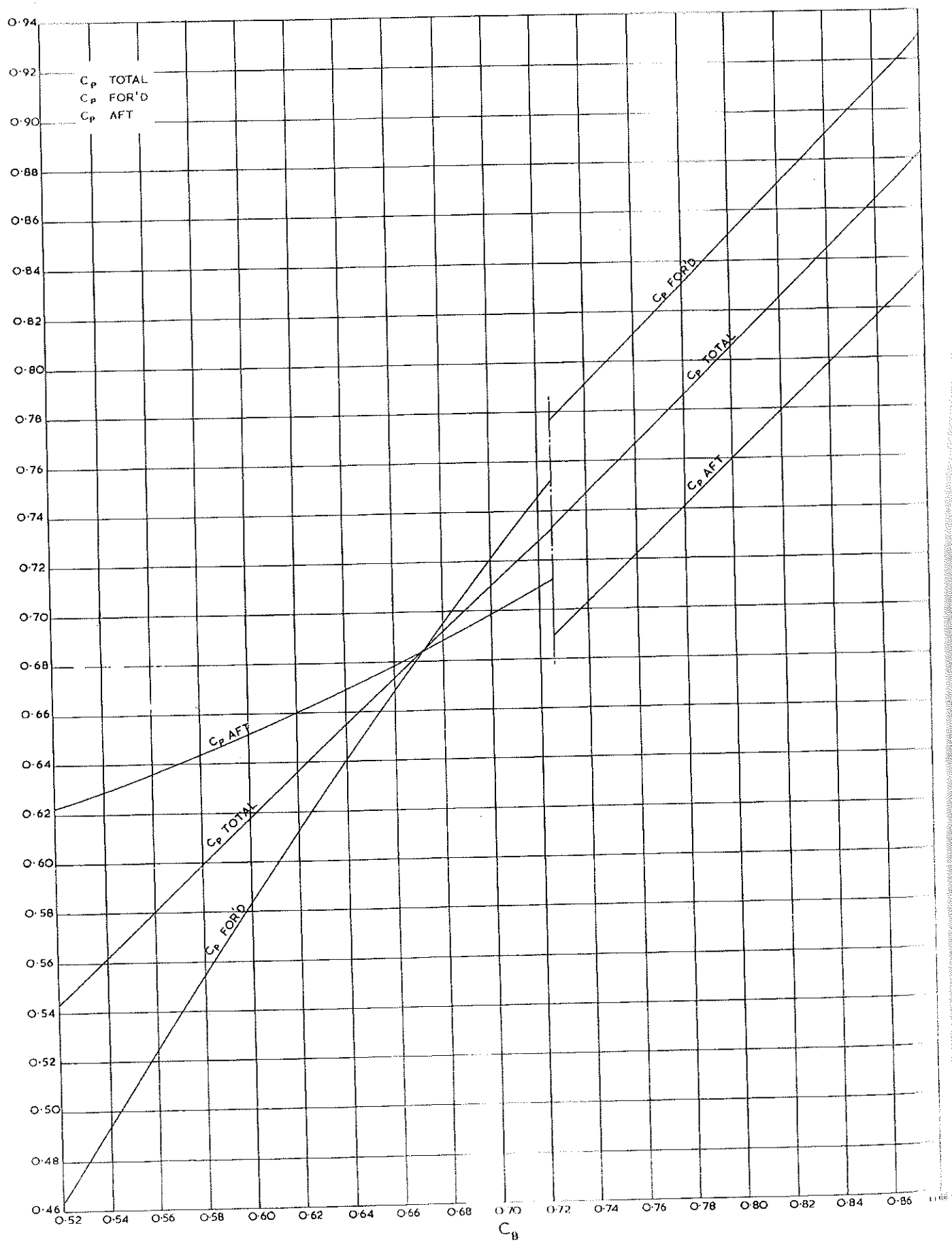

Fig. 58—Hydrostatic Particulars.
Prismatic Coefficient Total Based on L_{PP}, Fore Body and After Body Based on $\frac{1}{2}$ L_{PP}.

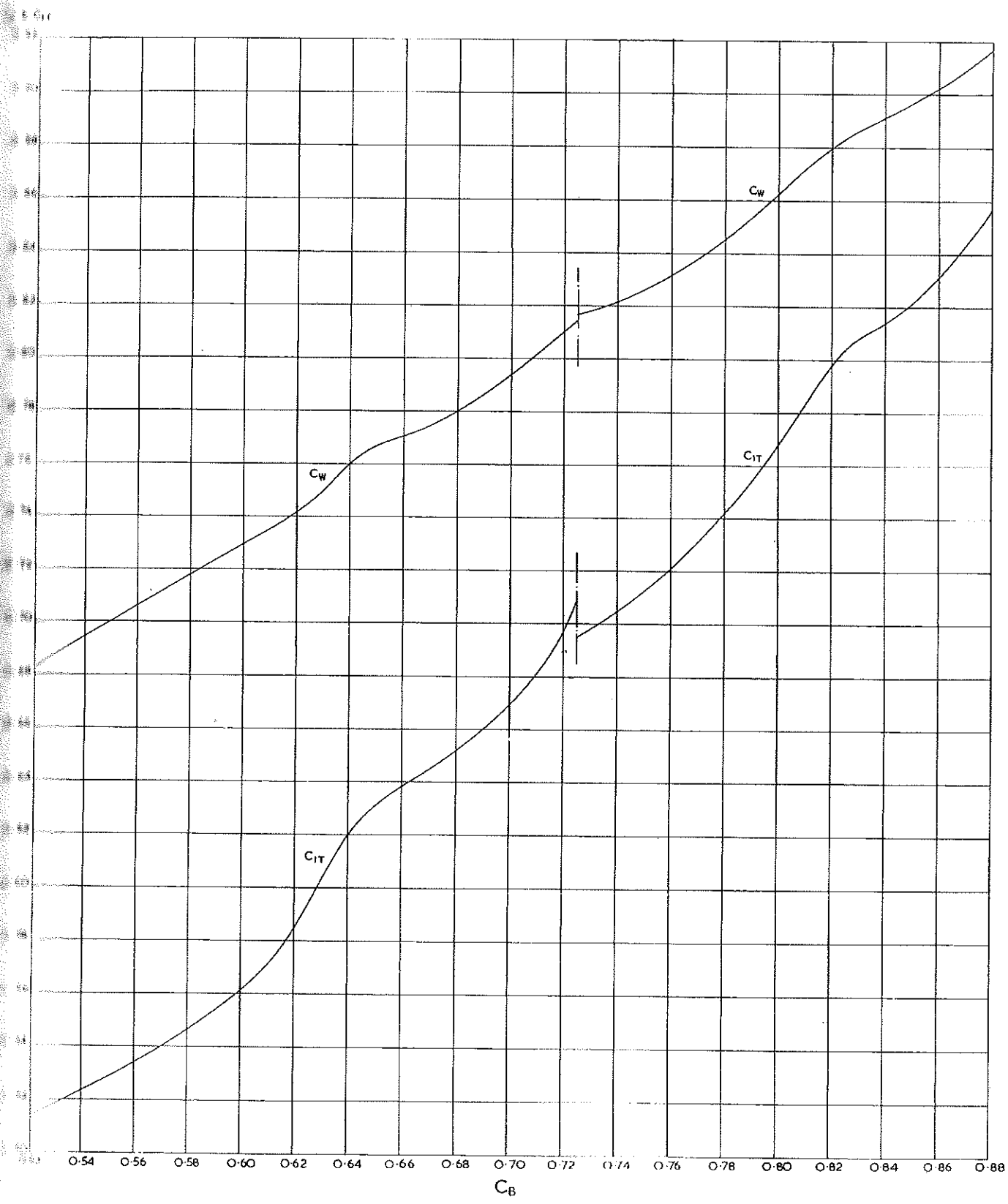

Hydrostatic Particulars.
Waterplane Area and Transverse Inertia Coefficients Based on Wetted Length.

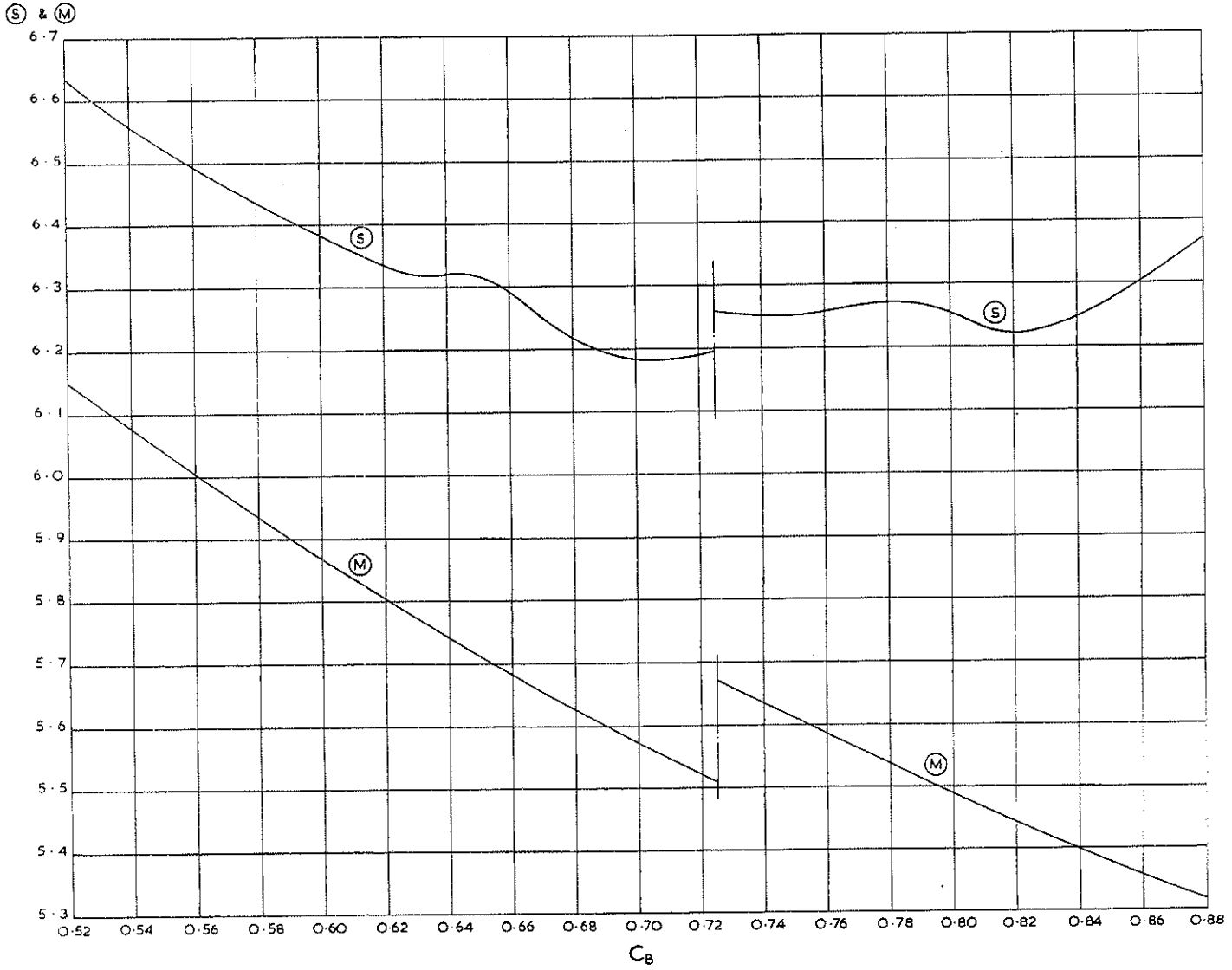

Fig. 60—Hydrostatic Particulars.
Wetted Surface Coefficient Ⓢ and Length-Displacement Ratio Ⓜ.

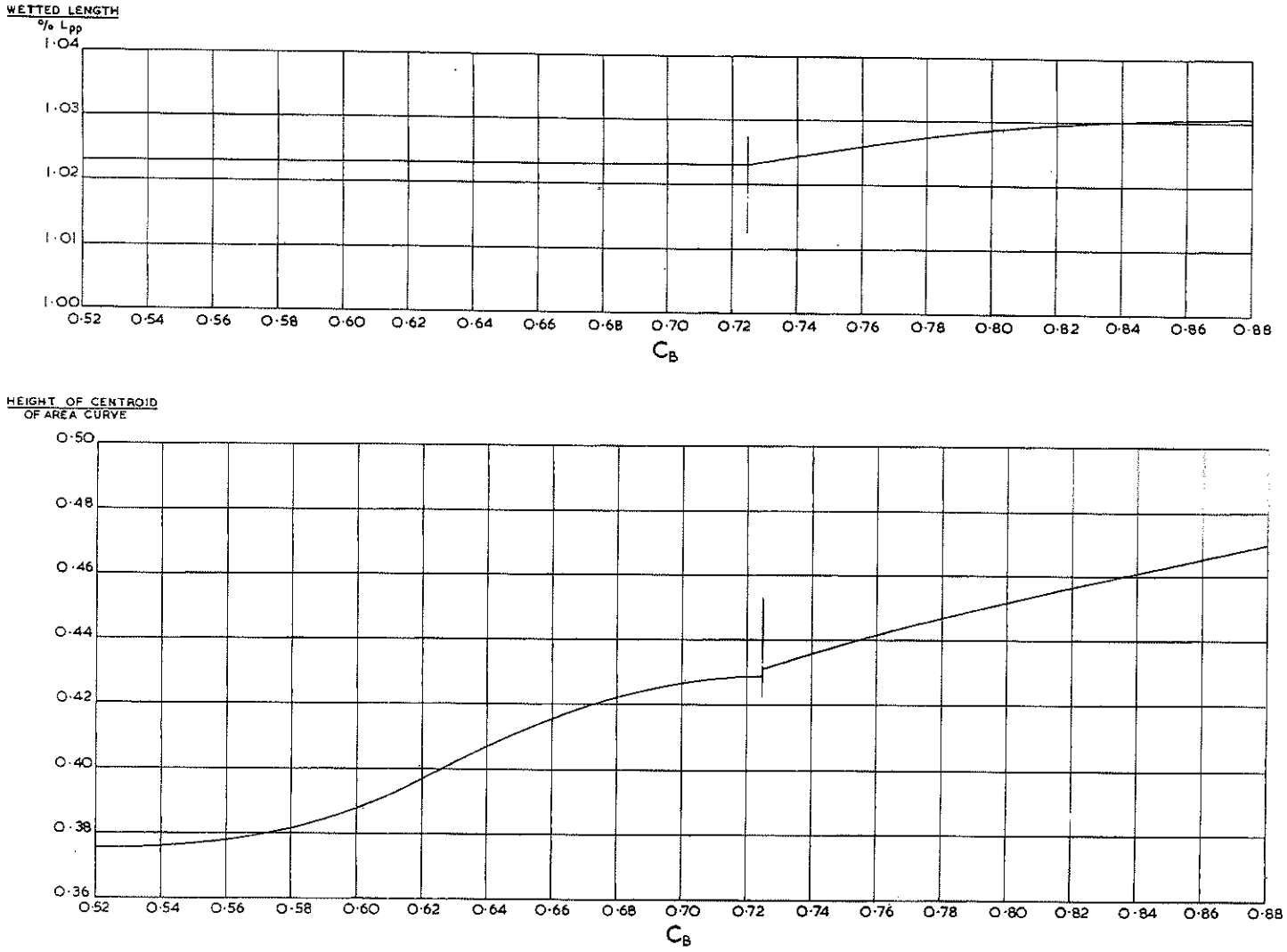

Fig. 61—Hydrostatic Particulars.
Wetted Length and Height of Centroid of Sectional Area Curve.

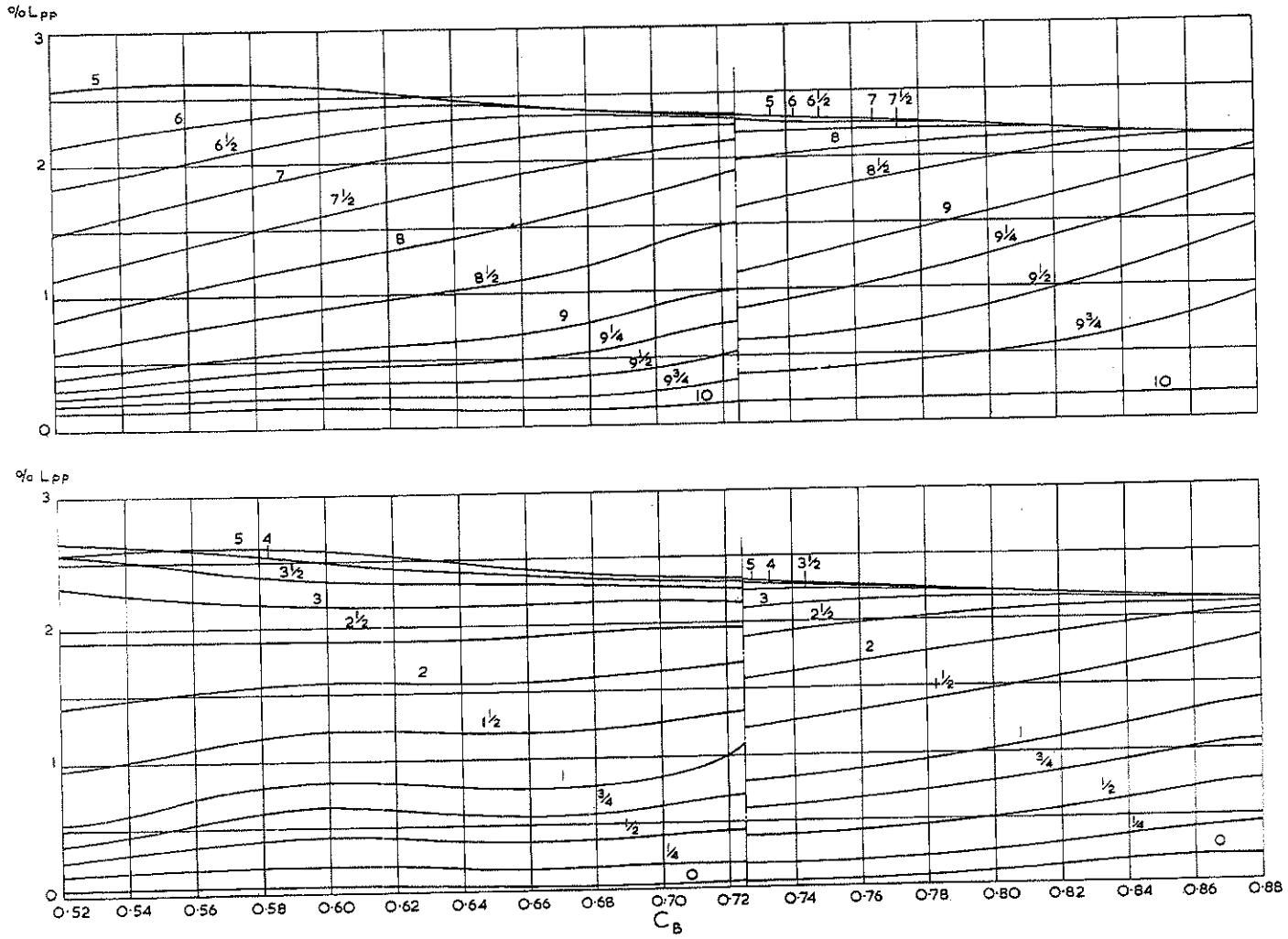

Fig. 62—Shift of Station For One Per Cent L_{pp} Movement of Longitudinal Centre of Buoyancy.

Resistance Data
for
Normal and Bulbous Bows

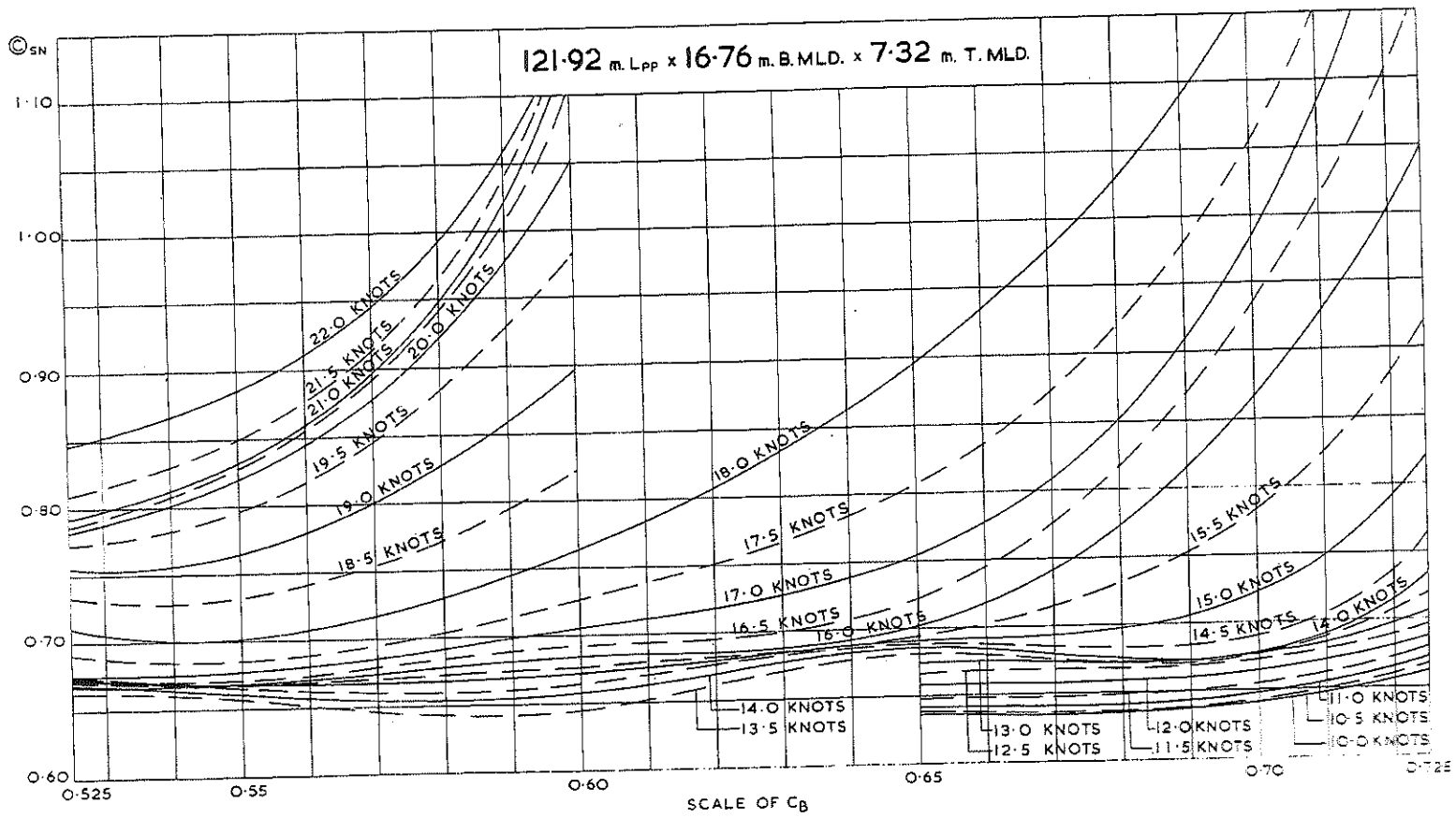

Fig. 63(a)—Cross Curves of Resistance Data for B.S.R.A. Methodical Series Forms: Normal Bows.

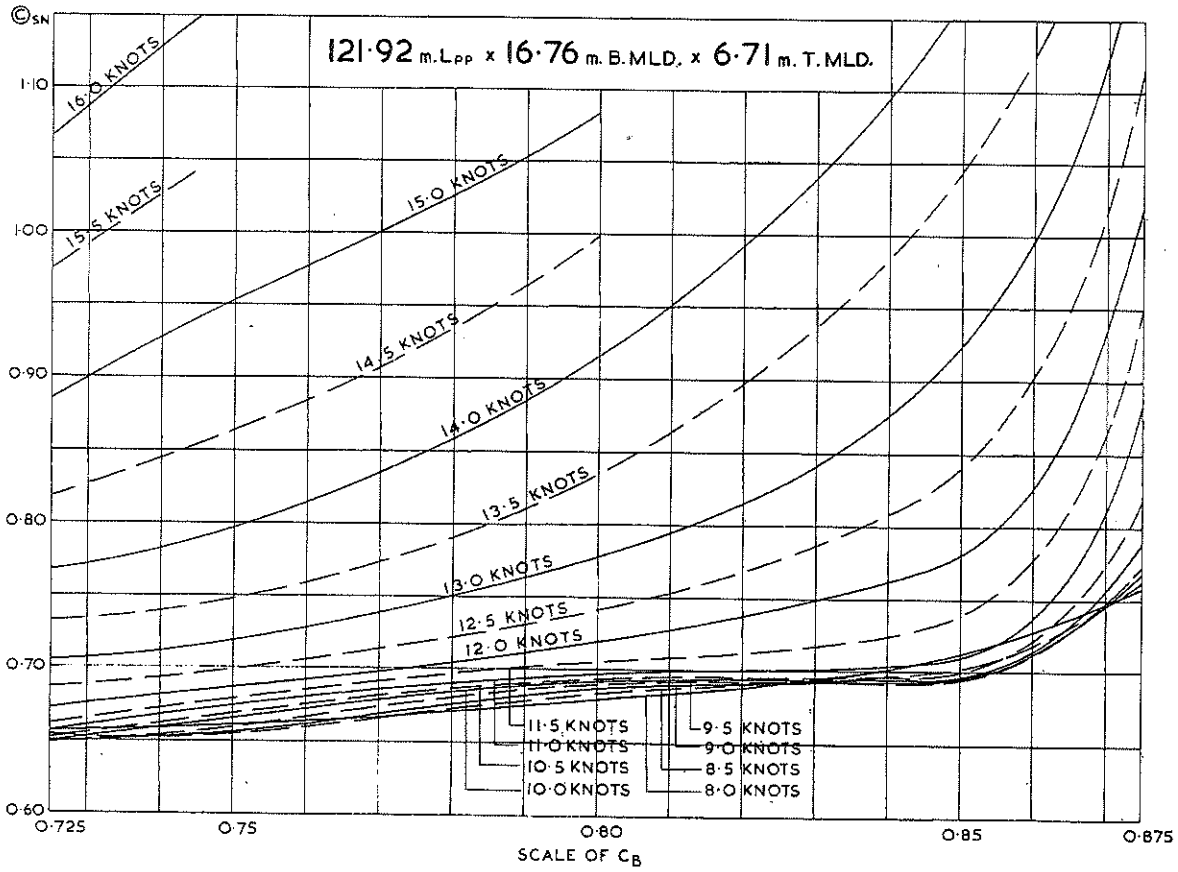

Fig. 63(b)—Cross Curves of Resistance Data for B.S.R.A. Methodical Series Forms: Normal Bows.

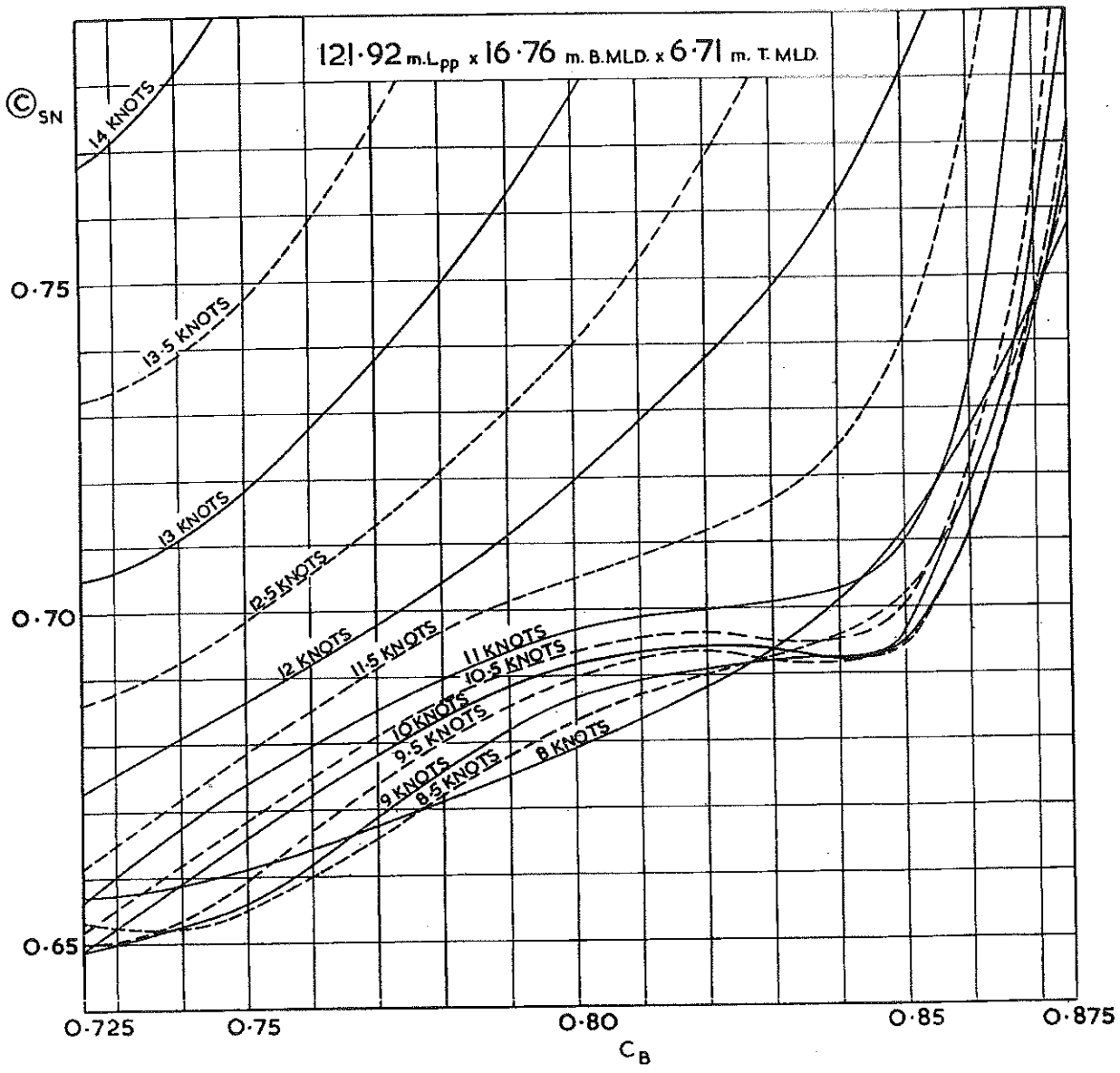

Fig. 63(c)—Cross Curves of Resistance Data for B.S.R.A. Methodical Series Forms: Normal Bows.
(Part enlargement of curves shown in Fig. 63(b))

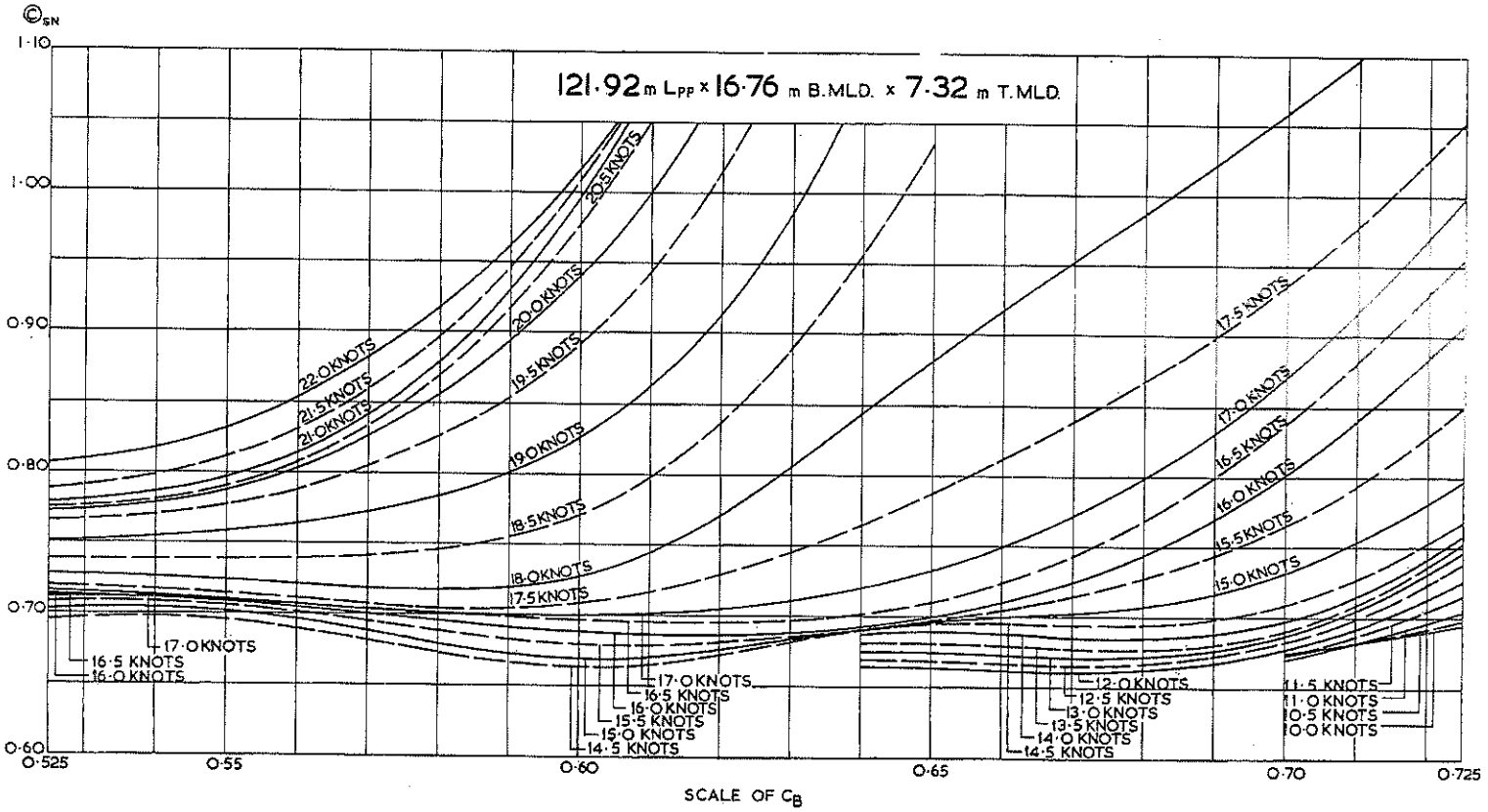

Fig. 64(a)—Cross Curves of Resistance Data for B.S.R.A. Methodical Series Forms: Bulbous Bows.

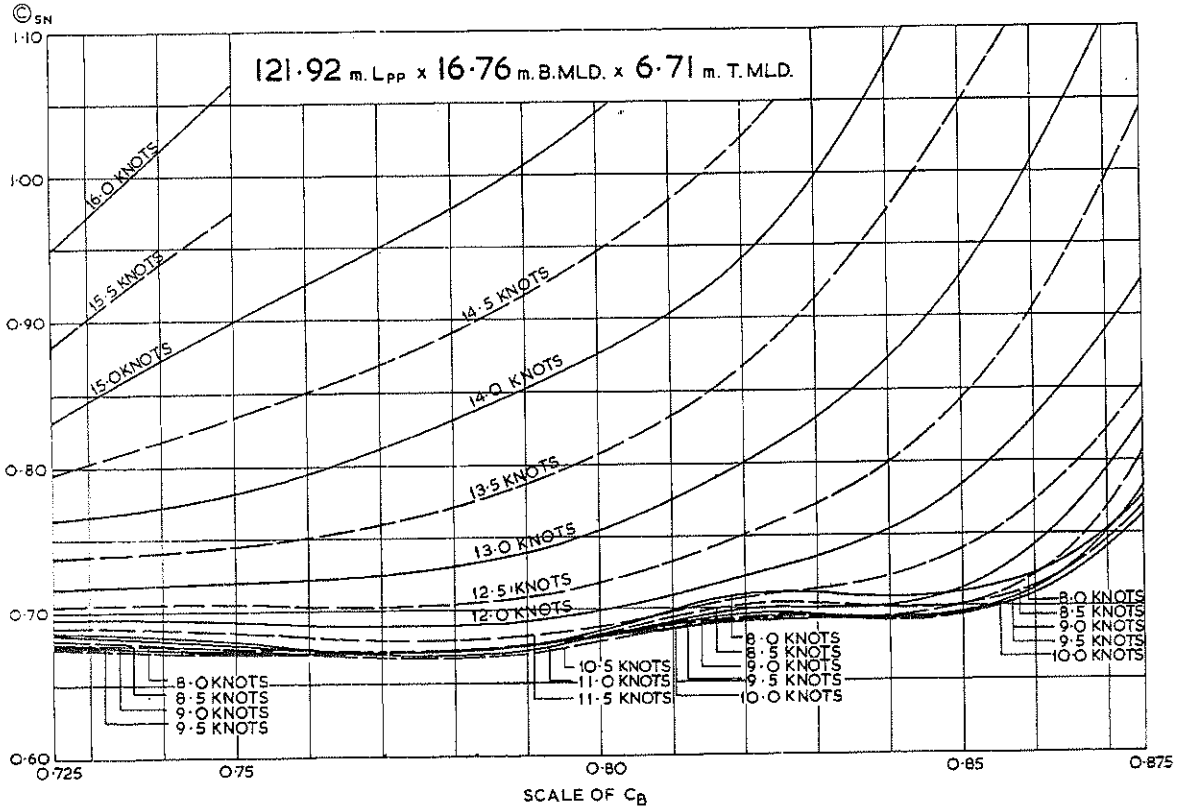

Fig. 64(b)—Cross Curves of Resistance Data for B.S.R.A. Methodical Series Forms: Bulbous Bows.

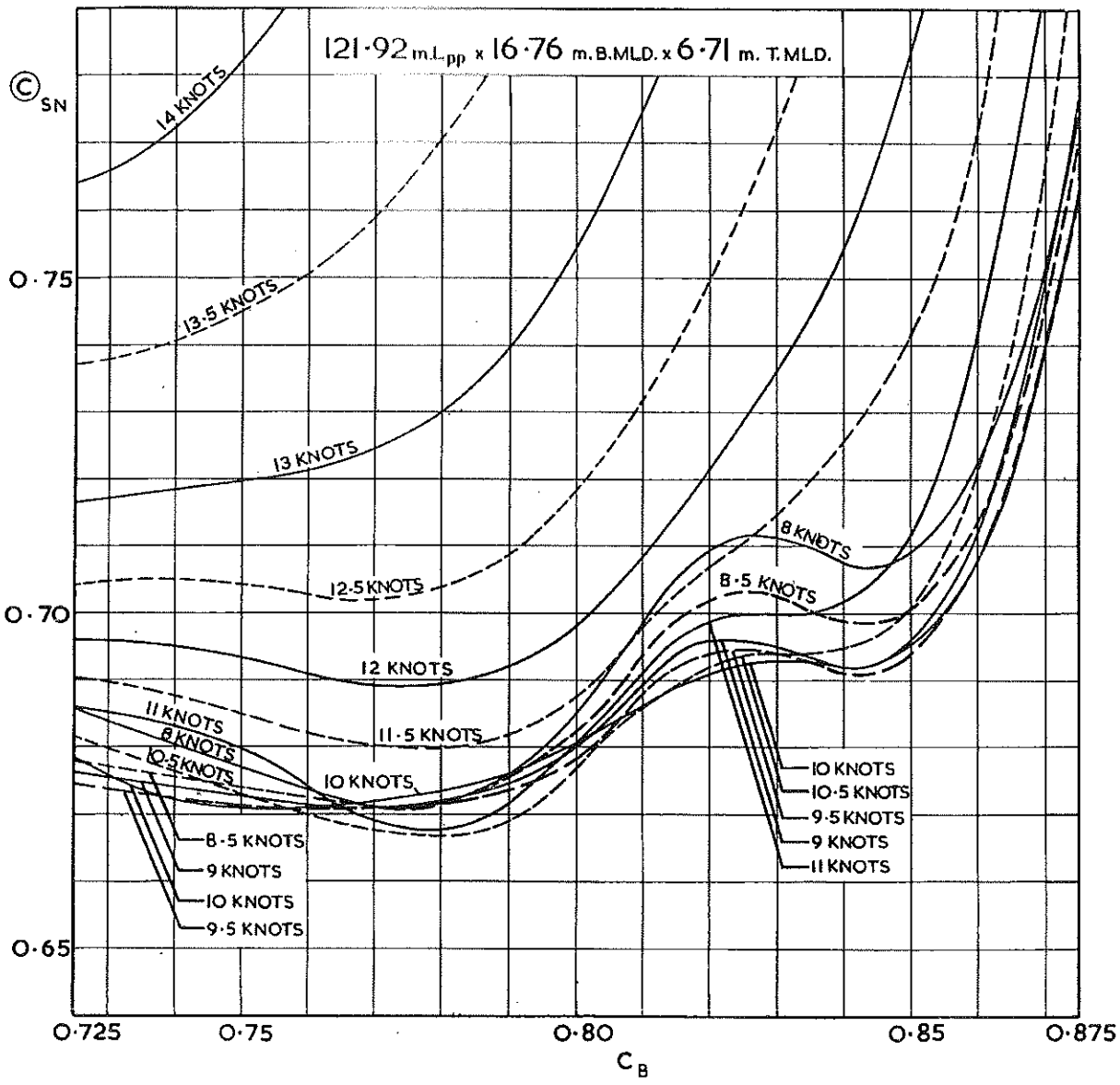

Fig. 64(c)—Cross Curves of Resistance Data for B.S.R.A. Methodical Series Forms: Bulbous Bows.
(Part enlargement of curves shown in Fig. 64(b))

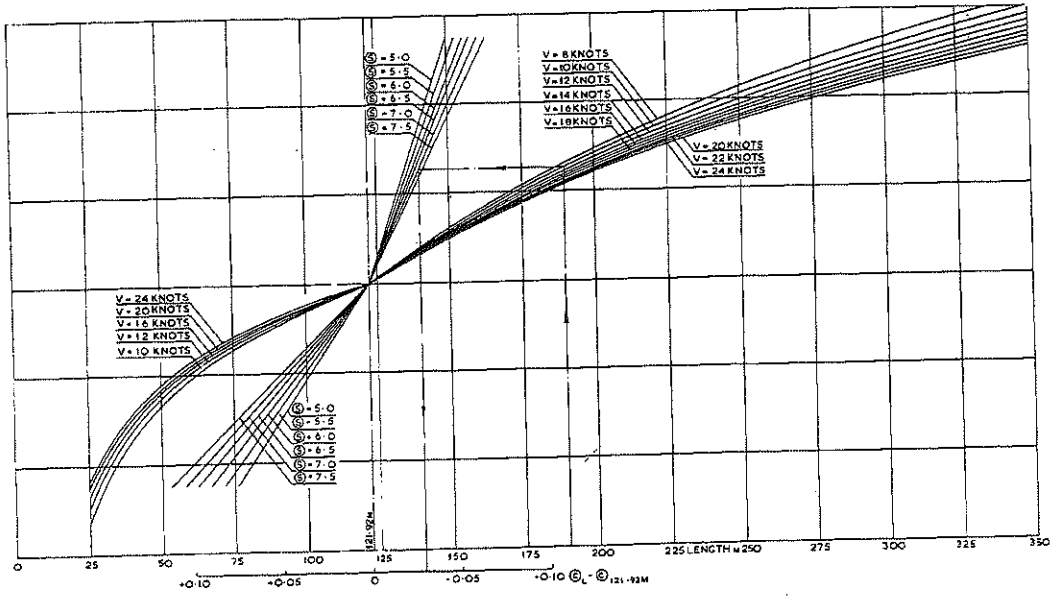

Fig. 65—Effect of Variation Length on © of Ship 121·92-m L_{PP}.

Note: Speeds indicated on the diagram correspond to the standard ship length of 121·92-m L_{PP}.

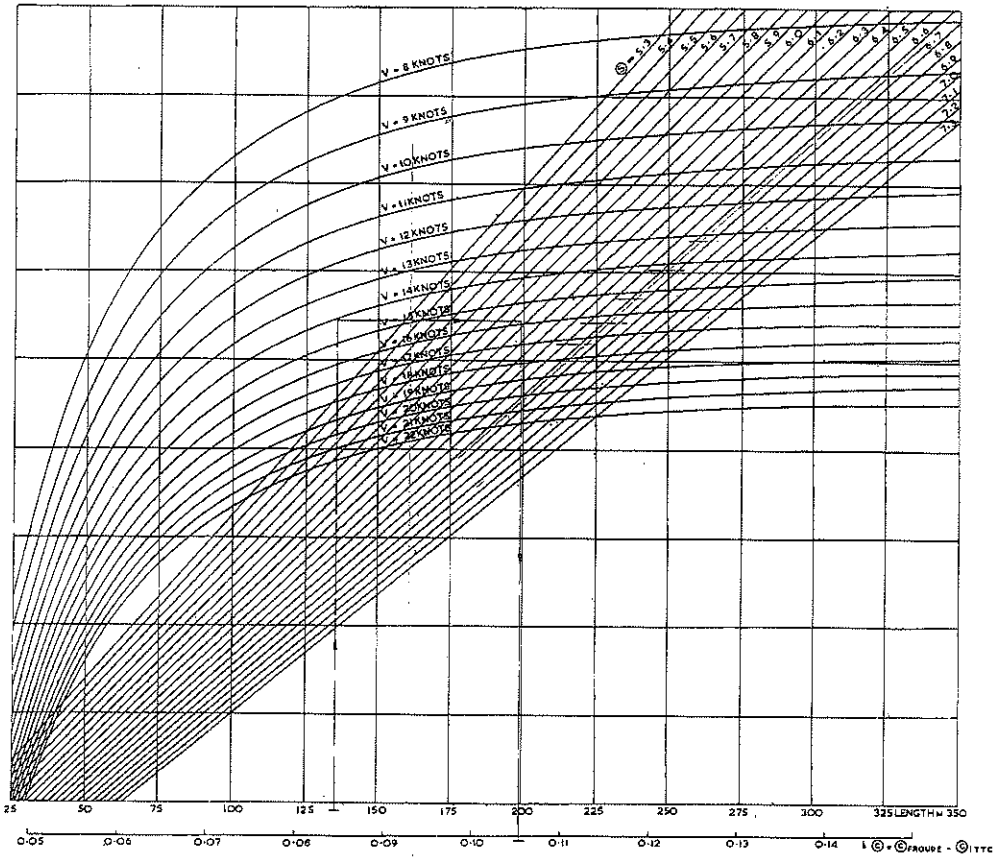

Fig. 66—Difference Between Ship Ⓒ Based on Froude and I.T.T.C. Skin-Friction Corrections.

Note: Speeds indicated on the diagram correspond to the standard ship length of 121·92-m L_{PP}.

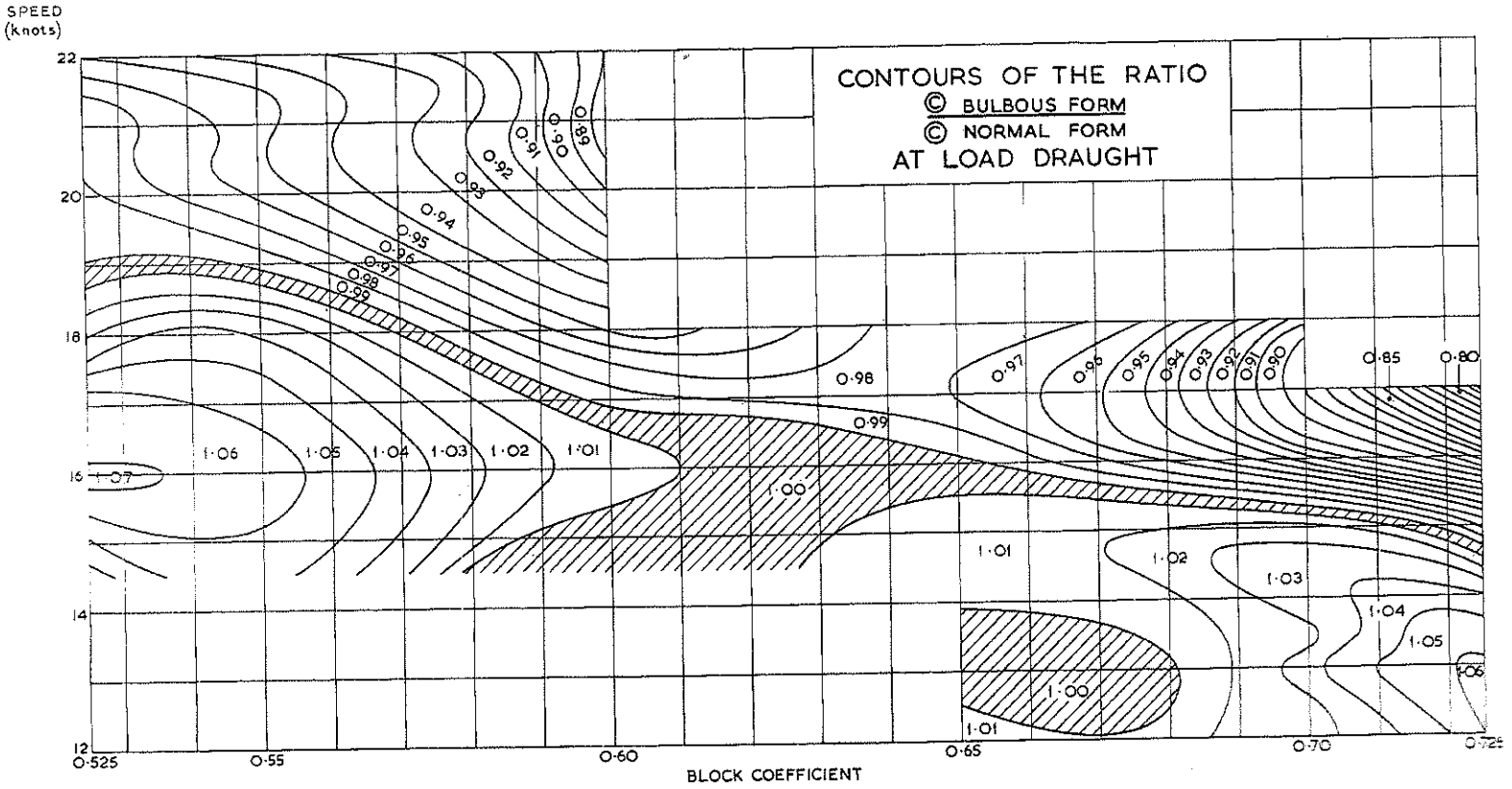

Fig. 67(a)—Contours of the Ratio $\frac{\text{© Bulbous Form}}{\text{© Normal Form}}$ at Load Draught.

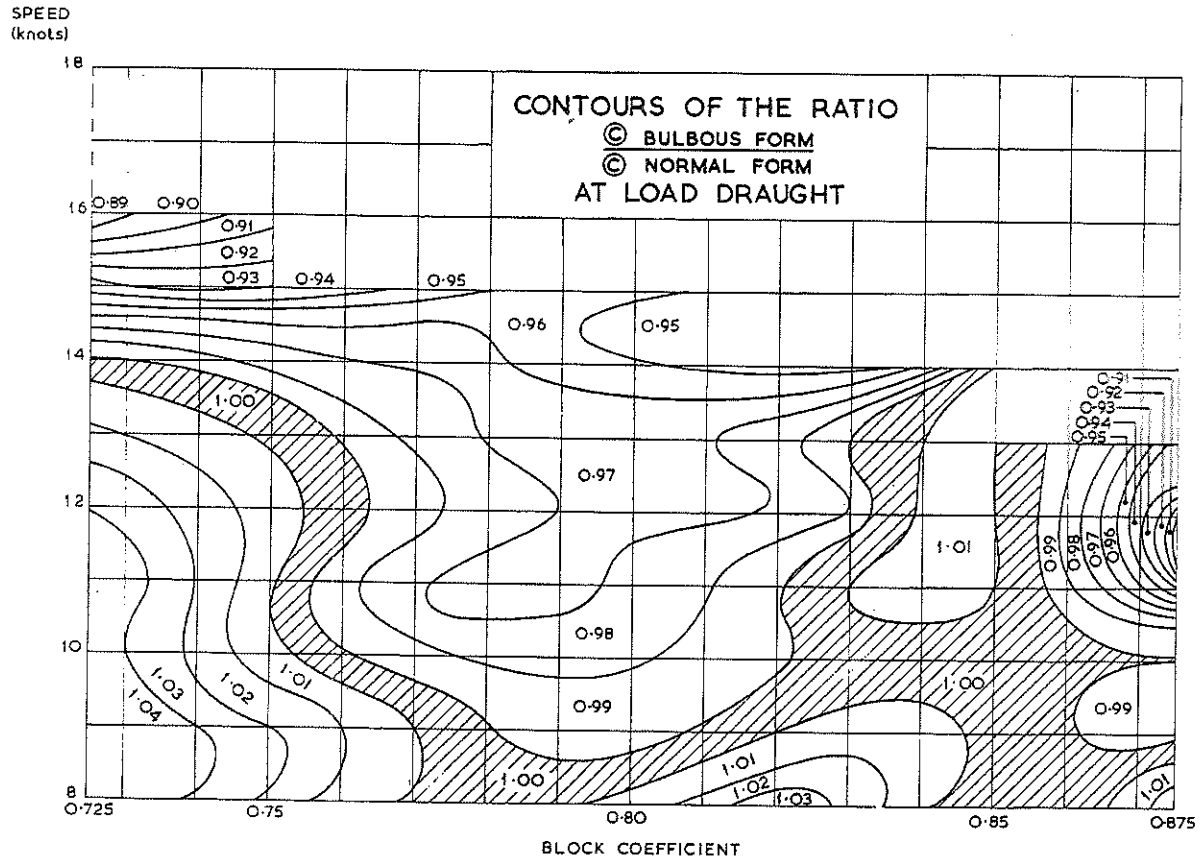

Fig. 67(b)—Contours of the Ratio $\frac{\text{© Bulbous Form}}{\text{© Normal Form}}$ at Load Draught.

PART II. VARIATION OF RESISTANCE WITH BEAM-DRAUGHT RATIO, LENGTH-DISPLACEMENT RATIO AND LONGITUDINAL POSITION OF CENTRE OF BUOYANCY

B. D. W. WRIGHT, C.Eng., M.R.I.N.A.

R. N. M. PATTULLO, C.Eng., F.R.I.N.A.

§ 8. INTRODUCTION

30 Part II of the report deals with the effect on resistance of variations in beam-draught ratio, length-displacement ratio, and longitudinal position of centre of buoyancy from the basis values associated with the parent forms given in Part I.

31 The results are presented in the form of correction factors to be applied to the Ⓒ values given in Part I and cover the range of block coefficients 0·55 to 0·85 for the load-draught condition.

32 Also presented are two simple expressions for the Froude wetted surface coefficient Ⓢ.

33 Over the range of block coefficients 0·65 to 0·80 the B/T and $L/\nabla^{1/3}$ correction factors are based on results of earlier work[8,10] and refer to hull forms which had normal bows. Over the extended range of fullness, however, the corresponding data have been derived from forms with bulbous bows. Nevertheless, it is considered that the correction factors presented should apply generally with acceptable accuracy to both the bulbous and non-bulbous forms and over the extended C_B range 0·55 to 0·85.

34 The effect of LCB variations was not investigated for the finer forms below 0·65 C_B and the corresponding correction factors are based on work by Moor on high-speed cargo liners.[6]

§ 9. DATA EMPLOYED

35 In general the variations from the parent form for a given block coefficient were made as follows:—

B/T Variations. Models had varying beam and draught but the same displacement, length, and LCB position as the parent form, i.e. the $L/\nabla^{1/3}$ ratio was constant.

$L/\nabla^{1/3}$ Variations. Models had the same B/T ratio and LCB position as the parent form, but the length was varied to keep the displacement constant.

LCB Variations. The models with varying LCB position differed from their parent only in that respect.

In the case of the B/T and $L/\nabla^{1/3}$ variations for the 0·85 C_B series, however, the model values for B/T and $L/\nabla^{1/3}$ were varied independently of the parent form.

36 The range of the B/T and the $L/\nabla^{1/3}$ ratios covered by the model results for the different block coefficients is shown in Fig. 68. The range of LCB position is illustrated in Fig. 69.

§ 10. PRESENTATION OF RESULTS

37 Correction-factor diagrams representing the effect on resistance of variations in B/T, $L/\nabla^{1/3}$ and LCB position are given in Fig. 70 to 80. The diagrams represent either a particular speed or a range of speeds and linear interpolation is considered to be sufficiently accurate for the intermediate speeds. The LCB contours corresponding to ship speeds of 21 and 22 knots were derived from an extrapolation of the LCB data from 20 knots.

38 The abscissae of the diagrams are a scale of block coefficient and the ordinates are either a scale of B/T ratio, $L/\nabla^{1/3}$ ratio, or in the case of the LCB variations a scale of deviation from the basis LCB position. The basis positions used with the LCB correction-factor diagrams are defined by the relationship 20 (C_B-0·675) over the range $0{\cdot}55 \leqslant C_B \leqslant 0{\cdot}725$. For higher block coefficients the basis LCB position is constant at 2% L_{PP} forward of midships. Each diagram consists of a set of contours indicating the correction-factor multiplier to be applied to the Ⓒ value obtained from the basic resistance diagram presented in Part I of this report. The individual values of the correction factors apply to the areas bounded by adjacent contours and are arranged in steps of one per cent. The shaded area indicates that no correction is required to the basis Ⓒ value, i.e. the correction-factor multiplier is unity. Included in the B/T and $L/\nabla^{1/3}$ diagrams are the actual values of these parameters defined by the model tests. In the diagrams these are indicated by the small circles.

39 Resistance estimates for vessels having proportions and LCB position differing from the basis ship may be readily made by applying these correction factors to the Ⓒ values obtained from the basic resistance diagrams given in Part I.

40 A length correction using the R.E. Froude skin-friction formula[9] can be made to give the required Ⓒ for the actual ship dimensions. For convenience a diagram for determining the skin-friction correction for a range of lengths, Ⓢ, and ship speed in knots corresponding to 121·92-m L_{PP} is presented in Fig. 65. In this connection the following two simple formulae have been obtained from the B.S.R.A. data for estimating the Froude wetted surface coefficient Ⓢ:-

(i) $Ⓢ = 2{\cdot}98 + 0{\cdot}58Ⓜ$

(ii) $Ⓢ = 1{\cdot}88 + 0{\cdot}941\ C_B + 0{\cdot}766Ⓜ - 0{\cdot}086\ L/B$

The first equation, which has a residual standard error of ±0·11, is similar to the R. E. Froude expression, $Ⓢ = 3{\cdot}4 + 0{\cdot}5Ⓜ$

41 Equation (ii) contains more terms, but it did give a slightly better fit to the data with a residual standard error ±0·08. For practical values of Ⓢ the error involved in using either of these B.S.R.A. formulae may be of the order of one per cent but in any case should not exceed two per cent.

§ 11. CONCLUDING REMARKS

42 The results obtained from the extended cross-fairing on the B/T and $L/\nabla^{1/3}$ variations suggest that any errors involved in using the correction-factor diagrams generally should be within two per cent over the normal design speed range. Errors of up to four per cent may occur when making corrections for B/T and $L/\nabla^{1/3}$ variations

from the Methodical Series parent forms at speeds corresponding to highly over-driven conditions. In the LCB correction-factor diagrams errors of the same magnitude may occur.

43 Worked examples illustrating the use of the correction factors are given in Appendix III.

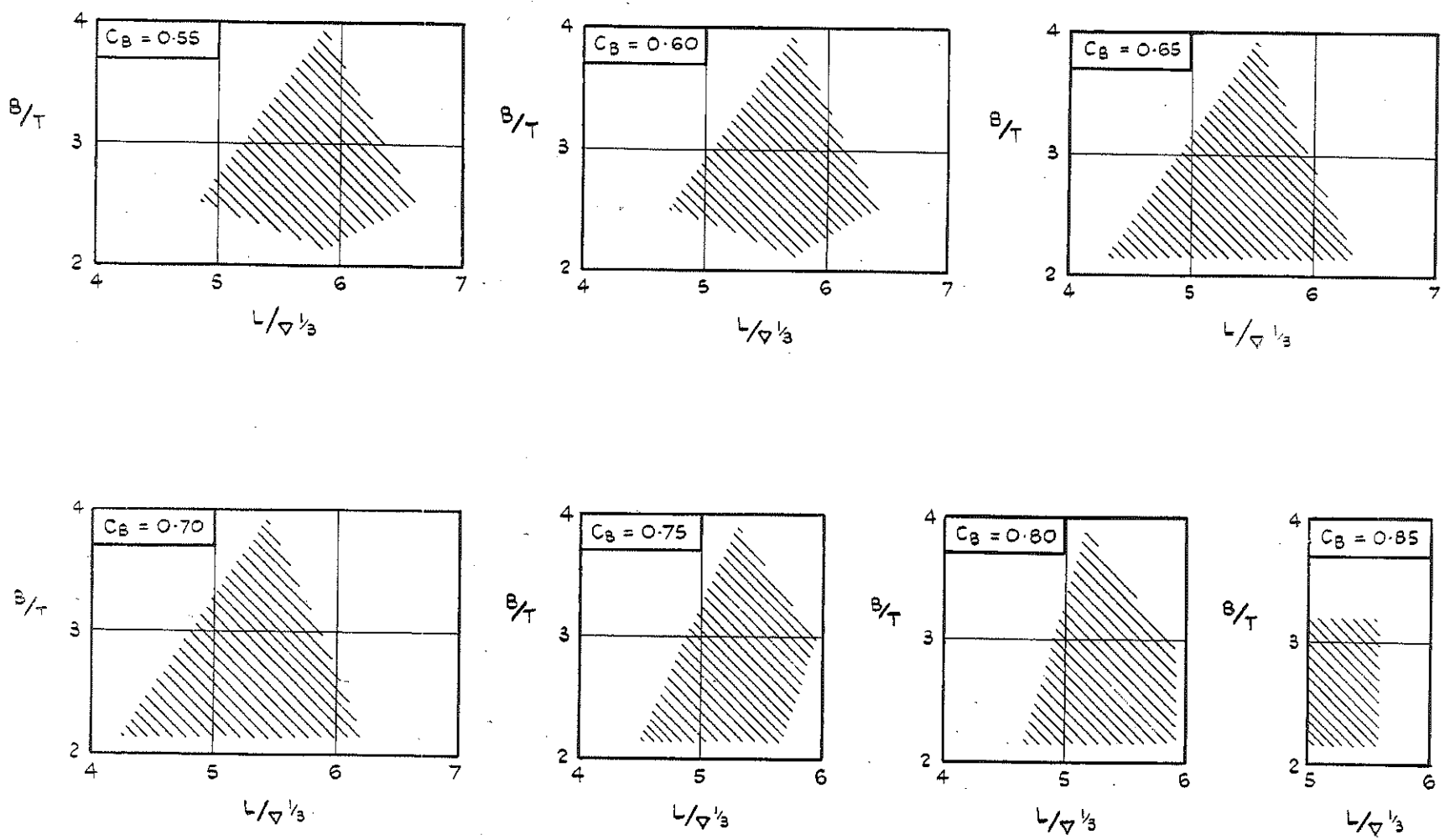

Fig. 68—Range of Beam-Draught and Length-Displacement Ratios Covered by Different Block Coefficients.

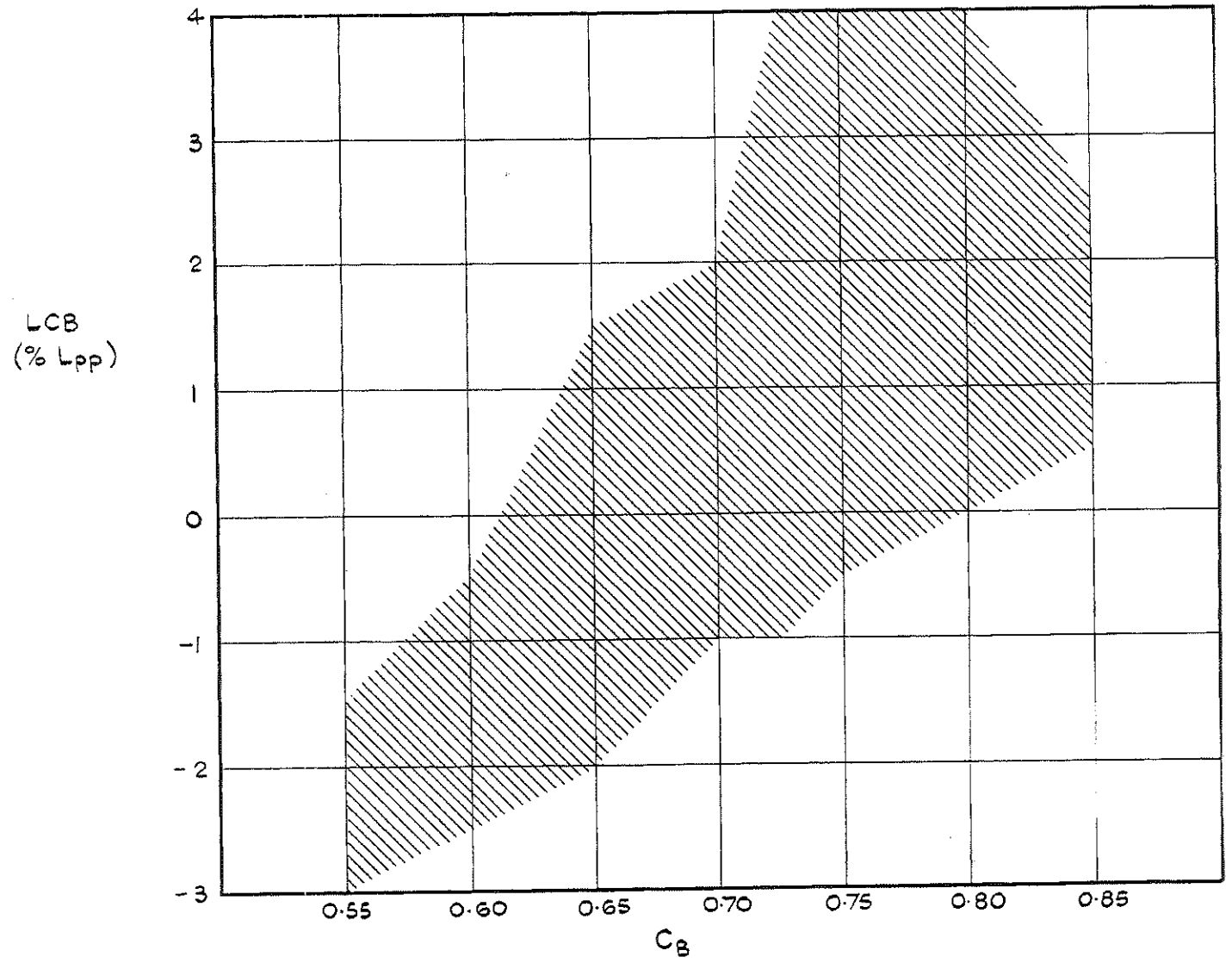

Fig. 69—Range of LCB Positions Covered by Different Block Coefficients.

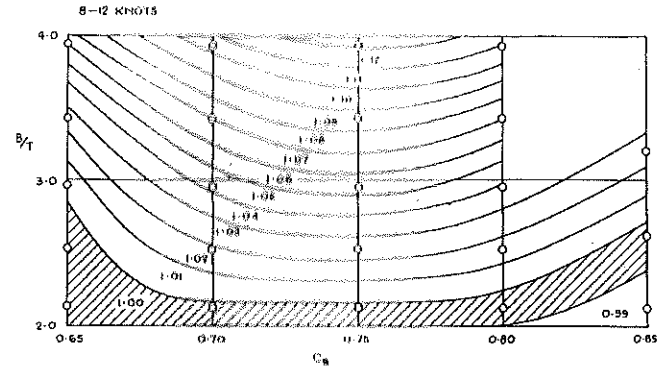

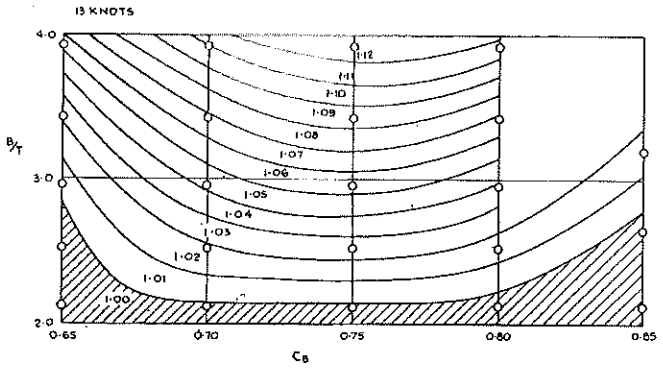

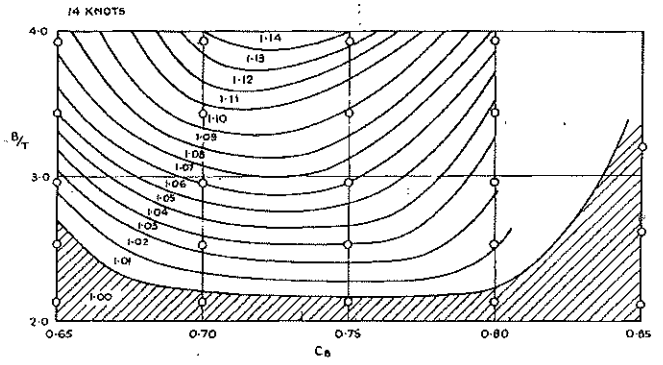

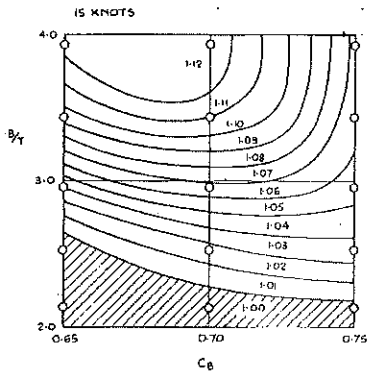

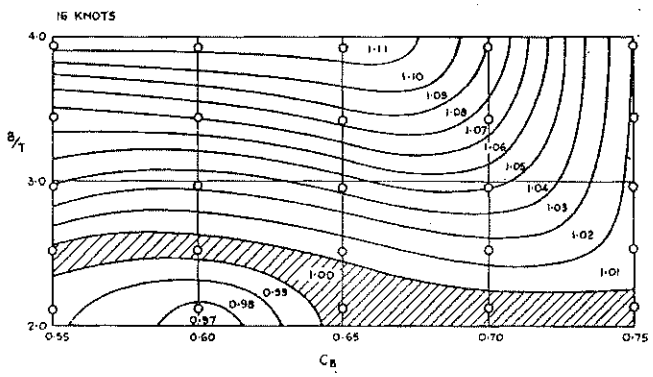

∘ B/T Ratios Defined by Model Tests

Fig. 70—Correction Factors for Variations in Beam-Draught Ratio. Ship Speed 8 to 16 knots.

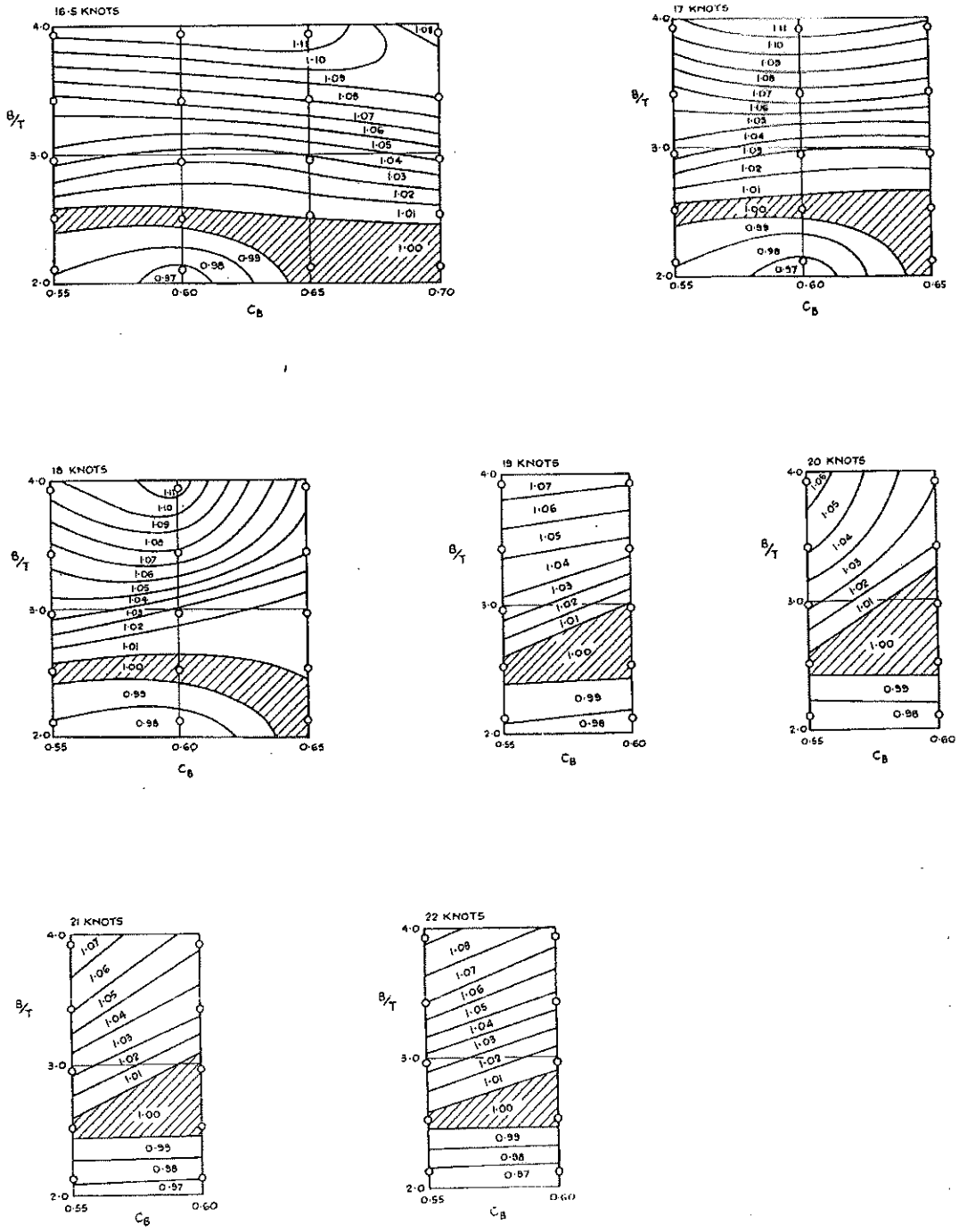

∘ B/T Ratios Defined by Model Tests

Fig. 71—Correction Factors for Variations in Beam-Draught Ratio. Ship Speed 16·5 to 22 knots.

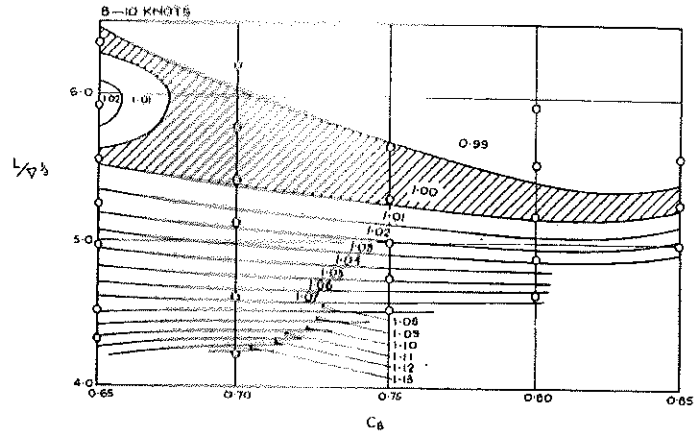

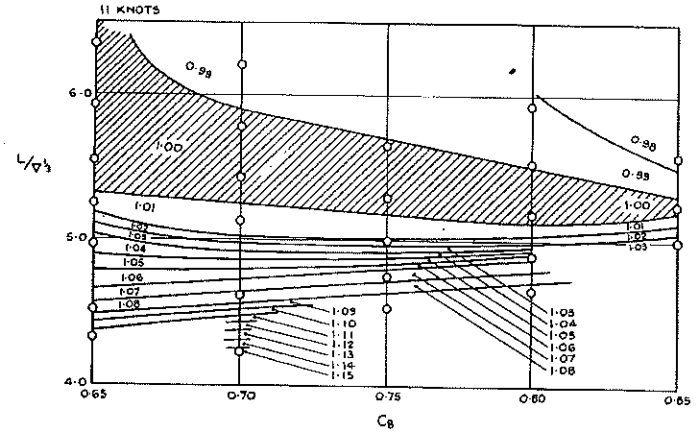

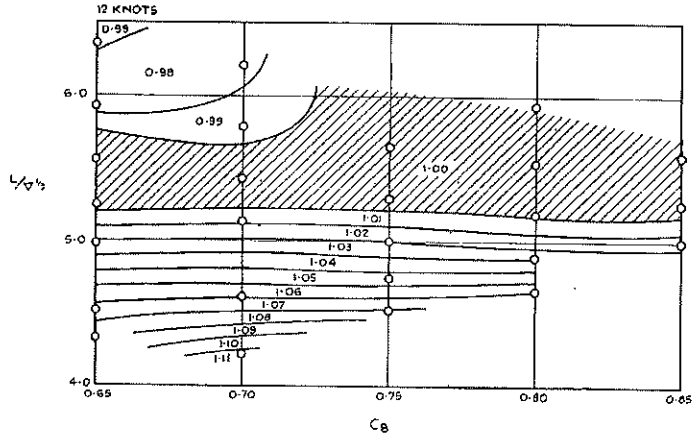

∘ $L/\nabla^{1/3}$ Ratios Defined by Model Tests

Fig. 72—Correction Factors for Variations in Length-Displacement Ratio. Ship Speed 8 to 12 knots.

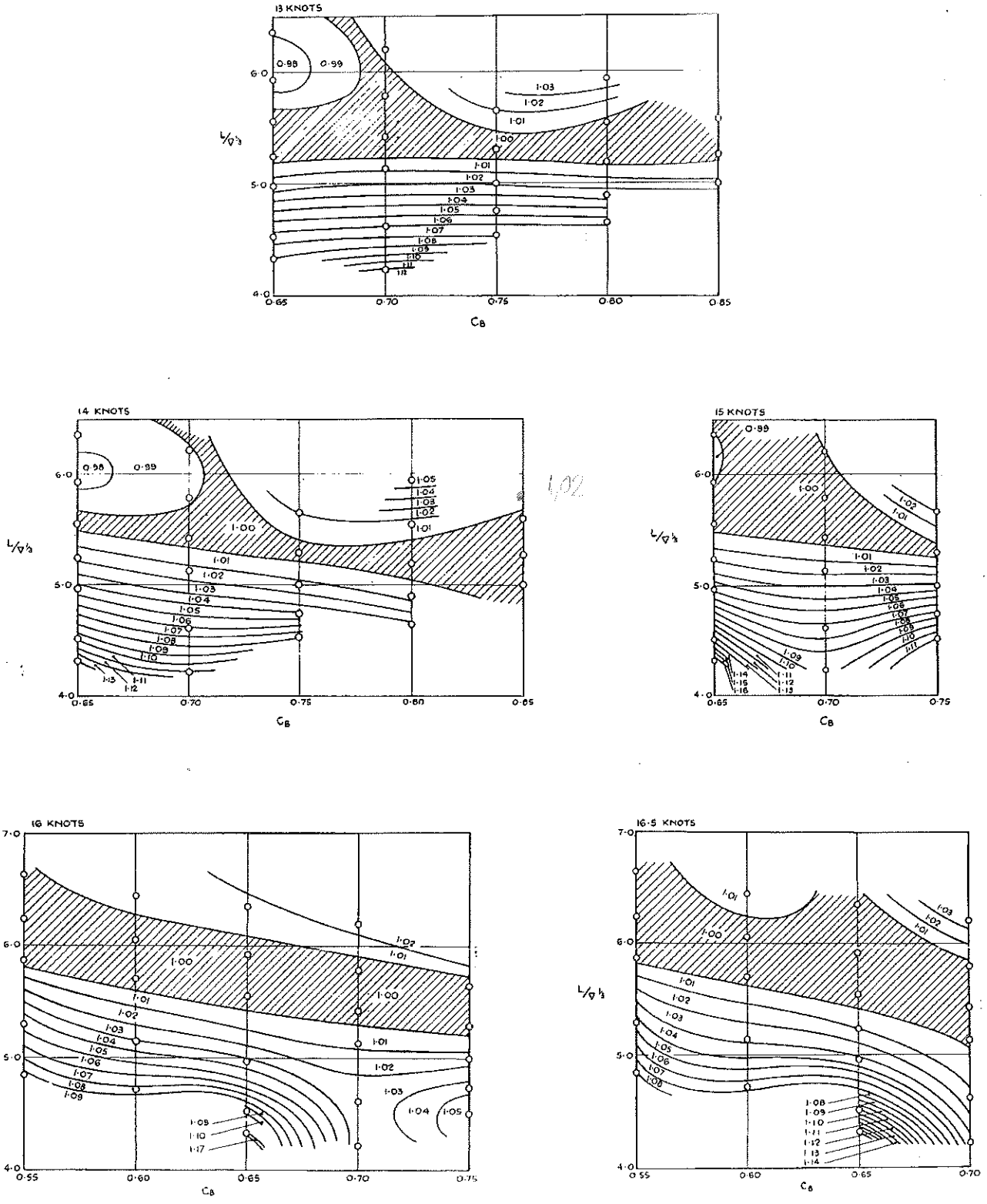

∘ $L/\nabla^{1/3}$ Ratios Defined by Model Tests

Fig. 73—Correction Factors for Variations in Length-Displacement Ratio. Ship Speed 13 to 16·5 knots.

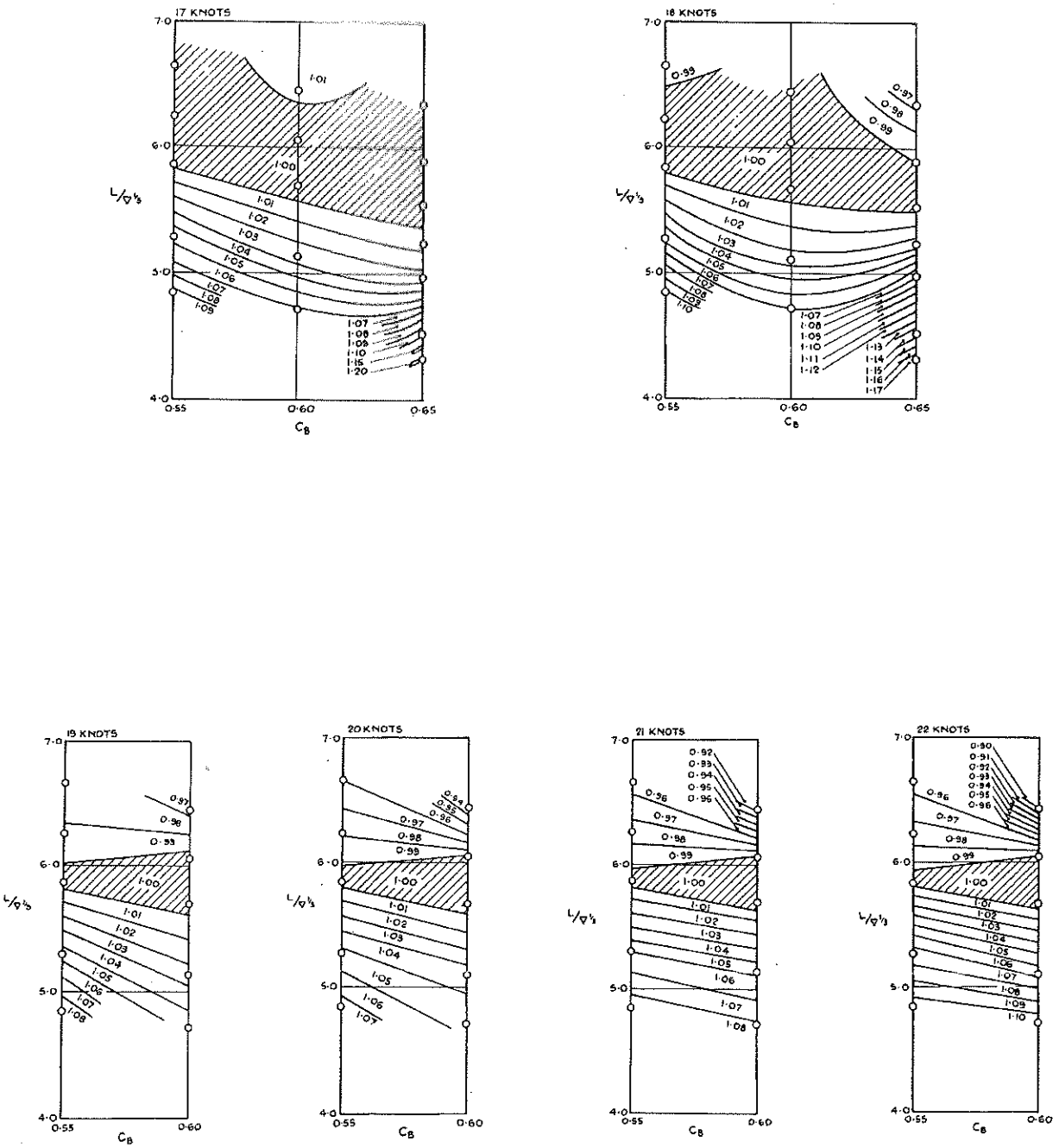

∘ $L/\nabla^{1/3}$ Ratios Defined by Model Tests

Fig. 74—Correction Factors for Variations in Length-Displacement Ratio. Ship Speed 17 to 22 knots.

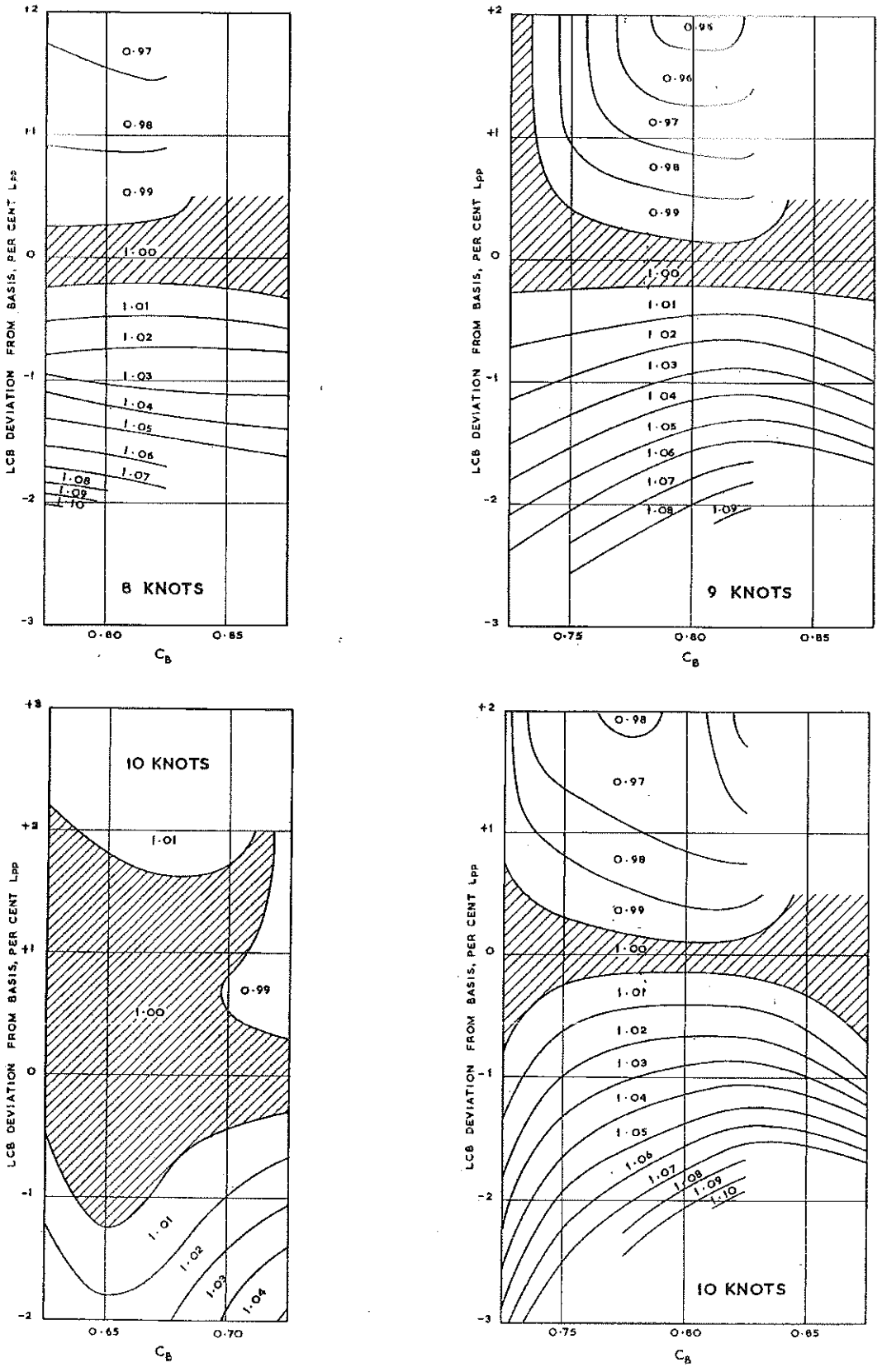

Deviation Expressed as Percentage of L_{PP} Forward (+) or Aft (—) of the Basis Position

Fig. 75—Correction Factors for Deviations From Basis LCB Position. Ship Speed 8 to 10 knots.

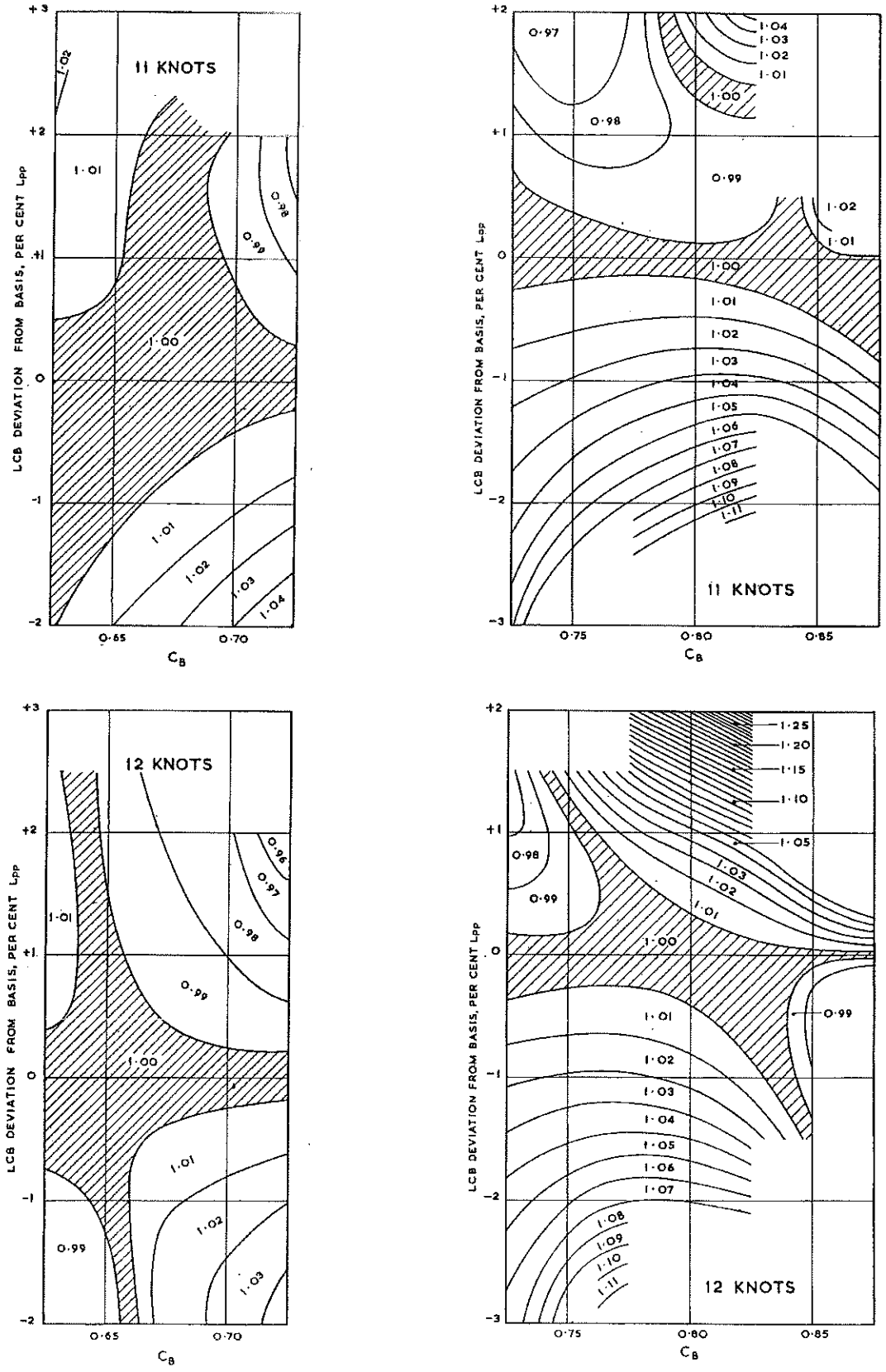

Deviation Expressed as Percentage of L_{PP} Forward (+) or Aft (—) of the Basis Position

Fig. 76—Correction Factors for Deviations from Basis LCB Position. Ship Speed 11 and 12 knots.

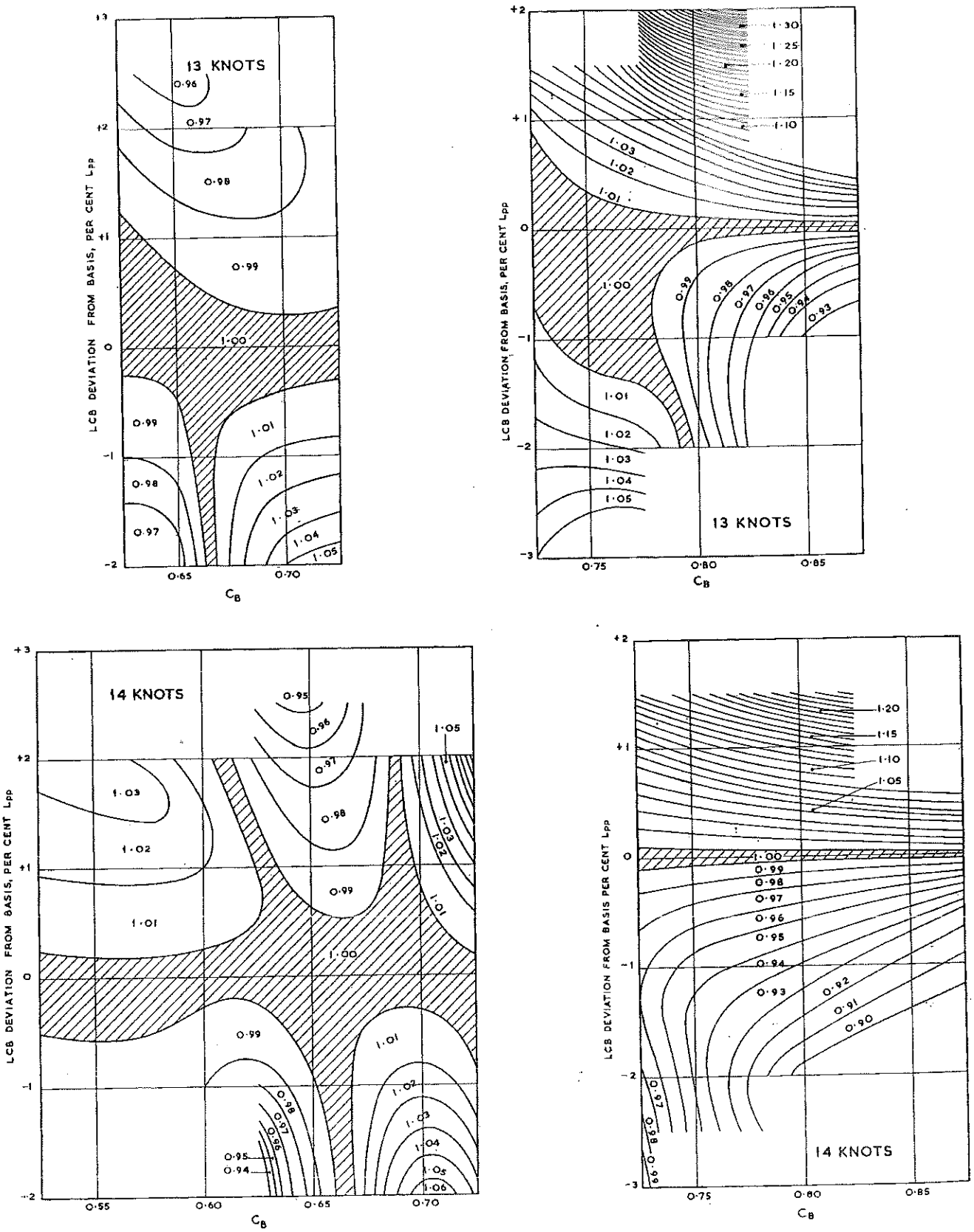

Deviation Expressed as Percentage of L_{PP} Forward (+) or Aft (−) of the Basis Position

Fig. 77—Correction Factors for Deviations from Basis LCB Position. Ship Speed 13 and 14 knots.

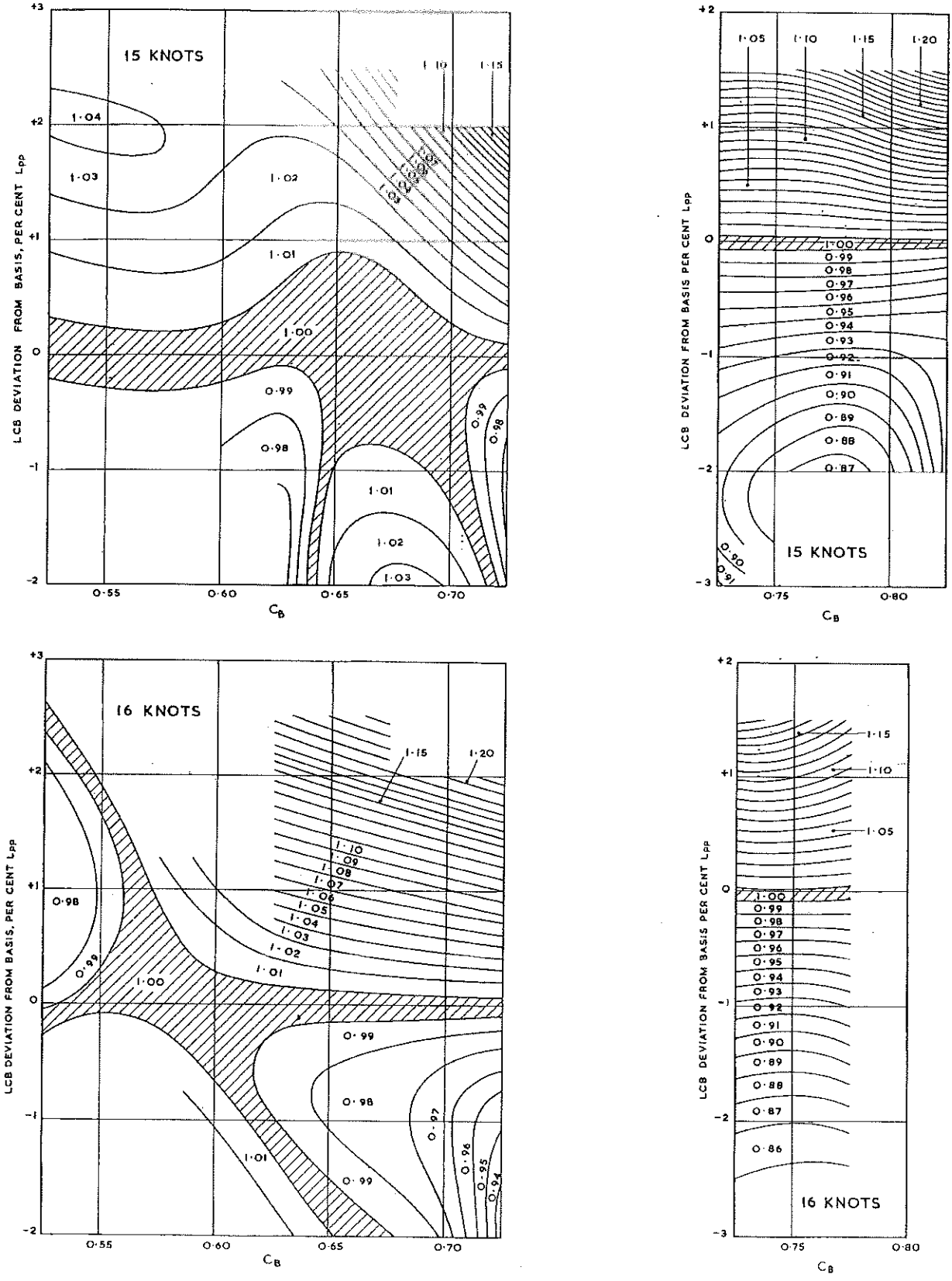

Deviation Expressed as Percentage of L_{PP} Forward (+) or Aft (–) of the Basis Position

Fig. 78—Correction Factors for Deviations from Basis LCB Position. Ship Speed 15 and 16 knots.

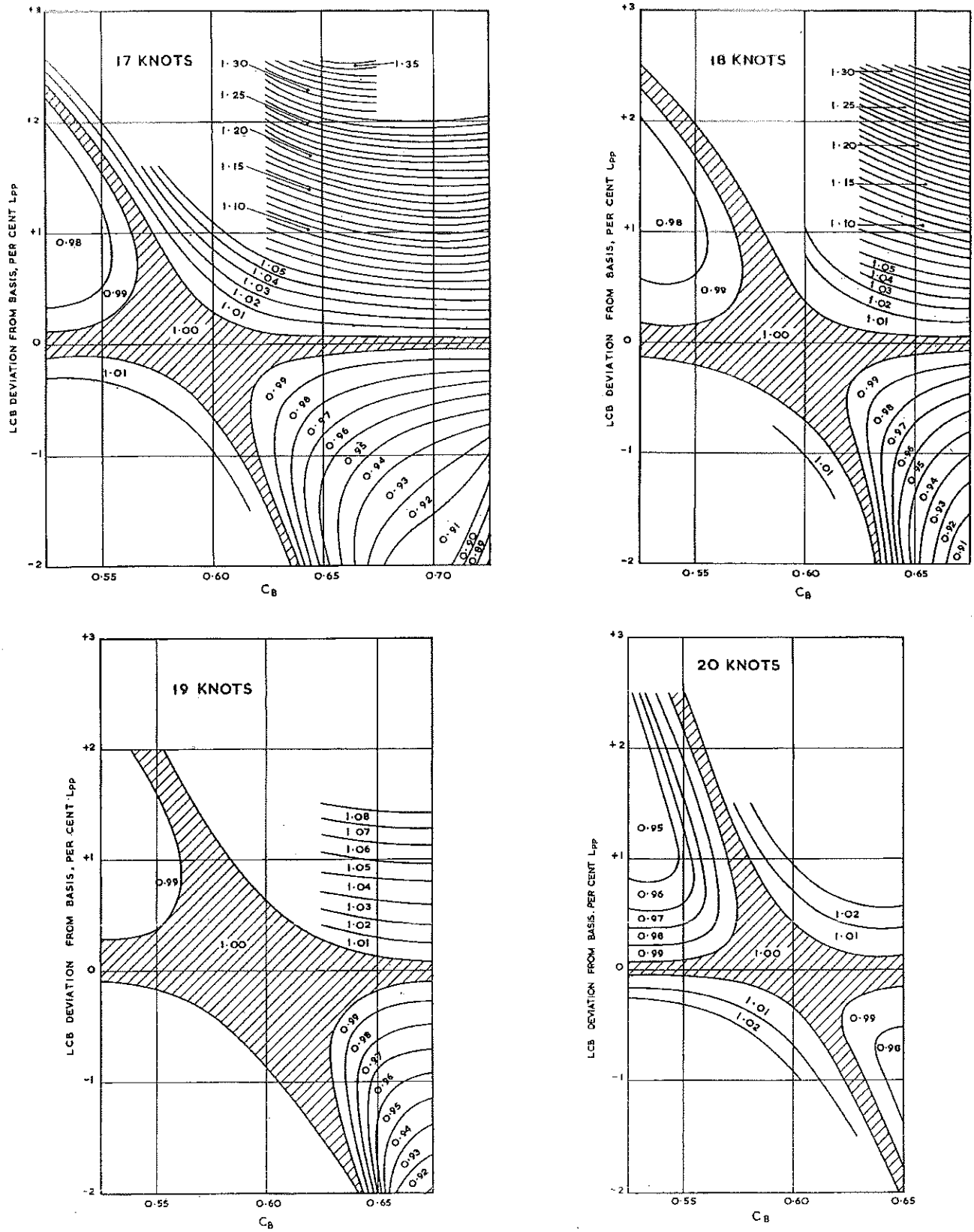

Deviation Expressed as Percentage of L_{pp} Forward (+) or Aft (−) of the Basis Position

Fig. 79—Correction Factors for Deviations from Basis LCB Position. Ship Speed 17 to 20 knots.

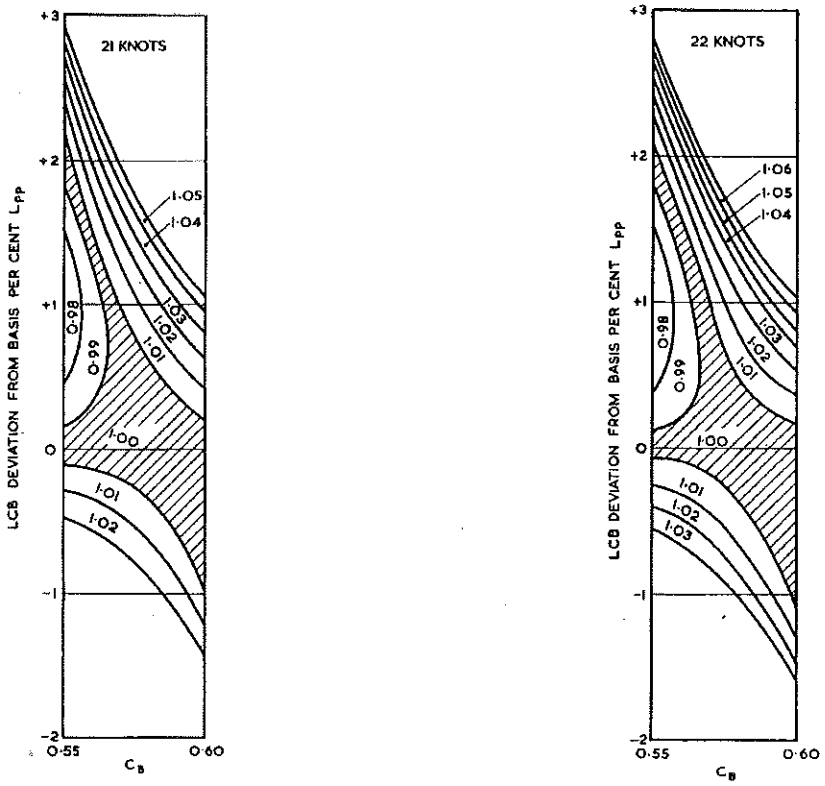

Deviation Expressed as Percentage of L_{PP} Forward (+) or Aft (—) of the Basis Position

Fig. 80—Correction Factors for Deviations from Basis LCB Position. Ship Speed 21 and 22 knots.

PART III. PROPULSION FACTORS

B. D. W. WRIGHT, C.Eng., M.R.I.N.A.

§ 12. INTRODUCTION

44 The third part of the report presents the results of an analysis of the effective-wake fractions, thrust-deduction fractions and relative rotative efficiencies obtained from the B.S.R.A. Methodical Series propulsion experiments with models of single-screw ocean-going merchant-ship forms in the load draught condition. This presentation, covering the range of block coefficients 0·55 to 0·85, is primarily an extension of earlier work.[21,22]

45 The propulsion data cover the variations in beam-draught ratio, length-displacement ratio, and LCB associated with the resistance experiments and ship geometry presented in Parts I and II of the present report. Also included in the present analysis are additional results obtained from models of improved performance developed over the range of block coefficients covered by the earlier presentation.

46 The propeller-hull interaction factors are presented in the form of design diagrams and the corresponding regression equations are given in Appendix I. Worked examples illustrating the use of the diagrams are given in Appendix III together with a specimen data sheet for design office use. The indications are that for a Methodical Series form any errors involved in estimating the qualified hull efficiency, $\eta_R \times \eta_H$, should not exceed five per cent when using the individual components w_T, t, and η_R.

47 A regression equation for estimating the quasi-propulsive coefficient, η_D has also been obtained in this analysis. This was facilitated by the greater number of propeller types and dimensions which were used in the extension of the Methodical Series experiments. A design diagram for estimating η_D is also given.

§ 13. DATA EMPLOYED

48 With the development of forms of improved performance over the range of block coefficients 0·65 to 0·80, and the overall extension of the range of fullness from 0·55 to 0·85, the data used in the present analysis are the combined results of propulsion experiments carried out at the National Physical Laboratory and at Vickers Ltd., St. Albans. The models were either the same as, or geometrically similar to, those used in the resistance experiments details of which may be found in earlier B.S.R.A. resistance and propulsion reports.[11-25]

49 Altogether 142 hull-propeller combinations of single-screw models were tested in the load-draught condition over the range of Froude numbers 0·12 to 0·36.

50 In the original series of experiments, the models were generally tested in turn with three standard propellers to cover a range of propeller revolutions. The exceptions were the models of more extreme proportions with limited draughts which did not permit the use of the largest propeller. The improved forms, however, were tested with individual propellers as were the 0·55, 0·60 and 0·85 block coefficient forms. Altogether twelve model propellers were used in the experiments, particulars of which are given in Table 13.

51 The various types of propeller and stern arrangements adopted for the series are given in Figs. 81 to 86, further details of which may be found in earlier propulsion reports.

TABLE 13

Particulars of Propellers

(Related to 121·92-m L_{PP} ship)

Nominal diameter (m)	Mean face-pitch ratio	Developed blade-area ratio	Number of blades	Boss dia. / Screw dia.	Model No.	Design of screw	Scale of model	Block coefficient series
3·21	0·664	0·775	5	0·204	W220	NPL	1/20	0·85
3·65	0·658	0·700	5	0·179	W221	NPL	1/20	0·85
3·70	0·879	0·771	5	0·206	STA207	Heliston	1/25	0·85
4·26	0·684	0·588	5	0·153	W222	NPL	1/20	0·85
4·26	0·720	0·529	4	0·176	STA357	Heliston	1/25	0·75
4·26	0·820	0·621	4	0·187	U302	NPL	1/22	0·55, 0·60
4·27	0·703	0·394	4	0·196	N84	Troost	1/22	0·65-0·80
4·65	0·786	0·400	4	0·180	N83A	Troost	1/22	0·65-0·80
4·72	1·088	0·700	4	0·169	W239	NPL	1/22	0·55
4·72	0·959	0·601	4	0·167	W238	NPL	1/22	0·60
4·93	0·841	0·547	4	0·217	STA302	Scimitar	1/25	0·65, 0·70
5·56	0·835	0·414	4	0·150	N82	Troost	1/22	0·65-0·80

52 The propulsion experiments were analysed at a nominal loading corresponding to Froude naked P_E plus 10% with the exception of those results for the improved forms which were analysed by St. Albans at a loading corresponding to a standard-ship condition of Froude naked P_E. The results for the improved forms, comprising two per cent of the data, were not corrected for this difference in loading as other model results have indicated the corrections involved generally to be small. The values of Taylor wake fraction and relative rotative efficiency were determined on the basis of thrust identity.

§ 14. METHOD OF ANALYSIS

53 Preliminary graphical analyses of the data suggested that a number of parameters were capable of producing a correlation with the dependent variables of interest. These were then used as a guide in developing the numerical analysis for the various factors subsequently described.

54 Fig. 87 shows the frequency distributions of the propulsion factors. Altogether 902 observations, from the 142 model hull-propeller combinations tested, were used in the analysis so that an investigation could be made into the possible effect of speed on the propulsion factors. Consideration was also given as to whether the bulbous-bow data, which represented 23% of the total observations, and the normal-bow data could be analysed separately. The bulbous results, however, were not amenable to a separate analysis because of the absence of systematic variations in proportions over the intermediate range of block coefficients 0·65 to 0·80. The analysis was, therefore, based on the combined data and the regression equations obtained generally give good agreement for models having either type of bow. Fig. 88 illustrates this point of view and suggests that the use of these equations in estimates for Methodical Series forms should rarely produce deviations in excess of two standard errors. The following is a brief account of the analysis carried out on each of the factors.

(1) WAKE FRACTION

55 Empirical formulae are already available for wake fraction requiring a knowledge of the geometry of both propeller and ship.[27,28] In the context of the B.S.R.A. Methodical Series experiments, similar expressions could equally well have been developed, but it was considered that the degree of accuracy obtained from a complex relationship would generally be out-weighed by the adoption of a simpler formula which may be found to give reliable estimates in practice. The present analysis was therefore mainly confined to a study of the parameters likely to be known at the design stage for preliminary powering estimates or for the analysis of voyage data.

56 Preliminary findings from a graphic analysis of the variables of interest led to a number of relatively simple regression equations of equal merit but containing different combinations of parameters. The simplest expression obtained, involving the single parameter block coefficient, is

$$w_T = 0{\cdot}535\ C_B - 0{\cdot}07.$$

The residual standard error of this equation is ±0·04.

57 Although this relationship is in good agreement with the well known Taylor formula, $w_T = 0{\cdot}50\ C_B - 0{\cdot}05$, the use of the fullness parameter alone, however, generally results in an underestimate of wake fraction in the case of very full forms and other parameters are necessary for an improved estimate.

58 The wake-fraction parameter, D_W, which was developed in the earlier analysis[21] has been retained as its use affords continuity with the earlier presentation and for the purposes of a graphical presentation it neatly combines three other highly significant

parameters namely B/D, $B/\nabla^{1/3}$, and $D/\nabla^{1/3}$. The design diagram for estimating wake fraction is shown in Fig. 89. In this analysis the LCB term although found significant in the statistical sense has been omitted as its contribution only affects the third decimal place. The equation finally adopted is given in Appendix I.

(2) THRUST-DEDUCTION FRACTION

59 The principal parameters found to represent the variation in thrust-deduction fraction were pitch ratio, $B/\nabla^{1/3}$, and LCB position. A number of trial regressions were made without the pitch-ratio term and an equation involving the D_t parameter used in the earlier analysis[21], has been developed. This is put forward as an alternative expression for use when pitch ratio is not available.

60 The inclusion of ship-speed terms in the regressions was found to affect only the third decimal place and have therefore been omitted from the two equations finally adopted and given in Appendix I.

61 Diagrams representing these equations are given in Figs. 90 and 91. Fig. 90 contains the pitch-ratio term whereas Fig. 91 assumes a knowledge of the propeller diameter.

(3) RELATIVE ROTATIVE EFFICIENCY

62 The best fit to these data was given by regression equations including both pitch ratio and blade-area ratio. In the regression equations ship speed was found to be significant but its contribution only affected the third decimal place and has therefore been omitted from the equation finally adopted and given in Appendix I.

63 For the purposes of a graphical presentation, two equations have been selected and are represented by the diagrams shown in Figs. 92 and 93. Fig. 92 assumes a knowledge of the pitch ratio and blade-area ratio whereas in Fig. 93 the only propeller term used is diameter in addition to the form parameters. As with thrust-deduction fraction the availability or otherwise of propeller dimensions will influence the use of one or other of these diagrams.

(4) QUASI-PROPULSIVE COEFFICIENT

64 In the earlier presentation of the Methodical Series data no analysis was carried out on quasi-propulsive coefficient, η_D, as only three propellers, which were of Troost design, were used and it was considered that the η_D results from the experiments would not be representative of the values likely to be obtained in practice. However, in the extension of the Methodical Series experiments a greater number of propellers was used and it was considered that a useful expression for η_D could be obtained from the data available.

65 In the first instance the following linear relationship, similar in form to the empirical formula given by Emerson and Witney[26], was obtained,

$$\eta_D = 0{\cdot}818 - 0{\cdot}000091\ N\sqrt{L_{PP}}$$

The residual standard error of this equation is ±0·040.

66 The best equation for the purposes of a graphical presentation, includes the parameters $N\sqrt{L_{PP}}$, blade-area ratio, beam-diameter ratio and block coefficient. A diagram representing an equation containing these parameters is given in Fig. 94 and details of the coefficients are given in Appendix I. This equation has in a number of instances given good agreement with results obtained from models outside of the B.S.R.A. Methodical Series.

67 It should be noted that the η_D values calculated correspond to a loading of Froude naked P_E plus 10%, i.e. the load factor $(1 + x) = 1{\cdot}10$. An analysis of Methodical Series and other model data suggests that values for other loadings may be approximated by making a 0·015 correction to the η_D value for every 0·10 change from the Methodical Series propeller loading, the correction being positive for a decrease in loading, i.e.

$$\eta_D \text{ (corrected)} = \eta_D + 0{\cdot}15\,[1{\cdot}10 - (1 + x)_{\text{Froude}}].$$

§ 15. CONCLUDING REMARKS

68 It is considered that the parameters adopted in the design diagrams adequately reflect the variations in the propeller–hull interaction factors over the extended range of hull and propeller dimensions covered by the B.S.R.A. Methodical Series experiments. The diagrams presented in Figs. 89 to 94 also serve to define the range of application of the parameters.

69 As stated earlier, the availability or otherwise of propeller dimensions will influence the choice of design diagram for use in estimating thrust-deduction fraction and relative rotative efficiency.

70 Estimates for quasi-propulsive coefficient η_D, derived from the component regressions for w_T, t, η_R in association with a propeller open-water efficiency determined from design diagrams are generally in good agreement with estimates obtained directly from the regression equation for η_D. It should be noted that although, in some cases, errors involved in estimating η_D from the individual component regressions may well be cumulative the indications are that they should not exceed five per cent. The two methods have their particular uses, for example if one is primarily interested in calculating the delivered power for a particular form the direct regression equation for η_D, which does not require a knowledge of propeller open-water efficiency, would be used. However, if one is interested in the effect of variation of hull and propeller parameters on the propeller-hull interaction factors, and ultimately η_D, then the component regression equations are required.

REFERENCES

1. Methodical Series Experiments on Ocean-Going Merchant-Ship Forms. Overall Analysis. Part I. Geometry of Forms. MOOR, D. I. and PATTULLO, R. N. M. B.S.R.A. Report No. 284 (1959) (Also Trans. Instn Nav. Archit., Lond., **103** (1961), p. 329).

2. A Proposed New Basis for the Design of Single-Screw Merchant Ship Forms and Standard Series Lines. TODD, F. H. and FORREST, F. X. Trans. Soc. Nav. Archit., N.Y., **59** (1951), p. 642.

3. Some Further Experiments on Single-Screw Merchant Ship Forms—Series 60. TODD, F. H. Trans. Soc. Nav. Archit., N.Y., **61** (1953), p. 516.

4. Model Resistance Tests on a Methodical Series of Forms. FERGUSON, J. M. and PARKER, M. N. Trans. Instn Nav. Archit., Lond., **98** (1956), p. 1.

5. On the Systematic Geometrical Variation of Ship Forms. LACKENBY, H. B.S.R.A. Report No. 12. (1947). (Also Trans. Instn Nav. Archit., Lond., **92** (1950), p. 289).

6. Resistance, Propulsion and Motions of High Speed Single-Screw Cargo Liners. MOOR, D. I. Trans. N.-E. Cst Instn Engrs Shipb., **82** (1966), p. 277.

7. The Effective Horsepower of Single-Screw Ships. Average Modern Attainment with Particular Reference to Variation of C_B and LCB. MOOR, D. I. and SMALL, V. F. B.S.R.A. Report No. 251. (1958) (Also Trans. Roy. Instn Nav. Archit., Lond., **102** (1960), p. 259).

8. Methodical Series Experiments on Ocean-Going Merchant-Ship Forms. Overall Analysis. Part III. Variation of Resistance with Breadth-Draught Ratio and Length-Displacement Ratio. LACKENBY, H. and PARKER, M. N. B.S.R.A. Report NS. 29. (1964) (Also Trans. Roy. Instn Nav. Archit., Lond., **108** (1966), p. 363).

9. On the 'Constant' System of Notation of Results of Experiments on Models used at the Admiralty Experiment Works. FROUDE, R. E., Trans. Instn Nav. Archit., Lond., **29** (1888), p. 304.

10. Methodical Series Experiments on Ocean-Going Merchant-Ship Forms. Overall Analysis. Part II. Variation of Resistance with Block Coefficient and Longitudinal Centre of Buoyancy. PATTULLO, R. N. M. and PARKER, M. N. B.S.R.A. Report No. 291. (1959). (Also Trans. Roy. Instn Nav. Archit., Lond., **103** (1961), p. 329).

Methodical Series Experiments on Ocean-Going Merchant-Ship Forms Variations in Breadth-Draught Ratio and Length-Displacement Ratio.

11. Results of Experiments with 0·55 Block Coefficient Series. B.S.R.A. Report NS. 200. 1968.

12. Results of Experiments with 0·60 Block Coefficient Series. B.S.R.A. Report NS. 168. 1967.

13. Part IV. Results of Further Resistance Experiments with 0·65 Block Coefficient Series. B.S.R.A. Report No. 108. 1952.

14. Results of Experiments with 0·65 Block Coefficient Series. B.S.R.A. Report No. 423. 1962.

15. Part VIII. Results of Resistance Experiments with a 0·70 Block Coefficient Form. B.S.R.A. Report No. 214. 1956.

16. Results of Experiments with 0·70 Block Coefficient Series. B.S.R.A. Report No. 413. 1962.

17. Part X. Experiments with a Re-Designed 0·75 Block Coefficient Form. B.S.R.A. Report No. 224. 1958.

18. Part XI. Results of Experiments with 0·80 Block Coefficient Form. B.S.R.A. Report No. 353. 1961.

Methodical Series Experiments with Ocean-Going Merchant-Ship Forms.

19. Length-Displacement and Breadth-Draught Variations with Models of 0·85 Block Coefficient. B.S.R. A. Report NS. 147. 1966.

20. Resistance and Propulsion Experiments with Models of 0·85 Block Coefficient. Variation of Longitudinal Position of Buoyancy. B.S.R.A. Report NS. 236. 1968.

Methodical Series Experiments on Ocean-Going Merchant-Ship Forms. Overall Analysis.

21. Part IV. Propulsion. PARKER, M. N. B.S.R.A. Report NS. 30. (1964) (Also Trans. Roy. Instn Nav. Archit., Lond., **108** (1966), p. 389).

22. Addendum to Part IV. Propulsion. Variation of Relative Rotative Efficiency. PARKER, M. N. and BOWDEN, B. S. B.S.R.A. Technical Memorandum No. 239. (1965) (Also Trans. Roy. Instn Nav. Archit., Lond., **108** (1966), p. 389).

Methodical Series Experiments with Ocean-Going Merchant-Ship Forms. Variations in Breadth-Draught Ratio and Length-Displacement Ratio.

23. Results of Experiments with a Re-Designed 0·75 Block Coefficient Form. B.S.R.A. Report No. 260. 1959.

24. Results of Experiments with 0·80 Block Coefficient Series. B.S.R.A. Report NS. 364. 1961.

25. Results of Experiments with 0·85 Block Coefficient Series. B.S.R.A. Report NS. 167. 1967.

26. A Review of Ship Model Data. EMERSON, A. and WITNEY, N. A. Trans. N.-E. Cst Instn Engrs Shipb., **66** (1949-1950), p. 295.

Methodical Series Experiments on Ocean-Going Merchant-Ship Forms Variations in Breadth-Draught Ratio and Length-Displacement Ratio.

11. Results of Experiments with 0·55 Block Coefficient Series. B.S.R.A. Report NS. 200. 1968.

12. Results of Experiments with 0·60 Block Coefficient Series. B.S.R.A. Report NS. 168. 1967.

13. Part IV. Results of Further Resistance Experiments with 0·65 Block Coefficient Series. B.S.R.A. Report No. 108. 1952.

14. Results of Experiments with 0·65 Block Coefficient Series. B.S.R.A. Report No. 423. 1962.

15. Part VIII. Results of Resistance Experiments with a 0·70 Block Coefficient Form. B.S.R.A. Report No. 214. 1956.

16. Results of Experiments with 0·70 Block Coefficient Series. B.S.R.A. Report No. 413. 1962.

17. Part X. Experiments with a Re-Designed 0·75 Block Coefficient Form. B.S.R.A. Report No. 224. 1958.

18. Part XI. Results of Experiments with 0·80 Block Coefficient Form. B.S.R.A. Report No. 353. 1961.

Methodical Series Experiments with Ocean-Going Merchant-Ship Forms.

19. Length-Displacement and Breadth-Draught Variations with Models of 0·85 Block Coefficient. B.S.R. A. Report NS. 147. 1966.

20. Resistance and Propulsion Experiments with Models of 0·85 Block Coefficient. Variation of Longitudinal Position of Buoyancy. B.S.R.A. Report NS. 236. 1968.

Methodical Series Experiments on Ocean-Going Merchant-Ship Forms. Overall Analysis.

21. Part IV. Propulsion. PARKER, M. N. B.S.R.A. Report NS. 30. (1964) (Also Trans. Roy. Instn Nav. Archit., Lond., **108** (1966), p. 389).

22. Addendum to Part IV. Propulsion. Variation of Relative Rotative Efficiency. PARKER, M. N. and BOWDEN, B. S. B.S.R.A. Technical Memorandum No. 239. (1965) (Also Trans. Roy. Instn Nav. Archit., Lond., **108** (1966), p. 389).

Methodical Series Experiments with Ocean-Going Merchant-Ship Forms. Variations in Breadth-Draught Ratio and Length-Displacement Ratio.

23. Results of Experiments with a Re-Designed 0·75 Block Coefficient Form. B.S.R.A. Report No. 260. 1959.

24. Results of Experiments with 0·80 Block Coefficient Series. B.S.R.A. Report NS. 364. 1961.

25. Results of Experiments with 0·85 Block Coefficient Series. B.S.R.A. Report NS. 167. 1967.

26. A Review of Ship Model Data. EMERSON, A. and WITNEY, N. A. Trans. N.-E. Cst Instn Engrs Shipb., **66** (1949-1950), p. 295.

27. The Wake and Thrust Deduction of Single-Screw Ships. TELFER, E. V. Trans. N.-E. Cst Instn Engrs Shipb., **52** (1935-1936), p. 179.

28. Principles of Naval Architecture. COMSTOCK, J. (ed.) Society Naval Architects and Marine Engineers. New York (1967), p. 394.

29. Decisions on Skin Friction and Turbulence Stimulation. Proceedings of the Eighth International Towing Tank Conference, Madrid, (1957), p. 324.

30. The N.S.M.B. Standard Series Propeller Data and their Applications. WRIGHT, B. D. W. B.S.R.A. Technical Memorandum No. 213. 1965.

31. Resistance and Propulsion Factors of Single-Screw Ships at Fractional Draught. MOOR, D. I., and O'CONNOR, F. R. C. Trans. N.-E. Cst Instn Engrs Shipb., **80** (1964), p. 185.

32. The Effective Horsepower of Single-Screw Ships. Average and Optimum Standards of Attainment 1969. MOOR, D. I. B.S.R.A. Report NS. 317. 1971.

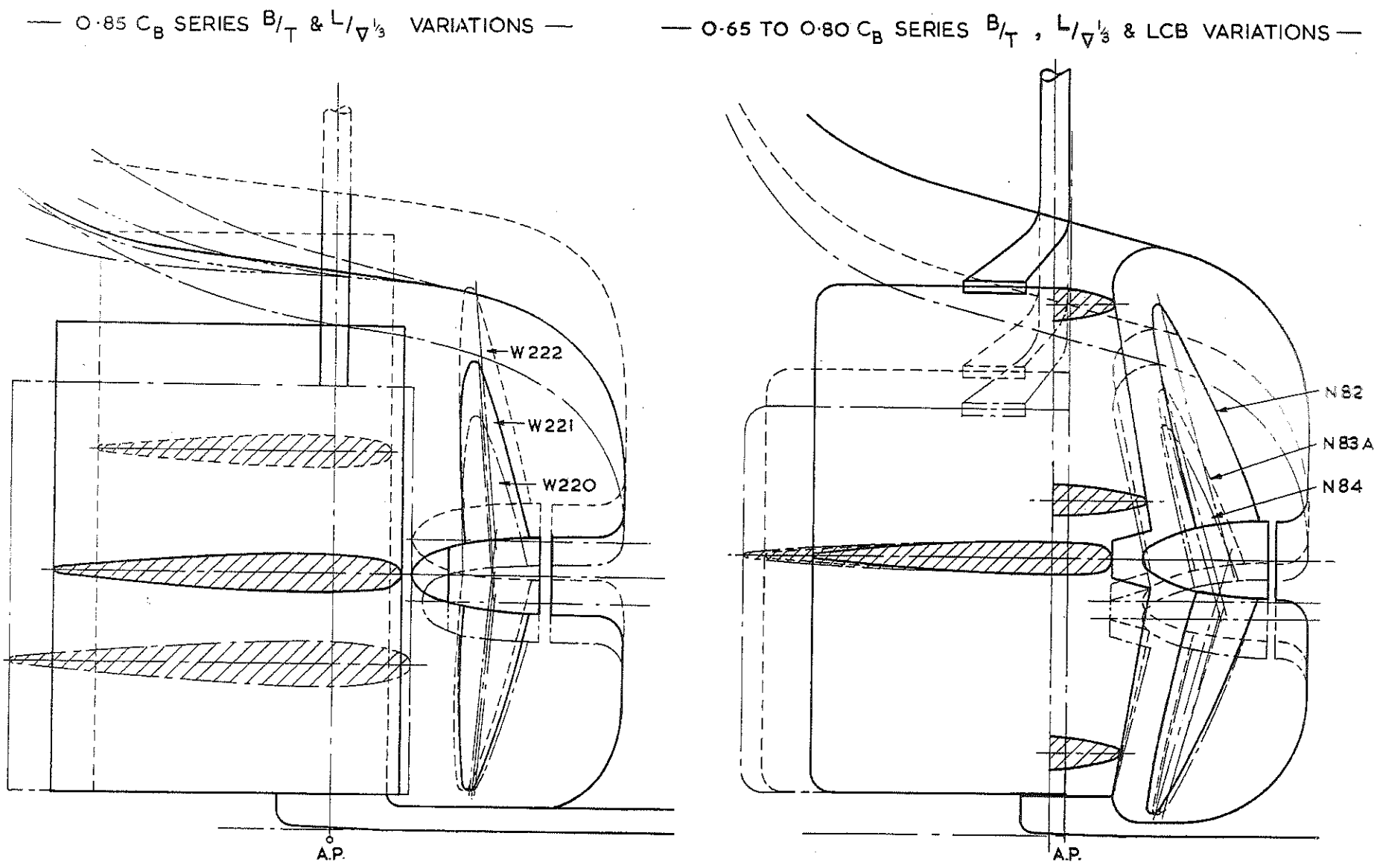

Fig. 81—Modified Stern Arrangements to Suit the Different Diameters of Propellers Tested.

— 0·55 & 0·60 C_B SERIES B/T & $L/\nabla^{1/3}$ VARIATIONS —

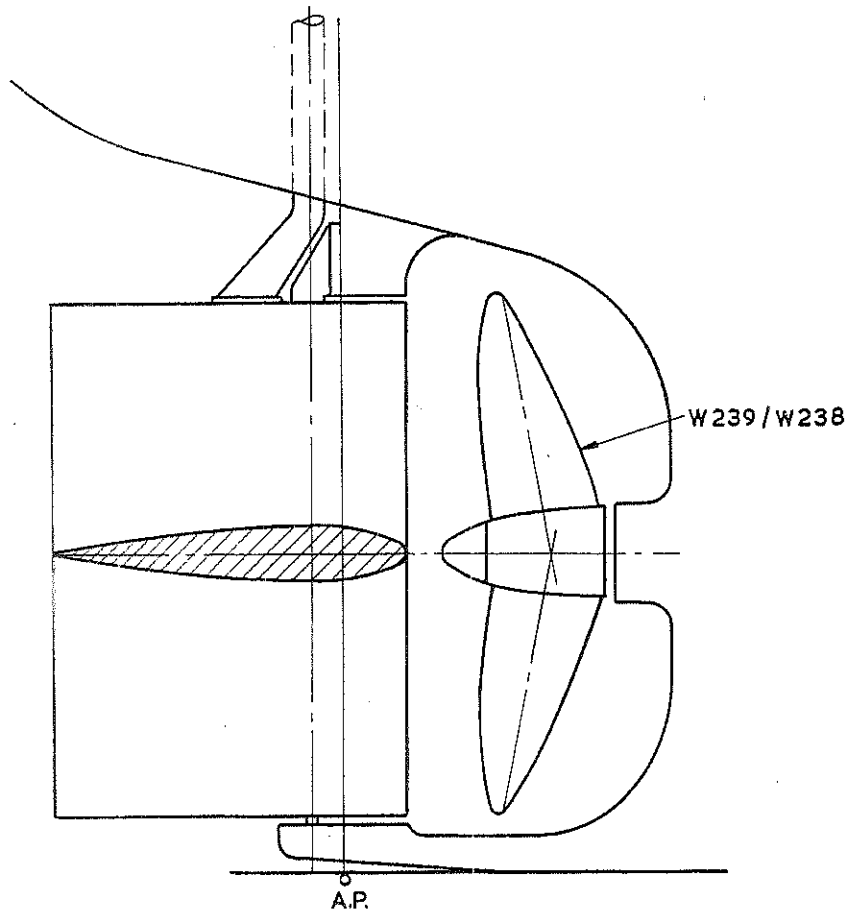

— 0·85 C_B SERIES LCB VARIATIONS —

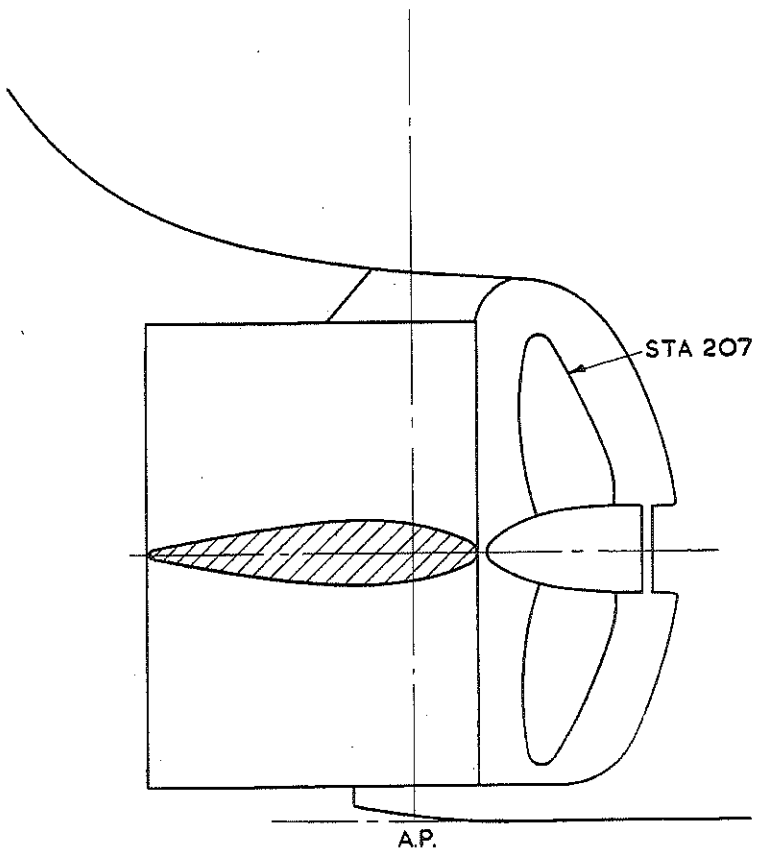

Fig. 82—Other Stern Arrangements.

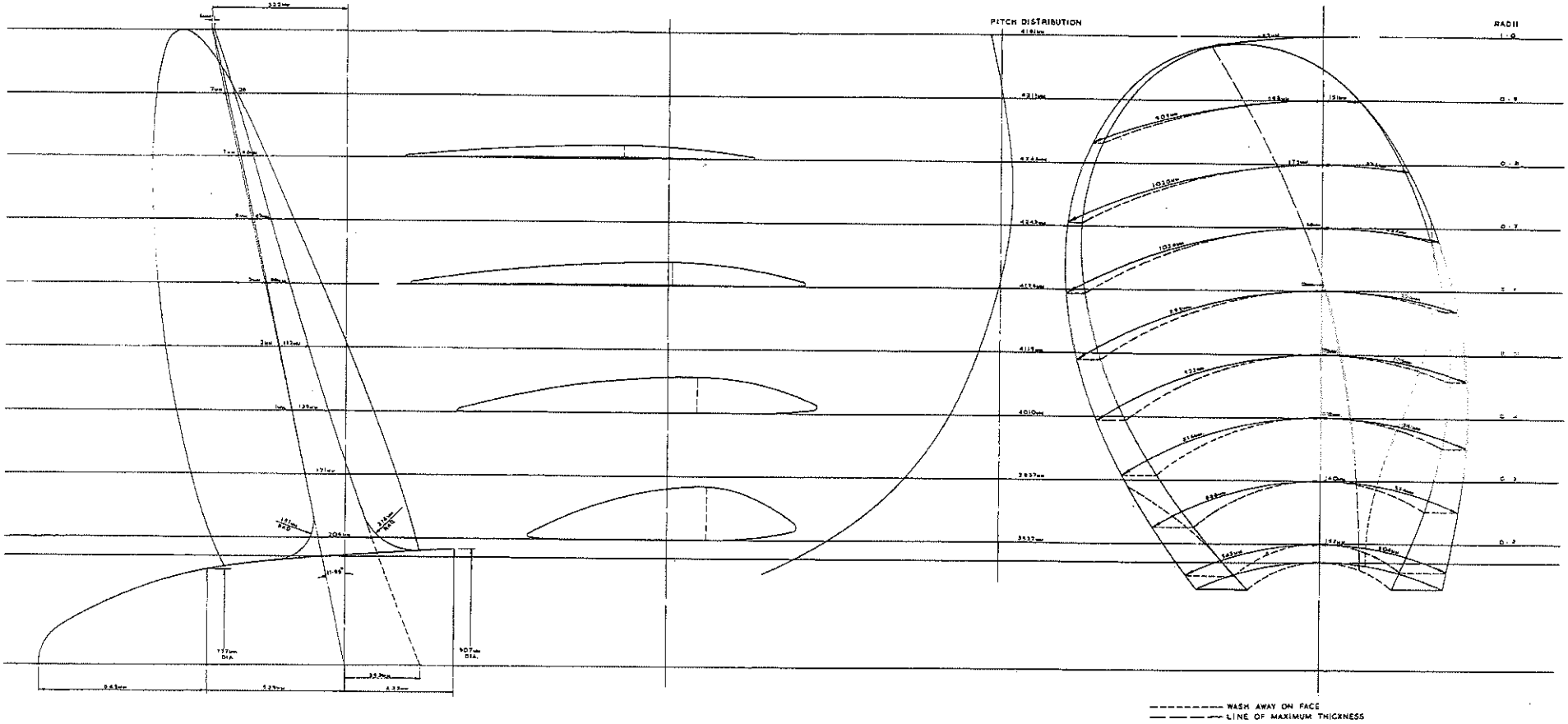

Fig. 83—Details of Four-Bladed Propeller, 4·93-m Diameter × 4·17-m Mean Pitch, Scimitar Design.

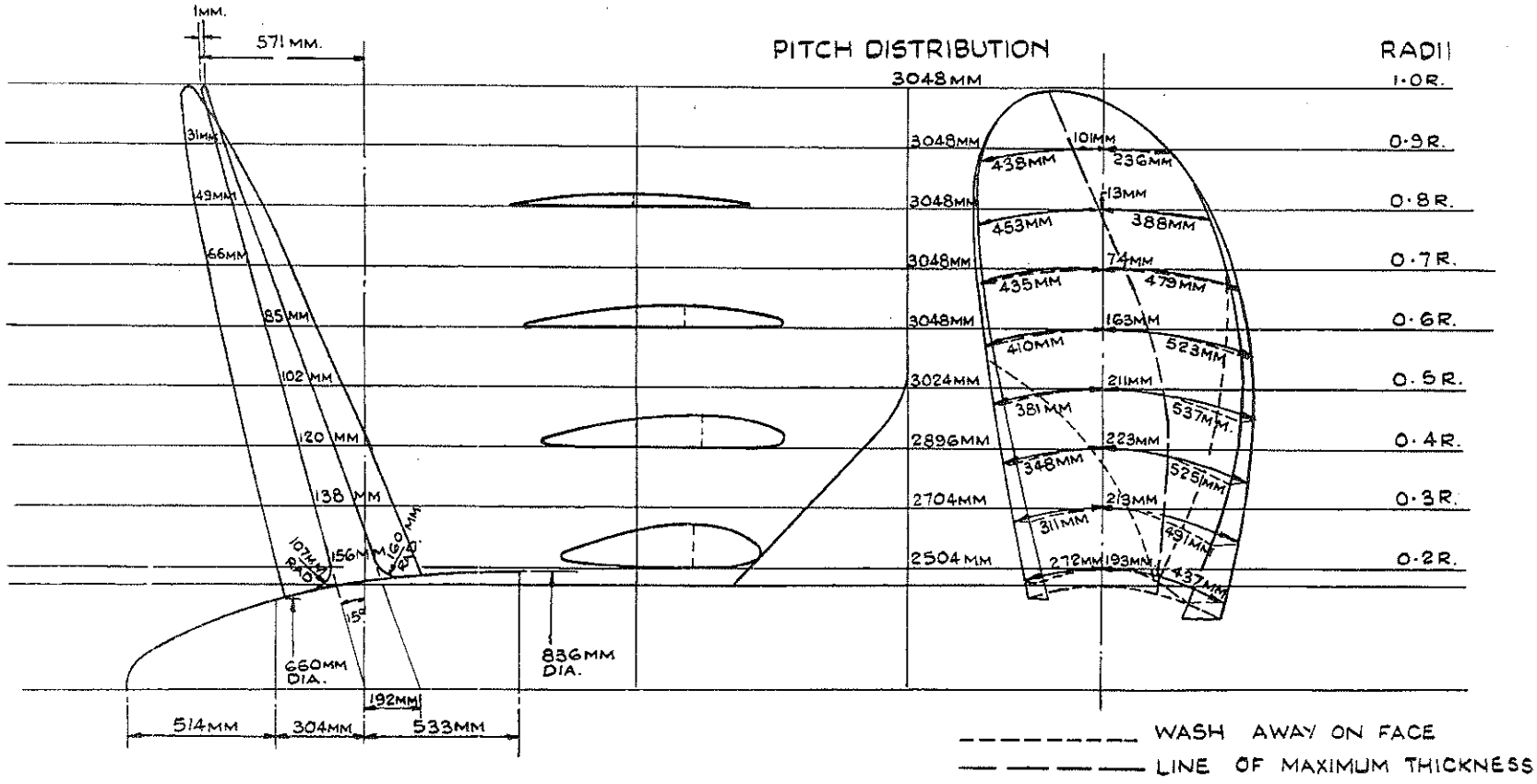

Fig. 84—Details of Four-Bladed Propeller, 4·27-m Diameter × 3·0-m Mean Pitch, Troost Design.

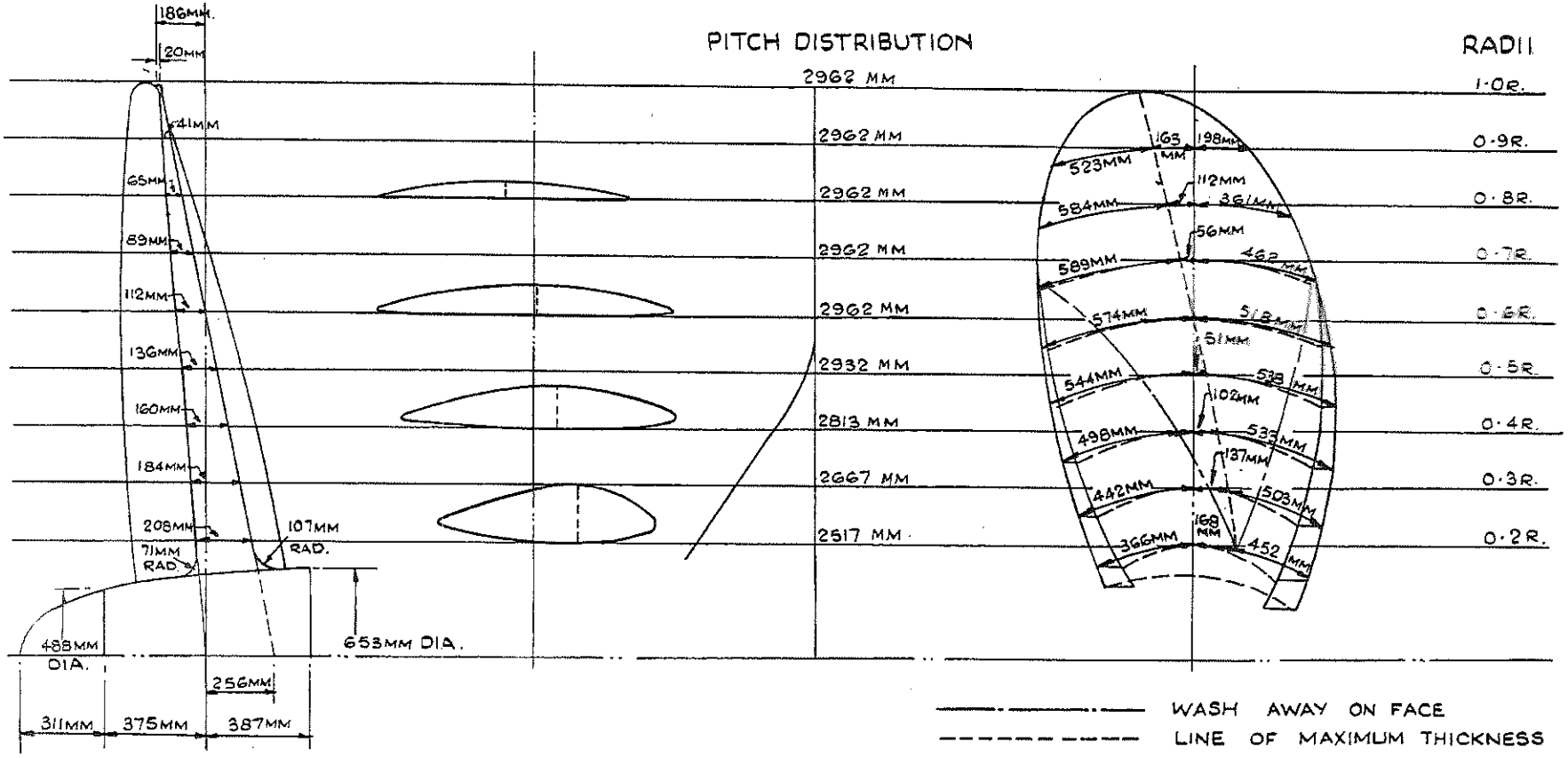

Fig. 85—Details of Five-Bladed Propeller, 4·26-m Diameter × 2·91-m Mean Pitch, NPL Design.

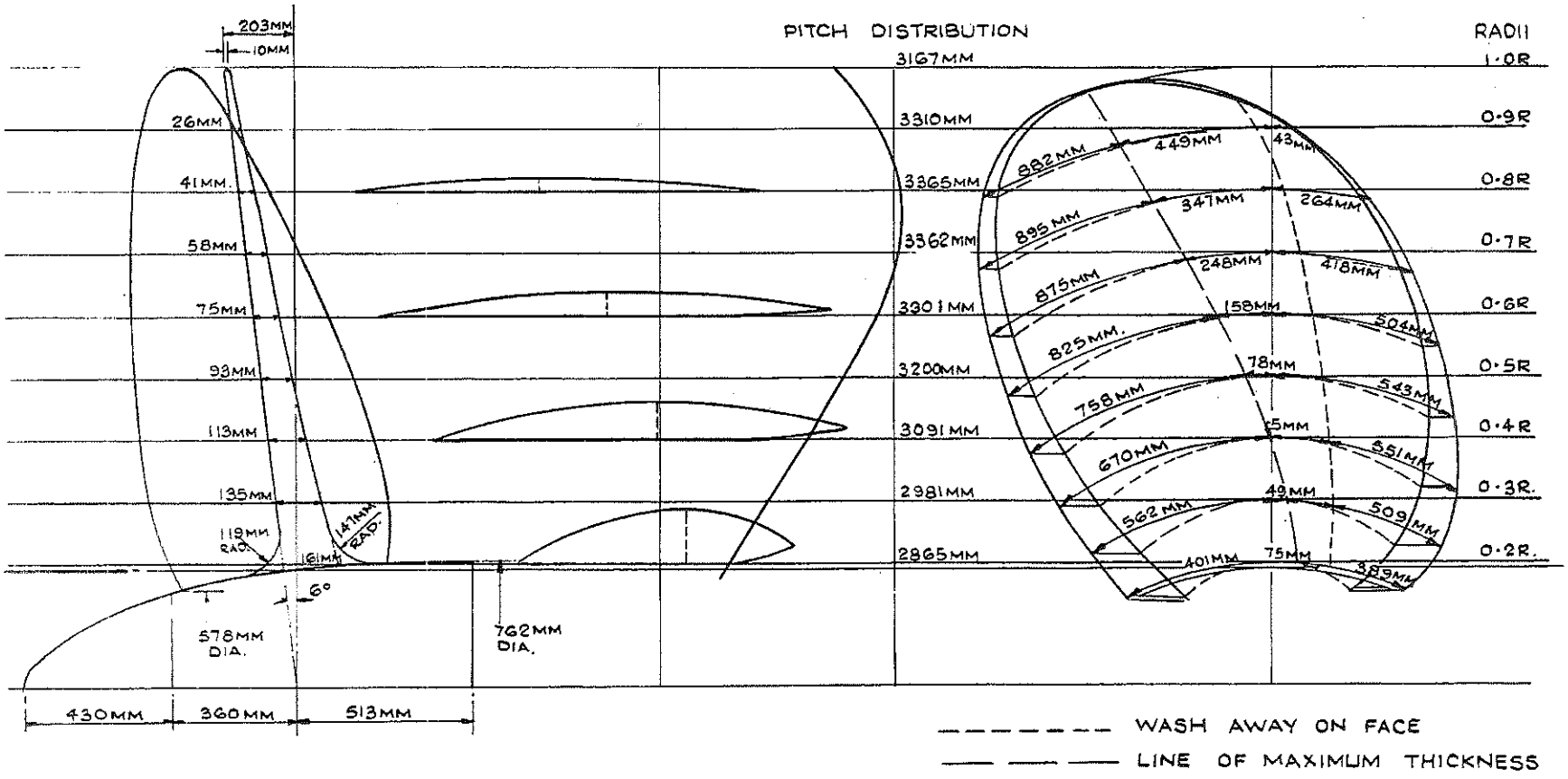

Fig. 86—Details of Five-Bladed Propeller, 3·7-m Diameter × 3·26-m Mean Pitch, Heliston Design.

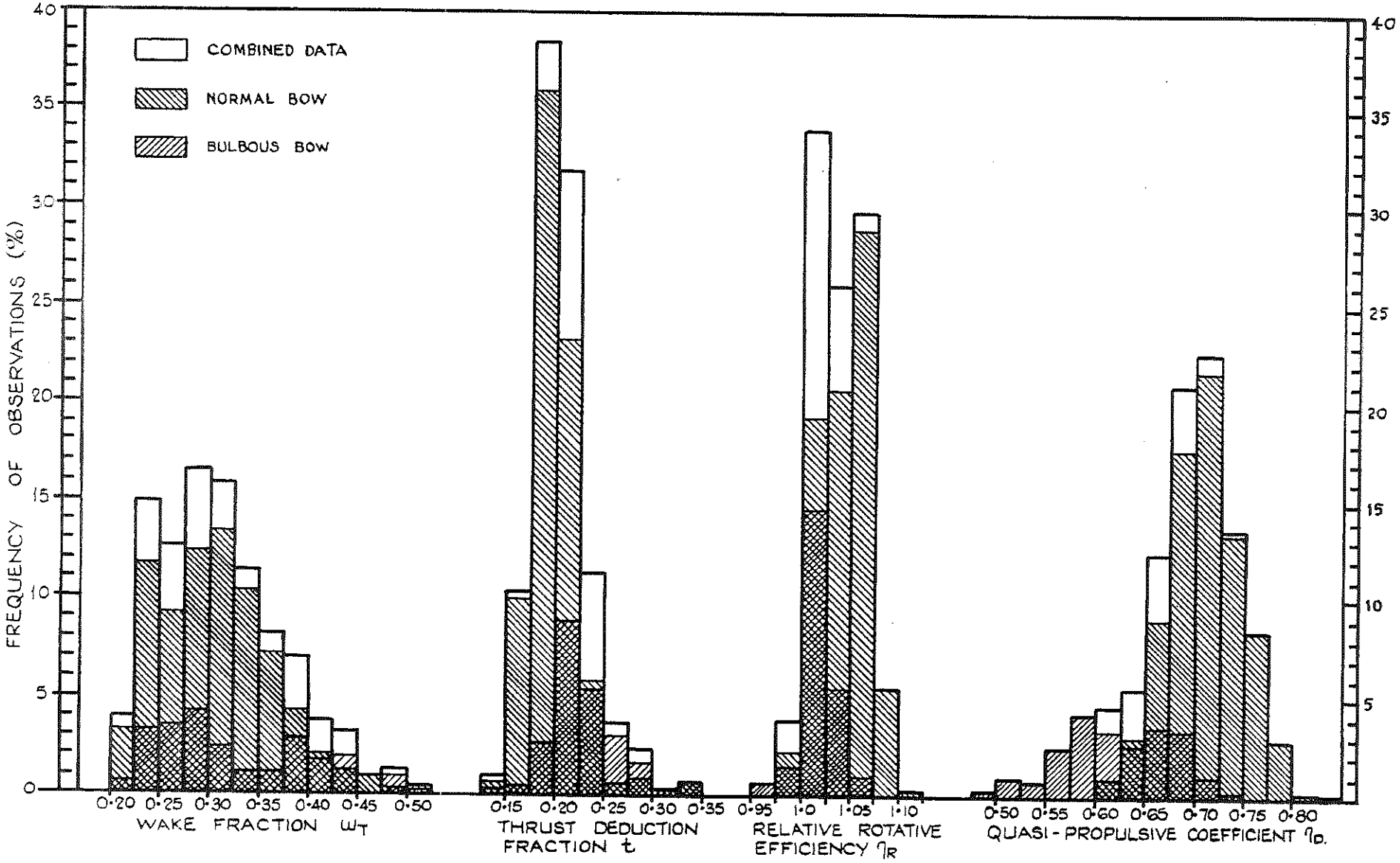

Fig. 87—Frequency Distributions of B.S.R.A. Propulsion Factors w_T, t, η_R, η_D.

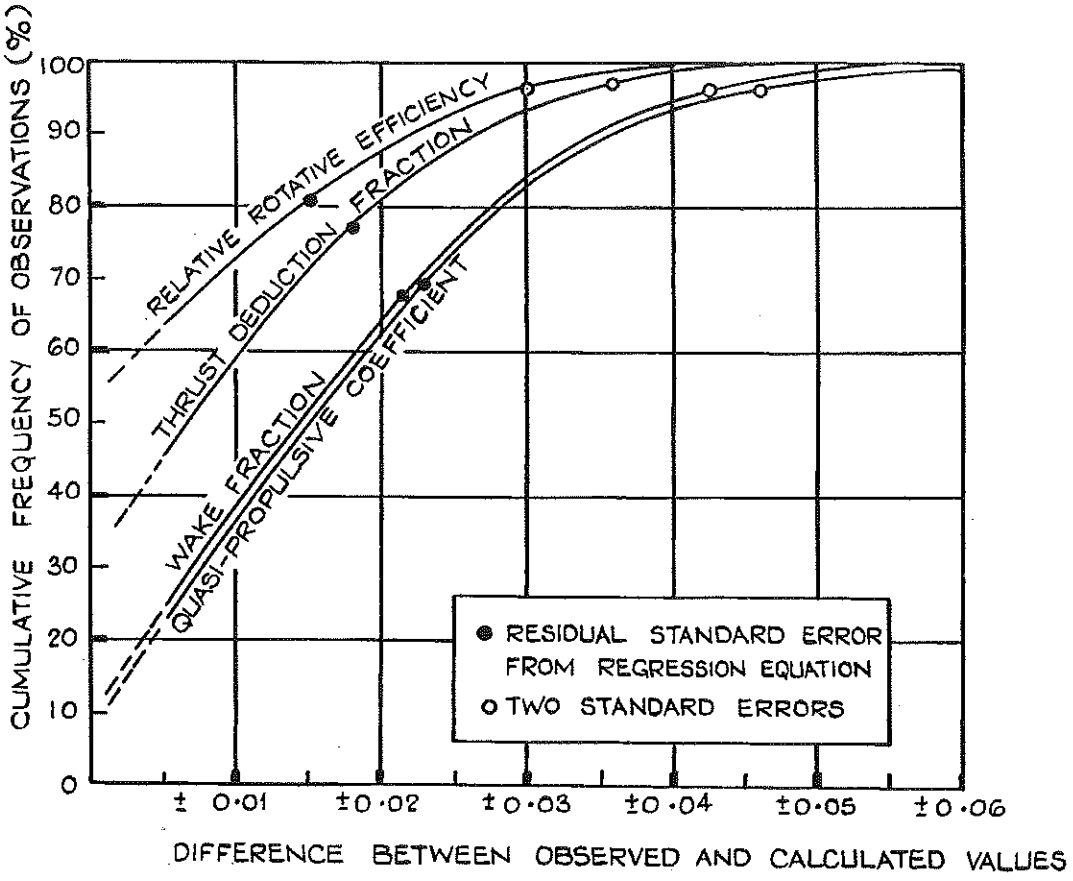

Fig. 88—Cumulative Frequency Diagram Showing Differences Between Calculated w_T, t, η_R, η_D Values and Experimental Results.

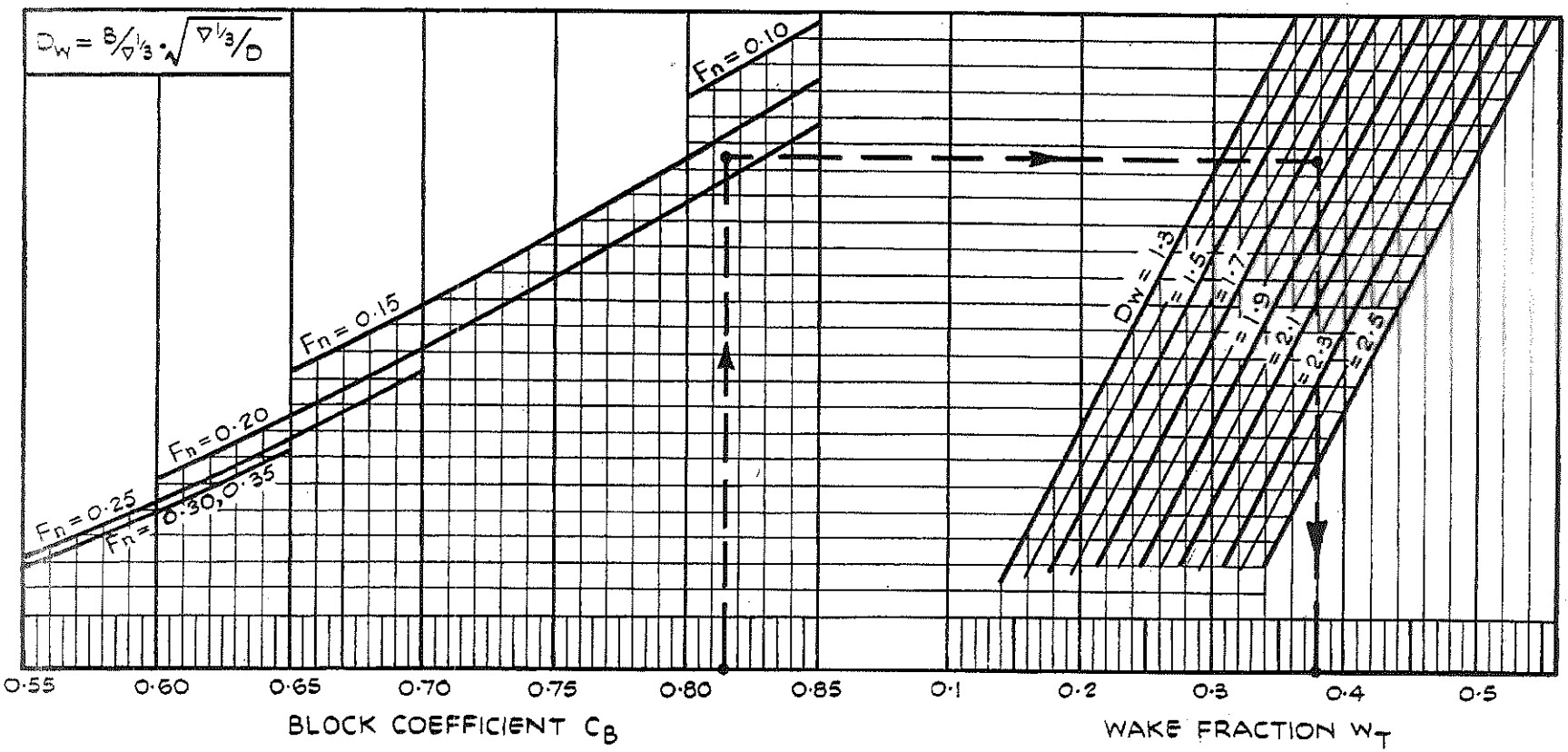

Fig. 89—Diagram for Estimating Wake Fraction.

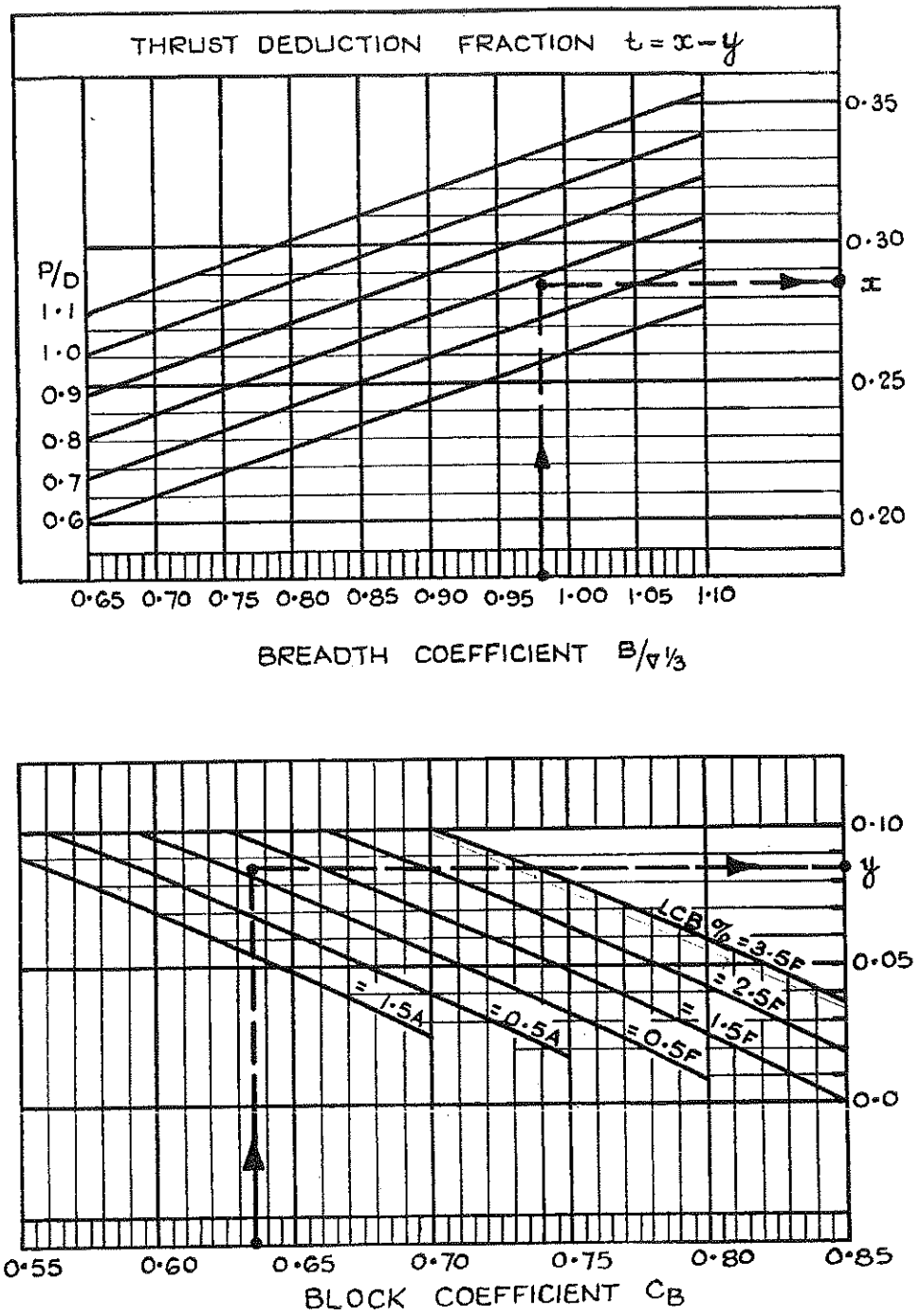

Fig. 90—Diagram for Estimating Thrust-Deduction Fraction.

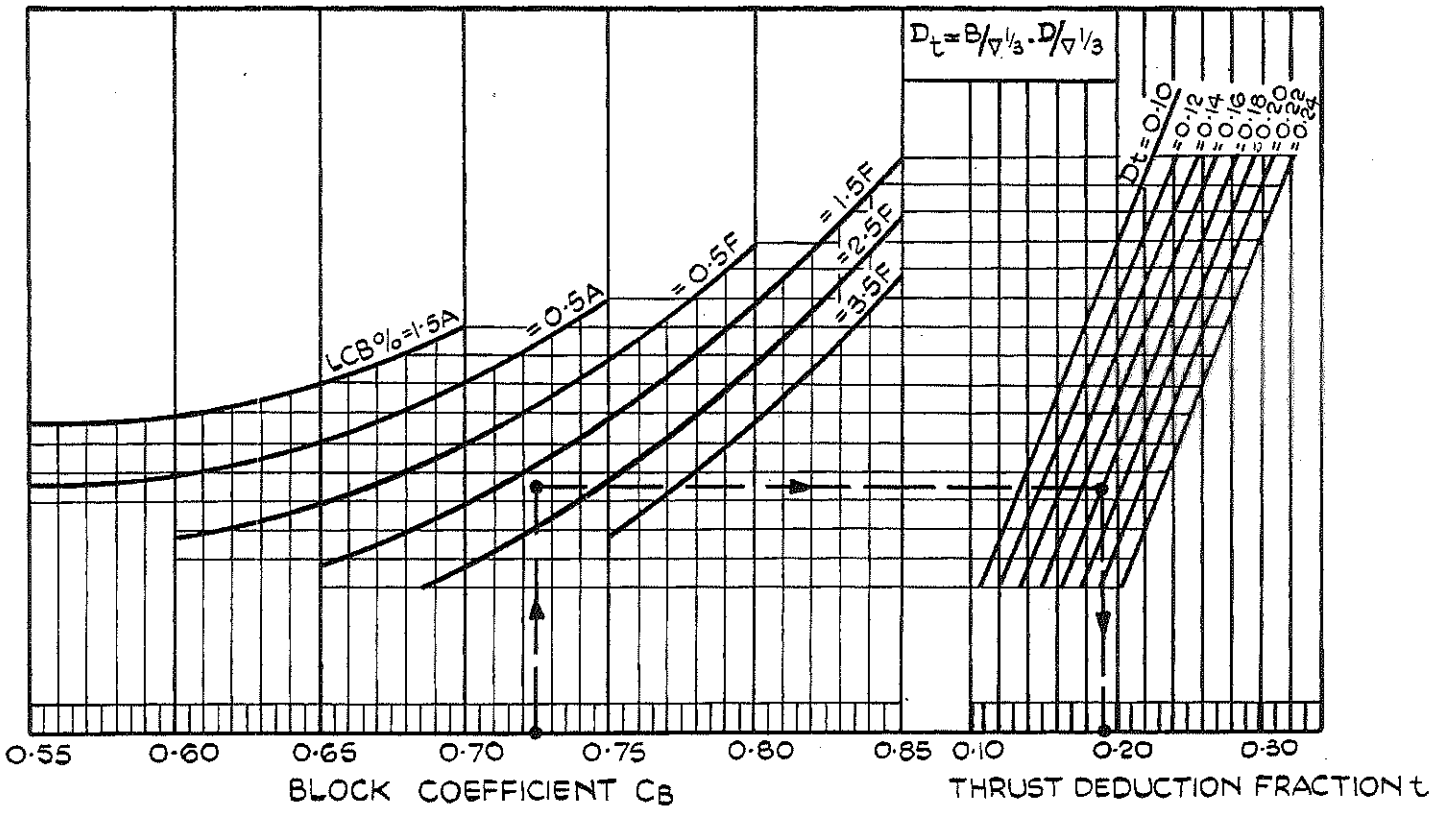

Fig. 91—Alternative Diagram for Estimating Thrust-Deduction Fraction.

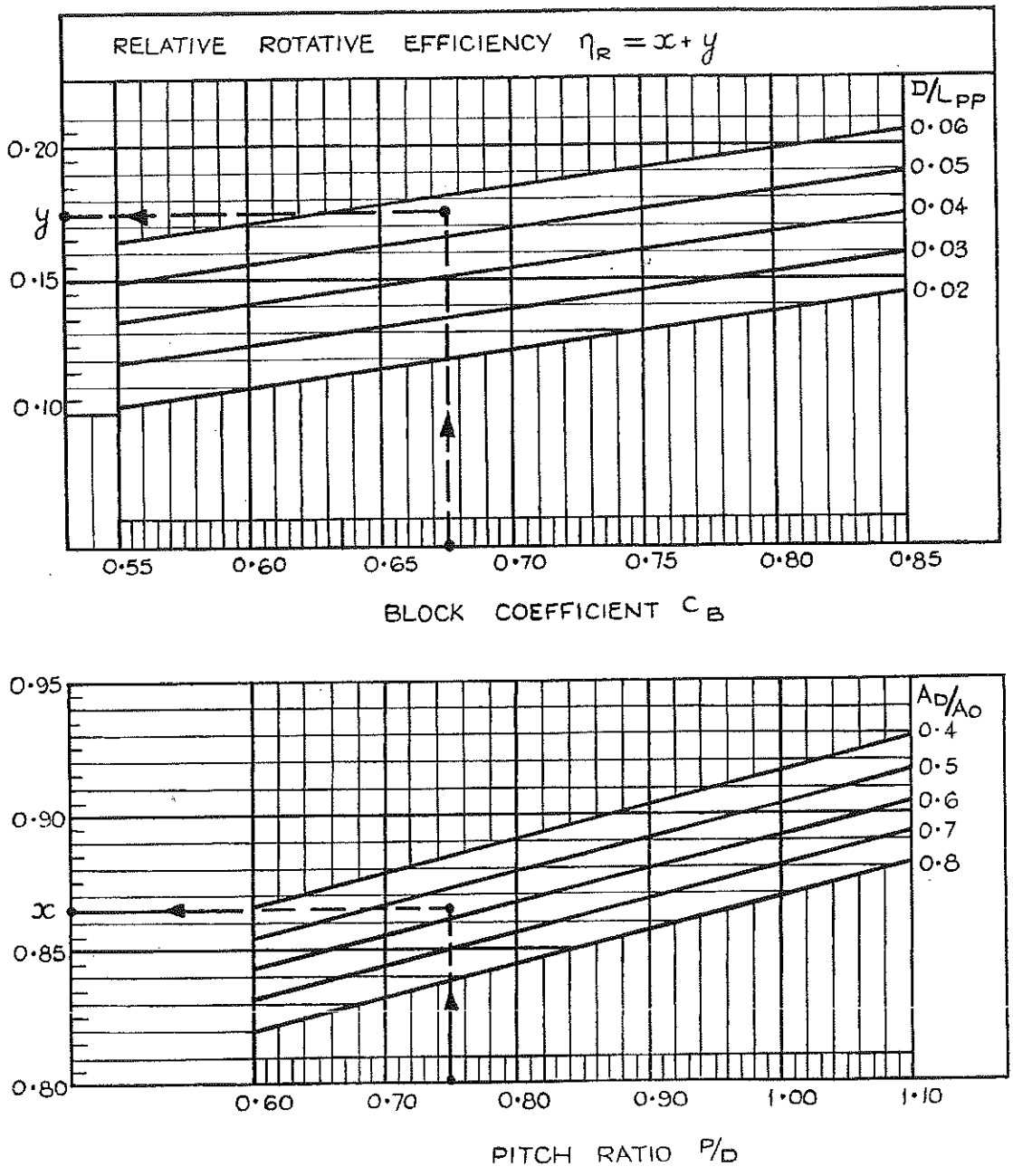

Fig. 92—Diagram for Estimating Relative Rotative Efficiency.

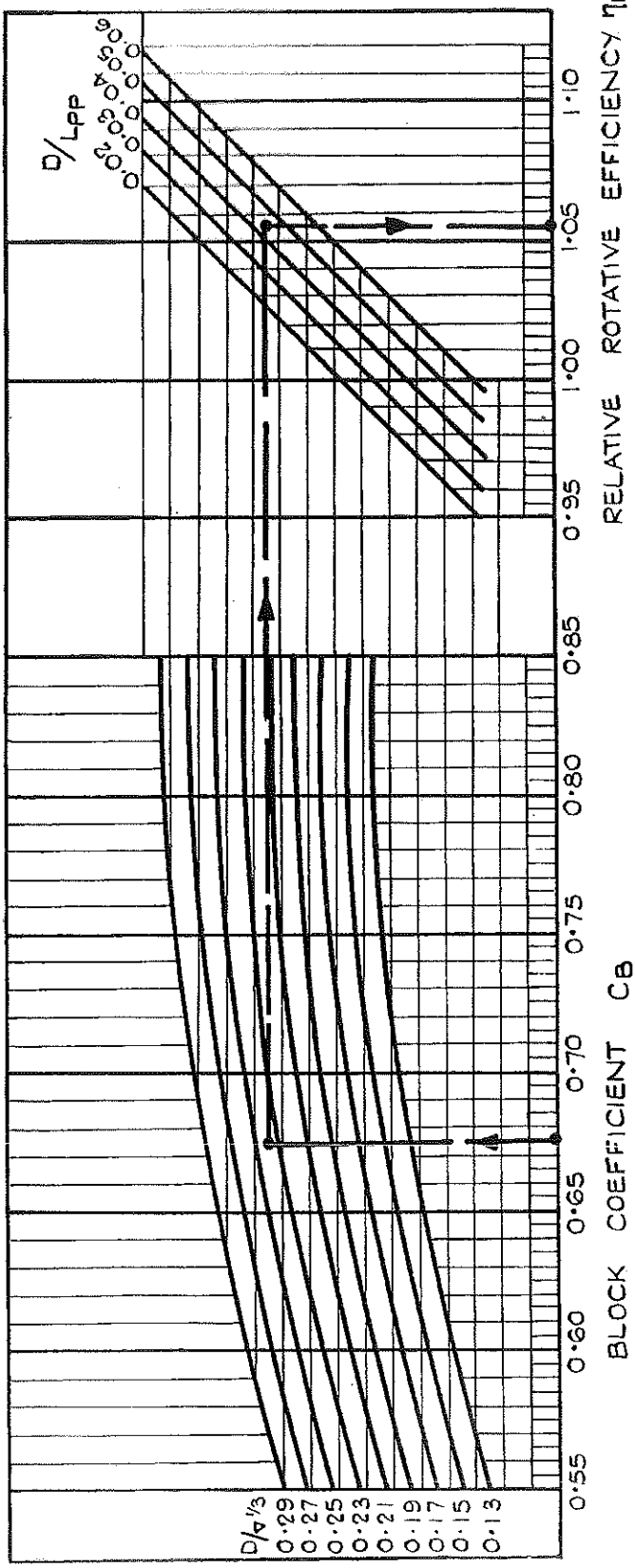

Fig. 93—Alternative Diagram for Estimating Relative Rotative Efficiency.

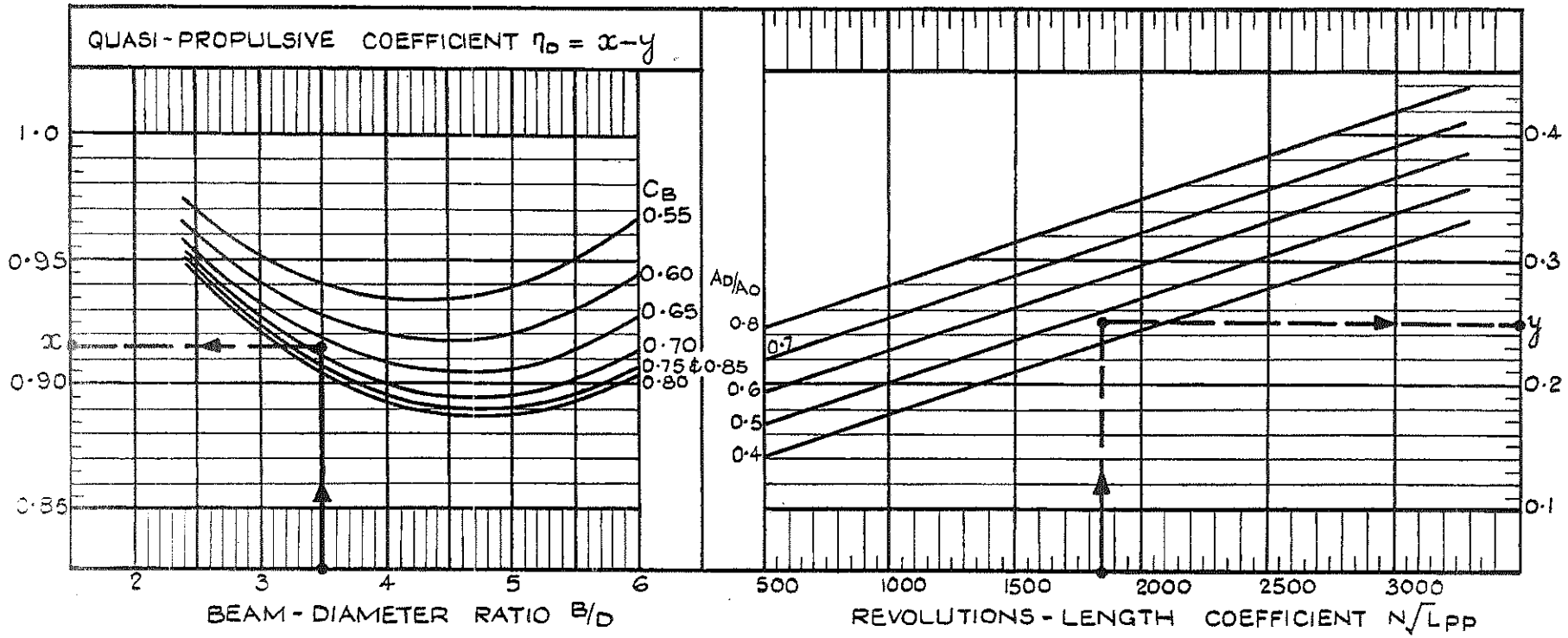

Fig. 94—Diagram for Estimating Quasi-Propulsive Coefficient.

APPENDIX I

FORMULAE FOR PROPULSION FACTORS*

71 A multiple-regression technique was employed for the analysis of the propeller-hull interaction factors.

72 The sets of equations in which all coefficients were found significant at the 0·1% level of probability were examined and those considered the best in terms of residual standard errors and Student's t-test values for wake fraction, thrust-deduction fraction, relative rotative efficiency and quasi-propulsive coefficient are given below. The last term in each equation is the residual standard error of the equation. Details of the individual standard errors of the coefficients are given in parentheses so that a measure of the reliability of each coefficient may be obtained. The multiple correlation coefficient (R) for each equation is also given.

(1) WAKE FRACTION

73 The minimum and maximum wake values were 0·204 and 0·518 respectively, with a mean of 0·311. The standard deviation of the experiment results was ± 0·063.

74 The regression equation finally adopted for wake fraction is as follows

$$w_T = a_1 C_B^2 + a_2 D_W + a_3 F_n + a_4 F_n^2 + a_5 \pm 0{\cdot}021. \quad \mathbf{(R = 0{\cdot}940)} \qquad (1)$$

where
$a_1 = 0{\cdot}3745$ $(0{\cdot}8989 \times 10^{-2})$
$a_2 = 0{\cdot}1590$ $(0{\cdot}3388 \times 10^{-2})$
$a_3 = -0{\cdot}8635$ $(0{\cdot}1022)$
$a_4 = 1{\cdot}4773$ $(0{\cdot}2129)$
$a_5 = -0{\cdot}0458$

(2) THRUST-DEDUCTION FRACTION

75 The minimum and maximum values of thrust-deduction fraction were 0·139 and 0·335 respectively with a mean of 0·204. The standard deviation of the experiment results was ±0·029.

76 Two equations are presented (2) and (3), equation (3) being an alternative to the preferred expression (2) if the pitch ratio of the propeller is not available.

It should be noted that when the LCB position is forward of midships its value is considered positive.

$$t = b_1 C_B^2 + b_2 C_B \, LCB/L_{PP} + b_3 B/\nabla^{1/3} + b_4 P/D + b_5 \pm 0{\cdot}018. \quad \mathbf{(R = 0{\cdot}784)} \qquad (2)$$

$$t = b_6 C_B + b_7 C_B^2 + b_8 LCB/L_{PP} + b_9 D_t + b_{10} \pm 0{\cdot}020. \quad \mathbf{(R = 0{\cdot}732)} \qquad (3)$$

where
$b_1 = 0{\cdot}3246$ $(0{\cdot}1044 \times 10^{-1})$
$b_2 = -2{\cdot}1504$ $(0{\cdot}1035)$
$b_3 = 0{\cdot}1705$ $(0{\cdot}8190 \times 10^{-2})$
$b_4 = 0{\cdot}1504$ $(0{\cdot}6854 \times 10^{-2})$
$b_5 = -0{\cdot}2064$

---

* *A glossary of the statistical terms used in this Appendix will be found on p. 136*

$b_6 = -1{\cdot}6837$ $(0{\cdot}1323)$

$b_7 = 1{\cdot}4935$ $(0{\cdot}9119 \times 10^{-1})$

$b_8 = -1{\cdot}6625$ $(0{\cdot}8585 \times 10^{-1})$

$b_9 = 0{\cdot}6688$ $(0{\cdot}3619 \times 10^{-1})$

$b_{10} = 0{\cdot}5352$

(3) RELATIVE ROTATIVE EFFICIENCY

77 The minimum and maximum values of relative rotative efficiency were 0·965 and 1·103 respectively with a mean of 1·036. The standard deviation of the experiment results was ±0·025.

78 Two equations are presented (4) and (5), equation (5) being an alternative to the preferred expression (4) if the blade area ratio and pitch ratio are not available.

$$\eta_R = c_1 C_B + c_2 D/L_{PP} + c_3 P/D + c_4 A_D/A_O + c_5 \pm 0{\cdot}015. \quad \mathbf{(R = 0{\cdot}781)} \qquad (4)$$

$$\eta_R = c_6 C_B + c_7 C_B{}^2 + c_8 D/L_{PP} + c_9 D/\nabla^{1/3} + c_{10} \pm 0{\cdot}016. \quad \mathbf{(R = 0{\cdot}757)} \qquad (5)$$

where $c_1 = 0{\cdot}1338$ $(0{\cdot}7887 \times 10^{-2})$

$c_2 = 1{\cdot}5188$ $(0{\cdot}1361)$

$c_3 = 0{\cdot}1240$ $(0{\cdot}9209 \times 10^{-2})$

$c_4 = -0{\cdot}1152$ $(0{\cdot}6704 \times 10^{-2})$

$c_5 = 0{\cdot}8372$

$c_6 = 0{\cdot}8443$ $(0{\cdot}1070)$

$c_7 = -0{\cdot}5054$ $(0{\cdot}7614 \times 10^{-1})$

$c_8 = 1{\cdot}1511$ $(0{\cdot}1786)$

$c_9 = 0{\cdot}4718$ $(0{\cdot}3934 \times 10^{-1})$

$c_{10} = 0{\cdot}5524$

(4) QUASI-PROPULSIVE COEFFICIENT

79 The minimum and maximum values for quasi-propulsive coefficient were 0·493 and 0·836 respectively with a mean of 0·690. The standard deviation of the experiment results was ±0·055.

80 The regression equation finally adopted for quasi-propulsive coefficient is as follows:

$$\eta_D = d_1 C_B\, B/D + d_2\, C_B{}^2 B/D + d_3\,(B/D)^2 + d_4\, N\sqrt{L_{PP}} + d_5\, A_D/A_O + d_6 \pm 0{\cdot}023. \quad \mathbf{(R = 0{\cdot}906)} \qquad (6)$$

where $d_1 = -0{\cdot}2690$ $(0{\cdot}2788 \times 10^{-1})$

$d_2 = 0{\cdot}1686$ $(0{\cdot}1966 \times 10^{-1})$

$d_3 = 0{\cdot}1130 \times 10^{-1}$ $(0{\cdot}1199 \times 10^{-2})$

$d_4 = -0{\cdot}6864 \times 10^{-4}$ $(0{\cdot}2255 \times 10^{-5})$

$d_5 = -0{\cdot}2627$ $(0{\cdot}8204 \times 10^{-2})$

$d_6 = 1{\cdot}1426$

GLOSSARY OF STATISTICAL TERMS

Variance, s^2

Variance is defined as the total sum of squares of the deviations of the observations y_i from their arithmetic mean $\bar{y}$, divided by $n - 1$ observations.

$$s^2 = \frac{1}{n-1} \sum_{i=1}^{n} (y_i - \bar{y})^2$$

Standard Deviation, s

Standard deviation is the positive square root of the variance.

Multiple Correlation Coefficient, R

The square of the multiple correlation coefficient, R^2 is the proportion of the total sum of squares

$$\sum_{i=1}^{n} (y_i - \bar{y})^2$$

which is accounted for by the regression equation.

Residual Standard Error, s_r

$$s_r = \left[\frac{1}{n-p-1} \sum_{i=1}^{n} (y_i - y_i')^2 \right]^{1/2}$$

where y_i' are values of the dependent variable obtained from the regression equation.

p is the number of independent variables in the regression equation.

For large n, $s_r = s\sqrt{1 - R^2}$

Student's t-statistic

The t-statistic for an independent variable is the ratio of its regression coefficient to the standard error of this coefficient. The contribution of a particular independent variable to the regression equation is considered significant, at a certain probability level, if its t-statistic exceeds the appropriate percentage point of the t distribution. These values are given in 'Biometrika Tables for Statisticians', by E. S. Pearson and H. O. Hartley, Cambridge University Press, London.

APPENDIX II

WORKED EXAMPLE: SHIP GEOMETRY

To determine the Methodical Series Lines for a 250 000-tonnes d.w. tanker

81 The vessel is required to have the following dimensions:-
330-m L_{PP} × 52-m moulded beam × 20-m moulded draught, 293 750 tonnes displacement, and LCB position 8·25m forward of midships.

Required Block Coefficient

$$C_B = \frac{293\,750}{330 \times 52 \times 20 \times 1{\cdot}025} = \mathbf{0{\cdot}835}$$

Deviation of LCB from Basis Position

Required LCB as percentage of L_{PP} forward of midships

$$= \frac{8{\cdot}25}{330} \times 100 = \mathbf{2{\cdot}5\%}$$

Basis LCB position = 2% L_{PP} forward of midships.

Deviation from basis = 2·5 — 2 = **0·5%** L_{PP} forward.

Adjustment of Basis Form to give Required LCB position

82 This is effected by a shift of the stations at which the waterline offsets are laid off. The shift of station (per cent L_{PP}) to give one per cent L_{PP} movement of LCB is given in Fig. 62. To give the required shift of stations in metres, these values must be multiplied by the factor

$$\text{(required movement)} \times \frac{L_{PP}}{100}$$

In this example $0{\cdot}5 \times \frac{330}{100} = \mathbf{1{\cdot}65}$.

83 Enter Fig. 62 at $C_B = 0{\cdot}835$, lift the shift of each station for one per cent movement, and multiply by the above factor, 1·65 as in Table 10. These shifts should be plotted and a curve of shifts run in.

Laying Out the Grid

84 Set out the equi-spaced displacement stations 0 to 10. For the half-breadth plan, add the auxiliary stations, shown as 0a, 1a, 2a, etc., in Fig. 95, displaced from the stations 0, 1, 2, etc., by the shifts determined above. Draw in the standard waterlines on the profile. These correspond to the A, B, C, ... , K waterlines which are percentages of the standard load draught, and their spacing must be adjusted in the ratio of the actual design load draught.

85 In this example the waterline heights corresponding to the load draught of 20 m are given in Table 11.

TABLE 10

Station	Shift of station in per cent L_{PP} for 1 per cent movement of LCB (from Fig. 62)	Shift of station in metres for 0·5 per cent L_{PP} movement of LCB
AP 0	0·16	0·264
1/4	0·35	0·578
1/2	0·61	1·007
3/4	0·91	1·502
1	1·17	1·931
1 1/2	1·62	2·673
2	1·94	3·201
2 1/2	2·09	3·449
3	2·15	3·548
3 1/2	2·18	3·597
4	2·18	3·597
5	2·18	3·597
6	2·18	3·597
6 1/2	2·18	3·597
7	2·18	3·597
7 1/2	2·18	3·597
8	2·18	3·597
8 1/2	2·09	3·449
9	1·77	2·921
9 1/4	1·48	2·442
9 1/2	1·08	1·782
9 3/4	0·63	1·040
FP 10	0·18	0·297

TABLE 11

Waterline	A	B	C	D	E	F	G	$H_{(LWL)}$	J	K
Height above keel expressed as percentage of load draught	7·69	15·38	23·08	38·46	53·85	69·23	84·62	100·0	115·38	130·77
Height above keel for load draught = 20m	1·54	3·08	4·62	7·69	10·77	13·85	16·92	20·0	23·08	26·15

Stem Profile

86 Fig. 51 gives the bulbous stem-profile offsets as percentages of L_{PP} relative to Station 10. Lift the offsets, given in Table 12, appropriate to the required block coefficient, i.e. $C_B = 0·835$, and lay off the profile. This profile applies to the basis LCB position. In this example the change in LCB is small and the basis profile has been used. In general, the fore-and-aft shifts of profile at any point to give the profile for the required LCB are obtained from the curve of shifts.

TABLE 12

Waterline	A	B	C	D	E	F	G	$H_{(LWL)}$	J	K
Percentage L_{PP} relative to station 10	0·69	1·17	1·39	1·38	0·91	0·48	0·10	0·0	0·14	0·41
Stem profile (m) relative to station 10	2·28	3·86	4·59	4·55	3·00	1·58	0·33	0·0	0·46	1·35

Stern Profile

87 The effect of the LCB position on the stern profile is small and may be neglected. The offsets taken from Fig. 52 are therefore used directly and are given in Table 13.

TABLE 13

Waterline	A	B	C	D	E	F	G	$H_{(LWL)}$	J	K
Percentage L_{PP} relative to station 0	1·48	1·67	1·78	1·80	1·63	0·48	—2·38	—3·00	—3·26	—3·43
Stern profile (m) relative to station 0	4·88	5·51	5·87	5·94	5·38	1·58	—7·85	—9·90	—10·76	—11·32

Waterline height above keel as percentages of load draught are as follows:-

Station 0 : 70·5%, i.e. **14·10m**

Station $-1/4$: 86·6%, i.e. **17·32m**.

Half-Breadth Plan

88 Enter Figs. 33 to 50 for the bulbous form at the required block coefficient i.e. $C_B = 0{\cdot}835$, and lift the offsets for the standard waterlines marked A, B, C, etc., on the diagrams, these being the levels corresponding to the standard load draught of 6·71m.

89 These offsets, the figures in parentheses in Table 14, are in terms of the full half-breadth and require to be multiplied by the full half-breadth (52m ÷ 2 = 26m) to give the actual offsets also listed in Table 14.

90 These offsets must be laid off at the auxiliary stations to give the required LCB position. The waterlines may then be run in.

Body Plan

91 Transfer the waterline offsets lifted at the displacement stations in the half-breadth plan to the standard waterlines in the body plan and draw in the body sections.

TABLE 12

Waterline	A	B	C	D	E	F	G	$H_{(LWL)}$	J	K
Percentage L_{PP} relative to station 10	0·69	1·17	1·39	1·38	0·91	0·48	0·10	0·0	0·14	0·41
Stem profile (m) relative to station 10	2·28	3·86	4·59	4·55	3·00	1·58	0·33	0·0	0·46	1·35

Stern Profile

87 The effect of the LCB position on the stern profile is small and may be neglected. The offsets taken from Fig. 52 are therefore used directly and are given in Table 13.

TABLE 13

Waterline	A	B	C	D	E	F	G	$H_{(LWL)}$	J	K
Percentage L_{PP} relative to station 0	1·48	1·67	1·78	1·80	1·63	0·48	—2·38	—3·00	—3·26	—3·43
Stern profile (m) relative to station 0	4·88	5·51	5·87	5·94	5·38	1·58	—7·85	—9·90	—10·76	—11·32

Waterline height above keel as percentages of load draught are as follows:-

Station 0 : 70·5%, i.e. **14·10m**

Station $-\frac{1}{4}$: 86·6%, i.e. **17·32m.**

Half-Breadth Plan

88 Enter Figs. 33 to 50 for the bulbous form at the required block coefficient i.e. $C_B = 0{\cdot}835$, and lift the offsets for the standard waterlines marked A, B, C, etc., on the diagrams, these being the levels corresponding to the standard load draught of 6·71m.

89 These offsets, the figures in parentheses in Table 14, are in terms of the full half-breadth and require to be multiplied by the full half-breadth (52m ÷ 2 = 26m) to give the actual offsets also listed in Table 14.

90 These offsets must be laid off at the auxiliary stations to give the required LCB position. The waterlines may then be run in.

Body Plan

91 Transfer the waterline offsets lifted at the displacement stations in the half-breadth plan to the standard waterlines in the body plan and draw in the body sections.

Table of Offsets

92 The offsets at the standard waterlines are given in Table 15. In practice it may be preferable to lift a set of offsets from the body plan at waterlines spaced in metres.

Check on Overall Accuracy of the Method

93 To check the accuracy of the method, the displacement and LCB position of the derived form have been calculated from the offsets using the B.S.R.A. hydrostatics computer program.

The results are as follows:-

Load displacement = 293 200 tonnes
(specified displacement = 293 750 tonnes; error 0·2%).

LCB position from midships = 8·16m or 2·47% L_{pp} forward of midships (specified position 8·25 m or 2·5 per cent forward; error 0·03% L_{pp}).

TABLE 14

Table of Waterline Offsets Corresponding to Auxiliary Stations
(Figures in parentheses are offsets in terms of the full half-breadth, other figures are actual offsets in metres.)

Waterline	Flat of bottom	A	B	C	D	E	F	G	$H_{(LWL)}$	J	K
Height above keel for load draught 20m		1·54	3·08	4·62	7·69	10·77	13·85	16·92	20·00	23·08	26·15
AP 0	— —	— —	— —	— —	— —	— —	(0·015) 0·39	(0·233) 6·06	(0·342) 8·89	(0·415) 10·79	(0·468) 12·17
¼	(0·021) 0·55	(0·023) 0·60	(0·025) 0·65	(0·031) 0·81	(0·040) 1·04	(0·070) 1·82	(0·204) 5·30	(0·385) 10·01	(0·496) 12·90	(0·574) 14·92	(0·630) 16·38
½	(0·024) 0·62	(0·073) 1·90	(0·104) 2·70	(0·132) 3·43	(0·178) 4·63	(0·247) 6·42	(0·379) 9·85	(0·522) 13·57	(0·621) 16·15	(0·692) 17·99	(0·744) 19·34
¾	(0·032) 0·83	(0·154) 4·00	(0·206) 5·36	(0·249) 6·47	(0·328) 8·53	(0·416) 10·82	(0·528) 13·73	(0·641) 16·67	(0·727) 18·90	(0·796) 20·70	(0·850) 22·10
1	(0·073) 1·90	(0·247) 6·42	(0·318) 8·27	(0·377) 9·80	(0·477) 12·40	(0·570) 14·82	(0·668) 17·37	(0·755) 19·63	(0·822) 21·37	(0·879) 22·85	(0·919) 23·89
1½	(0·210) 5·46	(0·471) 12·25	(0·561) 14·59	(0·626) 16·28	(0·730) 18·98	(0·805) 20·93	(0·861) 22·39	(0·898) 23·35	(0·932) 24·23	(0·959) 24·93	(0·981) 25·51
2	(0·436) 11·34	(0·681) 17·71	(0·763) 19·84	(0·817) 21·24	(0·893) 23·22	(0·938) 24·39	(0·962) 25·01	(0·978) 25·43	(0·987) 25·66	(0·992) 25·79	(0·998) 25·95
2½	(0·642) 16·69	(0·832) 21·63	(0·898) 23·35	(0·936) 24·34	(0·974) 25·32	(0·991) 25·77	(0·998) 25·95	(1·000) 26·00	(1·000) 26·00	(1·000) 26·00	(1·000) 26·00
3	(0·788) 20·49	(0·924) 24·02	(0·966) 25·12)	(0·987) 25·66	(1·000) 26·00	(1·000) 26·00	(1·000) 26·00	(1·000) 26·00	(1·000) 26·00	(1·000) 26·00	(1·000) 26·00
3½	(0·848) 22·05	(0·967) 25·14	(0·996) 25·12	(1·000) 26·00	(1·000) 26·00	(1·000) 26·00	(1·000) 26·00	(1·000) 26·00	(1·000) 26·00	(1·000) 26·00	(1·000) 26·00
4	(0·858) 22·31	(0·977) 25·40	(1·000) 26·00	(1·000) 26·00	(1·000) 26·00	(1·000) 26·00	(1·000) 26·00	(1·000) 26·00	(1·000) 26·00	(1·000) 26·00	(1·000) 26·00
5	(0·858) 22·31	(0·977) 25·40	(1·000) 26·00	(1·000) 26·00	(1·000) 26·00	(1·000) 26·00	(1·000) 26·00	(1·000) 26·00	(1·000) 26·00	(1·000) 26·00	(1·000) 26·00
6	(0·858) 22·31	(0·977) 25·40	(1·000) 26·00	(1·000) 26·00	(1·000) 26·00	(1·000) 26·00	(1·000) 26·00	(1·000) 26·00	(1·000) 26·00	(1·000) 26·00	(1·000) 26·00
6½	(0·858) 22·31	(0·977) 25·40	(1·000) 26·00	(1·000) 26·00	(1·000) 26·00	(1·000) 26·00	(1·000) 26·00	(1·000) 26·00	(1·000) 26·00	(1·000) 26·00	(1·000) 26·00
7	(0·858) 22·31	(0·977) 25·40	(1·000) 26·00	(1·000) 26·00	(1·000) 26·00	(1·000) 26·00	(1·000) 26·00	(1·000) 26·00	(1·000) 26·00	(1·000) 26·00	(1·000) 26·00
7½	(0·858) 22·31	(0·977) 25·40	(1·000) 26·00	(1·000) 26·00	(1·000) 26·00	(1·000) 26·00	(1·000) 26·00	(1·000) 26·00	(1·000) 26·00	(1·000) 26·00	(1·000) 26·00
8	(0·842) 21·89	(0·972) 25·27	(0·996) 25·12	(1·000) 26·00	(1·000) 26·00	(1·000) 26·00	(1·000) 26·00	(1·000) 26·00	(1·000) 26·00	(1·000) 26·00	(1·000) 26·00
8½	(0·716) 18·62	(0·884) 22·98	(0·933) 24·26	(0·956) 24·86	(0·967) 25·14	(0·972) 25·27	(0·979) 25·45	(0·991) 25·77	(1·000) 26·00	(1·000) 26·00	(1·000) 26·00
9	(0·483) 12·56	(0·679) 17·65	(0·755) 19·63	(0·797) 20·72	(0·833) 21·66	(0·835) 21·71	(0·840) 21·84	(0·856) 22·26	(0·895) 23·27	(0·942) 24·49	(0·976) 25·38
9¼	(0·312) 8·11	(0·535) 13·91	(0·610) 15·86	(0·646) 16·80	(0·683) 17·76	(0·698) 18·15	(0·699) 18·17	(0·722) 18·77	(0·775) 20·15	(0·838) 21·79	(0·909) 23·63)
9½	(0·143) 3·72	(0·362) 9·41	(0·428) 11·13	(0·478) 12·43	(0·514) 13·36	(0·514) 13·36	(0·514) 13·36	(0·540) 14·04	(0·594) 15·44	(0·662) 17·21	(0·742) 19·29
9¾	(0·030) 0·78	(0·175) 4·55	(0·252) 6·55	(0·294) 7·64	(0·321) 8·35	(0·312) 8·11	(0·290) 7·54	(0·299) 7·77	(0·336) 8·74	(0·389) 10·11	(0·463) 12·04
FP 10	— —	(0·086) 2·24	(0·130) 3·38	(0·157) 4·08	(0·158) 4·11	(0·100) 2·60	(0·053) 1·38	(0·011) 0·29	(0·000) 0·00	(0·024) 0·62	(0·076) 1·98

TABLE 15

Tables of Offsets at Displacement Stations

Waterline	Flat of bottom	A	B	C	D	E	F	G	$H_{(LWL)}$	J	K
Height above keel for load draught 20m		1·54	3·08	4·62	7·69	10·77	13·85	16·92	20·00	23·08	26·15
AP 0	—	—	—	—	—	—	0·39	6·06	8·89	10·79	12·17
1/4	0·53	0·51	0·60	0·74	0·94	1·69	5·16	9·91	12·81	14·83	16·29
1/2	0·61	1·79	2·54	3·23	4·36	6·10	9·55	13·33	15·93	17·78	19·13
3/4	0·80	3·71	5·01	6·07	8·04	10·29	13·26	16·29	18·57	20·39	21·82
1	1·67	5·96	7·72	9·19	11·72	14·15	16·78	19·16	21·00	22·55	23·65
1 1/2	4·82	11·37	13·69	15·40	18·17	20·24	21·85	22·94	23·93	24·74	25·39
2	10·04	16·67	18·88	20·36	22·55	23·90	24·65	25·17	25·49	25·68	25·89
2 1/2	15·39	20·75	22·62	23·73	24·95	25·55	25·81	25·94	25·96	25·98	26·00
3	19·77	23·55	24·78	25·44	25·93	25·98	26·00	26·00	26·00	26·00	26·00
3 1/2	22·02	25·11	25·88	26·00	26·00	26·00	26·00	26·00	26·00	26·00	26·00
4	22·31	25·40	26·00	26·00	26·00	26·00	26 00	26·00	26·00	26·00	26·00
5	22·31	25·40	26·00	26·00	26·00	26·00	26·00	26·00	26·00	26·00	26·00
6	22·31	25·40	26·00	26·00	26·00	26·00	26·00	26·00	26·00	26·00	26·00
6 1/2	22·31	25·40	26·00	26·00	26·00	26·00	26·00	26·00	26·00	26·00	26·00
7	22·31	25·40	26·00	26·00	26·00	26·00	26·00	26·00	26·00	26·00	26·00
7 1/2	22·31	25·40	26·00	26·00	26·00	26·00	26·00	26·00	26·00	26·00	26·00
8	21·91	25·28	25·91	26·00	26·00	26·00	26·00	26·00	26·00	26·00	26·00
8 1/2	19·69	23·74	24·80	25·24	25·43	25·52	25·64	25·85	26·00	26·00	26·00
9	14·19	19·10	20·94	21·94	22·71	22·78	22·93	23·33	24·13	24·97	25·58
9 1/4	9·65	15·24	17·24	18·23	19·21	19·49	19·55	20·09	21·36	22·89	24·37
9 1/2	4·46	10·33	12·07	13·33	14·27	14·36	14·39	15·07	16·49	18·25	20·32
9 3/4	0·96	4·89	6·86	7·89	8·71	8·48	7·98	8·23	9·33	10·65	12·60
FP 10	—	2·24	3·38	4·08	4·11	2·60	1·38	0·29	0·00	0·62	1·98

PRINCIPAL DIMENSIONS

LENGTH BETWEEN PERPENDICULARS	=	330 m
BEAM	=	52 m
DRAUGHT, LOAD CONDITION	=	20 m
LCB POSITION FORWARD OF MIDSHIPS	=	8·25 m
BLOCK COEFFICIENT	=	0·835

SCALE :- 1, 500

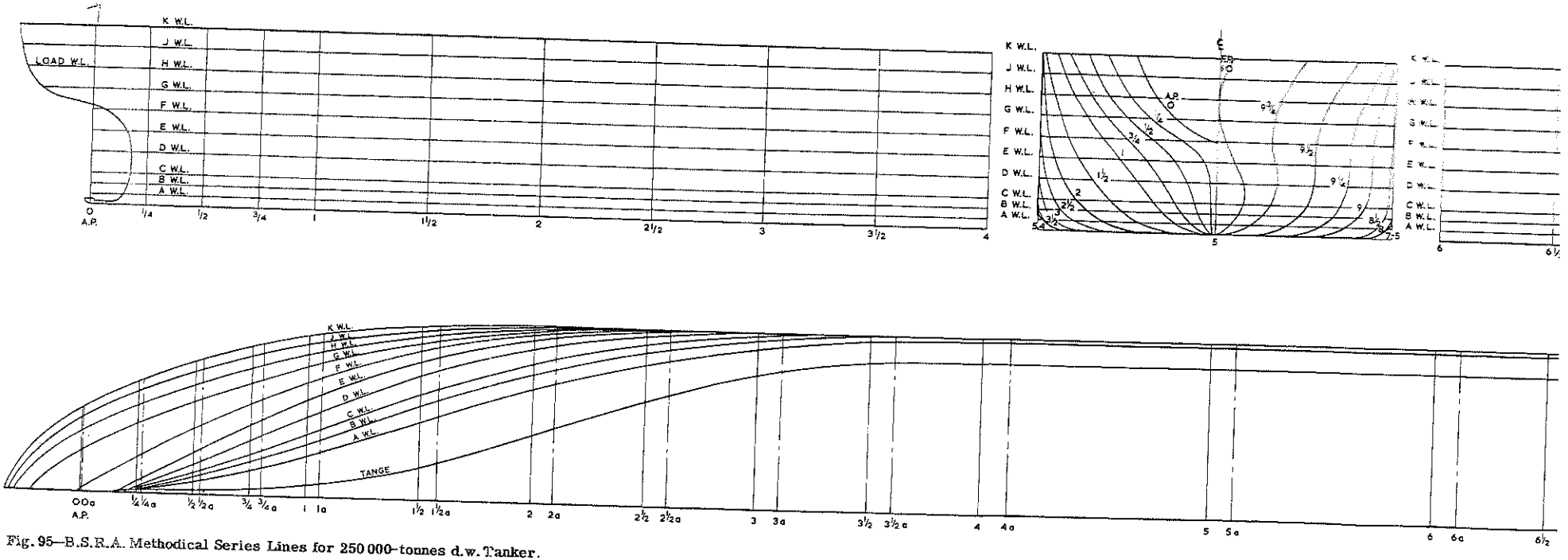

Fig. 95—B.S.R.A. Methodical Series Lines for 250 000-tonnes d.w. Tanker.

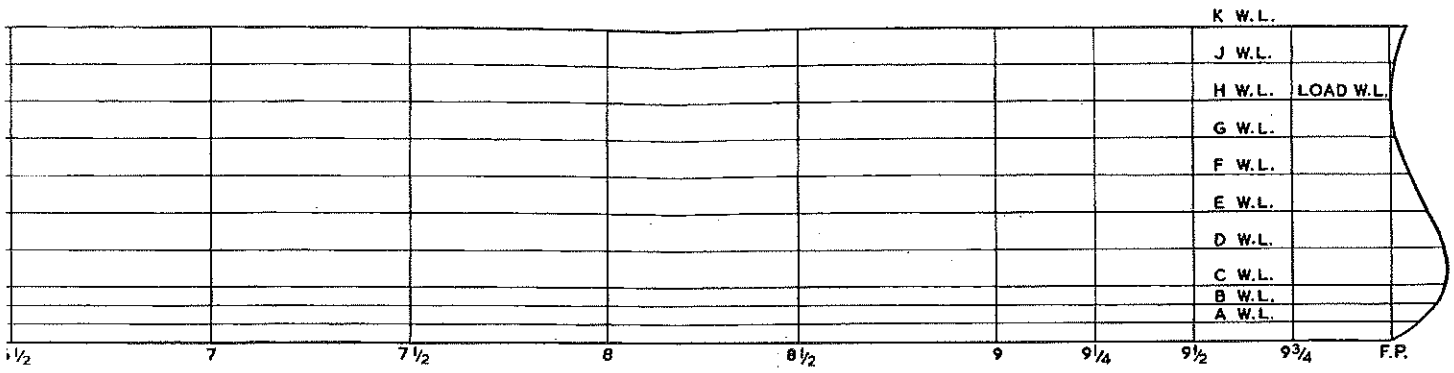
K W.L.
J W.L.
H W.L.
LOAD W.L.
G W.L.
F W.L.
E W.L.
D W.L.
C W.L.
B W.L.
A W.L.
6½
7
7½
8
8½
9
9¼
9½
9¾
F.P.

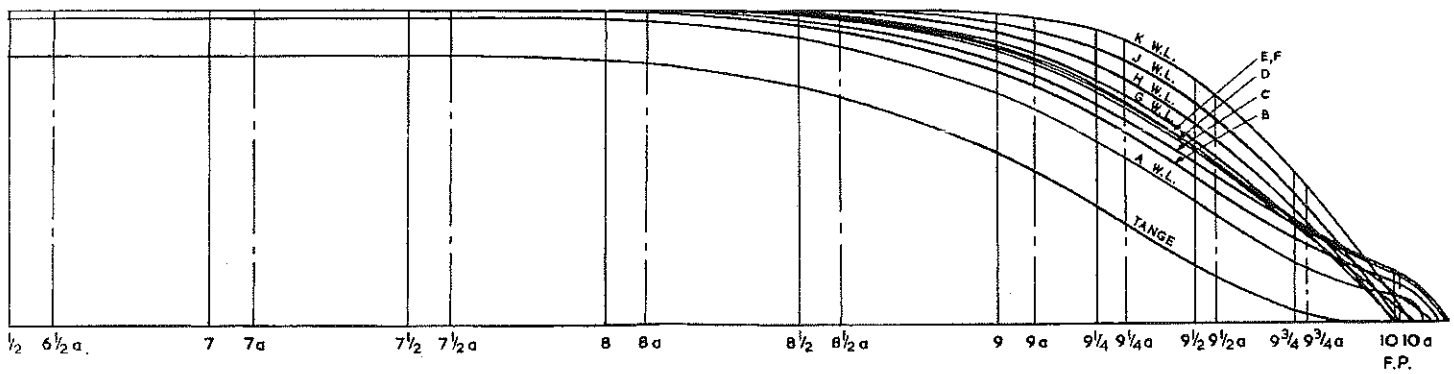
K W.L.
J W.L.
H W.L.
G W.L.
F
A W.L.
TANGE
E,F
D
C
B
½
6½a
7
7a
7½
7½a
8
8a
8½
8½a
9
9a
9¼
9¼a
9½
9½a
9¾
9¾a
10
10a
F.P.

APPENDIX III

WORKED EXAMPLES: RESISTANCE AND PROPULSION

94 The following worked examples demonstrate the use of the design diagrams for determining the resistance coefficient © and the propeller-hull interaction factors for a supertanker and a fast cargo liner. The first example is set out in detail.

95 Specimen data sheets for design office use are given after the worked examples.

EXAMPLE 1

To determine (1) the resistance coefficient © (2) the wake fraction (3) thrust-deduction fraction (4) relative rotative efficiency and (5) the quasi-propulsive coefficient for a supertanker having the following particulars:

Length between perpendiculars	= 330 m
Beam moulded	= 52 m
Load draught	= 20 m
Block coefficient	= 0·835
LCB position forward of midships	= 8·25 m
Propeller diameter	= 9·35 m
Mean face-pitch ratio	= 0·675
Developed blade-area ratio	= 0·60
Propeller revolutions per minute	= 85
Service Speed	= 14·75 knots
Approximate deadweight	= 250 000 tonnes

(1) CALCULATION OF FROUDE RESISTANCE COEFFICIENT ©

(i) 121·92-m L_{pp}© Values for Basis Form

96 The resistance © value for a service speed corresponding to the dimensions of the 121·92 × 16·76 × 6·71 m basis ship may be taken from the basic resistance diagram for bulbous forms presented in Figure 64(c). For the basis ship the corresponding speed is $14{\cdot}75 \times \sqrt{\frac{121{\cdot}92}{330}} = \mathbf{8{\cdot}97\ knots.}$

From the basic resistance diagram, © = **0·694** at 8·97 knots.

(ii) Corrections for B/T Ratio and $L/\nabla^{1/3}$ Ratio

97 In the present example

$$B/T = \frac{52}{20} = \mathbf{2{\cdot}6.}$$

Volume of displacement $\nabla = L_{pp} \times B \times T \times C_B$

$$\nabla = 330 \times 52 \times 20 \times 0{\cdot}835$$

$$\nabla = 286,500\ m^3$$

$$\nabla^{1/3} = \mathbf{65{\cdot}93\ m,}$$

$$\text{and } L/\nabla^{1/3} = \frac{330}{65{\cdot}93} = \mathbf{5{\cdot}0.}$$

The correction-factor multipliers required for these values are taken from the contours presented in Figs. 70 and 72. The correction-factor multipliers for B/T and $L/\nabla^{1/3}$ are **1·01** and **1·025** respectively.

(iii) Corrections for LCB Position

98 The basis LCB position is 2 per cent forward of midships and in this example the actual LCB position is 2·5 per cent forward. The deviation from the basis position is **+ 0·5%** and the necessary LCB correction to be made to the basis ship © value is taken from the contours presented in Fig. 75. The correction-factor multiplier for LCB is **0·99**.

(iv) 121·92-m L_{PP}© Value for Required Form

99 The total correction to be applied to the basis © value is the product of the corrections obtained in (ii) and (iii) for the basis ship speed. In this example $©_{121·92m} = 0·99 \times 1·01 \times 1·025 \times 0·694 = \mathbf{0·711}$.

(v) © Value for Required Form

100 The final correction required is that for the difference in ship size from L_{PP} 121·92m to 330m. For this purpose the R.E. Froude skin-friction correction may be taken from Fig. 65 or from the formula

$$©_{121·9m} - ©_{330m} = (0_{121·9m} - 0_{330m})ⓈⓁ^{-0·175}$$

The wetted surface coefficient Ⓢ may be estimated from either of the formulae given in para 40, the values being **5·95** and **5·88** (the latter value obtained from the Froude-type equation).

The R.E. Froude skin-friction 'O'—values for 121·92m and 330m may be obtained from Reference 9 the values being **0·0741** and **0·0658** respectively. The R.E. Froude speed-length coefficient Ⓛ = $3·545F_n$. In this example

Froude number $= \dfrac{14·75 \times 1852}{3600} \Big/ \sqrt{9·81 \times 330} = \mathbf{0·133}$ and the © correction for length is **−0·045**, i.e.

$©_{330m} = 0·711 - 0·045 = \mathbf{0·666}$.

A conversion diagram is given in Fig. 66 from which ship © values based on the I.T.T.C. 1957 model-ship correlation line[29] may be taken.

(2) CALCULATION OF TAYLOR WAKE FRACTION

101 The parameters required for estimating wake fraction are C_B, D_W, and F_n.

$$B/\nabla^{1/3} = \frac{52}{65·93} = \mathbf{0·789}.$$

$$D/\nabla^{1/3} = \frac{9·35}{65·93} = \mathbf{0·142}.$$

The wake fraction parameter $D_W = B/\nabla^{1/3} \times \sqrt{\nabla^{1/3}/D} = \dfrac{0·789}{\sqrt{0·142}} = \mathbf{2·09}$.

Entering the diagram for wake fraction, Fig. 89, at $C_B = 0·835$ and $F_n = 0·133$ the value for Taylor wake fraction $w_T = \mathbf{0·451}$.

(3) CALCULATION OF THRUST-DEDUCTION FRACTION

102 Two diagrams are available for estimating t. In the first instance the preferred diagram, presented in Fig. 90, is used. The parameters required are C_B, LCB, $B/\nabla^{1/3}$, and P/D. The LCB position expressed as a percentage of L_{PP} is **2·5F**. Entering the sub-

diagram at $C_B = 0{\cdot}835$ the partial value for t is **y = 0·025.** Entering the other diagram at $B/\nabla^{1/3} = 0{\cdot}789$ the partial value for t is **x = 0·237.**

The difference between the partial values x and y gives the thrust-deduction fraction **t = 0·212.** The alternative presentation requires the parameters C_B, LCB, and the thrust-deduction parameter D_t.

$$D_t = B/\nabla^{1/3} \times D/\nabla^{1/3}$$
$$= 0{\cdot}789 \times 0{\cdot}142 = \mathbf{0{\cdot}112}.$$

Entering the diagram for thrust-deduction fraction, Fig. 91, at $C_B = 0{\cdot}835$, the value for **t = 0·204.**

(4) CALCULATION OF RELATIVE ROTATIVE EFFICIENCY

103 Two diagrams are available for estimating η_R. The preferred diagram, presented in Fig. 92, is used in the first instance. The parameters required are P/D, A_D/A_O, C_B, and D/L_{PP}.

$$D/L_{PP} = \frac{9{\cdot}35}{330} = \mathbf{0{\cdot}028}.$$

Entering the sub-diagram at $P/D = 0{\cdot}675$ the partial value for η_R is **x = 0·853.** Entering the other diagram at $C_B = 0{\cdot}835$ the partial value for η_R is **y = 0·155.** The summation of the partial values x and y gives the relative rotative efficiency, η_R = **1·008.**

The alternative presentation requires the parameters C_B, D/L_{PP}, and $D/\nabla^{1/3}$.

Entering the diagram for relative rotative efficiency, Fig. 93, at $C_B = 0{\cdot}835$ the value for η_R **= 1·02.**

(5) CALCULATION OF QUASI-PROPULSIVE COEFFICIENT

104 Entering the Troost B6 series propeller diagrams[30] at a value of advance coefficient

$$\delta = \frac{ND}{V_A} = \frac{85 \times 9{\cdot}35 \times 3{\cdot}28}{14{\cdot}75 \times (1-0{\cdot}451)} = \mathbf{321}$$ and pitch ratio = **0·675**

the open water efficiency η_O **= 0·429.**

(i) Using the preferred design diagrams in conjunction with the open-water efficiency, the quasi-propulsive coefficient is given by

$$\eta_D = \eta_H \times \eta_R \times \eta_O$$
$$= \frac{1-0{\cdot}212}{1-0{\cdot}451} \times 1{\cdot}008 \times 0{\cdot}429 = \mathbf{0{\cdot}622}.$$

(ii) Using the alternative design diagrams for t and η_R

$$\eta_D = \frac{1-0{\cdot}204}{1-0{\cdot}451} \times 1{\cdot}02 \times 0{\cdot}429 = \mathbf{0{\cdot}635}.$$

(iii) The diagram for estimating quasi-propulsive coefficient directly, presented in Fig. 94, requires the parameters B/D, C_B, $N\sqrt{L_{PP}}$, and A_D/A_O.

$$B/D = \frac{52}{9{\cdot}35} = 5{\cdot}56$$

$$N\sqrt{L_{PP}} = 85 \times \sqrt{330} = \mathbf{1545}.$$

Entering the sub-diagram at B/D = 5·56 the partial value for η_D is **x = 0·896.** Entering the other diagram at $N\sqrt{L_{PP}} = 1545$ the partial value for η_D is **y = 0·276.**

The difference between the partial values x and y gives the quasi-propulsive coefficient, η_D = **0·620.** The values obtained in (i) to (iii), correspond to a propeller loading $(1 + x)_{Froude} = 1{\cdot}10$ and should be corrected to the appropriate loading of the ship as suggested in para. 67.

EXAMPLE 2.

A fast cargo liner has the following particulars

Length between perpendiculars	= 155 m
Beam moulded	= 23 m
Load draught	= 9 m
Block coefficient	= 0·550
LCB position abaft midships	= 2·35 m
Propeller diameter	= 6·35 m
Mean face-pitch ratio	= 0·975
Developed blade-area ratio	= 0·60
Propeller revolutions per minute	= 122
Service speed	= 22 knots
Approximate deadweight	= 13 000 tonnes

Details of this calculation are presented in an abbreviated form. In the propulsion estimates the values obtained from the alternative regression equations for t and η_R are given in parentheses.

(1) CALCULATION OF FROUDE RESISTANCE COEFFICIENT ©

(i) 121·92-m L_{PP} © Value for Basis Form

105 From Fig. 64(a) the resistance © value, for a service speed corresponding to the dimensions of the basis bulbous form, i.e. 19·5 knots, is **0·776.**

(ii) Corrections for B/T Ratio and $L/\nabla^{1/3}$ Ratio

106 The values for B/T and $L/\nabla^{1/3}$ are **2·55** and 5·95 respectively. From Figs. 71 and 74 the correction-factor multipliers for B/T and $L/\nabla^{1/3}$ are both **unity.**

(iii) Corrections for LCB Position

107 The LCB position for the ship is 1½ per cent abaft midships which represents a positive deviation from the basis ship of 1 per cent. From Fig. 79 the correction-factor multiplier for LCB is **0·97.**

(iv) 121·92-m L_{PP} Value for Required Form

108 The total correction applied to the basis © value is therefore **0·97.** In the present example $©_{121{\cdot}9m} = 0{\cdot}97 \times 0{\cdot}776 = \mathbf{0{\cdot}753}$.

(v) © Value for Required Form

109 The estimated wetted surface coefficient Ⓢ = 6·37 and from Fig. 65 the R.E. Froude skin-friction correction is **−0·012** and hence the Froude resistance coefficient © for the required form is

$$©_{155m} = ©_{121·9m} - 0·012$$

$$©_{155m} = 0·753 - 0·012 = \mathbf{0·741}.$$

(2) CALCULATION OF TAYLOR WAKE FRACTION

Volume of displacement $\nabla = 17,660\ m^3$,

$$\nabla^{1/3} = \mathbf{26·04\ m}.$$

$B/\nabla^{1/3} = \mathbf{0·883}$ and $D/\nabla^{1/3} = \mathbf{0·244}$ hence $D_W = \mathbf{1·79}$.

Froude number = **0·29** and from Fig. 89 $w_T = \mathbf{0·225}$.

(3) CALCULATION OF THRUST-DEDUCTION FRACTION

$D_t = \mathbf{0·216}$ and LCB = **1·5%A**

From Fig. 90 $t = 0·296 - 0·091$

$t = \mathbf{0·205}$ ($t = 0·228$ from Fig. 91).

(4) CALCULATION OF RELATIVE ROTATIVE EFFICIENCY

$D/L_{pp} = \mathbf{0·041}$ and from Fig. 92

$\eta_R = 0·889 + 0·136 = \mathbf{1·025}$ ($\eta_R = \mathbf{1·028}$ from Fig. 93).

(5) CALCULATION OF QUASI-PROPULSIVE COEFFICIENT

$N\sqrt{L_{pp}} = \mathbf{1520}$ and $B/D = \mathbf{3·63}$

From the Troost B4 series propeller diagrams[30], the open-water efficiency = **0·65** at $\delta = \mathbf{149·2}$ and $P/D = \mathbf{0·975}$.

(i) From the preferred design diagrams

$$\eta_D = \frac{1-0·205}{1-0·225} \times 1·025 \times 0·65 = \mathbf{0·682}.$$

(ii) From the alternative diagrams for t and η_R

$$\eta_D = \frac{1-0·228}{1-0·225} \times 1·028 \times 0·65 = \mathbf{0·666}.$$

(iii) From the design diagram for η_D given in Fig. 94

$\eta_D = 0·939 - 0·263 = \mathbf{0·676}$

As mentioned in the previous example, the values obtained in (i) to (iii) correspond to a propeller loading of $(1 + x)_{Froude} = 1·10$.

SPECIMEN DATA SHEET FOR USE IN CALCULATING RESISTANCE OF A B.S.R.A. METHODICAL SERIES FORM

SHIP NUMBER..... DATE.....

Bulbous/Normal bow

L_{PP} (m)	B (m)	T (m)	C_B	LCB (%)*	B/T	$L/\nabla^{1/3}$	Basis LCB Position

Froude Wetted Surface Coefficient Ⓢ = 1·88 + 0·941 C_B + 0·766 $L/\nabla^{1/3}$ − 0·086 L/B =

Naked Effective Power (kW) = $\frac{© \Delta^{2/3} V^3}{579 \cdot 9}$

1	2	3	4	5	6	7	8	9	10	11	12	13	14	15
Speed in knots for basis ship 121·92-m L_{FP}	Froude $©_{121 \cdot 9}$ m from basis diagram (vide Figs. 63 and 64)†	Correction-factor multipliers (vide Figs. 70 to 80)			Total © correction factor multiplier (3 × 4 × 5)	Froude © without length correction (2 × 6)	Froude skin-friction correction (vide Fig. 65)	Speed V in knots for actual ship.	V^3	Froude Basis		δ © for ship (vide Fig. 66)	1957 I.T.T.C. Basis	
		B/T	$L/\nabla^{1/3}$	LCB						© for ship (7 + 8)	Naked effective power (kW)		© for ship (11-13)	Naked effective power (kW)

* *LCB position considered positive when forward of midships.*

† *Figure numbers refer to those given in B.S.R.A. Report NS. 333, 1971.*

SPECIMEN DATA SHEET FOR USE IN CALCULATING B.S.R.A. METHODICAL SERIES PROPULSION FACTORS

Ship No.....
Date.....

L_{pp} (m)	B (m)	T (m)	C_B	LCB (%) (see note 1)	Propeller particulars		
					Diameter D (m)	Pitch ratio P/D	A_D/A_O

Ship speed V (knots)	Froude number ($0{\cdot}164\ V/\sqrt{L_{pp}}$)	Taylor wake fraction w_T (Fig. 89) see note 2	Thrust-deduction fraction				Relative rotative efficiency η_R			
			Preferred diagram (Fig. 90)			Alternative diagram for t (Fig. 91)	Preferred diagram (Fig. 92)			Alternative diagram for η_R (Fig. 93)
			x	y	$t = x - y$		x	y	$\eta_R = x + y$	

Ship speed V (knots)	Speed of advance $V_A = V(1 - w_T)$	Propeller rpm, N	Taylor advance coeff. $\delta = \frac{3{\cdot}28\ ND}{V_A}$	Propeller efficiency η_O (see note 3)	Revolutions length coefficient $N\sqrt{L_{pp}}$	Quasi-propulsive coefficient η_D (see note 4)			
						Design diagram (Fig. 94)			$\frac{(1-t)}{(1-w_T)} \times \eta_R \times \eta_O$
						x	y	$\eta_D = x - y$	

Parameters required

$B/\nabla^{1/3} =$

$D/\nabla^{1/3} =$

$D_W = B/\nabla^{1/3} \cdot \sqrt{\nabla^{1/3}/D}$

$=$

$D_t = B/\nabla^{1/3} \cdot D/\nabla^{1/3}$

$=$

$D/L_{pp} =$

$B/D =$

Notes: 1. LCB position considered positive when forward of midships.
2. Design diagrams are given in Part III of B.S.R.A. Report NS. 333. 1971.
3. Propeller open-water efficiency η_O may be taken from the NSMB (Troost) B series diagrams given in B.S.R.A. Technical Memorandum No. 213. 1965.
4. The value of η_D corresponds to a propeller loading of $(1 + x)_{Froude} = 1{\cdot}10$. A correction for other propeller loadings may be made as suggested in B.S.R.A. Report NS. 333 i.e. η_D (corrected) $= \eta_D + 0{\cdot}15[1{\cdot}10 - (1 + x)_{Froude}]$.

CONVERSION FACTORS TO ASSIST COMPARISON WITH DATA IN IMPERIAL UNITS

(Correct to 5 significant figures)

Length

1 km	= 0·53961 UK nautical mile
1 km	= 0·53996 International nautical mile
1 m	= 0·54681 fathom
1 m	= 3·2808 ft
1 mm	= 0·039370 in.
1 μm	= 0·039370 mil

Area

1 m^2	= 10·764 ft^2
1 mm^2	= 0·0015500 $in.^2$

Volume

1 m^3	= 35·315 ft^3
1 l	= 0·21998 gal

Section Modulus

1 m cm^2	= 0·50853 $in.^2$ ft
1 cm^3	= 0·061024 $in.^3$

Second Moment of Area

1 m^2 cm^2	= 1·6684 $in.^2$ ft^2
1 cm^4	= 0·024025 $in.^4$

Frequency

1 Hz	= 1 c/s

Speed

1 km/h	= 0·53961 UK knot
1 km/h	= 0·53996 International knot
1 m/s	= 3·2808 ft/s

Acceleration

1 m/s^2	= 3·2808 ft/s^2

Mass

1 tonne	= 0·984207 ton
1 kg	= 2·2046 lb

Specific Volume

1 m^3/tonne	= 35·881 ft^3/ton
1 l/kg	= 0·016018 ft^3/lb

Mass Flow

1 tonne/h	= 0·98421 ton/h
1 kg/h	= 2·2046 lb/h

Volume Flow

1 m^3/min	= 35·315 ft^3/min
1 m^3/h	= 3·6662 gal/min
1 l/h	= 0·21998 gal/h

Density

1 g/cm^3	= 0·036127 $lb/in.^3$
1 g/l	= 0·062428 lb/ft^3

Moment of Inertia

1 kg m^2	= 23·730 lb ft^2
1 kg cm^2	= 0·34172 lb $in.^2$

Momentum

1 kg m/s	= 7·2330 lb ft/s

Moment of Momentum and Angular Momentum

1 kg m^2/s	= 23·730 lb ft^2/s

Force

1 kN	= 0·10036 tonf
1 N	= 0·22481 lbf

Moment of Force

1 kN m	= 0·32927 tonf ft
1 N m	= 0·73756 lbf ft

Pressure

1 MN/m^2	= 9·8693 atm
1 MN/m^2	= 145·04 $lbf/in.^2$
1 kN/m^2	= 0·29530 in. Hg.
1 kN/m^2	= 4·0147 in. w.g.
1 N/m^2	= 10 dyne/cm^2
1 bar	= 10^5 N/m^2 = 14·504 $lbf/in.^2$

Stress

1 N/mm^2	= 0·064749 $tonf/in.^2$
1 N/mm^2	= 145·04 $lbf/in.^2$

Absolute or Dynamic Viscosity

1 cP	= 10^{-3} N s/m^2
1 kg/m s	= 0·67197 lb/ft s

Kinematic Viscosity*

1 cSt	= 10^{-6} m^2/s
1 m^2/s	= 10·764 ft^2/s

Energy (Work, Heat)

1 kWh	= 1·3410 hp h
1 kJ	= 0·94782 Btu
1 J	= 0·73756 ft lbf

Power

1 kW	= 1·3410 hp
1 W	= 0·73756 ft lbf/s
1 W	= 3·4121 Btu/h

Fuel Consumption Rate

1 kg/kWh	= 1·6440 lb/hp h

Absolute Temperature

°F	= 9/5 K − 459·7
°R	= 9/5 K

Celsius Temperature

°F	= 9/5 °C + 32

Temperature Interval (°C)

1 °C	= 9/5 °F

Linear Expansion Coefficient

1 $°C^{-1}$	= 5/9 $°F^{-1}$

Heat Flow Rate

1 kW	= 0·94782 Btu/s

Specific Energy, Calorific Value, Specific Latent Heat

1 kJ/kg	= 0·42992 Btu/lb

Specific Heat Capacity

1 kJ/kg °C	= 0·23885 Btu/lb °F

Specific Entropy

1 kJ/kg K	= 0·23885 Btu/lb °R

Density of Heat Flow Rate

1 W/m^2	= 0·31700 Btu/ft^2 h

Volumetric Heat Release Rate

1 W/m^3	= 0·096622 Btu/ft^3 h

Coefficient of Heat Transfer

1 W/m^2 °C	= 0·17611 Btu/ft^2 h °F

Thermal Conductivity

1 W/m °C	= 6·9335 Btu in./ft^2 h °F

Prefixes (in order of magnitude)

tera	T	= 10^{12}
giga	G	= 10^9
mega	M	= 10^6
kilo	k	= 10^3
hecto	h	= 10^2
deca	da	= 10
deci	d	= 10^{-1}
centi	c	= 10^{-2}
milli	m	= 10^{-3}
micro	μ	= 10^{-6}
nano	n	= 10^{-9}

**Diagrams for converting Redwood and Saybolt seconds, Engler degrees, and Barber fluidity are given in standard text books, e.g. H.M. Spiers' 'Technical Data on Fuel.'*

Unchanged Factors

Plane angle — Angular velocity
Time — Angular acceleration
Rotational speed

Revised July 1971

RECENT B.S.R.A. REPORTS

283 Review of Data-Logging Equipment in Two Tankers
284 Automatic Tack Welding
285 Fatigue Behaviour of Steel Specimens with Square Openings
286 Paints for Wet Surfaces
287 Piston-Ring Breakages
288 Internal Fault Protection of a.c. Marine Generators
289 Prefabrication Primers. Period of Protection
290 Tests on Cuno Fuel-Oil Filter
291 Tests using Lubricating Oil on an Alfa-Laval Vacuum Centrifuge
292 Survey of Marine Sewage Systems
293 Reliability Analysis in Ships' Engineering Systems
294 External Cathodic Protection and External Paint Trials
295 Manœuvring Trials with 193,000-tonne d.w. Tanker *Esso Bernicia*
296 Review of Materials for Heat-Exchanger Water Boxes
297 Preventing Marine Growth by the Use of Predatory Bacteria
298 Painting Under Adverse Conditions
299 Evaluation of Anti-Corrosive Coatings
300 Numerical Assessment of Hull Condition
301 Plastic Pipes for Hot-Water Service on Board Ship
302 Production Sequencing of Accommodation Bulkhead Panels
303 Forming Mild Steel by Heat-Line Bending
304 Improving Mooring Methods. Cargo Vessels. New Construction
305 Study of Marine Fouling Organisms
306 Photogrammetry as Aid to Ship-Piping Manufacture
307 Materials for Salt-Water Circulating Pumps
308 Evaluation of AUTOKON Computer System. Part II. Part Generation
309 Plate and Section Handling. Part 2. Controlled Magnets for Lifting
310 Simulation of a Diesel-Engine Jacket Water-Cooling System
311 Trials of Anti-Fouling Compositions
312 B.S.R.A. Pipe to Flange Friction-Welding Machine
313 Behaviour of a Double-Bottom Structure under Load
314 Water-Ballast System Design for Dry Bulk Carriers
315 Methodical Series Resistance and Propulsion Experiments. 0·65 Block Coefficient Series. Variations in Parallel Middle Body
316 Methodical Series Resistance and Propulsion Experiments. 0·70 Block Coefficient Series. Variations in Parallel Middle Body
317 Effective Horsepower of Single-Screw Ships. Standards of Attainment 1969
318 Corrosion of Bronze Propellers
319 Removal of Fouling and Exhausted Anti-Fouling Composition by 'Soft-Blasting'
320 Methodical Series Resistance and Propulsion Experiments. 0·75 Block Coefficient Series. Variations in Parallel Middle Body
321 Experience in Use of Steel-Plate Ordering Technique (SPOT)
322 Computer System in the *Queen Elizabeth 2*
323 Oxygen Cutting of Shipbuilding Steel
324 Service trial on a Jungner Power Meter
325 Operational Experience with a Heavy Fuel-Oil Homogeniser
326 Evaluation of Tellurometer MRB 201 System as a Means of Measuring Ship Speed
327 Inhibiting Marine Fouling with the Cychlor Electrolyser
328 Project Control System for Use with Network Analysis
329 Reliability Study of Alternative Electrical Power Generation Systems in Motor Ships
330 B.S.R.A. Materials Coding System for the Shipbuilding Industry
331 Review of the Use of Data Loggers in Merchant Ships
332 Study of the Decca ISIS 300 A Second-Generation Supervisory Data Logger